DEVELOPMEMT OF TETRAPHENYLBORATE-BASED PHOTOBASE GENERATORS AND SACRIFICIAL POLYCARBONATES FOR RADIATION CURING AND PHOTORESIST APPLICATIONS

by

Xun Sun, B.Eng.

A thesis submitted to the

Faculty of Graduate Studies and Research

in partial fulfillment of the requirements for the degree of

Doctor of Philosophy

Department of Chemistry

Carleton University

Ottawa, Ontario

November 2008

Your file Votre référence
ISBN: 978-0-494-47492-1
Our file Notre référence
ISBN: 978-0-494-47492-1

ABSTRACT

Aiming at the development of new photobase generators (PBGs) and photoimageable sacrificial materials for radiation curing and photoresist applications, this thesis research explores the potential of tetraphenylborate salts as a new class of PBGs and their uses as photocatalysts in photoinitiated base-catalyzed polymerizations, polymer cross-linking and polymer thermal degradation. The thesis work also investigates the structure-performance relationship in thermodegradable polycarbonates (PCs).

The design strategy for new PBGs involves the use of a protonated amine with tetraphenylborate as a counter ion. The photolysis of the tetraphenylborate chromophore leads to the release of free amine bases. A variety of amines can be used and converted into the corresponding PBGs. Specifically, triethylamine, 1,8-diazabicyclo[5.4.0]undec-7-ene (DBU), 1,5,7-triaza-bicycle[4.4.0]dec-5-ene (TBD) and tert-butylimino-tris(dimethylamino)phosphorane [*t*-BuP_1(dma)] are readily converted into the tetraphenylborate salts, which all can release the base upon irradiation below 280 nm in the solid state and in solution. The quantum yields of these PBGs are comparable to most of commercially available cationic photo-initiators. TBD·$HBPh_4$ and *t*-BuP_1(dma)·$HBPh_4$ are able to release TBD and *t*-BuP_1(dma) that are 100 and 1000 times more basic, respectively, than the strongest base ever generated among all previously reported PBGs. TBD·$HBPh_4$ is found to be an efficient photocatalyst for the living ring-opening polymerization of cyclic esters, photo-cross-linking of polymeric materials containing the hydroxyl-ester groups, and base-amplified thermolysis of poly(propylene carbonate) (PPC). Using TBD·$HBPh_4$ as a PBG, a dry-developing

photoresist material based on PPC is successfully formulated and the positive images with a resolution better than 80 μm and an aspect ratio of 3:1 have been demonstrated.

In addition, thermodegradable PCs are functionalized to contain the photo-cross-linkable acrylate, metal-binding (e.g., amine, disulfide, pyrrolidinone and diether) and water-soluble carboxylic acid groups. The metal-binding PCs are highly labile to heat and can be completely degraded to volatile compounds at 320-380 ^{o}C in an inert atmosphere. The degradation temperatures are further lowered, even close to room temperature, in the presence of acid or amine groups due to chemical amplification effect. The PCs containing pyrrolidinone or cross-linked acrylate groups can not be cleanly burned off, because their thermolysis by-products are non-volatile and become char-like ashes (> 1 wt.%). In comparison with DuPont Fodel® silver conductor paste, the PCs-based photoimageable sacrificial paste has comparable photo-patterning ability and a lower burning temperature for image development.

ACKNOWLEDGMENTS

First of all, I would like to express my deepest thanks to my supervisor, Dr. Zhi Yuan (Wayne) Wang. He motivated me by his example and knowledge, and provided me firm and decisive guidance. Without his support, this thesis could not be completed successfully.

I would also like to thank Dr. Jane Gao for her assistance and advice. Her calm, unruffled and pleasant style of dealing with most trying problems one encounters during research has taught me much. My sincere thanks also go to the late Dr. Oliver E. Edward. His knowledge and passion for chemistry always inspires me.

It was a great pleasure for me to work with all the members of Dr. Wang's lab: Dr. Y. W. Bai, Dr. N. H. Song, Dr. L. Kuang, J. D. Zhang, Dr. S. D. Xun, Dr. X. G. Wu, Dr. E. Todd, Dr. G. LeClair, Mr. Y. X. Cui, Mr. Huy, Mrs. W. H. Hao, Mr. D. Li, Mrs. Z. H. Wang. They treated me like their brother. Special thanks to Dr. Bai and Dr. Song whose extensive help was more appreciated than they would ever know.

My thanks also go to many others in the department and the technicians who work at the NMR and MS facilities at Carleton University and the University of Ottawa. They have done a lot for me to finish my thesis.

Finally, I want to thank my family, my parents, uncle, brother and sister for their unconditional supports and care throughout the years and in particular my wife for her love and understanding during my study in Canada.

TABLE OF CONTENTS

List of Tables

List of Figures

List of Schemes

LIST OF SYMBOLS AND ABBREVIATIONS

Φ	Quantum yield
λ_{max}	Maximum absorption wavelength
ε	Molar absorption coefficient
n	Refractive index
AAPO	Acryloyl acetophenone oxime
AN	Acetonitrile
AOI	*O*-Acyloximes
BOC	Benzyloxycarbonyl
CL	Caprolactone
COI	*O*-Carbamoyloximes
DABCO	1,4-diazabicyclo [2.2.2]octane
DBN	1,5-diazabicyclo [4.3.0]non-5-ene
DBU	1,8-diazabicyclo[5.4.0]undec-7-ene
DMAP	*N,N*-dimethylaminopyridine
DMF	*N,N*-dimethylformamide
DMSO	Dimethyl sulfoxide
DP	Degree of polymerization
DSC	Differential scanning calorimetry
FMOC	9-fluorenylmethyl carbamates
HEC	2-hydroxyethyl cellulose
HPA	Hydroxypropyl acrylate
MMA	Methyl methacrylate
M_n	Number-average molecular weight
M_v	Viscosity-average molecular weight
NBOC	*O*-nitrobenzyloxycabonyl
P(GMA-co-EA)	Poly[glycidyl methacrylate-co-ethyl acrylate]
PBGs	Photobase generators
PEG	Polyethylene glycol
PIs	Photoinitiators
pK_a	Negative logarithm of the acid dissociation constant
PL	Photoluminescence
PMMA	Poly(methyl methacrylate)
QA	Quaternary Ammonium
ROP	Ring-opening polymerization
SET	Single electron transfer
St	Styrene
TBD	1,5,7-Triaza -bicyclo[4.4.0]dec-5-ene

TBD•$HBPh_4$	1,5,7-triazabicyclo[4.4.0]dec-5-enyltetraphenylborate
t-BuP1(dma)	*tert*-Butylimino-tris(dimethylamino)phosphorane
t-BuP_1(dma)•$HBPh_4$	*tert*-butylimino-tris(dimethylamino)phosphoranyltetraphenyl borate
T_d	Decomposition temperature with 5% weight loss
TGA	Thermogravimetric analysis
THF	Tetrahydrofuran
UV-vis	Ultraviolet-visible
VOC	Volatile organic compound
VP	*N*-vinylpyrrolidone
PPC	poly(propylene carbonate)
M_{res}	Ash content
$T_{burn\text{-}off}$	Clean-burn-off temperature
T_d	The onset temperature with 5% weight loss
PS	Polystyrene
PE	Polyethylene
BTC	Bis(trichloromethyl)carbonate
MIM	N-methylimidazole

CHAPTER I

INTRODUCTION TO PHOTOBASE GENERATORS

Photobase generators (PBGs) are compounds capable of in situ generating basic species by irradiation, e.g., mostly by ultraviolet-visible (UV-vis) irradiation. The study of PBGs starts twenty years ago. As a new generation of photoinitiators (PIs), PBGs have been applied to initiate base-catalyzed polymer cross-linking and modifications, and show great potentials in coatings and micro-electronics industry.[1] The rapid growth of PBGs is due to their unique advantages over traditional PIs. The reactive species released from PBGs are organic nitrogen bases, which are stable in air and inert to metal corrosion. Therefore, comparing with the widely used free-radical PIs, PBGs do not experience oxygen inhibition. In contrast to the commercially available cationic PIs, which produce strong acidic species, PBGs are much better fit for applications involving metallic substrates, such as coatings in automobile and electronic industries.

I.1 History of Photobase Generators

The first PBG was reported in 1987,[2] as an outcome of the fast expansion of UV curing technology and urgent needs for new PIs. Making clear the notions of UV curing and PIs helps to better understand the development of PBGs.

I.1.1 UV Curing

UV curing uses UV light to solidify a photochemically reactive and usually

solvent-free coating material through polymerization or cross-linking.[3] The UV light is typically in a range from 400 to 100 nanometers (nm) with three categories: UV-A (400 ~ 315 nm), UV-B (315 ~ 280 nm), and UV-C (280 ~ 100 nm).[4] The intensity of irradiance falling on a surface is measured in milliwatts per square centimeter (mW/cm^2). The UV curing technology appeared in the middle of 20^{th} century. The first patent in this area was a UV-curable ink disclosed in 1946 from Inmont Corp. in the US.[5] In 1967, the Bayer AG in Germany developed the first generation of UV-curable coating for wooden furniture with a trademark of Roskydal®. A new industry featured by "Faster curing, faster manufacture" took shape. The UV curing technology grew rapidly in the 1990s, stemmed from the existence of commercial photoinitiators covering most wavelengths of the UV spectrum. Nowadays, UV curing has become to a well-accepted technology that enables an increasingly large number of industrial uses, from protective and decorative coatings to graphic arts applications such as UV-curable printing or ink jet inks and to the production of electronic materials.[6-9]

Driving forces for this fast growth are due to some unique features of the UV curing technology. (1) Generally, with irradiation by a UV lamp in the range of several hundred watts per square centimeter, the coating can be completely solidified in seconds or minutes, which may take several hours and even days for traditional coatings. This high curing speed considerably increases the manufacturing efficiency and reduces the unit costs. (2) The long shelf life of the ready-to-use property in combination with "cure on demand" triggered by light gives a full control over the curing process, providing

advantages such as easy handling and very little loss of material due to premature gelation. (3) The use of solvent-free formulations with very low volatile organic compound (VOC) emissions meets the increasingly stringent legal regulations required for all the industrial applications. Thus, the UV curing technology offers both economic and environmental advantages.

I.1.2 Photoinitiators

The UV curing systems normally consist of four parts: photoinitiators, monomers, oligmer resins and additives, such as stabilizers, adhesion promoters, pigments, etc.[6] The key component is photoinitiator (PI), since it is responsible for efficient transformation of energy of photons into chemical energy in the form of reactive species that are capable of initiating the chemical reaction. The initiation process may be described in two steps (Scheme I.1). The PI goes to the excited state by absorbing a photon, which then produces one or many reactive species ($R^{\bullet}$, R^{+}) that may be the free radical, ion or radical ion; the reactive species then initiates the chemical reaction or polymerization. With an appropriated light source, efficient photoinitiation of the PI depends upon several factors, including: (1) suitable absorption coefficient and wavelength sensitivity, (2) initiation quantum yield, e.g., in a range of 0.1 ~ 1.0, and (3) reactivity of photogenerated species.[8]

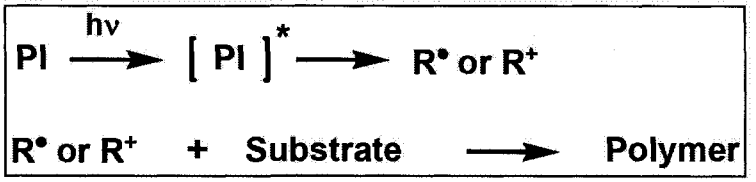

Scheme I.1. Initiation process of photoinitiator

Traditional PIs can be generally classified into free-radical photoinitiators and cationic photoinitiators, based on the type of photogenerated reactive species. Benzoin and its derivatives, benzil ketals, substituted acetophenone and benzophenone, acylphosphine oxides, and thioxanthone derivatives are the common free-radical photoinitiators.[10-15] They produce free radicals to initiate radical polymerization of acrylate systems upon irradiation. Cationic photoinitiators generate Lewis acid or protonic acids to initiate cationic polymerization of monomers, such as epoxides and vinyl ethers, when excited with UV light. The commercial cationic photoinitiators include onium salts belonging to the diaryliodonium and triarylsulfonium families, 2-nitrobenzyl esters, and phosphonium salts.[16-19]

Free-radical photopolymerization is by far the most widely used process in UV curing. Cationic photopolymerization has also found industrial applications. Both technologies have inherent advantages and limitations closely related to the mechanism of polymerization. While radically polymerizing systems allow very fast curing at ambient temperature, the process can be seriously affected by oxygen inhibition. The resulted polymeric coatings exhibit severe shrinkage, which may cause stress and poor adhesion. Cationic systems are not inhibited by atmospheric oxygen, but residual acids may migrate and corrode metal substrates, especially for applications in the automotive and microelectronic industries.

Another curing process free of oxygen inhibition and metal corrosion uses the base-catalyzed reactions. A wide variety of formulations suitable for such a process are

available, based on the base-catalyzed addition of polyols to isocyanates to yield polyurethanes,[20-23] the ring-opening of epoxides by nucleophiles such as amino, thiol, or carboxylate groups[24,25], and a base-catalyzed Michael reaction of acetoacetate or malonate containing polyesters and acrylates.[26,27] A new type of PIs capable of producing a base is thus required, which lead to the development of photobase generators.

I.1.3 Photobase Generators (PBGs)

The first example of PBG was reported in 1987. Ammonia, generated by the photolysis of Co(III)-amine complex, was employed as a cross-linker for polymers with pendant epoxy groups.[26] One year later, it was reported that the amino groups could be generated by the photochemical transformation of the acyloxyimino groups. These amino groups were also used for cross-linking epoxy resins.[27] Since then, many other PBGs and their applications have been documented.[28-33] As PBGs, *O*-acyloximes, *O*-cabamoyloximes, *O*-nitrobenzyloxycabonyl derivatives, substituted benzoin carbamates, quaternary ammonium salts and benzyl bicyclic amidines were investigated.

General Chemistry of PBGs

The PBGs are in essence photosensitive compounds that, upon absorption of photons, undergo photochemical reactions, producing basic species. The whole process may be generally divided into three stages: (1) the *absorptive act*, which consists of the interaction of a photon and a PBG molecule, resulting in absorption of the photon and formation of an electronically excited PBG molecule, (2) the *primary photochemical*

process, which involves the excited PBG molecule to produce reactive intermediates, such as radicals or ions, ready to trigger the base generation, and (3) the *secondary or "dark" process*, which occurs from the intermediates to release the free bases.

Molecular Composition

To realize the base generation, a molecule of PBG is essentially composed of two parts: (1) the *chromophore*, which is the light absorbing moiety, responsible for transformation of energy of photons into chemical energy, and (2) the *latent base*, which is the moiety that is able to block and release the actual base on demand.

Characteristics

- Catalytic activity of released bases

So far, the bases generated from all the reported PBGs are organic nitrogen bases. Their activities are governed by both basicity and nucleophilic strength. The basicity of a compound is normally described by the pK_a value. A higher pK_a value represents a higher basicity. PBGs that are capable of releasing the nitrogen bases with a higher pK_a value and a strong electron-donating power are more powerful photocatalysts and thus more desirable for practical applications.

- Quantum yield of base generation

The quantum yield (Φ) of base generation at a particular wavelength (λ) is defined as: $\Phi(\lambda)$ = (number of released free base) / (number of absorbed photons). The quantum yield is preferably higher than 0.1 to ensure that exposure dose necessary for base

formation will not be so high that uncontrolled photochemical side reactions occur extensively.

- Absorption

It is desirable for PBGs to be capable of being used over a broad range of exposure wavelengths. For example, in UV curing, PBGs absorbing the UV-A light are preferred, since longer wavelength light means lower energy consumption, thus lower cost. In application as photoresist, PBGs having short-wavelength absorption are required, since the long-wavelength light may limit the photo-patterning resolution.

- Thermal stability

The PBG itself is required to be neutral and thermally stable. The neutral nature ensures the "curing on demand" feature of PBGs. Good thermal stability prevents the PBG from decomposition during the pre-treatment in applications.

All these properties are related to the structure of PBG molecule. In the following section, some PBGs will be examined, in order to probe the structure-property relationship for better understanding and designing of new photobase generators.

I.2 Family of Photobase Generators

I.2.1 Co(III)-amine complex

The transition metallic complexes, introduced by Kutal et al. in 1987, were the first member in the family of PBGs for photogeneration of ammonia and methylamine.[34-37]

Nitrogen bases coordinate to transition metals via their lone-pair electrons, thus masks the basic properties of these molecules.

Mechanism

Exemplary in this regard are acidopentaamminecobalt(III) complexes with the general formula of $Co(NH_3)_5X^{2+}$, where X^- is a uninegative ligand such as Cl^-, Br^-, or NCS^-. These complexes are thermally inert (~ 250°C) and strongly absorbing in the UV-C region (λ_{max} = 252 nm, $\varepsilon = 1.83\times10^5$ $M^{-1}cm^{-1}$ for $[Co(NH_3)_5Br](ClO_4)_2$ in water) owing to the X-to-Co charge transfer excited states. Populating these ligand-to-metal charge transfer states creates a labile Co(II) center that, in solution, undergoes rapid substitution of its original ligands by solvents, and consequently, releases the free bases. The outcome of this photoredox process is the generation of three reactive species: a cationic Lewis acid (Co^{2+}), uncharged Lewis bases (NH_3), and a radical ($X^{\bullet}$). (Scheme I.2)[38, 39]

$$Co(III)(NH_3)_5X^{2+} \overset{h\nu}{\rightleftharpoons} Co(II)(NH_3)_5^{2+}, X^{\bullet} \xrightarrow{H_2O} Co^{2+}_{(aq)} + 5NH_3 + X^{\bullet}$$

Scheme I.2. Photoredox process of Co(III)-amine complex

Table I.1. Quantum yields for photoredox decomposition of Co(III) complexes in poly[glycidyl methacrylate-co-ethyl acrylate] films exposed to 254-nm irradiation

Complex		$\Phi_{Co^{2+}}$
$[Co(NH_3)_5Br](ClO_4)_2$ [a]	**(1)**	0.0089±0.001
$[Co(NH_2CH_3)_5Br](ClO_4)_2$ [a]	**(2)**	0.0079±0.002
$[Co(NH_2CH_3)_5Cl](ClO_4)_2$ [a]	**(3)**	0.0129±0.004
$[Co(NH_3)_5Br](BPh_4)_2$ [b]	**(4)**	0.309±0.01
$[Co(NH_3)_6](BPh_4)_3$ [b]	**(5)**	0.349±0.04

[a] *Data from reference [36];* [b] *Data from reference [40].*

Quantum Yield

The quantum yields of photodissociation of Co(III)–amine complexes change with different counterions (Table I.1). With perchlorate anions (ClO_4^-), the quantum yields are quiet low. This inefficiency arises from rapid back-electron transfer between the primary photoproducts (e.g. $Co(NH_3)_5^{2+}$ and $X^{\bullet}$). The unwanted cage effect can be reduced by coupling the photoredox step with rapid secondary reactions that consume the photoproducts. In the photolysis of **5**, the primary photoproducts, which are the radical pair ($Co(NH_3)_6^{2+}$ and $BPh_4^{\bullet}$), undergo rapid reactions that favour irreversible decomposition (Scheme I.3). Thus, the quantum yields of Co(III)–amine tetraphenylborate complexes are much improved. However, the metallic complexes are inorganic salts. Their solubility in organic solvents and polymers are somewhat limited.

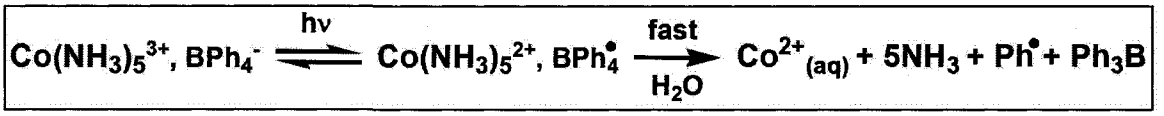

$$Co(NH_3)_5^{3+}, BPh_4^- \rightleftharpoons Co(NH_3)_5^{2+}, BPh_4^{\bullet} \xrightarrow[H_2O]{fast} Co^{2+}_{(aq)} + 5NH_3 + Ph^{\bullet} + Ph_3B$$

Scheme I.3. Photolysis of Co(III)-amine tetraphenylborate complex

I.2.2 *O*-Acyloximes (AOI)

In 1988, *O*-acyloximes were reported to be highly photoreactive PBGs releasing primary amines.[41] *O*-acyloximes are organic compounds. They have good compatibility in common organic solvents and polymers, thus minimizing aggregation and phase separation in polymer matrix.

Mechanism

At first, the photo-transformation of acyloxyimino groups into amino groups in a polymer matrix took place, as described by Tsunooka et al. (Scheme I.4).[42-47] In the copolymer of acryloyl acetophenone oxime (AAPO) with styrene (St) or methyl methacrylate (MMA), doped with 10 wt. % benzophenone as a sensitizer, after irradiation at 366 nm at room temperature, imino radicals, carbon dioxide and carbon radicals are introduced as primary photoproducts. These reactive species undergo two secondary reactions: 1) the radical recombination producing the alkylimino groups, then, converting into amino groups by hydrolysis with water; and the side reaction, 2) hydrogen

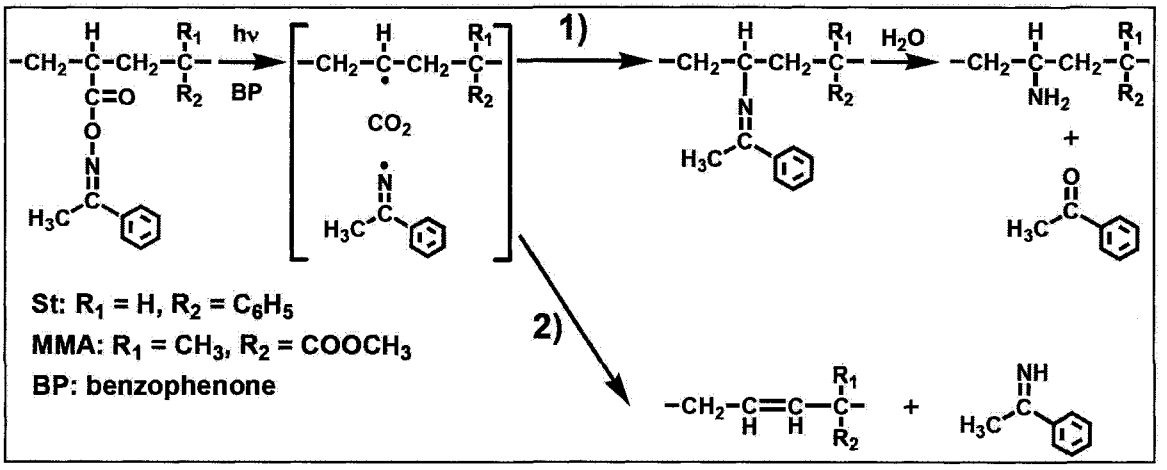

Scheme I.4. Photoreaction of polymeric *O*-acyloximes

abstraction by the imino radicals from methylene units in the main chain resulting in the formation of double bonds. Under the same condition, the yield of amino pendant groups depends on the content of AOI groups in the copolymers: the yield decreased with an increase of AOI groups (Table I.2). This is explained by that the increase in the content of

Table I.2. Contents of AAPO in copolymers versus yield of amino groups

Copolymer		Content of AAPO (mol.%)	Yield of amine groups
AAPO(26.3)-co-St	**(6)**	26.3 %	15%
AAPO(51.0)-co-St	**(7)**	51.0 %	25%
P(AAPO)	**(8)**	100 %	22%

AOI groups facilitating the formation of acetophenone azine by the recombination of imino radicals, which consequently depresses the formation of alkylimino groups (Scheme I.5).[41]

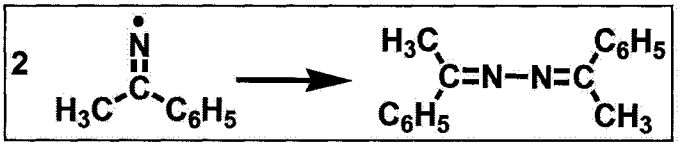

Scheme I.5. Recombination of imino radicals in polymeric *O*-acyloximes

Later on, small-molecule *O*-acyloximes were reported as PBGs (Table I.3).[48,49] These compounds show a strong absorption in the UV-C region (λ_{max} = ~240-250 nm, ε= 1.2~2.8 $\times 10^5$ $M^{-1}cm^{-1}$ in CH_3OH) with a π-π* character depending on the substituted groups attached on the oxime moiety. Their thermal stability is poor, starting to decompose around 130°C.

Table I.3. Quantum yields of amines generation from *O*-acyloximes

O-Acyloximes		Amines	Quantum Yield
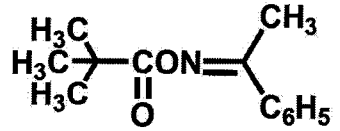	**(9)**	t-butylamine	0.049
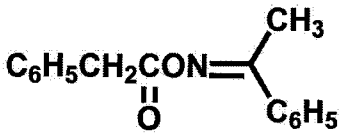	**(10)**	benzylamine	0.504

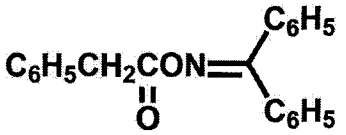	**(11)**	benzylamine	0.357
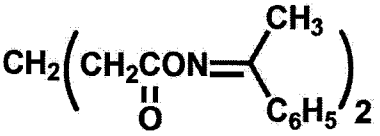	**(12)**	1,3-propane-diamine	0.091
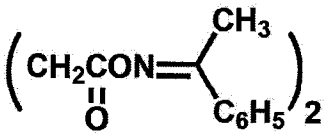	**(13)**	ethylenediamine	0.476
AAPO(26.3)-co-St	**(6)**	amine groups	0.490

Quantum Yield

The quantum yields of amines generation from *O*-acyloximes depend on the structure of acyl moiety.[49] Table I.3 shows the relation between structure and quantum yield. The decrease in the yields of **9** and **12** are explained by the presence of a hydrogen-bonded six-member ring, which facilitates the hydrogen abstraction by the resulting imino radicals and consequently depresses the amine generation (Scheme I.6).

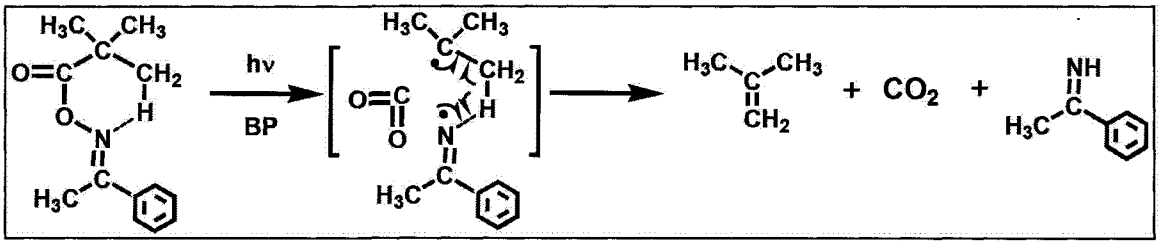

Scheme I.6. Photolysis of *O*-Acyloximes **9**

Due to the requirement for water in the amine generation, the application of *O*-acyloximes in water-labile materials is severely limited.

I.2.3 *O*-Carbamoyloximes

Tsunooka et al. also developed a group of *O*-carbamoyloximes as PBGs releasing primary amines (Figure I.1).[50-53] These compounds have the onset of decomposition temperatures in a range of 140-150 °C, and absorb UV-C light (λ_{max} = ~240-250 nm, ε= 1.4~4.3×10^5 M^{-1}cm^{-1} in CH_3OH), similar to *O*-acyloximes.

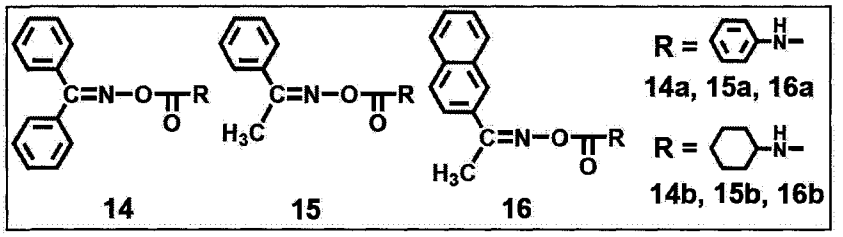

Figure I.1. Structures of *O*-carbamoyloximes

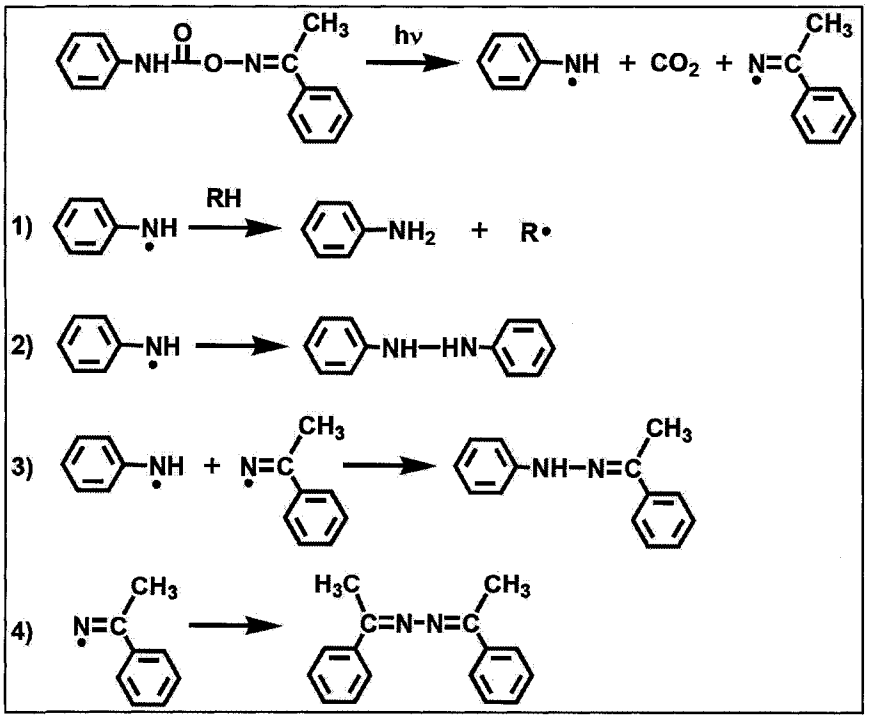

Scheme I.7. Photolysis of *O*-carbamoyloximes **15a**

Mechanism

Photolysis of *O*-carbamoyloximes is not as simple as that of O-acyloximes.[54] Scheme I.7 shows reactions which occur in the direct or sensitized photolysis of **15a**. With four secondary reactions, aniline, diphenylhydrazine, phenylhydrazine, and acetophenone azine are generated as main photoproducts. Comparing with *O*-acyloximes (Scheme I.5), the carbamoyl moieties enable direct hydrogen abstraction from hydrogen donors, like solvents or polymer matrix, resulting in the direct formation of amine.

Quantum Yield

Table I.4 shows quantum yields of amines generated from *O*-carbamoyloximes at 366 nm with benzophenone sensitizer in benzene.[50] It is clear that photolysis strongly depends on the substituents. For a given oxime, the cyclohexylcarbamoyl derivatives always give the lower quantum yield than the phenylcarbamoyl derivatives. The reason is the involvement of an in-cage reaction influencing the overall efficiency of base generation. This in-cage reaction occurs prior to the separation of the photoproduced radical pair, which are iminyl radical ($R_1R_2N\bullet$) and acyloxyl radical ($RCO_2\bullet$). As the decarboxylation of the cyclohexylcarbamoyl radical is not fast enough, this radical pair has enough time to recombine and gives the starting oxime. And therefore the global efficiency of the amine generation is decreased.

Table I.4. Quantum yields of amines generated from *O*-carbamoyloximes

Compound	**14a**	**14b**	**15a**	**15b**	**16a**	**16b**
$\Phi_{(366\ nm)}$	0.58	0.18	0.91	0.46	0.94	0.63

Although *O*-carbamoyloximes and *O*-acyloximes show high efficiency in the amines generation, their thermal stabilities are poor, decomposing around 140-150 °C. In the formulation of coating or imaging materials, the standard processing conditions usually include heating to temperatures as high as 150 °C, for removing of residue solvents or effective post exposure baking. Thus, thermally inert organic PBGs are needed.

I.2.4 Benzyloxycarbonyl & *O*-nitrobenzyloxycabonyl-derived Carbamates

Benzyloxycarbonyl (BOC) and *o*-nitrobenzyloxycabonyl (NBOC) groups are photo-reactive and are effective for protecting amino groups in polypeptide syntheses.[55] The photochemical deprotonation is sufficiently rapid and efficient, in some case the efficiency of deprotection reaching 100%. Thus, the photochemistry of BOC and NBOC is a basis for PBG design.

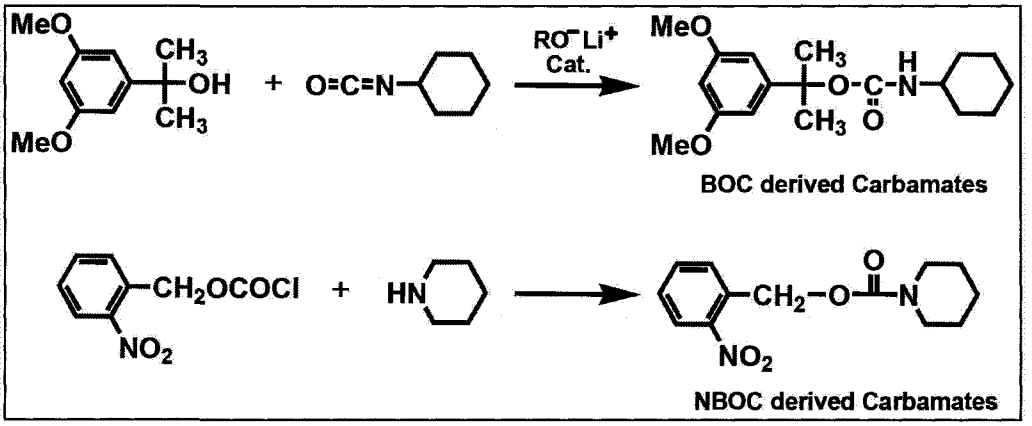

Scheme I.8. Preparation of BOC or NBOC-derived carbamates

In 1990, Frechet et al. first reported the BOC or NBOC-derived carbamates as PBGs releasing primary and secondary amines.[56-66] The compounds are prepared by direct addition of isocyanate to tertiary alcohols in the presence of a lithium alkoxide catalyst or

reactions between chloroformates with target amines (Scheme I.8). They have good thermal stability, decomposing around 200-240°C. The BOC-derived carbamates show a moderate absorption in UV-C region (λ_{max} = ~270-285 nm, ε= 1.2~3.0×10^3 M^{-1}cm^{-1}), while the NBOC-derived carbamates absorb UV light below 400 nm (λ_{max} = ~250-260 nm, ε= 0.5~1.3×10^4 M^{-1}cm^{-1}) both in solid state and solution.

Mechanism

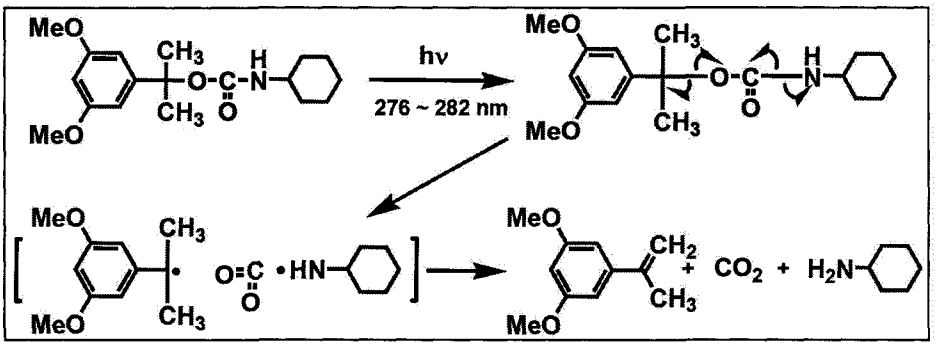

Scheme I.9. Photolysis of BOC-derived carbamates

The photolysis of BOC-derived carbamates proceeds as shown in Scheme I.9, with initial heterolytic cleavage of the benzyloxy bond to afford the fragments, which, on subsequent elimination liberate the styrenic product, CO_2, and free cyclohexylamine.

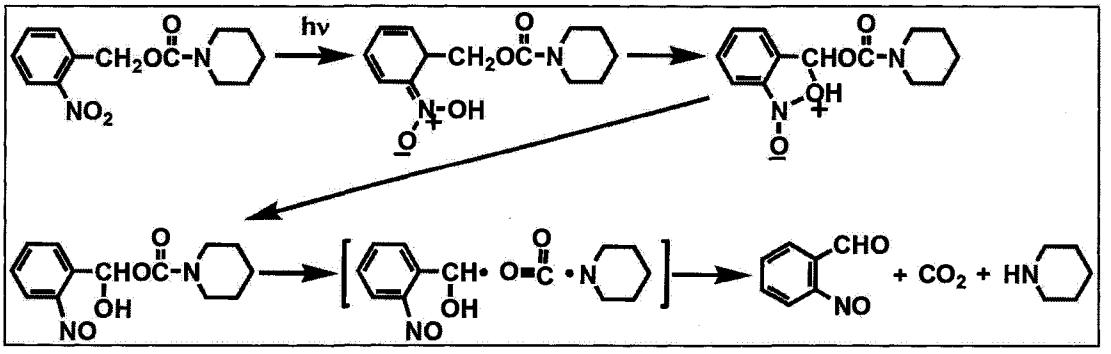

Scheme I.10. Photolysis of NBOC-derived carbamates

In contrast, the photochemistry of the NBOC-derived carbamates is particularly complex (Scheme I.10). The primary photochemical process is the intramolecular hydrogen abstraction by the excited nitro group. This is followed by an electron-redistribution process to the *aci*-nitro form, which rearranges to the nitroso product. And this intermediate undergoes the secondary reaction, further decomposing to produce free amines, CO_2 and benzaldehyde or ketones.

Table I.5. Quantum yields for amine formation in the photolysis of BOC and NBOC-derived carbamates in poly(methyl methacrylate) films

BOC-derived Carbamates		$\Phi_{280\ nm}$
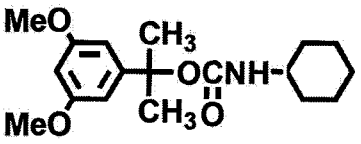	**(17)**	0.10
NBOC-derived Carbamates		$\Phi_{254\ nm}$
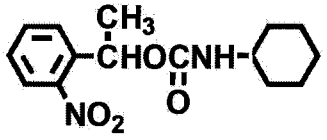	**(18)**	0.11
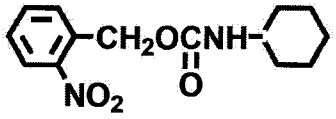	**(19)**	0.13
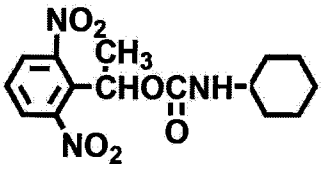	**(20)**	0.35
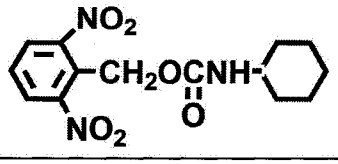	**(21)**	0.62

Quantum Yield

Quantum yields for amine formation in the photolysis of BOC and NBOC-derived carbamates are summarized in Table I.5.[57] The NBOC derivatives always show a higher photo-efficiency than BOC derivatives, due to their much higher absorption coefficient. Furthermore, in the NBOC-derived carbamates, the highest quantum yield, 0.62, is obtained from the photolysis of 2,6-dinitrobenzyl-substituted derivatives. Since the rate-determining step is the primary photochemical process involving the intramolecular hydrogen abstraction from the benzylic C-H bond by the excited nitro group as shown in Scheme I.10, this high efficiency results from two factors: (1) the presence of additional *o*-nitro groups in the chromophore increases the probability of this abstraction occurring, and (2) the absence of bulky α-substituents (R = methyl or larger) raises the number of abstractable hydrogen atoms and removes unfavourable steric hindrance in the solid-state hydrogen abstraction reaction. Thus, in the BOC and NBOC-derived carbamates, the absorption nature resulted from chromophore, and the structures possessing steric and electronic effects, which are in favour to the primary photochemical process and prevent the back electron transfer to go back to starting materials, play an important role to increase the quantum yields.

In addition, Toya et al. reported photogeneration imidazole from the NBOC-derived carbamates.[67] The compounds are synthesized by the reaction of *N,N'*-carbonyl-diimidazole with nitrobenzyl alcohols in acetonitrile (Scheme I.11). As the chromophore

is still the NBOC group, their UV absorption remains the same (λ_{max} = ~250-260 nm, ε= 0.5~1.3 $\times 10^4$ $M^{-1}cm^{-1}$). Unfortunately, quantum yields are not present in the literature.

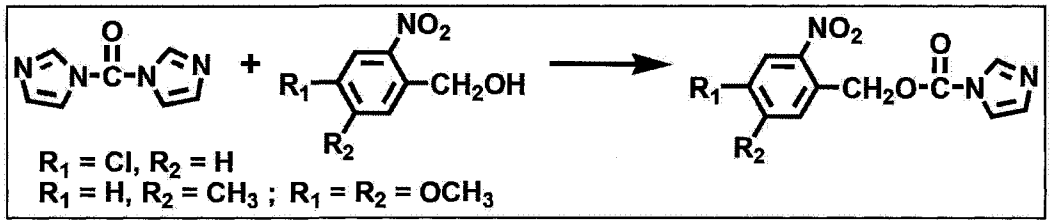

Scheme I.11. Synthesis of NBOC-derived carbamates containing imidazole

Although the BOC and NBOC-derived carbamates are thermally stable compounds and show high photo-efficiency in base generation, they still suffer from some restrictions. For instance, the utility of the *o*-nitrobenzyl class of PBGs is limited by the formation of reactive *o*-nitrosobenzaldehyde, which may react in situ with the liberated amine to form an imine or undergo other deleterious side reactions.[64,68] In BOC class of PBGs, severe anti-bleaching is a significant problem. The resulting photoproducts, absorbing UV light at the same wavelength as the starting materials, act as internal light filters and ultimately restrict the use to thin film applications.[69-72]

I.2.5 Benzoinyl Carbamates

In 1996, Frechet developed a different kind of carbamate-based PBGs, using benzoinyl groups as the chromophore.[73-76] In the photolysis, the substituted benzoin undergoes a photocyclization to form the corresponding benzo[*b*]furans, which are inert to amines. The benzoin absorbs UV-C light at 240~260 nm, which is quiet different from the absorption of photoproducts (280~340 nm) (Scheme I.12), thus, solving the

anti-bleaching problem. Benzoinyl carbamates are also thermally inert (T_d: 200~230°C). Their photo-efficiencies are comparable to that of NBOC-derived carbamates.

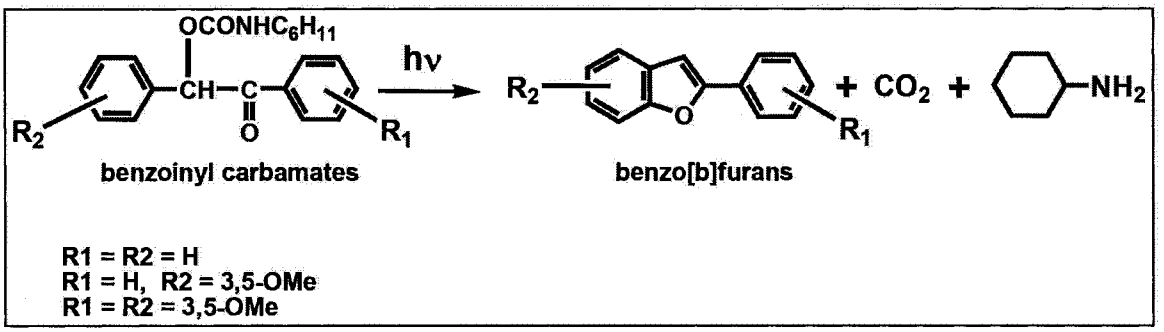

Scheme I.12. Photoreaction of benzoinyl carbamates

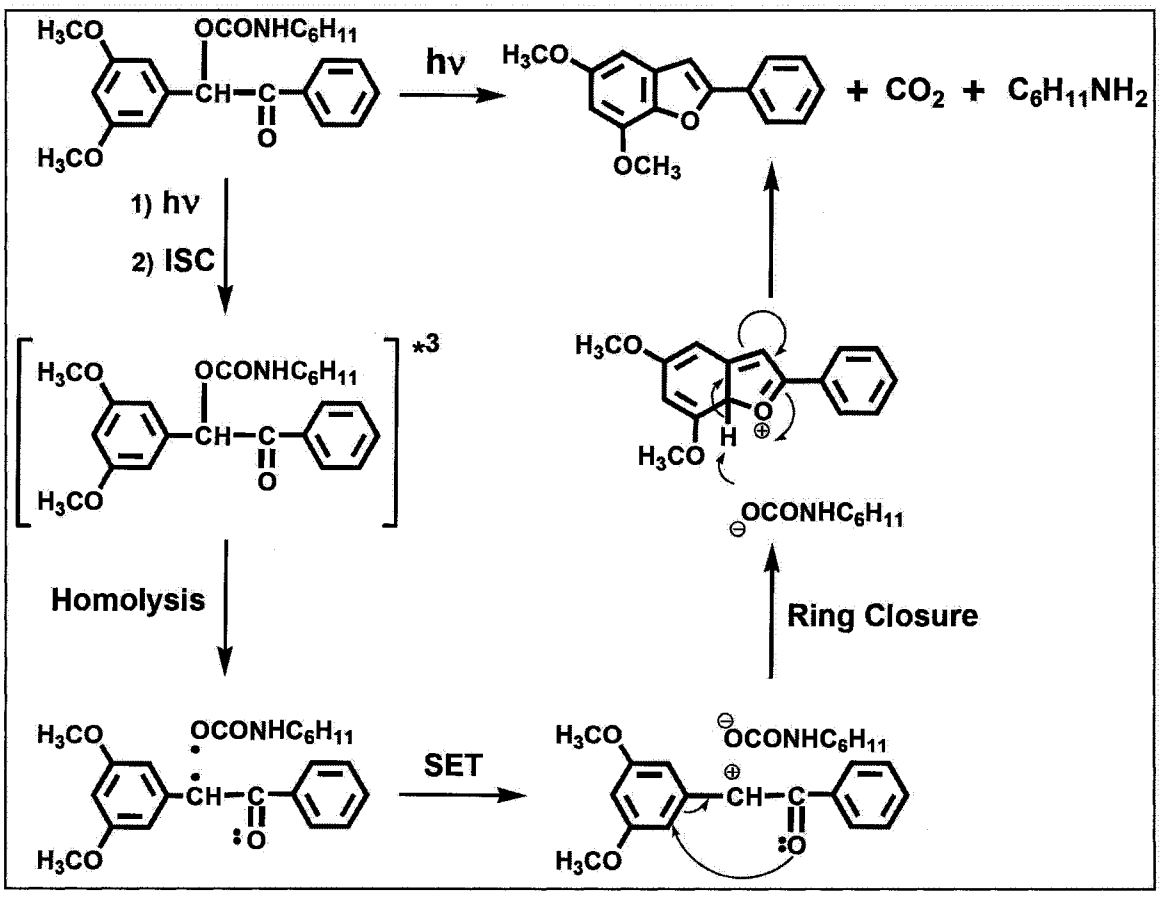

Scheme I.13. Mechanism of photolysis of benzoinyl carbamate

Mechanism

The benzoinyl carbamates are synthesized by reaction of the corresponding benzoin with cyclohexyl isocyanate.[74] The mechanism of photolysis is shown in Scheme I.13. Upon irradiation, benzoinyl chromophore is excited to the triplet excited state. Subsequent homolysis produces a radical pair which undergoes rapid electron transfer to yield an ion pair. After ring closure, the liberated carbamate anion acts as a base and abstracts the bridgehead proton from the bicyclic ring, forming the benzo[*b*]furan. The unstable carboxylated amine then ejects CO_2, liberating the free amine.

I.2.6 Fluorenylmethyl Carbamates

Instead of using benzoinyl chromophore, Ichimura et al. introduced another method, involving photoinduced base proliferation reactions, to improve the performance of carbamate-based PBGs.[77-80] They reported the thermally stable 9-fluorenylmethyl carbamates (FMOC) as PBGs capable of releasing primary and secondary amines (Scheme I.14). The FMOC are base sensitive compounds. The free amines released from photolysis are strong enough to catalyze β–elimination reaction of FMOC, which produce the same aliphatic amines and CO_2, realizing the base proliferation effect. Facilitated by this auto-catalytic reaction, an amount of generated amines increase in a geometric progression, and consequently maximize the quantum yield. However, details of mechanism and kinetics are still under investigation.

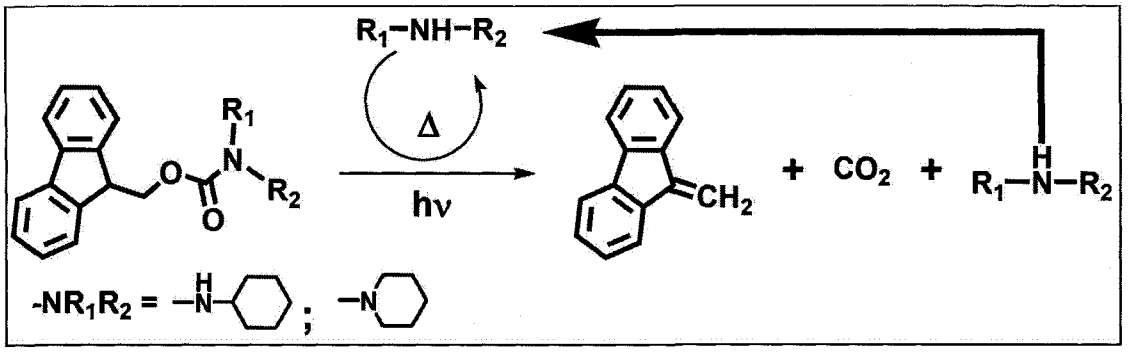

Scheme I.14. Photoreaction and base proliferation reaction in FMOC

I.2.7 Quaternary Ammonium (QA) Salts

Comparing with primary and secondary amines, tertiary amines have much higher catalytic activity and more in demand for practical applications. Thus, starting in the early 2000, research on PBGs is focused on photogeneration of stronger nitrogen bases.

The photogeneration of tertiary amines is considerably more difficult than that of primary or secondary amines, and only a few examples of photolatent tertiary amines are reported in the literature. In a tertiary amine, the nitrogen atom is fully substituted. Introduction of an additional photocleavable substituent result in the formation of quaternary ammonium (QA) salts. The QA salts reported in the literature as PBGs are normally composed of three parts: (1) the chromophore, which absorbs energy of photos, and then triggers the rapid bond-cleavage reaction to generate free bases, (2) the precursor of the tertiary amine, which is connected to the chromophore through the photocleavable C-N bond, and (3) the counter anion, which stabilizes the molecule. The QA salts can be classified into two categories based on their structures and photolysis mechanisms (Figure I.2). The type I QA salts are compounds containing phenacyl groups

as chromophore and undergoing the single electron transfer photoprocess in the photolysis. The type II QA salts include compounds bearing benzhydryl or fluorenyl groups as chromophore and produce tertiary amines through a photochemical heterolysis reaction.

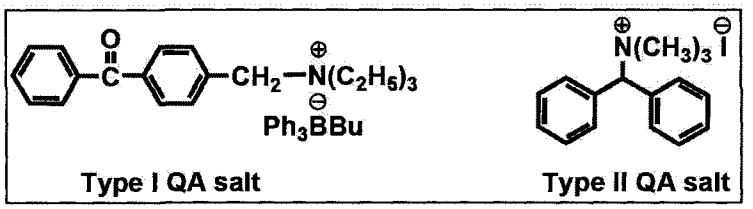

Figure I.2. Type I and type II QA salts

I.2.7.1 Type I - QA salts

Neckers et al. did much work on the type I QA salts (Figure I.3).[81-87] These QA salts have good thermal stability (T_d = 214~246°C). Their UV-Vis spectra show nearly identical absorption to that of chromophore with n-π* transitions centered at 334~340 nm ($\varepsilon = \sim 2.0\times10^3 M^{-1}cm^{-1}$).

Mechanism

The mechanism of photocleavage reaction is shown in Scheme I.15.[87] The primary photochemical process goes through the single electron transfer (SET) from the borate anions to excited chromophore, leading to secondary reactions of homolytic C-N bond scission and concomitant formation of tertiary amine. It can be predicted from the mechanism that type I QA salts having chromophore and anion that are in favour of the SET process and steric amine possess the maximal photo-efficiency of base generation.

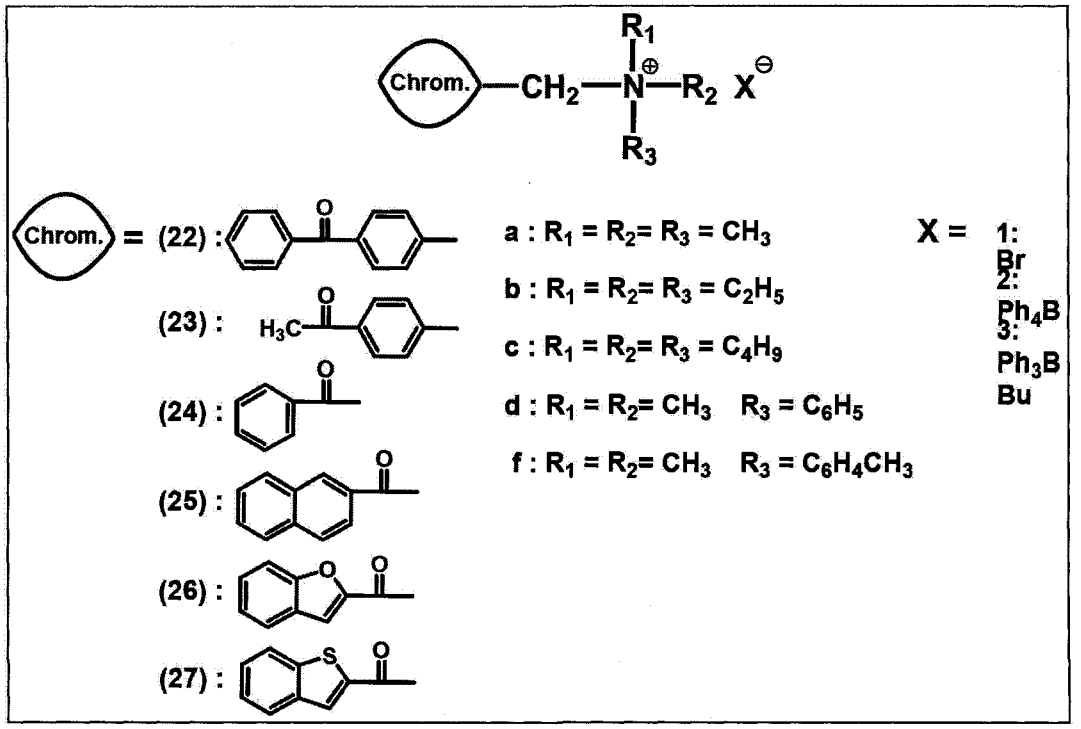

Figure I.3. Structures of type I QA salts

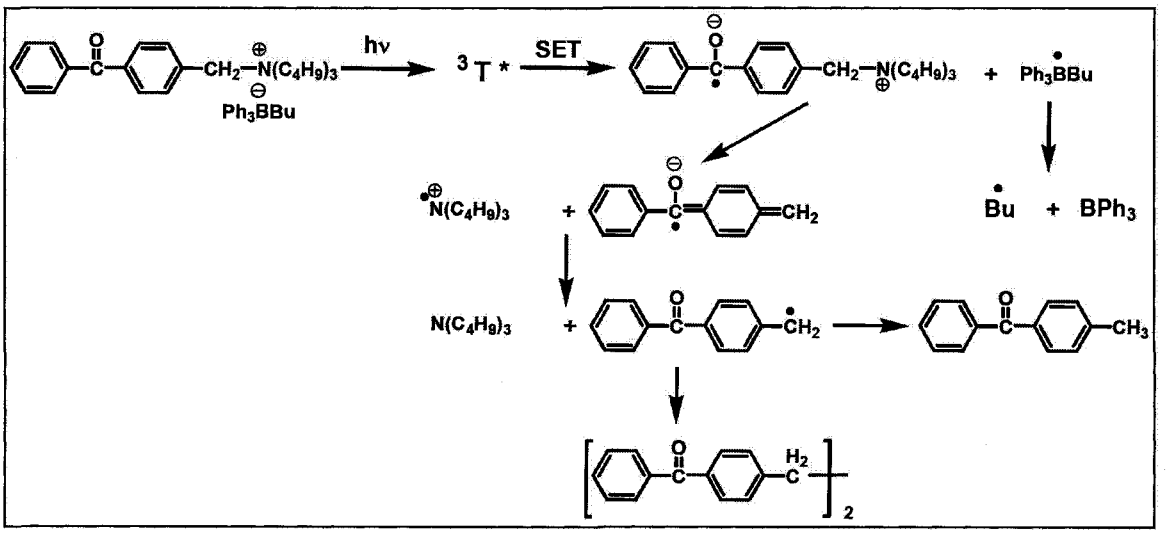

Scheme I.15. Mechanism of photolysis of the type I QA salt **22C3**

Quantum Yield

By modifying the structures of type I QA salts, Neckers et al. studied the influence of electronic and steric effects on efficiency of the base photogeneration.[88-96] Values of quantum yields are summarized in Table I.6. As expected from the mechanism, for type I QA salts possessing the same chromophore, enhanced efficiency is achieved with a triphenylbutylborate (Ph_3BBu^-) as the counter anion over those with a tetraphenylborate (Ph_4B^-) counter anion, since the Ph_3BBu^- anion is more easily oxidized than the Ph_4B^- anion which speeds up the SET process. And, the presence of bulky substituents on the quaternary nitrogen increases the efficiency of the base generation by promoting the C–N bond cleavage due to the release of strain energy. For compounds containing the same borate counter anion, efficiency differ with different chromophores. This difference reflects the overall effect of both photophysical and photochemical processes in the chromophore, including the following: (1) the rate of intersystem crossing (ISC) from excited singlet state to triplet state, the efficiency of which depends on how much of the excitation energy is lost by fluorescence, internal conversion to ground state, and/or other routes; (2) competition between back electron transfer and the SET in the primary photochemical process; (3) other side reactions not leading to release free amines, such as the coupling reaction between the chromophore radicals before the C–N bond cleavage.

Neckers et al. also prepared a polymeric type I QA salt.[97,98] With irradiation at 350 nm, through the same mechanism of photocleavage, pendant tertiary amine groups are released from QA moieties and butyl radicals are generated from Ph_3BBu^- anions. This

polymeric QA salt works as a hybrid PI, which is capable of simultaneously catalyzing cross-linking of epoxy resins and initiating polymerization of acrylates.

Table I.6. Quantum yields of base generation from type I QA salts

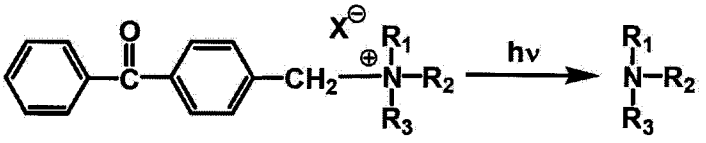

1 X = Br
2 X = Ph_4B
3 X = Ph_3BBu

Sample	R_1	R_2	R_3	Φ
1c	**Bu**	**Bu**	**Bu**	0.06
2a	**Me**	**Me**	**Me**	0.38
2b	**Et**	**Et**	**Et**	0.52
2c	**Bu**	**Bu**	**Bu**	0.61
2f	**Me**	**Me**	**$C_6H_4CH_3$**	0.32
3c	**Bu**	**Bu**	**Bu**	0.98
3d	**Me**	**Me**	**C_6H_5**	0.71

In 2006, Tsunooka et al. further studied type I QA salts.[99-101] They introduced the thiocyanate as the counter anion to minimize the anti-bleaching problem (Scheme I.16). In the photocleavage reaction of modified QA salts, 1,4-diazabicyclo[2.2.2]octane (DABCO) and N,N-dimethylaminopyridine (DMAP) are generated with quantum yields of 0.11 and 0.043 respectively in acetonitrile with a 254-nm irradiation. The photoproduct, namely phenacylthiocyanate (PnSCN), can cyclize to form 5-phenyloxazole-2-thione (POT) that absorbs at 330 nm and thus does not affect the 254-nm irradiation for unreacted QA salts.

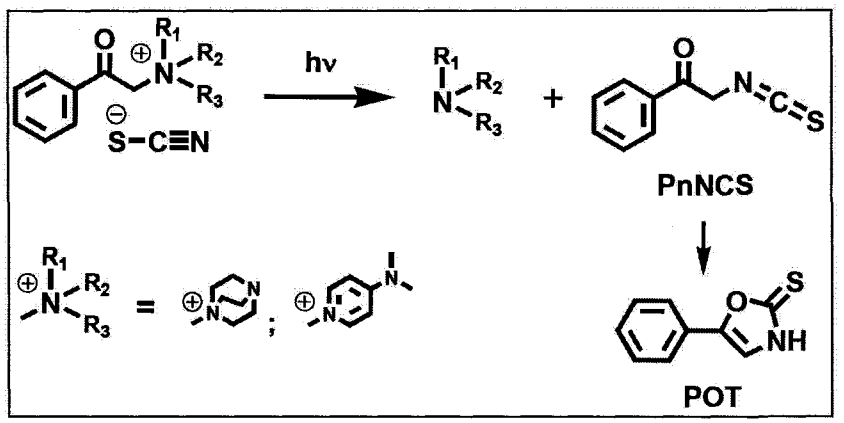

Scheme I.16. Photocleavage reaction of QA salts containing thiocyanate

I.2.7.2 Type II - QA salts

The type II QA salts were first reported as PBGs by Hanson et al. in 2002. With benzhydryl or fluorenyl groups as chromophore, and halide or triflate anion as counterion, these QA salts are able to generate triethylamine (Et_3N), quinuclidine, and DABCO upon UV irradiation.[102] They are prepared by methylation of benzhydrylamine with iodomethane or reaction of 9-bromofluorene with tertiary amines (Scheme I.17). These salts are thermally stable (T_d = 188~193°C) and absorb around 240-260 nm.

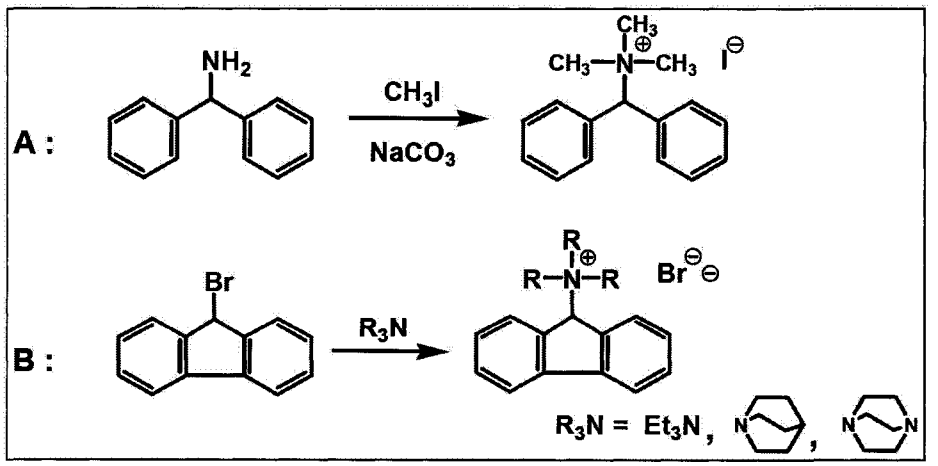

Scheme I.17. Preparation of type II QA salts

Mechanism

In the mechanistic study, Hanson et al. found that changing the counter anions had no influence on the base generation. The parallel photo-efficiency was even obtained in the QA salts with triflate anion, which is a well-known poor electron donor. Based on these results, they eliminated the possibility of the photoinduced SET process happened in the type I QA salts, which was sensitive to the changes of counter anions. Meanwhile, they isolated benzhydryl methyl ether as the primary photoproduct from the photolysis of trimethylbenzhydryl ammonium iodide in methanol. As the nucleophilic attack of the benzhydryl cation by methanol was the only way to produce this photoproduct, it indicated that carbon cations were the main reactive species generated in the photolysis. Thus, they proposed the mechanism consisting of a photochemical heterolytic cleavage of C-N bond to give the tertiary amine and the carbon cation, followed by reaction of the carbon cation with a nucleophile (Scheme I.18).

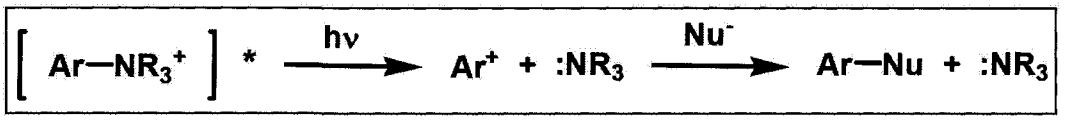

Scheme I.18. Mechanism of photolysis of type II QA salts

I.2.8 Benzyl Bicyclic Amidines

In late 2007, Dietliker et al. reported benzyl bicyclic amidines as PBGs.[103-106] Amidines including 1,8-diazabicyclo[5.4.0]undec-7-ene (DBU) and 1,5-diazabicyclo [4.3.0]non-5-ene (DBN) can be obtained from photolysis of these PBGs (Scheme I.19). Comparing with tertiary amines such as triethylamine (^{AN} pK_a = 18.8), DBU (^{AN} pK_a =

24.3) and DBN (^{AN} pK_a = 23.8) are much stronger bases. The basicity is attributed to the conjugative interaction of the two nitrogen atoms via the carbon-nitrogen double bond. Alkylation of the carbon-nitrogen double bond breaks the conjugation, and consequently masks the basic properties of amidines. By using this strategy, Dietliker et al. prepared the PBGs through the alkylation of the amidines with substituted benzyl groups. The resulting benzyl bicyclic amidines with isolated nitrogen atoms possess a lower basicity. The benzyl group works as a chromophore.

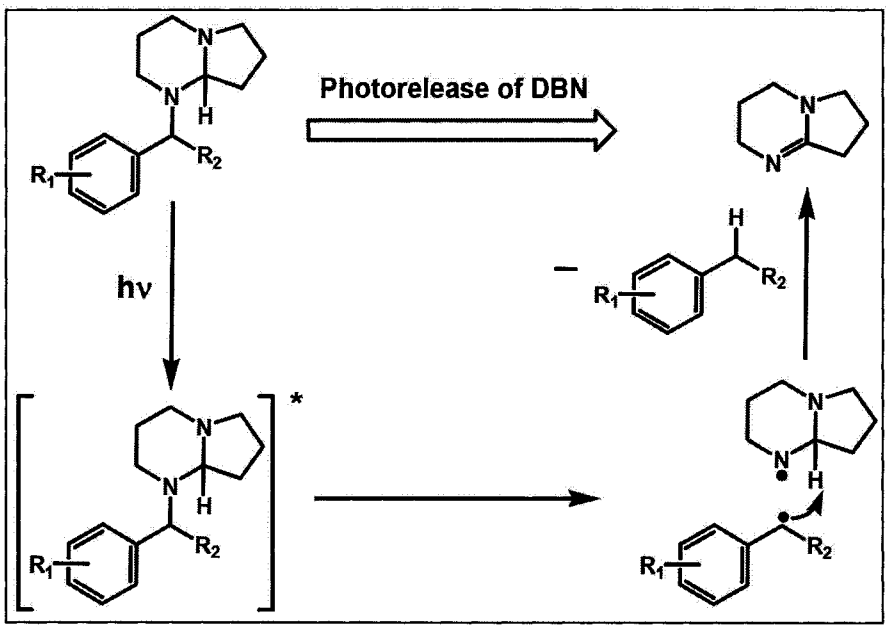

Scheme I.19. Photogeneration of DBN from benzyl bicyclic amidines

Mechanism

The proposed photolysis mechanism of benzyl bicyclic amidines is shown in Scheme I.19. Upon direct irradiation or sensitization, the PBG molecule jumps to its excited state, followed by the primary photochemical process, which is the homolytic cleavage of the benzylic carbon–nitrogen bond. The resulting carbon-centered radical

subsequently abstracts a hydrogen atom from the tertiary carbon atom activated by the two adjacent amino substituents, thereby introducing the amidine conjugation and release the free DBN. This mechanism is supported by photochemical investigations and ^{1}H NMR CIDNP (chemically induced dynamic nuclear polarization) spectroscopic study, which gave strong evidence for radical intermediates.

Benzyl bicyclic amidines have been evaluated as photocatalysts for curing a variety of resins. However, their applications as PBGs are severely restricted to systems that are inert to tertiary amines. Since the basicity of the benzyl bicyclic amidines is similar to ordinary tertiary amines, even before irradiation, the PBG itself can catalyze reactions for example the ring-opening of epoxy resins and thus is lacking of the unique "curing on demand" feature as PBGs.

I.3 Applications of Photobase Generators

All the reported PBGs are mainly employed for either base-catalyzed cross-linking of polymers or base-catalyzed polymer modification. The former is widely used in coating industry including protective and decorative coatings, graphic arts applications such as UV-curable printing or ink jet inks.

I.3.1 Photoinduced Cross-linking of Polymers

Cross-linking of epoxy resins

Amine-initiated curing of epoxy polymers is a general formula used in coating industry. However, the curing rate is often too fast to control. Cross-linked gel is formed

once mixing amines with epoxides. By applying PBGs as photocatalysts, the "curing on demand" feature triggered by light gives a full control over the curing process.

The PBGs capable of releasing primary amines, for example Co(III)-amine complexes, oximes and carbamates derivatives, are effective photoinduced cross-linkers in the UV curing of epoxy polymers, such as poly[glycidyl methacrylate-co- ethyl acrylate] P(GMA-co-EA) (Scheme I.20).[34-36] Normally, 20~40 mol.% of PBGs are required to obtain the efficient conversion of cross-linking, since released primary amines undergo addition reactions instead of working as real catalysts. And the cross-linking is usually further amplified by post-baking around 70 °C for 10 min after UV irradiation.

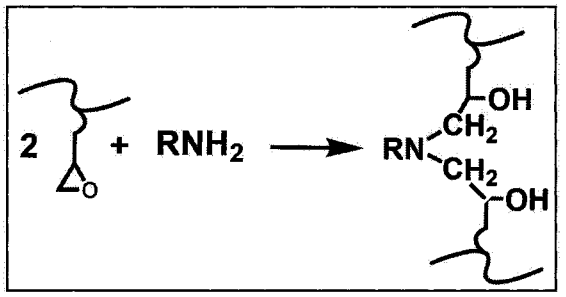

Scheme I.20. Cross-linking of P(GMA-co-EA) by amines

The activities of different PBGs vary by their own nature. Co(III)–amine complexes have poor compatibility with epoxy polymers. Oximes and carbamates derivatives show much better dispersion in epoxy resins, and the metal-free residue is desired for application in microelectronics. However, in the photo-cross-linking of thick films (e.g. 10~30 μm) by *O*-acyloximes, the films need to be kept under saturated water vapor at room temperature before post-baking to accelerate the curing rate, which limits its application. The best curing result is obtained by using FMOC. Facilitated by the base

proliferation effect, the curing rate is five times higher than other PBGs, under similar conditions.

QA salts can also be used as efficient photocatalysts in the cross-linking of epoxy polymers.[89,93-96] In this case, instead of acting as photoinduced cross-linker, they work as a real catalyst, since the released tertiary amines are much stronger nucleophile than primary or secondary amines. With less than 5 mol % of QA salts, P(GMA-co-EA) copolymer can be cross-linked after irradiation and post-baking.

O-Acyloxime-containing cross-linkable polymers

The *O*-acyloxime-containing polymers, so-called "AAPO copolymers", including acryloyl acetophenone oxime with styrene (AAPO-co-St) or methyl methacrylate (AAPO-co-MMA), are proved to be self-photo-cross-linkable with benzoquinone (Scheme I.21).[44] Irradiation of these copolymers produce amines and free radicals that react readily with quinones (e.g. 1,4-benzoquinone). Thus, AAPO copolymer films containing benzoquinone become insoluble by UV irradiation at 366 nm and post-baking. Benzoquinone acts as a cross-linker in this system.

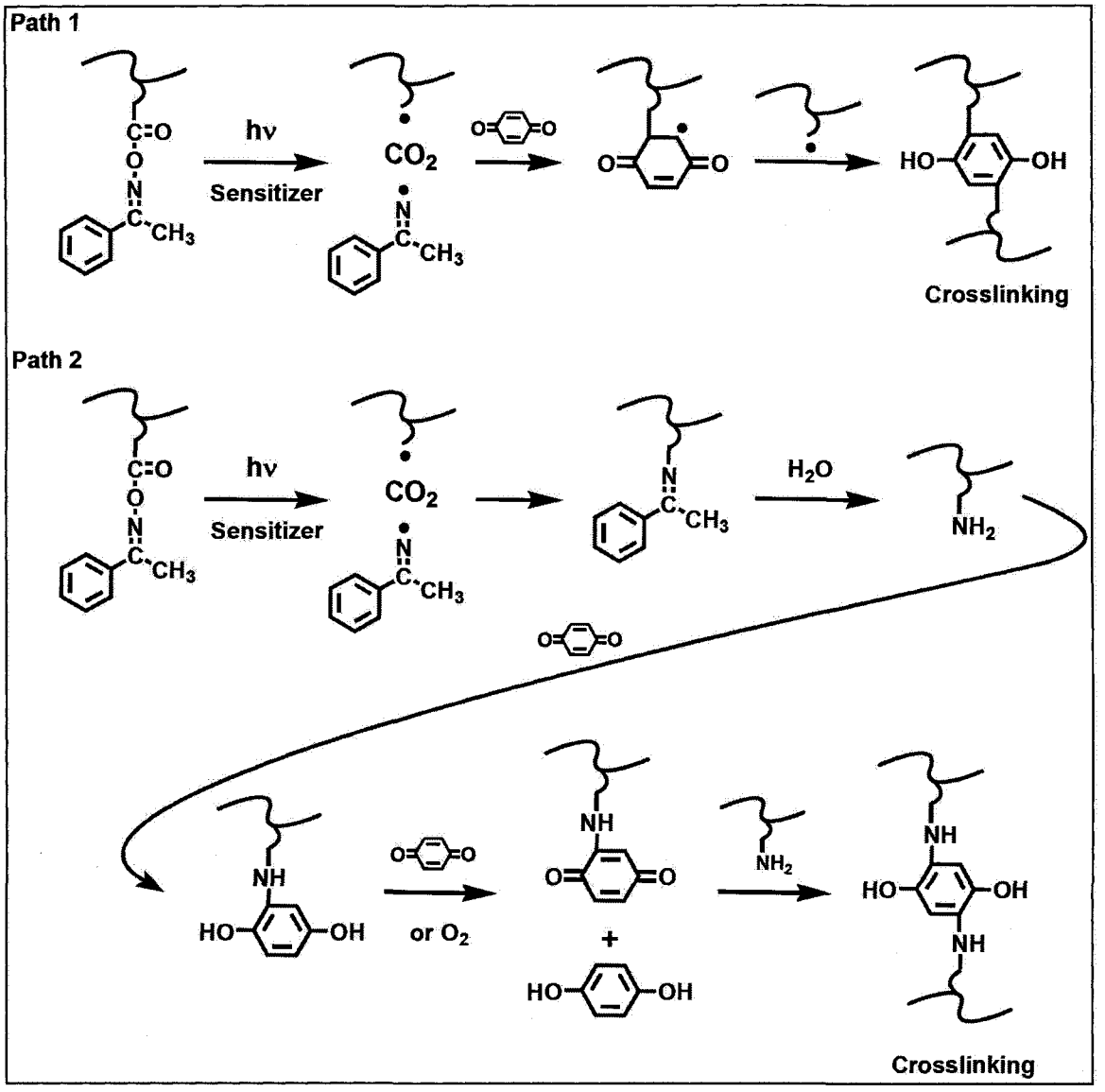

Scheme I.21. Photoinduced cross-linking of AAPO polymers

Cross-linking via Michael addition

Benzyl bicyclic amidines, which are able to release DBU and DBN, are effective photocatalysts for cross-linking via base-catalyzed Michael reaction.[107] The Michael addition of an anion of acetoacetate or malonate catalyzed by base to the bis-acrylate cross-linker (Scheme I.22), can be applied in UV-curable coating systems. Tack-free

coatings are obtained in the presence of 5 mol % benzyl bicyclic amidine as photocatalyst with irradiation and post-baking in less than one hour.

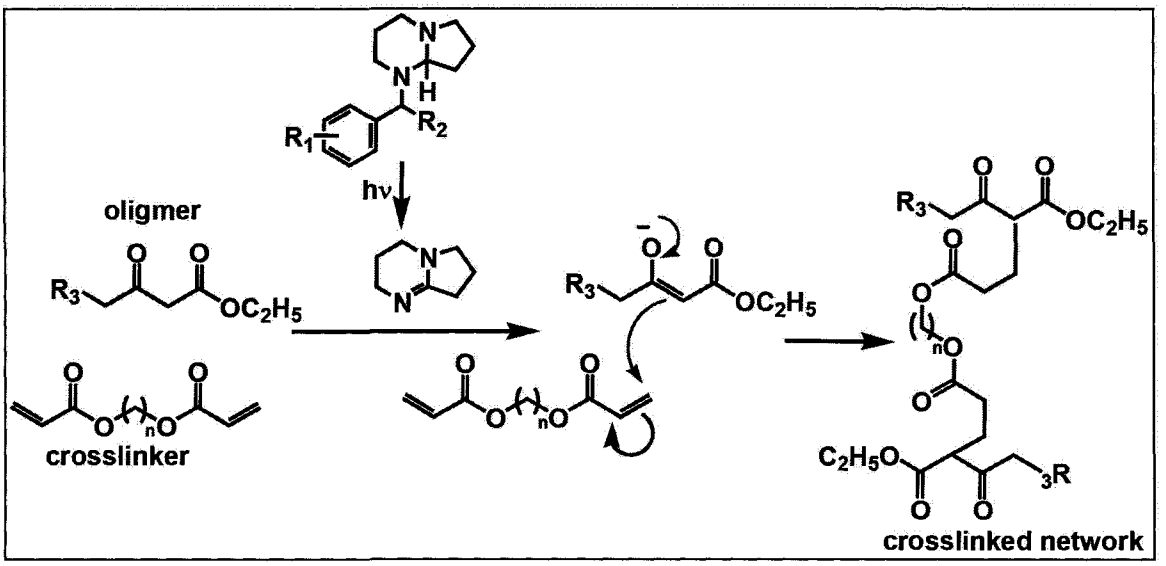

Scheme I.22. Photoinduced cross-linking via Michael addition

I.3.2 Photoinduced Polymer Modification

Photoresists

The AAPO copolymers with styrene or methyl methacrylate can be employed as dual-tone photoresists.[43-45] As shown in Scheme I.23, the pendant *O*-acyloxyimino (AOI) groups in copolymer (AAPO-co-MMA) or (AAPO-co-St) can be transformed into the ammonium salts by treatment with aqueous HCl after irradiation. The copolymers are originally soluble in non-polar organic solvents before irradiation and they become soluble in water or methanol after irradiation followed by acid treatment. Using methanol as a developer, a positive-tone photoresist has been established. Well-resolved patterns

with about 1 μm minimum features were obtained with an exposure dose of 50 mJ/cm^2 for AAPO-co-MMA.[43]

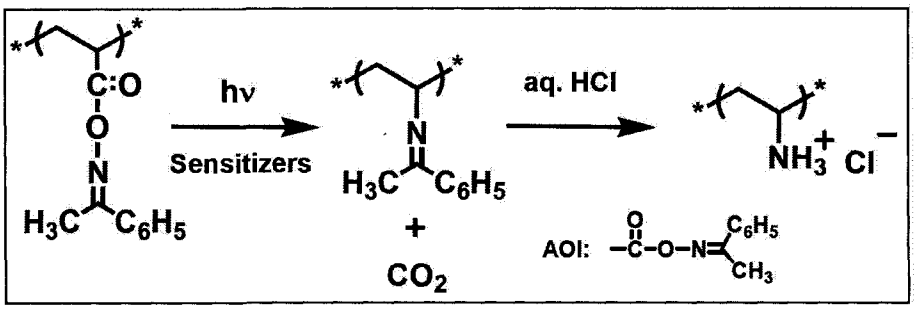

Scheme I.23. Photo-transformation of pendant AOI groups in AAPO polymers

Photopatterning Protein on Polymer Surface

The photo-transformation of the pendant AOI groups to amine groups is also used to modify surface properties of polymers. The irradiated AAPO polymer surfaces, after hydrolysis, can be stained with an acid dye (e.g., acid blue 40).[108] The adsorption of acid dyes on the films can be controlled by changing the irradiation time.

In addition, the selective photogeneration of amine groups creates a hydrophobically different surface, with the amine-rich regions selectively repelling protein adsorption, realizing a negative tone protein pattern (Figure I.4). This patterning method is applied to biochip fabrication.

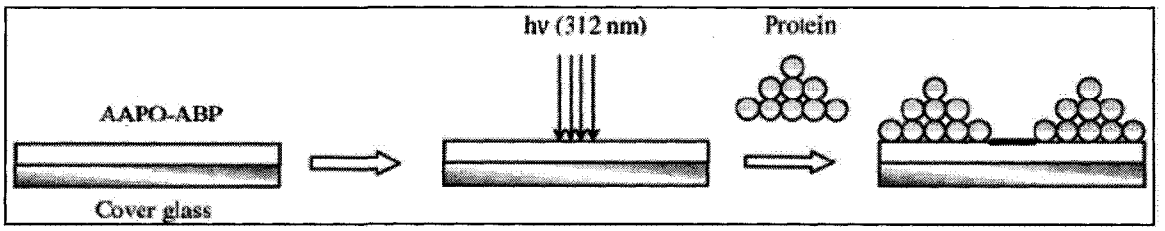

Figure I.4. Schematic illustration of protein patterning on AAPO copolymer

Photopatterning Polyimides

A route to a photoinduced imidization catalyzed by *O*-nitrobenzyloxy-carbonyl-derived carbamates was reported (Scheme I.24).[109] The process involves the amine-catalyzed conversion of soluble polyamic esters into relatively insoluble, partially imidized polymers. Upon 254-nm irradiation, images with 1–2 μm resolution can be formed.

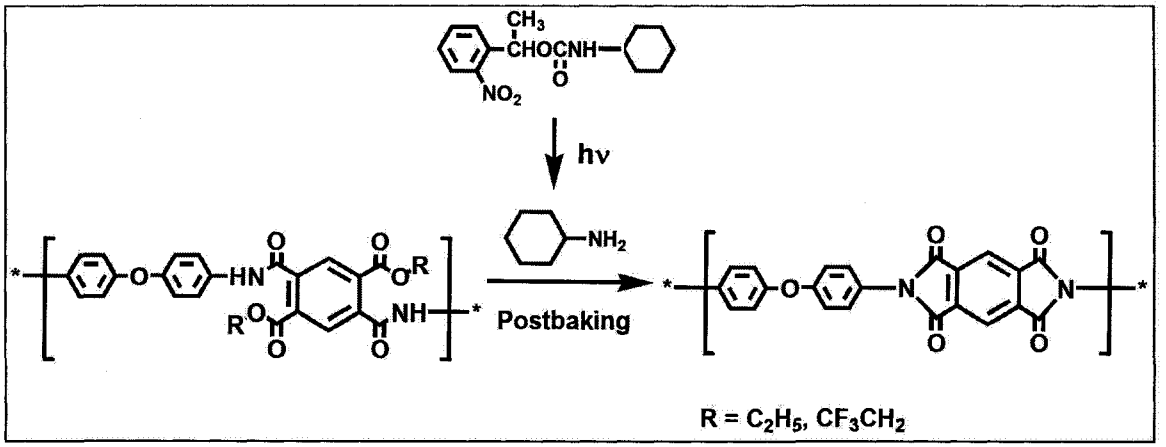

Scheme I.24. Photoinduced imidization of polyimides

I.3 Rationale and Objectives

Through the history of PBGs research, the focus has changed from optimization of photo-efficiency by slight structural variation to exploring photochemistry and developing new types of PBGs for stronger bases. The driving force of this transformation comes from the need for applications.

The PBGs releasing primary and secondary amines are often used as photoinduced reactants in chemical curing reactions. Although QA salts and benzyl bicyclic amidines can release tertiary amines and DBU, and act as a true photocatalyst, their applications in

UV curing are limited to epoxy system or Michael addition. Other base-catalyzed formulations are still unavailable in UV curing.

Furthermore, up to now, very little was known about the photobase-catalyzed living anionic ring-opening polymerization (ROP) of cyclic esters. Such a process would show a great potential in UV curing and compete well with the free-radical polymerization and cationic polymerization, because (1) the living nature can maximize the conversion of curing even without enough irradiation, (2) the anion is much less sensitive to oxygen and moisture in air, and (3) the ROP character prevents shrinkage after curing.

However, none of the known photogenerated bases, including DBU, the strongest base with $^{AN}pK_a$ = 24.3, are powerful enough to initiate the anionic living ROP. In comparison, a bicyclic guanidine, namely 1,5,7-triaza-bicyclo [4.4.0]dec-5-ene (TBD), is a strong base with $^{AN}pK_a$ = 26.03 and has been proved to be a very effective bifunctional catalyst for transesterification and ROP of cyclic monomers, such as σ-valerolactone (VL) and ε-caprolactone (CL).[110-112] It can simultaneously activate the ester through acyl transfer and trigger the alcohol with hydrogen bonding. TBD also catalyzes the reactions between isocyanates with alcohols to form urethanes, which is also suitable base-catalyzed reactions for polymer curing. Therefore, it would be both fundamentally interesting and practically useful to realize PBGs that can generate TBD and other stronger bases for photoinduced living polymerizations and polymer curing.

A PBG molecule is normally composed of two parts, the masked base and the chromophore. To design a PBG for a given base, a method to mask its basicity is needed, and then, a chromophore with suitable photochemistry capable of triggering the base liberation must be selected.

Previous experience in designing PBGs suggests some critical features to be considered: (1) efficient photoprocess to trigger the base generation, (2) favourable UV absorption characteristics, (3) solid-state photoreactivity, (4) none or less energy loss through other transitions for example emission, (5) stability of photo by-products, (6) thermal stability, (7) solubility in organic solvents and compatibility in polymeric materials, (8) facile synthesis.

Bearing all these in mind, we use protonation as the method to mask the target base and choose tetraphenylborate as the chromophore. Protonation is a simple and effective way to mask a base. It is a good choice, provided that a proper photochemical reaction that can trigger the deprotonation and liberate the target base is available. Furthermore, if a protonated base is used, a counterion must be selected. The counterion should be or contain the chromophore. It is known that photolysis of sodium tetraphenylborate ($NaBPh_4$) leads to protons abstraction from other molecules, such as water and alcohols. This fact has been confirmed through deuterium labelling experiments.[113,114] By comparing pK_a values of TBD, or the acidity of its conjugated acid ($TBD{\bullet}H^+$), with water, methanol and ethanol ($^{water}pK_a$ = 13.6 vs. 15.5~16.1),[115] it is clear that $TBD{\bullet}H^+$ is a much better proton donor than water and alcohols. Therefore, $TBD{\bullet}HBPh_4$ should be

photochemically reactive and able to liberate TBD upon irradiation even in the presence of alcohols and water.

Accordingly, the objectives of the part one of this thesis research are:

1. to develop a new family of PBGs capable of releasing stronger nitrogen bases than bicyclic amidines,
2. to characterize and evaluate the new PBGs under various conditions, and
3. to explore potential applications of the new PBGs .

I.4 References

1. Tsunooka, M.; Suyama, K.; Shirai, M. *J. Photopolym. Sci. Technol.* **2006**, *19*, 65.
2. Kutal, C.; Willson, C. Grant. *J. Electrochem. Soc.* **1987**, *134*, 2280.
3. Schwalm, R. (eds.), *UV Coatings: Basics, Recent Developments and New Applications*; Elsevier Publishers, **2006**.
4. ISO 21348 *Process for Determining Solar Irradiances*.
5. Paul, W.; Harry, L. US Patent 2406878 (**1946**).
6. Fouassier, J. P.; Rabek, J. F. (eds.), *Radiation Curing in Polymer Science and Technology-Vol, 4: Practical Aspects and Applications*; Elsevier Applied Science Publishers: London, **1993**.
7. Koleske, J. V. (eds.), *Radiation Curing of Coatings*; ASTM, Radtech International Publishers: North America, **2002**.
8. Roffey, C. G. (eds.), *Photopolymerization of Surface Coatings*; Wiley Interscience

Publishers: New York, **1982**.

9. Allen, N. S.; Edge, M.; Bellobono, I. R.; and Selli, E. (eds.), *Current Trends in Polymer Photochemistry*; Ellis Horwood Publishers: Hemel Hempstead, **1995**.
10. Liska, R.; Wendrinsky, J. *Nucl. Instrum. Methods Phys. Res.: B*, **1999**,*151*, 290.
11. Angiolini, L.; Caretti, D.; Carlini, C.; Corell, E. *Polymer* **1999**, *40*, 7197.
12. Segurola, J.; Allen, N. S.; Edge, M.; Parrondo, A.; Roberts, I. *J. Photochem. Photobiol. A: Chem.* **1999**, *122*, 115.
13. Stephen, D. R.; Illsley, D. *J. Photochem. Photobiol. A: Chem.* **1995**, *89*, 75.
14. Lougnot, D. J.; Turck, C.; Fouassier, J. P. *Macromolecules* **1989**, *22*, 108.
15. Encinas, M. V.; Rufs, A. M.; Corrales, T.; Catalina, F.; Peinado, C.; Schmith, K.; Neumann, M. G.; Allen, N. S. *Polymer* **2002**, *43*, 3909.
16. Kayaman-Apohan, N.; Amanoel, A.; Arsu, N.; Gungor, A. *Prog. Org. Coat.* **2004**, *49*, 23.
17. Zhou, W.; Kuebler, S. M.; Carrig, D.; Perry, J. W.; Marder, S. R. *J. Am. Chem. Soc.* **2002**, *124*, 1897.
18. Sanrame, C. N.; Brandao, M. S. B.; Coenjarts, C.; Scaiano, J. C.; Pohlers, G.; Suzuki, Y.; Cameron, J.. F. *J. Photochem. Photobiol. Sci.* **2004**, *3*, 1052.
19. Aoai, T.; Kodama, K.; Yagihara, M. *J. Photopolym. Sci. Technol.* **1998**, *11*, 409.
20. Stoye, D.; Freitag W.; Lackharze, Hanser (Munich), **1996**, pp. 186.
21. Erdle, W.; K.-H. Vogel, R.G. Tinsley, *Farbe Lack* **2004**, *110*, 22.
22. Barton, J.M. *Adv. Polym. Sci.* **1985**, *72*, 11.

23. Birbaum, J.L.; Kunz, M.; Kimura, A.; Nakashima, H. Eur. Patent 898202 (**1997**).

24. Clemens, R.J.; Del Rector, F. *J. Coat. Technol.* **1989**, *61*, 83.

25. Noomen, A.; *Prog. Org. Coat.* **1997**, *32*, 137.

26. Kutal, C.; Willson, C. Grant. *J. Electrochem. Soc.* **1987**, *134*, 2280.

27. Song, K. H.; Urano, A.; Tanaka, M. *J. Polym. Sci. Part C,* **1987**, *25*, 417.

28. Cameron, J. F.; Frechet, J. M. J.; *J. Org. Chem.* **1990**, *55*, 5919.

29. Winkle, M. R.; Graziano, K. A.; *J. Photopolym. Sci. Technol.* **1990**, *3*, 419.

30. Frechet, J. M. J.; Cameron, J. F. *Polym. Muter. Sci. Eng.* **1991**, *64*, 55.

31. Cameron J. F.; Frechet, J. M. J. *Polym. Mater. Sci. Eng.* **1991**, *64*, 71.

32. Nishikubo, T.; Takehara, E.; Kameyama, A. *Polym. J.* **1993**, *25*, 421.

33. Frechet, J. M. J. *Pure Appl. Chem.* **1992**, *64*, 1239.

34. Weit, S. K.; Kutal, C. *Inorg. Chem.* **1990**, *29*, 1455.

35. Weit, S. K.; Grutsch, P. A.; Kutal, C. *Inorg. Chem.* **1991**, *30*, 2819.

36. Weit, S. K.; Kutal, C.; Allen, R. D. *Chem. Mater.* **1992**, *4*, 453.

37. Davies, J. D.; Wang, Z.; Kutal, C. *Chem. Mater.* **1996**, *8*, 850.

38. Balzani, V.; Carassiti, V. *Photochemistry of Coordination Compounds*, Chapter 11, Academic Press, London, **1970**.

39. Endicott, J. F. in: Adamson, A.W.; Fleischauer, P.D. (Eds.), *Concepts of Inorganic Photochemistry*, Chapter 3, Wiley Interscience, New York, **1975**.

40. Kutal, C.; Palmer, B. J.; Wang, Z. in: *Advances in Resist Technology and Processing XII, Proc. SPIE*, 2438, **1995**, pp. 795.

41. Song, K. H.; Tsunooka, M. *J. Photochem. Photobiol. A: Chem.* **1988**, *44*, 197.

42. Song, K. H.; Tsunooka M. *Makromol. Chem., Rapid Commun.* **1988**, *9*, 519.

43. Song, K. H.; Tonogai, S.; Tsunooka, M.; Tanaka, M. *J. Photochem. Photobiol. A: Chem.* **1989**, *49*, 269.

44. Tachi, H.; Tsunooka, M. *Eur. Polym. J.* **2000**, *36*, 2395.

45. Suyama, K.; Miyamoto, Y.; Matsuoka, T.; Wada, S.; Tsunooka, M. *Polym. Adv. Technol.* **2000**, *11*, 589.

46. Nishimura, M.; Tsunooka, M. *J. Polym. Sci. A: Polym. Chem.* **1994**, *32*, 2177.

47. Lalevee, J.; Allonas, X.; Fouassier, J. P.; Tachi, H.; Izumitani, A.; Shirai, M.; Tsunooka, M. *J. Photochem. Photobiol., A: Chem.* **2002**, *151*, 27.

48. Ito, K.; Nishimura, M.; Sashio, M.; Tsunooka, M. *Chem. Lett.* **1992**, *7*, 1153.

49. Ito, K.; Nishimura, M.; Sashio, M.; Tsunooka, M. *J. Polym. Sci., A: Polym. Chem.* **1994**, *32*, 1793.

50. Lalevee, J.; Allonas, X.; Fouassier, J. P.; Tachi, H.; Izumitani, A.; Shirai, M.; Tsunooka, M. *J. Photochem. Photobiol. A: Chem.* **2002**, *151*, 27.

51. Chae, K. H.; Song, H. B. *Polym. Bullet.* **1998**, *40*, 667.

52. Hwang, H.; Chae, K. H. *J. Photochem. Photobiol., A: Chem.* **1999**, *126*, 37.

53. Chae, K. H.; Gwark, J. C.; Chang, T. *Macromol. Rapid Commun.* **2000**, *21*, 1007.

54. Tsunooka, M.; Tachi, H. K. *J. Photoscience* **1999**, *6*, 145.

55. Binkley, R. W.; Flechtner, T. W. *Synthetic Organic Photochemistry* (W. M. Horspool Ed.), pp. 407-417, Plenum Press, New York, **1984**.

56. Cameron, J. F.; Frechet, J. M. J. *J. Org. Chem.* **1990**, *55*, 5919.

57. Cameron, J. F.; Frechet, J. M. J. *J. Am. Chem. Soc.* **1991**, *113*, 4303.

58. Cameron, J. F.; Frechet, J. M. J. *J. Photochem. Photobiol., A: Chem.* **1991**, *59*, 105.

59. Urankar, E. J.; Frechet, J. M. J. *Chem. Mater.* **1997**, *9*, 2861.

60. Frechet, J. M. J.; Matuszczak, S.; Reck, B.; Stover, H. D. H.; Willson, C. G. *Macromolecules* **1991**, *24*, 1746.

61. Stover, H. D. H.; Matuszczak, S.; Willson, C. G.; Frechet, J. M. J. *Macromolecules* **1991**, *24*, 1741.

62. Frechet, J. M. J.; Leung, M.; Urankar, E. J.; Willson, C. G.; Cameron, J. F.; MacDonald, S. A.; Niesert, C. P. *Chem. Mater.* **1997**, *9*, 2887.

63. Frechet, J. M. J.; Cameron, J. F., *Polym. Muter. Sci. Eng.* **1991**, *64*, 55.

64. Beecher, J. E.; Frechet, J. M. J. *Polym. Mater. Sci. Eng.* **1991**, *64*, 71.

65. Frechet, J. M. J. *Pure Appl. Chem.* **1992**, *64*, 1239.

66. Cameron, J. F.; Frechet, J. M. J.; *J. Photochem. Photobiol., A: Chem.* **1991**, *59*, 105.

67. Nishikubo, T.; Kameyama, A.; Toya, Y. *Polym. J.* **1997**, *29*, 450.

68. Beecher, J. E.; Cameron, J. F.; Frechet, J. M. J. *J. Mater. Chem.* **1992**, *2*, 811.

69. Matuszczak, S.; Cameron, J. F.; Frechet, J. M. J.; Willson, C. G. *J. Mater. Chem.* **1991**, *1*, 1045.

70. Willson, C. G.; Cameron, J. F.; MacDonald, S. A.; Niesert, C. P.;Frechet, J. M. J.; Leung, M. K.; Ackmann, A. *Proc. S.P.I.E. Advances in Resist Technology and Processing X* **1993**, *1925*, 354.

71. Leung, M. K.; Frechet, J. M. J.; Cameron, J. F.; Willson, C. G. *Polym. Mater. Sci. Eng.* **1993**, *68*, 30.

72. Willson, C. G.; Cameron, J. F.; MacDonald, S. A.; Niesert, C. P.; Frechet, J.M. J.; Leung, M. K.; Ackmann, A. *Polym. Mater. Sci. Eng.* **1993**, *68*, 60.

73. Cameron, J. F.; Willson, C. G.; Frechet, J. M. J. *J. Chem. Soc.* **1997**, *16*, 2429.

74. Cameron, J. F.; Willson, C. G.; Frechet, J. M. J. *J. Am. Chem. Soc.* **1996**, *118*, 12925.

75. Cameron, J. F.; Frechet, J. M. J. *Polym. Mater. Sci. Eng.* **1996**, *74*, 323.

76. Cameron, J. F.; Frechet, J. M. J. *Polym. Mater. Sci. Eng.* **1996**, *74*, 284.

77. Arimitsu, K.; Ichimura, K. *J. Photopolym. Sci. Technol.* **2000**, *13*, 157

78. Arimitsu, K.; Ito, Y.; Ichimura, K. *J. Photopolym. Sci. Technol.* **2005**, *18*, 227.

79. Arimitsu, K.; Miyamoto, M.; Ichimura, K. *Angew. Chem., Int. Ed.* **2000**, *39*, 3425.

80. Arimitsu, K.; Ichimura, K. *J. Mater. Chem.* **2004**, *14*, 336.

81. Polykarpov, A. Y.; Neckers, D. C. *Tetrahedron Letters* **1995**, *36*, 5483.

82. Sarker, A. M.; Polykarpov, A. Y.; Marino, T. L.; Neckers, D. C. *J. Polym. Sci., A: Polym. Chem.* **1996**, *34*, 2817.

83. Polykarpov, A. Y.; Hassoon, S.; Neckers, D. C. *Macromolecules* **1996**, *29*, 8274.

84. Hu, S.; Neckers, D. C. *Tetrahedron* **1997**, *53*, 2751.

85. Sarker, A. M.; Nikolaitchik, A. V.; Neckers, D. C. *J. Phy. Chem. A* **1998**, *102*, 5375.

86. Popielarz, R.; Sarker, A. M.; Neckers, D. C. *Macromolecules* **1998**, *31*, 951.

87. Sarker, A. M.; Lungu, A.; Mejiritski, A.; Kaneko, Y.; Neckers, D. C. *J. Chem. Soc.,*

Perkin Trans. 2, **1998**, *10*, 2315.

88. Hu, S.; Sarker, A. M.; Kaneko, Y.; Neckers, D. C. *Macromolecules* **1998**, *31*, 6476.

89. Hassoon, S.; Sarker, A.; Neckers, D. C. *J. Am. Chem. Soc.* **1995**, *117*, 11369.

90. Hassoon, S.; Neckers, D. C. *J. Phy. Chem.* **1995**, *99*, 9416.

91. Hassoon, S.; Sarker, A.; Polykarpov, A. Y.; Rodgers, M. A. J.; Neckers, D. C. *J. Phy. Chem.* **1996**, *100*, 12386.

92. Murphy, S. T.; Zou, C.; Miers, J. B.; Ballew, R. M.; Dlott, D. D.; Schuster, G. B. *J. Phy. Chem.* **1993**, *97*, 13152.

93. Sarker, A. M.; Neckers, D. C. *J. Photochem. Photobiol., A: Chem.* **1998**, *117*, 67.

94. Sarker, A. M.; Neckers, D. C. *J. Photochem. Photobiol., A: Chem.* **1999**, *121*, 83.

95. Kaneko, Y.; Sarker, A. M.; Neckers, D. C. *Chem. Mater.* **1999**, *11*, 170.

96. Sarker, A. M.; Kaneko, Y.; Neckers, D. C. *Chem. Mater.* **2001**, *13*, 3949.

97. Mejiritski, A.; Sarker, A. M.; Neckers, D. C. *Chem. Mater.* **1996**, *8*, 1360.

98. Sarker, A. M.; Lungu, A.; Neckers, D. C. *Macromolecules* **1996**, *29*, 8047.

99. Suyama, K.; Fuke, K.; Yamamoto, T.; Kurokawa, Y.; Tsunooka, M.; Shirai, M. *J. Photochem. Photobiol., A: Chem.* **2006**, *179*, 87.

100. Tachi, H.; Yamamoto, T.; Shirai, M.; Tsunooka, M. *J. Polym. Sci., A: Polym. Chem.* **2001**, *39*, 1329.

101. Tsunooka, M.; Yamamoto, T.; Kurokawa, Y.; Suyama, K.; Shirai, M. *J. Photopolym. Sci. Technol.* **2002**, *15*, 47.

102. Jensen, K. H.; Hanson, J. E. *Chem. Mater.* **2002**, *14*, 918.

103. Baudin, G.; Dietliker, K.; Jung, T. PCT Pat. Appl. WO 200333500 (**2001**).

104. Tsunooka, M.; Okamura, H.; Shirai, M. *J. Photopoly. Sci. Technol.* **2006**, *19*, 65.

105. Dietliker, K.; Jung, T.; *J. Benkhoff, RadTech USA 2004, in: Technical Conference,Proceedings,* Charlotte NC, USA, **2004**, pp. 217.

106. Tsunooka, M.; Okamura, H.; Shirai, M. *J. Photopolym. Sci. Technol.* **2006**, *19*, 65.

107. Studer, K.; Jung, T.; Dietliker, K.; Benkhoff, J.; Dogan, N. *PU Mag.* **2006**, *3*, 2.

108. Choi, W. S.; Noh, Y.; Chae, K. H. *Adv. Mater.* **2005**, *17*, 833.

109. Frechet, J. M. J.; Cameron, J. F.; Chung, C. M.; Haque, S. A.; Willson, C. G. *Polym. Bullet.* **1993**, *30*, 369.

110. Pratt, R. C.; Lohmeijer, B. G. G.; Long, D. A.; Waymouth, R. M.; Hedrick, J. L. *J. Am. Chem. Soc.* **2006**, *128*, 4556.

111. Zhang, L.; Hedrick, J. L.; Wade, C. G. *Macromolecules* **2007**, *40*, 4154.

112. Pibre, G.; Chaumont, P.; Fleury, E.; Cassagnau, P. *Polymer* **2008**, *49*, 234.

113. Williams, J. L. R.; Doty, J. C.; Grisdale, P. J.; Searle, R.; Regan, T. H.; Happ, G. P.; Maier, D. P. *J. Am. Chem. Soc.* **1967**, *89,* 5153.

114. Wilkey, J. D.; Schuster, G. B. *J. Org. Chem.* **1987**, *52*, 2117.

115. Room, E.; Kiitt, A.; Kaljurand, I.; Koppel, I.; Leito, I.; Koppel, I. A.; Mishima, M.; Goto, K.; Miyahara, Y. *Chem. Eur. J.* **2007**, *13*, 7631.

CHAPTER II

TETRAPHENYLBORATE SALTS: A NEW CLASS OF PHOTOBASE GENERATORS

II.1 Introduction to the New Photobase Generators

II.1.1 Rationale and Strategy

As outlined in the preceding chapter, we chose tetraphenylborate as the chromophore to design new PBGs, and propose the photogeneration of TBD from its tetraphenylborate salt (TBD•$HBPh_4$) via a photoinduced proton transfer reaction. Actually, not limited to the photogeneration of the bicyclic guanidine TBD, tetraphenylborate salts refers to a whole new class of PBGs, capable of releasing tertiary amines, amidines, guanidines and even phosphazenes.

The photochemistry of $NaBPh_4$ or $KBPh_4$ has been well examined. Williams et al. did the photolysis of $NaBPh_4$ in aqueous solution and alcohols with the 254-nm UV light,[1,2] and found 1-phenyl-1,3-cyclohexadiene as the principal photoproduct. Yields higher than 95 % were obtained both in nitrogen and air-saturated solutions (Table II.1). By deuterium tagging, they proved that two protons, added to the rings to form the diene, came from solvents. Later on, Schuster et al. furthered this study, and proposed the mechanism of photolysis (Scheme II.1).[3]

Table II.1. Photolysis of sodium tetraphenylborate in water with 254 nm irradiation

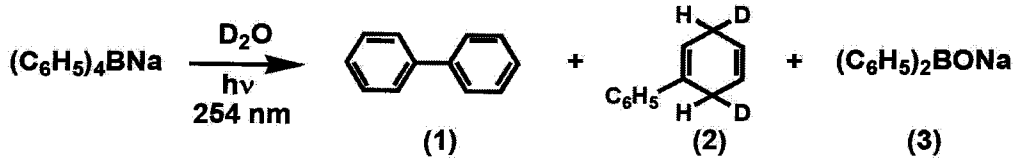

Borates	Atmosphere	Yield (%)	
		(1)	(2)
$NaBPh_4$	Air[a]	3	97
$NaBPh_4$	N_2[b]	2	97

[a] Irradiation was stirred under an air atmosphere, [b] Irradiation was stirred under an nitrogen atmosphere

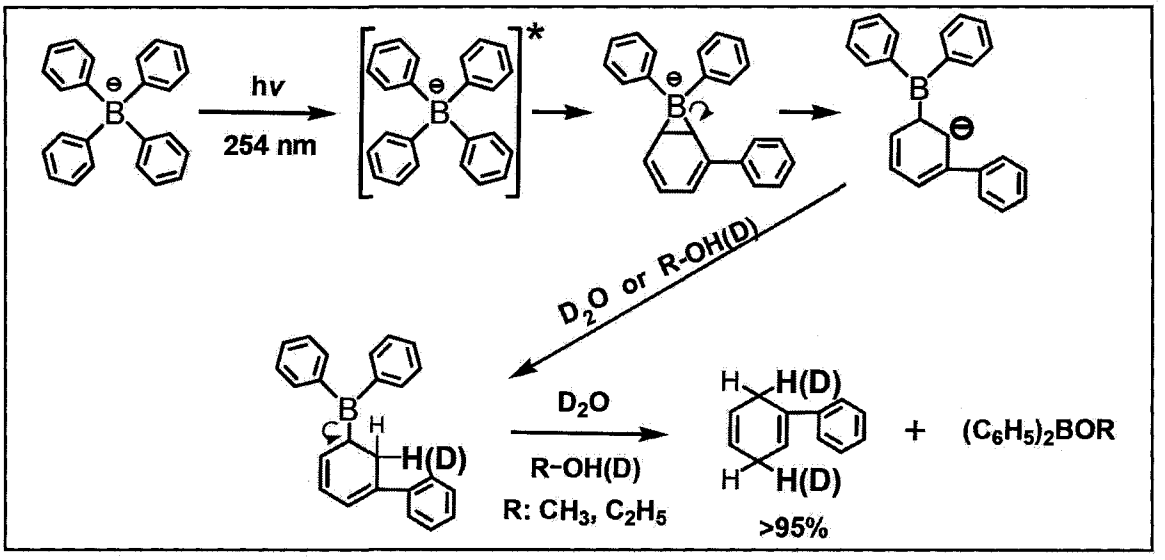

Scheme II.1. Photolysis mechanism of tetraphenylborate

The primary photochemical process involves the rearrangement of tetraphenylborate and cleavage of a boron-carbon bond. The resulting intermediate carbon anion can effectively abstract protons from adjacent proton donors, such as water and alcohols (e.g., methanol and ethanol). In comparison with water or alcohols, the conjugate acids of nitrogen bases ($B{\cdot}H^+$), including amines, amidines, guanidines and some phosphazenes, have much lower pK_a values and are thus better proton donors (Table II.2). The $B{\cdot}H^+$ should go through the same deprotonation process as water or alcohols during the

photolysis of tetraphenylborate, and consequently release the corresponding free bases. Therefore, tetraphenylborate salts can be used as latent precursors for a variety of nitrogen bases, which have pK_a values lower than water and alcohols.

Table II.2. pK_a values of water, alcohols and conjugated acids of nitrogen bases

Proton Donors	**MeOH H_2O**	***t*-BuP$_1$dma·H$^+$**	**TBD·H$^+$**	**DBU·H$^+$**	**Et_3N·H$^+$**
pK_a (H_2O)[a]	16.1-15.7	13.9	13.6	12.3	10.7
pK_a (AN)[b]	N.A.	26.98	26.03	24.34	18.82
	Alkoxide	Phosphazene	Guanidine	Amidine	Tertiary Amine
Corresponding Bases	MeO^- OH^-	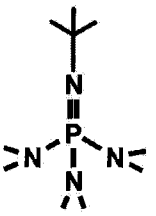 *t*-BuP$_1$dma	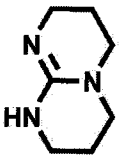 TBD	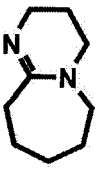 DBU	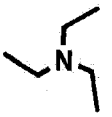 Et_3N

[a] pK_a values tested in aqueous solution, data from reference [4], [b] pK_a values tested in acetonitrile solution, data from reference [5]

Meanwhile, the photochemistry of tetraphenylborate offers two desirable features which render it particularly attractive for base photogeneration. (1) The photolysis of tetraphenylborate is quite efficient. Williams et al. reported the quantum yield of photodecomposition up to 0.26 in water at 254 nm. Since the yield of 1-phenyl-1,3-cyclohexadiene is around 95 %, representing that decomposition of one mole of tetraphenylborate produces nearly one mole of diene by abstracting two moles of protons, thus, the quantum yield for the base generation should be double, as 0.52. The quantum yield of 0.1 is usually acceptable for PIs in practical applications. Therefore, the photochemistry of tetraphenylborate is efficient enough to trigger the base generation in

PBGs. (2) All of the photoproducts resulting from the photolysis of tetraphenylborate are inert to nitrogen base. For example, the tetraphenylborate has been used as the counterion in both Co(III)-amine complex and type I QA salts. And its photoproducts have been proved to be chemically inert to the generated nitrogen bases.

Accordingly, any nitrogen bases having pK_a values lower than water or alcohols should be generated from photolysis of their tetraphenylborate salts. At present, all the reported PBGs, limited by their nature of chemistry, can only release one or at most two kinds of nitrogen bases. For example, QA salts only produce tertiary amines, and carbamate derivatives can just generate primary and secondary amines. Thus, if the proposed tetraphenylborate salts are proved to be efficient PBGs, it will be the first PBG that is able to generate a wide range of nitrogen bases and some bases much stronger than DBU, which is the strongest base generated among all the previously reported PBGs.

II.1.2 Goals

In this chapter, our work focuses on the photochemistry of new tetraphenylborate PBGs and their applications as photocatalysts in polymerization and polymer modification. Four tetraphenylborate salts were prepared (Figure II.1). These salts are chosen because: (1) they possess different types of bases, including phosphazene, bicyclic guanidine, bicyclic amidine and tertiary amine, allowing us to test the base-generating ability of tetraphenylborate salts, and (2) particular attention will concentrate on TBD•HBPh$_4$, since the target generated base TBD has an extraordinary catalytic activity

in polymerization and transesterification reactions.

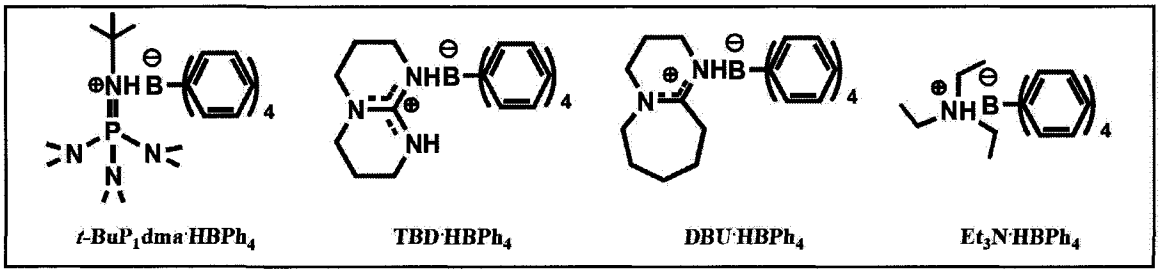

Figure II.1. Four tetraphenylborate salts prepared in this work

II.2 Synthesis and Characterization

II.2.1 Synthesis, Structural Characterization, Stability and Solubility

Synthesis

The selected tetraphenylborate salts were prepared by a two-step reaction (Scheme II.2).[6] The nitrogen bases were firstly acidified with hydrochloric acid (HCl) in aqueous solution and then transformed into tetraphenylborate salts by anion exchanges with $NaBPh_4$. The products precipitated out from aqueous solution and purified by recrystallization from a mixture of MeOH and $CHCl_3$ (4:1) (Table II.3).

Yields of tetraphenylborate salts are around 80-90 %. However, lower yields resulted by using an excess amount of concentrated HCl. The reason is that the tetraphenylborate anions decompose in solution at pH values less than 3.0. The decomposition is believed to be the electrophilic attack by proton at the carbon bonded to boron leading to formation of triphenylborane and benzene.[7,8] Thus, adjusting the pH value of reaction solutions before adding $NaBPh_4$ is important in the preparation of tetraphenylborate salts.

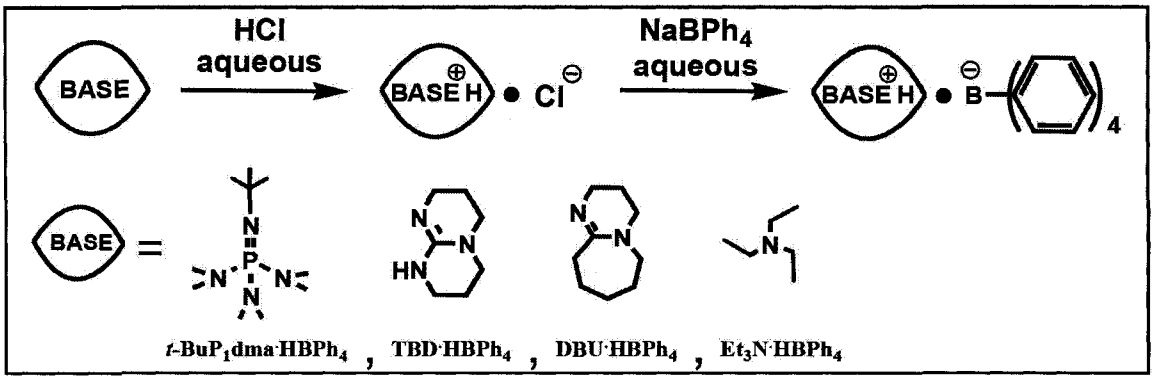

Scheme II.2. Synthesis of tetraphenylborate salts

Table II.3. Physical appearance of synthesized tetraphenylborate salts

Tetraphenylborate Salts	***t*-BuP$_1$(dma)·HBPh$_4$**	**TBD·HBPh$_4$**	**DBU·HBPh$_4$**	**Et$_3$N·HBPh$_4$**
Physical Appearance	white needle crystals	colorless cubic crystals	colorless plate crystals	white needle crystals

Structural Characterization

The ^{1}H, ^{13}C NMR spectra and IR spectra of the prepared tetraphenylborate salts are consistent with the expected structures. The purity of these salts is estimated to be around 98-99 % from their NMR data.

Figure II.2 shows the ^{1}H NMR spectra of prepared tetraphenylborate salts and the peaks are assigned. The peaks of α–methylene protons, which are adjacent to the nitrogen atoms in tetraphenylborate salts, always appear in the lower field comparing to the same methylene protons in the free bases, indicating that the bases are successfully protonated. The protons on the tetraphenylborate anion at 6.79, 6.93 and 7.18 ppm are present in a correct ratio to the protons on the protonated form of base, indicating that the anion is effectively changed from the chloride to the tetraphenylborate.

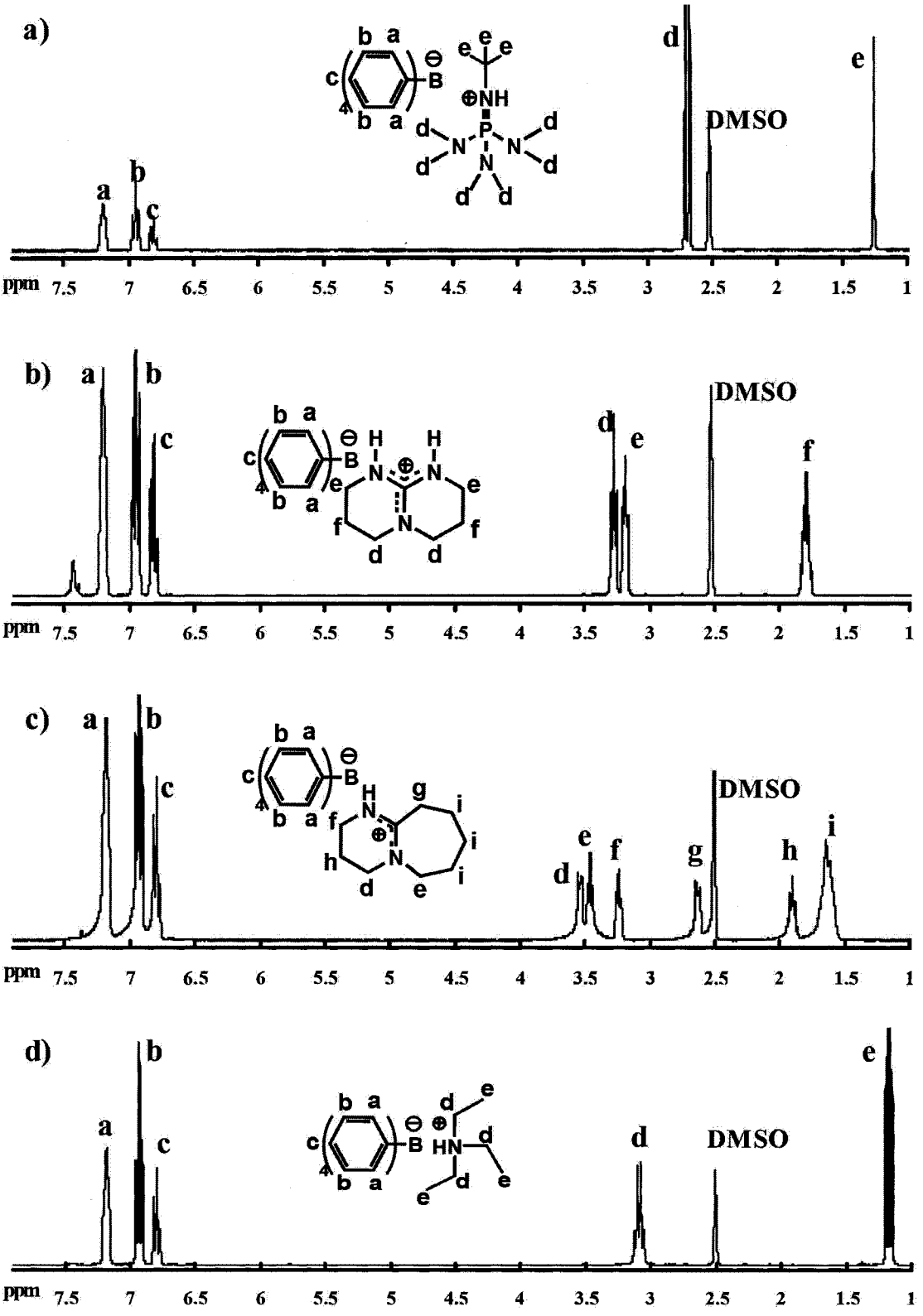

Figure II.2. ^{1}H NMR spectra (300MHz) of (a) *t*-BuP$_1$(dma)·HBPh$_4$, (b) TBD·HBPh$_4$, (c) DBU·HBPh$_4$, and (d) Et$_3$N·HBPh$_4$ in DMSO-d_6

Figure II.3 displays the IR spectra of the prepared tetraphenylborate salts. Peaks are observed around 1580 and 1500 cm^{-1} representing the stretching vibrations of the C=C double bonds on phenyl rings from the tetraphenylborate anion, and peaks at 1300 cm^{-1} indicating the C-N bonds from the protonated nitrogen base.

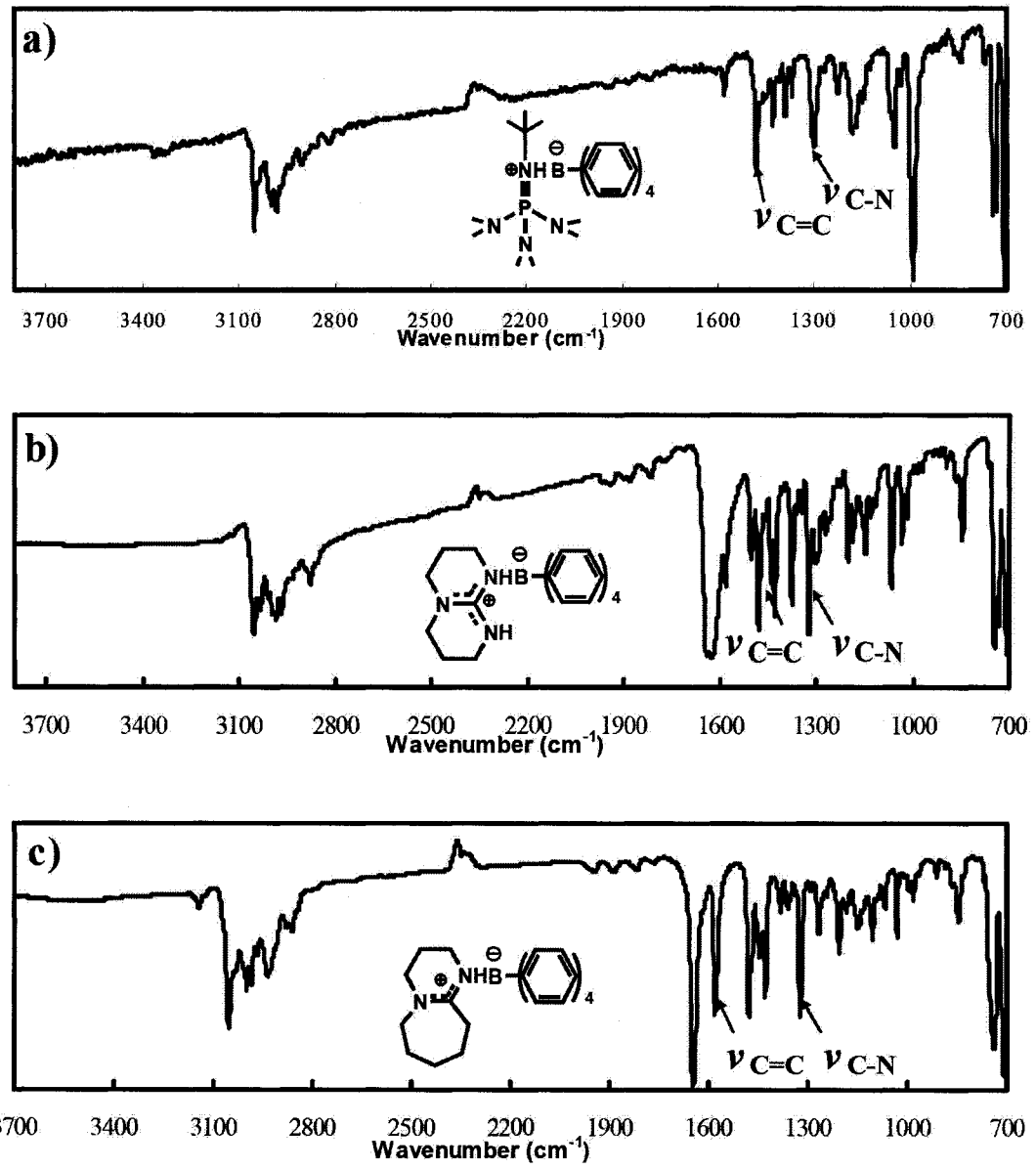

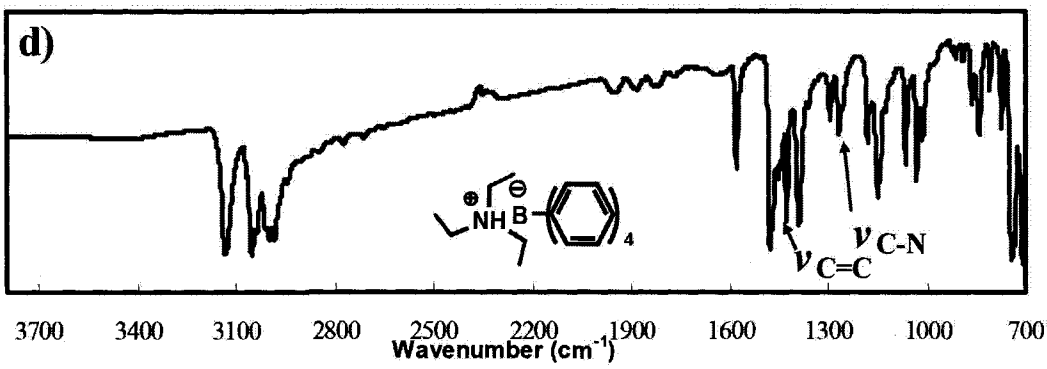

Figure II.3. IR spectra of (a) *t*-BuP_1(dma)·$HBPh_4$, (b) TBD·$HBPh_4$, (c) DBU·$HBPh_4$, and (d) Et_3N·$HBPh_4$ (KBr pellet)

Solubility

All prepared tetraphenylborate salts are readily soluble in polar aprotic solvents including acetonitrile (AN), dimethyl sulfoxide (DMSO), *N,N*-dimethylformamide (DMF), tetrahydrofuran (THF), chloroform ($CHCl_3$), dimethyl ether and acetone, but less soluble in protic solvents such as methanol (CH_3OH) and ethanol (C_2H_5OH), and insoluble in water and hexane.

These salts also show a good compatibility with polymers such as poly(methyl methacrylate) (PMMA), 2-hydroxyethyl cellulose (HEC) and polyethylene glycol (PEG). No phase separation was observed in thin films with thickness of 1-3 μm at a 10-15 wt % doping level. This feature will facilitate their applications as photocatalysts in polymeric systems.

Stability

The thermal properties of the synthesized tetraphenylborate salts are determined by differential scanning calorimetry (DSC) and thermogravimetric analysis (TGA).

As shown in Table II.4, three of these salts, including *t*-BuP_1(dma)·$HBPh_4$, TBD·$HBPh_4$ and DBU·$HBPh_4$, have good thermal stability with the onset temperatures for 5 % weight loss in the range of 250°C and the starting decomposition temperatures around 240°C in a nitrogen atmosphere. Considering that these tetraphenylborate salts might be utilized as photocatalysts in open to air systems, we also tested their thermal stability in air. Their decomposition temperatures are normally around 10-20 °C lower than those in nitrogen.

Table II.4. Thermal properties of synthesized tetraphenylborate salts

Tetraphenylborate Salts	Melting Point (°C)	Decomposition Temperature (°C)			
		5 % weight loss		1 % weight loss	
***t*-BuP_1(dma)·$HBPh_4$**	206-208	276[a]	244[b]	253[a]	238[b]
TBD·$HBPh_4$	223-234	251[a]	239[b]	246[a]	221[b]
DBU·$HBPh_4$	200-201	252[a]	223[b]	244[a]	215[b]
Et_3N·$HBPh_4$	136-138	188[a]	169[b]	175[a]	155[b]

[a] tested in nitrogen, [b] tested in air

In addition, the physical properties of these tetraphenylborate salts remain unchanged for at least six months when being stored at room temperature in the dark. Such stability meets the requirements for standard material processing conditions in UV curing or imaging systems, which may include prolonged heating at temperatures as high as 150 °C.

Et_3N·$HBPh_4$ possesses relatively lower thermal stability comparing with the other three tetraphenylborate salts. It can be explained by the relatively weaker intermolecular

forces in $Et_3N{\cdot}HBPh_4$. The N-H···π hydrogen bonds between the aromatic π-systems of tetraphenylborate and the cation is the principal intermolecular interaction in tetraphenylborate salts.[9, 10] In the other three salts, for example $TBD{\cdot}HBPh_4$, all three nitrogen lone pairs cooperate to donate electrons to hold the proton, thus the N-H···π hydrogen bond is much stronger, and consequently resulted in higher thermal stability (Figure II.4).

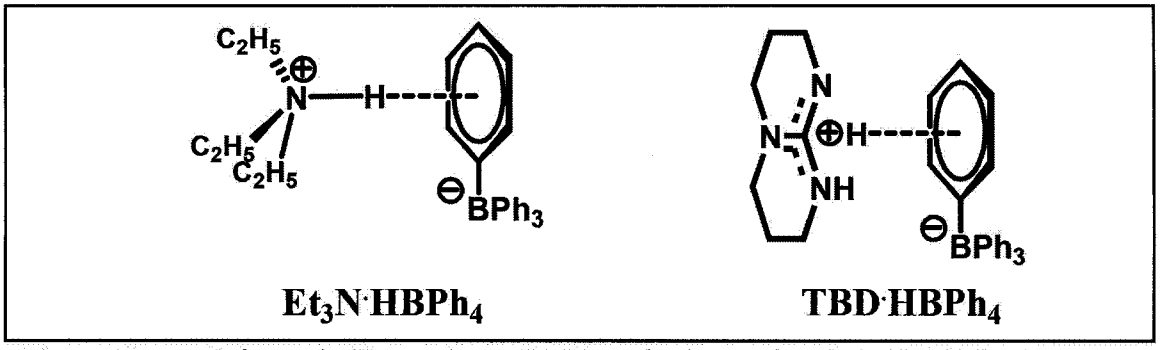

Figure II.4. Schematic illustration of N-H···π hydrogen bonds in $Et_3N{\cdot}HBPh_4$ versus $TBD{\cdot}HBPh_4$

II.2.2 Photophysical Properties – Absorption and Emission

The electronic absorption and emission spectra of a molecule provide important information concerning the structure, energetics and dynamics of electronically excited states. The excited state is the starting point for all the photochemical processes. Thus, our research on photochemistry of tetraphenylborate salts begins with the study of their absorption and emission spectra.

II.2.2.1 UV-vis Absorption

The synthesized tetraphenylborate salts absorb the light within the UV-C region (100-280 nm) in acetonitrile (Figure II.5), with an intense peak centered at 195 nm (ε_{195nm}

= 1.0-1.2 × 10^5 $M^{-1}cm^{-1}$) and a weak broad peak in 220-280 nm (ε_{254nm} = 4.9-5.0 × 10^3 $M^{-1}cm^{-1}$).

In addition, we studied the influences on UV-vis absorption of these salts caused by changing (1) the concentration of solutions, (2) structures of cations and (3) solvents with different polarity. Based on these data, the 254-nm light was selected for the photolysis tests.

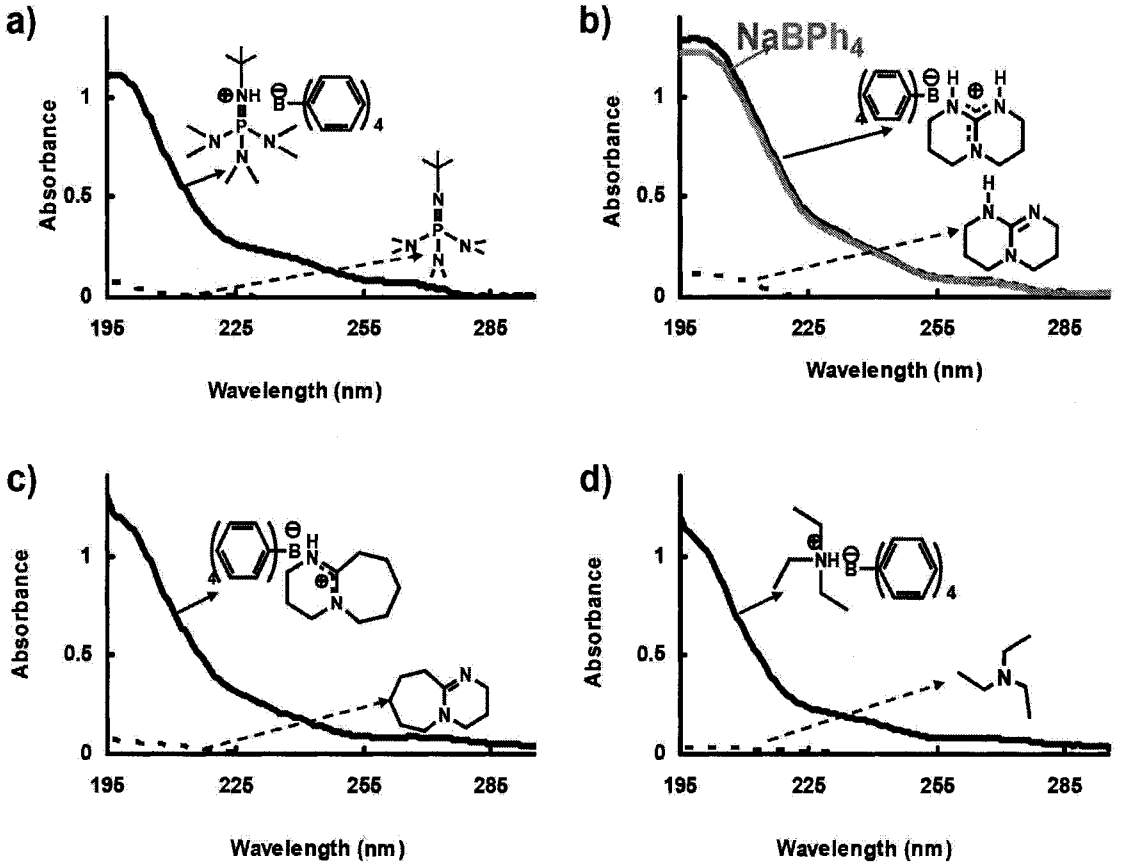

Figure II.5. UV-vis absorption spectra of (a) *t*-BuP_1(dma)·$HBPh_4$ and *t*-BuP_1(dma), (b) TBD·$HBPh_4$, TBD and $NaBPh_4$, (c) DBU·$HBPh_4$ and DBU, and (d) Et_3N·$HBPh_4$ and Et_3N in acetonitrile solution with concentration of 2.0×10^{-5} M.

Concentration Effect

In concentrated acetonitrile solutions, the absorption spectra of all the synthesized

tetraphenylborate salts are similar in shape to those in dilute solutions, as seen for TBD·HBPh$_4$ (Figure II.6). It indicates that no absorption due to the formation of excimer in these tetraphenylborate salts. Thus, one-photon absorption results in the formation of a single excited molecule of tetraphenylborate salts.

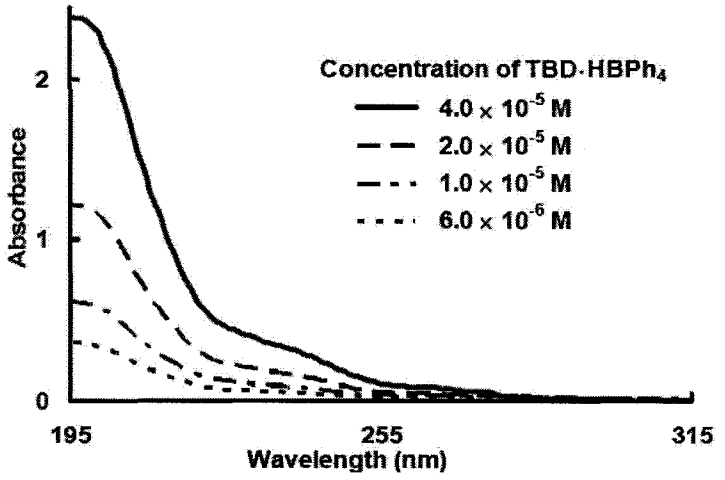

Figure II.6. UV-vis absorption spectra of TBD·HBPh$_4$ in AN with different concentrations.

Cation Effect

All the absorption spectra are independent to the types of cations and essentially identical to that of NaBPh$_4$ (Figure II.5b). In comparison, *t*-BuP$_1$(dma), TBD, DBU, and Et$_3$N only absorb weakly at 190-230 nm (ε_{193nm} = 3.2-6.9 × 10^3 $M^{-1}cm^{-1}$). Thus, UV-vis absorption of the synthesized tetraphenylborate salts are not affected by cations, but governed by the chromophore which is the tetraphenylborate anion.

In addition, although the tetraphenylborate anion, with low ionization potential, is proved to be an efficient electron donor,[11] no charge-transfer absorption bands were observed in these four tetraphenylborate salts.

Solvatochromic Effect

Due to the nature of the chromophore, these tetraphenylborate salts should have two excitation transitions: the $\sigma_{C\text{-}B}$-$\sigma_{C\text{-}B}^*$ transition and the $\pi_{benzene}$-$\pi_{benzene}^*$ transition.[11, 12] This fact is verified in the solvatochromism study (Table II.5). The sign of solvatochromism depends on the difference in dipole moment of the chromophore between its ground state and excited state. The polarity of excited $\sigma_{C\text{-}B}^*$ and $\pi_{benzene}^*$ states are different, thus, two distinct solvatochromic shifts should be observed corresponding to the two excitation transitions. As shown in Figure II.7, by changing the solvent from ethanol to more polar acetonitrile (polarity index: 5.2 vs. 5.8, dielectric constant: 24 vs. 37),[13] the spectral changes of TBD·$HBPh_4$ shown two types of solvatochromism: (1) in the deep UV region (195 nm<λ<236 nm), the absorption band shifts hypsochromically, which suggests the σ-σ^* excitation transition, and (2) at longer wavelength (236 nm<λ<290 nm), the absorption band shifts bathochromically, which indicates the π-π^* excitation transition.

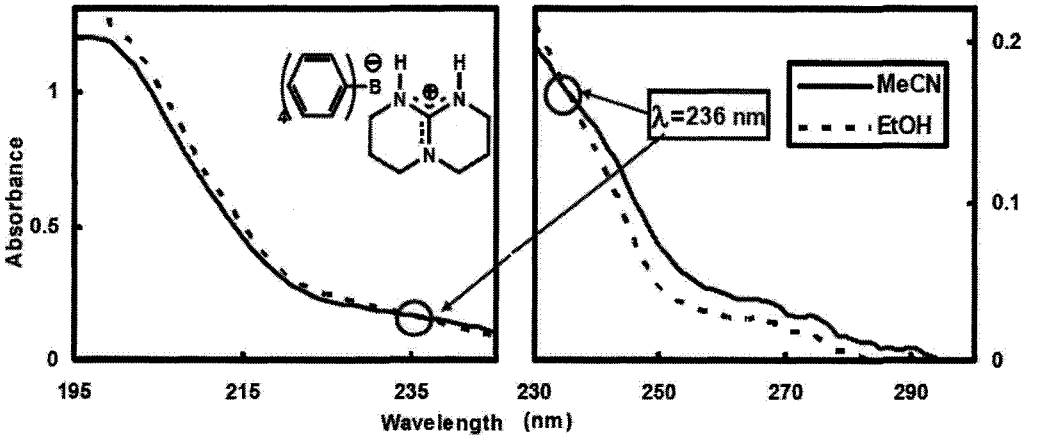

Figure II.7. UV-vis absorption spectra of TBD·$HBPh_4$ in different solvents (2×10^{-5} M).

Table II.5. Absorption data of synthesized tetraphenylborate salts in acetonitrile

Transition Types	$\sigma_{C\text{-}B}$-$\sigma_{C\text{-}B}^*$ Transition		$\pi_{benzene}$-$\pi_{benzene}^*$ Transition	
	Absorption Range (nm)	ε_{max} ($M^{-1}cm^{-1}$)	Absorption Range (nm)	ε_{max} ($M^{-1}cm^{-1}$)
***t*-BuP$_1$(dma)·HBPh$_4$**	195 - 235	105,509	235 - 285	4,990
TBD·HBPh$_4$	195 - 236	126,740	236 - 295	5,051
DBU·HBPh$_4$	195 - 233	111,782	233 - 295	5,355
Et$_3$N·HBPh$_4$	195 - 234	99,577	234 - 285	4,714

As shown in the Schuster's mechanism (Scheme II.1), the photoinduced proton transfer reaction, involving the carbon anion as the reactive intermediate, is triggered by the heterolysis of a boron-carbon bond. Since both the $\sigma_{C\text{-}B}$-$\sigma_{C\text{-}B}^*$ and the $\pi_{benzene}$-$\pi_{benzene}^*$ excitation lead to the B-C bond cleavage, the light below 280 nm down to the deep UV can be used to test the base generation. We selected the irradiation at 254 nm, based on the facts that (1) at this wavelength, the absorption coefficients of the synthesized tetraphenylborate salts are comparable to those of some widely used cationic PIs, also namely as photoacid generators (PAGs), such as arylonium salts and arylsulfonium salts (e.g., 3.0-7.0 × 10^3 $M^{-1}cm^{-1}$ at 254 nm)[14], and (2) this light source is readily available in our lab.

II.2.2.2 Emission

Generally, there are two energy-transfer pathways of the light absorbed by a photosensitive compound (Figure II.8): (1) radiationless transition, involving the transformation of electronic excitation energy into vibrational/rotational energy and

producing new chemical species, and (2) radiative transition, which refers to the photoluminescence (PL).

For the synthesized tetraphenylborate salts to be potentially useful as PBGs, they are required to have a low PL emission, since more energy transferred through the radiative transition tend to lead inefficiency in the photochemical process. Additionally, the emitted light may affect other components in UV curing or imaging systems, thus limited their applications.

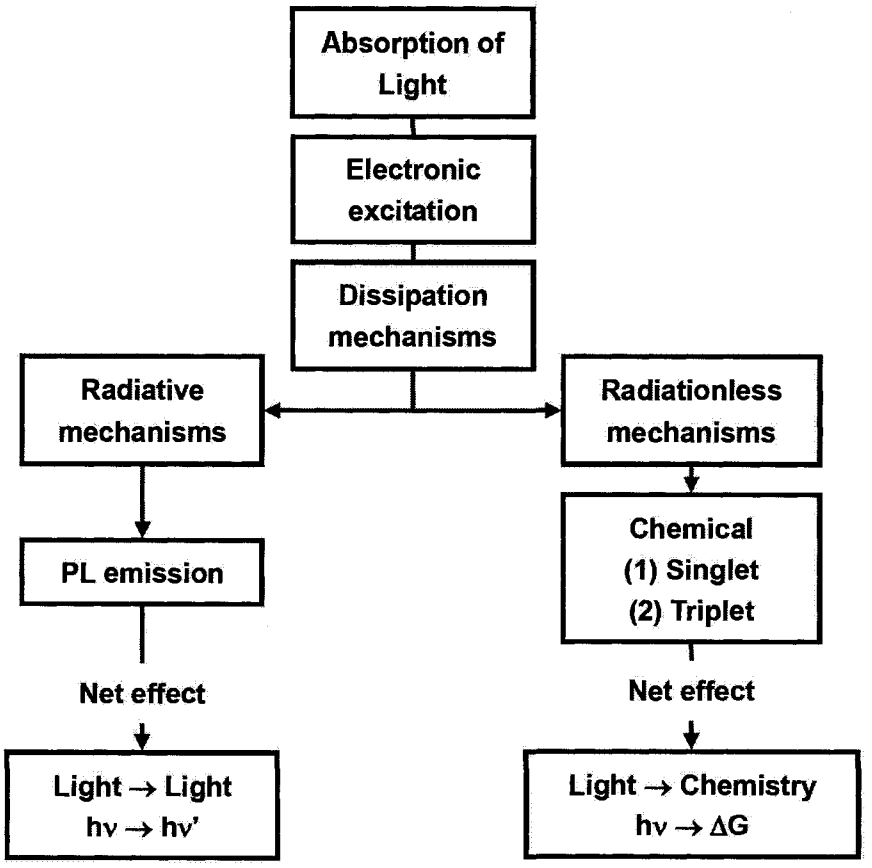

Figure II.8. Overview of energy transitions in photosensitive compounds

Photoluminescence

We examined the PL emission of synthesized the tetraphenylborate salts in acetonitrile and measured the quantum yields. As 254-nm irradiation is selected for the photolysis, we are particularly interested in emission excited by the light in a range of 220-280 nm.

As shown in Figure II.9 for TBD·$HBPh_4$, all the salts have the same PL spectra with a band centered at 313-317 nm on excitation with 244-250 nm UV light. Changing the concentration of solution does not introduce new PL bands, and all the PL spectra still kept the similar shape (Figure II.10). These results further support that (1) photophysical properties of the synthesized salts are controlled by the chromophore, and (2) there is no excimer formation.

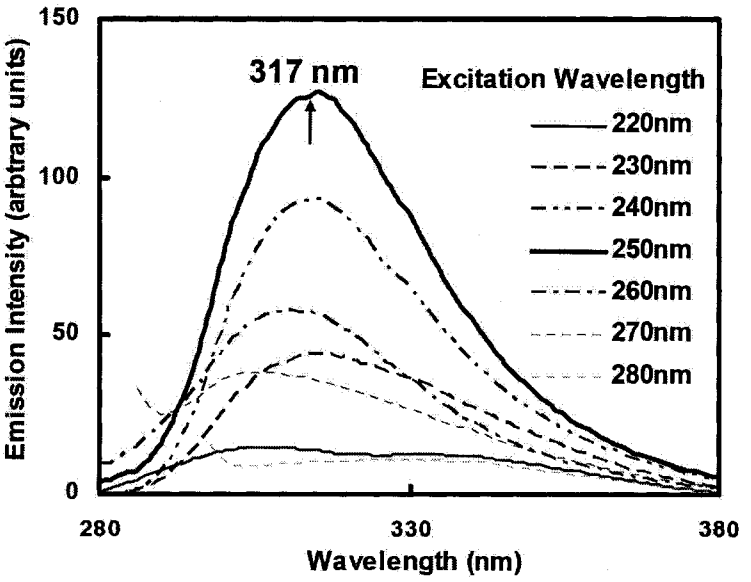

Figure II.9. PL spectra of TBD·$HBPh_4$ in AN (6×10^{-5} M) excited at 220-280 nm

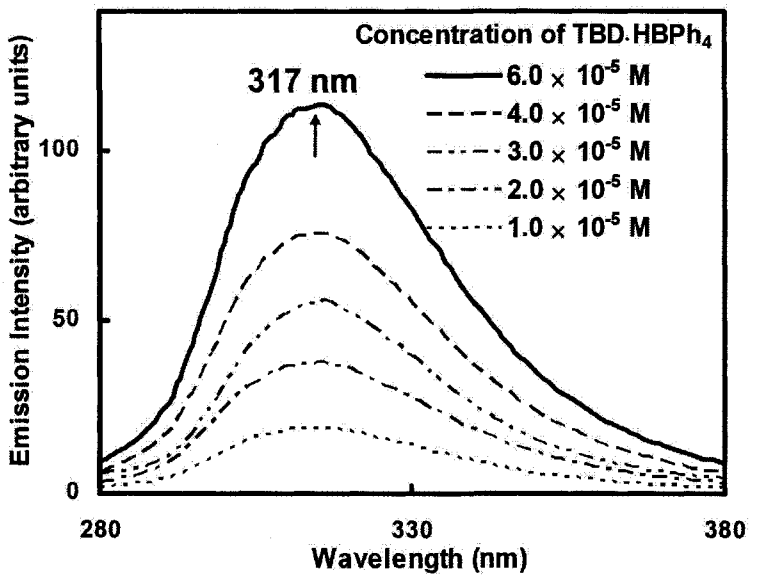

Figure II.10. PL spectra of TBD·$HBPh_4$ in acetonitrile with different concentration excited at 248 nm

Quantum Efficiency

In the measurement of quantum efficiency of PL emission (Φ_E), we used standard samples with known Φ_E as references and followed the comparative method of Williams et al.[15] To ensure the resulting data are accurate and reliable, we take the following into considerations. (1) The standard should absorb at same the excitation wavelength as the synthesized tetraphenylborate salts, and emit in the same spectral region. We chose quinine sulphate because its quantum yield is proved to be constant with excitation from 240 through 320 nm,[16] which perfectly fits the excitation wavelength (244-250 nm) for tetraphenylborate salts. (2) Quinine sulphate is cross-calibrated with another standard (naphthalene). (3) In order to minimize re-absorption effects, absorbance in the 10-mm cuvette should not exceed 0.1 at and above the excitation wavelength.

As shown in Table II.6, Φ_E of all the tetraphenylborate salts are less than one-tenth

of the quantum yield of benzene, indicating quite low energy loss through radiative transition in the synthesized tetraphenylborate salts with 254-nm irradiation.

Table II.6. Emission properties of the synthesized tetraphenylborate salts, benzene as the reference and quinine sulfate and naphthalene as standards

Compounds	Excitation λ_{max} (nm)	Emission λ_{max} (nm)	Quantum yield (Φ_E)
***t*-BuP$_1$(dma)·HBPh$_4$** [a]	246	313	0.0176±0.0003
TBD·HBPh$_4$ [a]	248	317	0.0183±0.0003
DBU·HBPh$_4$ [a]	249	315	0.0194±0.0004
Et$_3$N·HBPh$_4$ [a]	250	315	0.0191±0.0004
Benzene [b]	254	320	0.18±0.1
Quinine sulfate [c]	254	454	0.55±0.02
Naphthalene [d]	254	328	0.205±0.014

[a] in acetonitrile at room temperature, [b] in cyclohexane at room temperature, data from reference [17], [c] in 1.0 *N* H_2SO_4 at room temperature, data from reference [18], [d] in ethanol at room temperature, data from reference [18].

II.2.3 Photochemical Property

II.2.3.1 Photogeneration of Bases

Detection of Bases by pH Indicator

The base-generating ability of the synthesized tetraphenylborate salts was first tested by irradiation of their degassed acetonitrile solutions at 254 nm, followed by analysis using a pH indicator, namely phenol red, to detect the basic species in the resulting photoproducts. The aqueous solution of phenol red shows an absorption band at 400 nm at pH < 7.0 and the absorption band shifts to 570 nm due to formation of a quinoid structure at pH > 7.0 (Scheme II.3).[19]

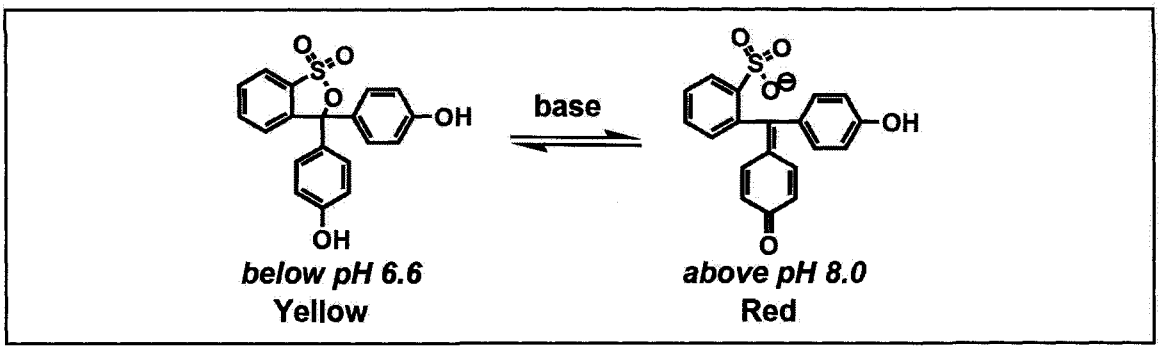

Scheme II.3. Structural changes of phenol red at different pH

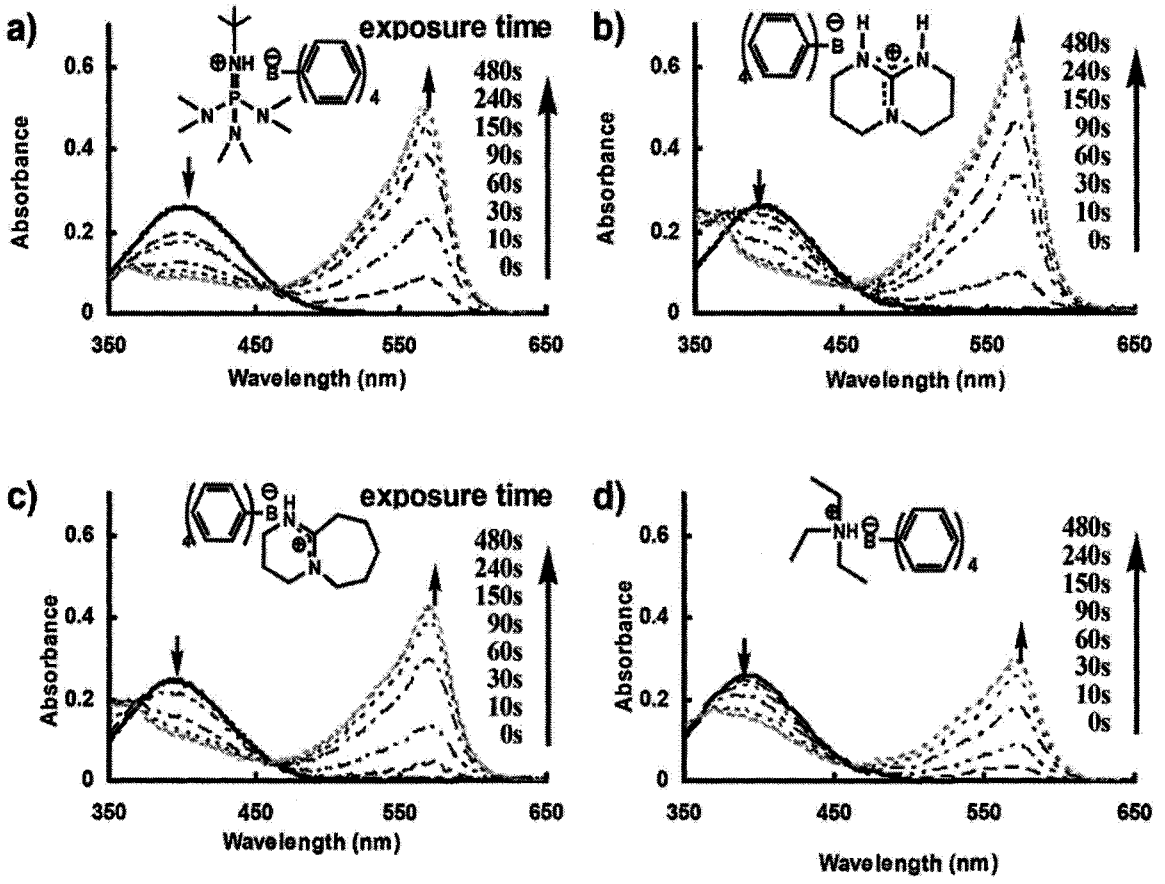

Figure II.11. Changes of UV-vis spectra of phenol red solution upon addition of a degassed solution of (a) *t*-BuP_1(dma)·$HBPh_4$, (b) TBD·$HBPh_4$, (c) DBU·$HBPh_4$, and (d) Et_3N·$HBPh_4$, that were irradiated over time.

Figure II.11 shows UV-vis absorption spectral changes of phenol red in aqueous solution upon addition of the unirradiated and irradiated tetraphenylborate salts. We observed only one absorption band centered at 400 nm in the spectra of phenol red solution upon addition of the unirradiated tetraphenylborate salts. This indicates that these tetraphenylborate salts are neutral. Upon addition of the irradiated solution of tetraphenylborate salts to the aqueous solution of phenol red, a new absorption band at 570 nm appeared, assigned to the deprotonated phenol red after reaction with the released basic species. The intensity increased with an increase of irradiation time. Therefore, basic compounds can be produced in the photolysis of tetraphenylborate salts.

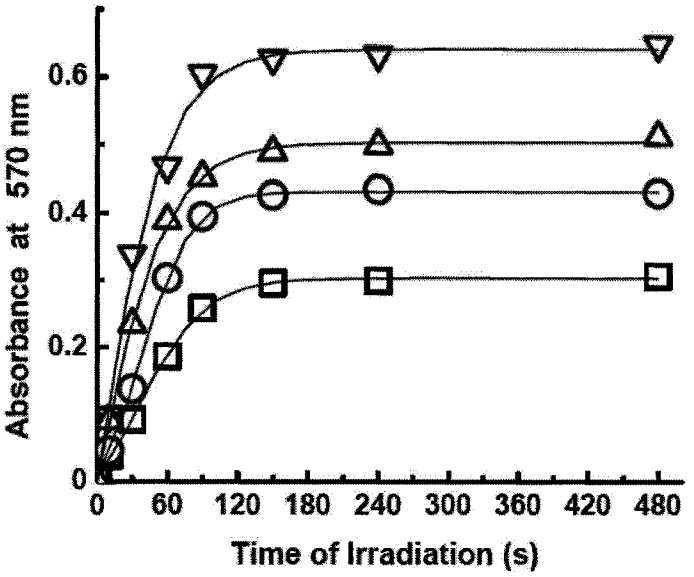

Figure II.12. Plot of the absorbance at 570nm due to deprotonation of phenol red in presence of bases against exposure time for (▽) TBD·HBPh$_4$, (△) *t*-BuP$_1$(dma)·HBPh$_4$, (○) DBU·HBPh$_4$ and (□) Et$_3$N·HBPh$_4$.

To compare the base-generating ability among these four synthesized tetraphenylborate salts, the intensity of the new absorption band centered at 570 nm was

plotted against irradiation time (Figure II.12). The intensity of absorption band at 570 nm gradually increased with longer irradiation time and became constant when the exposure time was more than 2 min. This indicated that most of basic species were already released after 2-min irradiation. The final intensities of the absorption bands at 570 nm were quite different in the tests for these four tetraphenylborate salts under the same condition, suggesting that the fully irradiated solutions of these salts had distinct pH values. Thus, photolysis of different tetraphenylborate salts generated different types of basic species. Furthermore, this result also described qualitatively the difference in basicity of released basic species. Photolysis of TBD·$HBPh_4$ produced the relatively stronger basic species than other three salts. It should be noted that all the tests were run under same conditions. To ensure the reliability of the results and minimize human errors, the data in Figure II.12 were averaged from three tests. The relative standard deviations of the three tests were less than 5 %.

Determination of Base Structures by ^1H and ^{31}P NMR

To determine the structures of generated basic species, the course of photolysis of the synthesized tetraphenylborate salts with a different amount of irradiation dosage at 254 nm were monitored by ^1H or ^{31}P NMR spectroscopy.

Figure II.13 shows ^1H NMR spectral changes in TBD•$HBPh_4$ upon irradiation at 254 nm under nitrogen. Protons H_d (3.26 ppm) and H_e (3.16 ppm, Figure II.13a) adjacent to the nitrogen atoms in TBD•H^+ were gradually disappearing and shifting to 3.08 ppm

(Figure II.13b) after irradiation at 254 nm. In comparison, the same characteristic methylene protons in TBD appeared at 3.01 ppm (Figure II.13d). However, since triarylborane is the main product in photolysis of $NaBPh_4$,[1] the in situ formation of an ate-complex between TBD and triarylborane (Ph_3B) during the photolysis of TBD•$HBPh_4$ should be expected. Apparently, the ex-situ formed ate-complex displays the same protons at 3.08 ppm (Figure II.13c), identical to the in situ formed TBD-Ph_3B complex (Figure II.13b). Therefore, the NMR studies confirmed the liberation of TBD from the photolysis of TBD•$HBPh_4$.

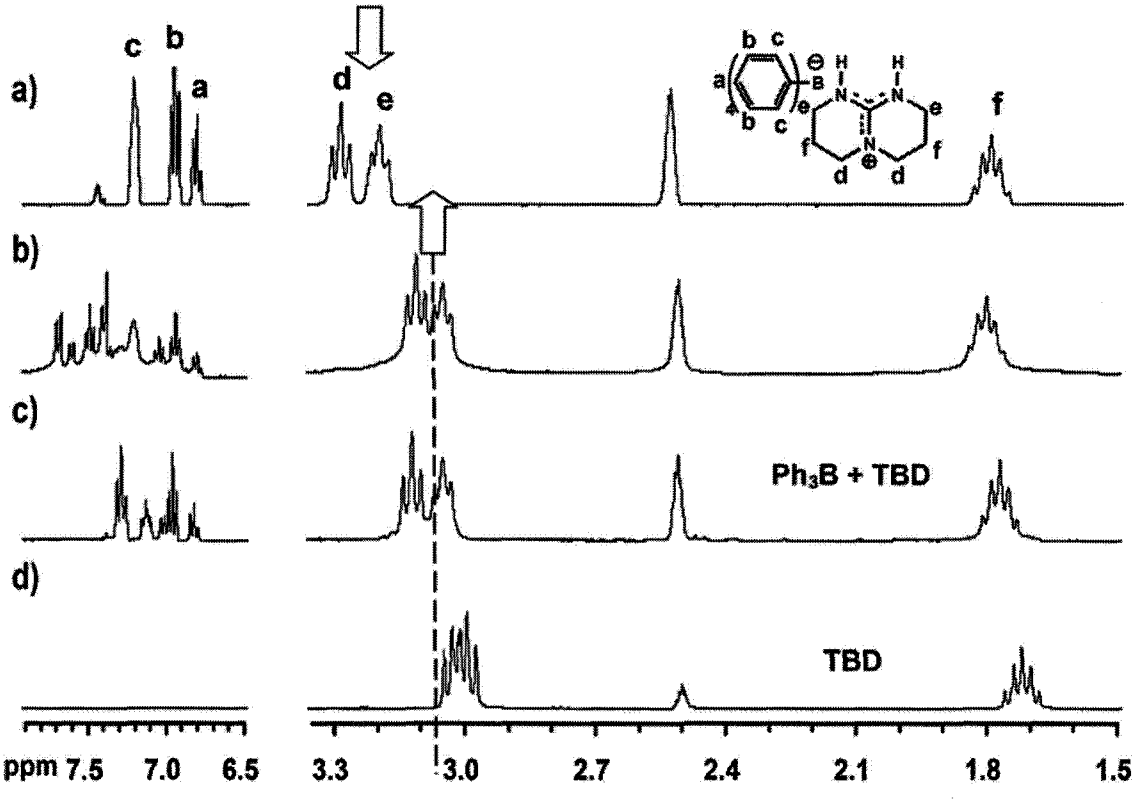

Figure II.13. ^1H NMR spectra (DMSO-d_6) of TBD•$HBPh_4$ after irradiation at 254 nm with a dose of a) 0, b) 92×10^{-6} Einstein, and as well of c) a mixture of Ph_3B and TBD and d) TBD

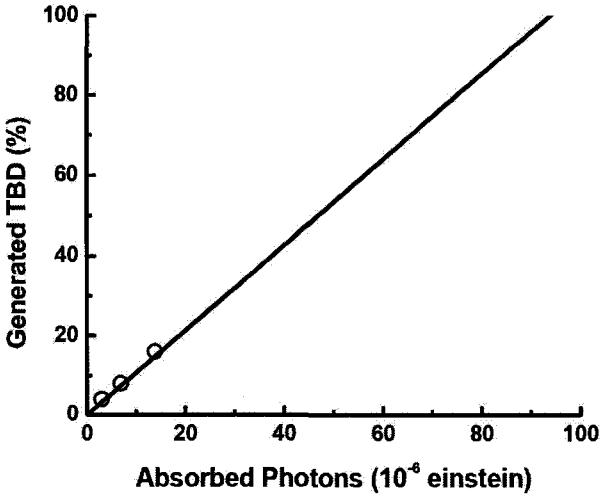

Figure II.14. Changes of generated TBD on irradiation of TBD•$HBPh_4$ based on the area changes of the peak at 3.08 ppm

Furthermore, based on the area of the new peak at 3.08 ppm, the degree of photogeneration of TBD form TBD•$HBPh_4$ was plotted as a function of the absorbed photons (Figure II.14). The slope gives the quantum yield (Φ) for TBD generation, which is 0.182 ± 0.012 (Φ is averaged from three tests in acetonitrile at room temperature upon irradiation at 254 nm). The peak f (Figure II.13a) was used as the internal standard to normalize the area of the new peak at 3.08 ppm in different spectra, since its area was always constant during the photolysis. To avoid the contribution of light absorption of the photoproducts, only the initial conversions (< 20 %) were taken into account. The quantum efficiency is wavelength dependent, and a higher efficiency for TBD generation from TBD•$HBPh_4$ can be expected at a shorter wavelength via the $\sigma_{C\text{-}B}$-$\sigma_{C\text{-}B}^*$ excitation, such as at 193 nm or 187 nm, due to its much higher absorption coefficient (ε_{195nm} = 1.26 × 10^5 $M^{-1}cm^{-1}$ vs. ε_{254nm} = 5.05 × 10^3 $M^{-1}cm^{-1}$).

Similar ^{1}H NMR spectral changes were observed for DBU·HBPh$_4$, and Et$_3$N·HBPh$_4$ after irradiation, as shown in Figure II.15 and II.16 respectively. Upon UV exposure at 254 nm, peaks due to the phenyl rings of the tetraphenylborate at 6.7-7.2 ppm decreased, suggesting the photodissociation of the anion. Meanwhile, peaks assigned to the protons adjacent to the nitrogen atoms in DBU•H$^+$ or Et$_3$N·H$^+$ (Figure II.15a and II.16a) were gradually depleted with the concomitant appearance of new peaks in the upper fields (Figure II.15b and II.16b), which had the chemical shifts identical to the same methylene protons in the ex-situ formed Ph$_3$B-DBU or Ph$_3$B-Et$_3$N complexes (Figure II.15c and II.16c). Thus, free nitrogen bases (DBU or Et$_3$N) are generated upon photolysis of their tetraphenylborate salts.

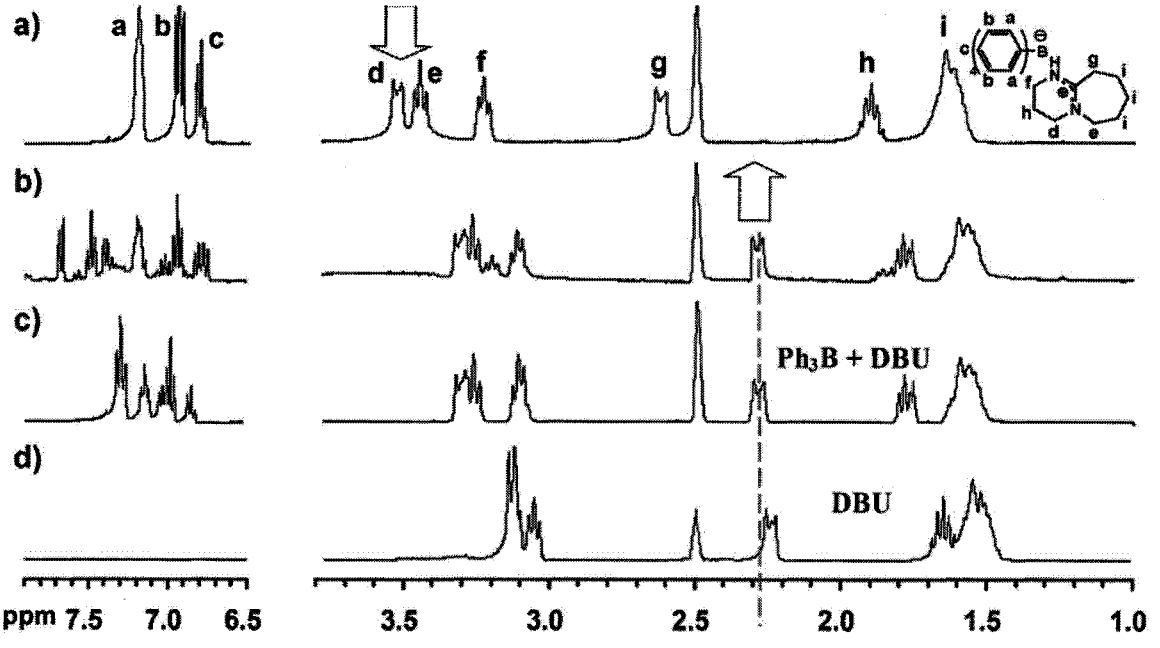

Figure II.15. ^{1}H NMR spectra (DMSO-d_6) of DBU•HBPh$_4$ after irradiation at 254 nm with a dose of a) 0, b) 81 × 10^{-6} Einstein, and as well of c) a mixture of Ph$_3$B and DBU and d) DBU

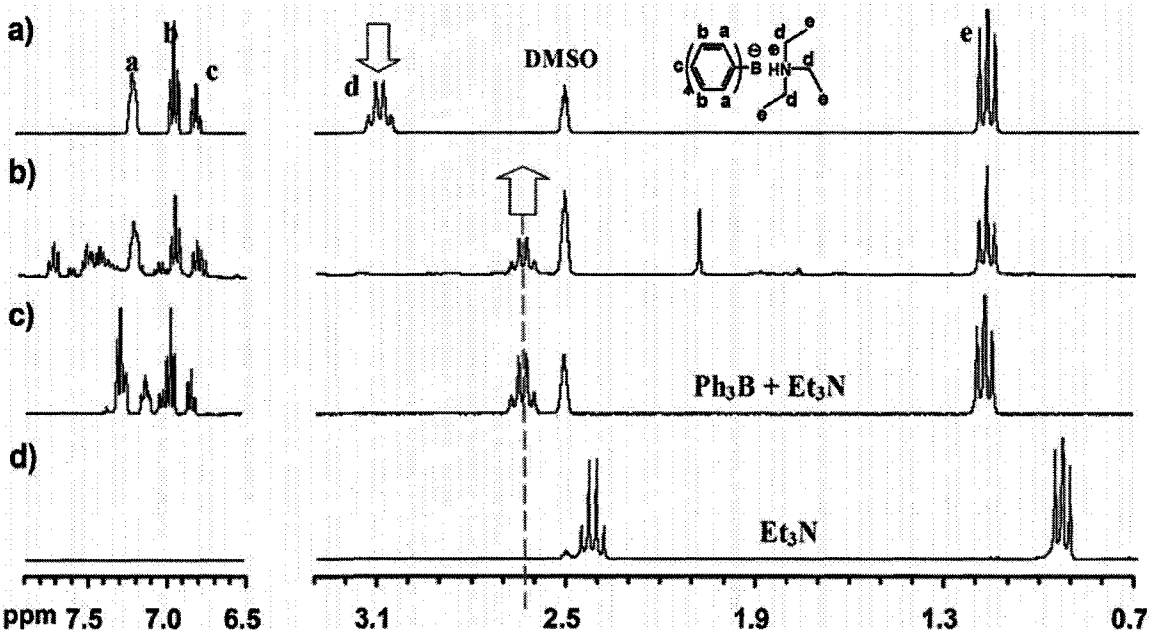

Figure II.16. ^{1}H NMR spectra (DMSO-d_6) of Et_3N•$HBPh_4$ after irradiation at 254 nm with a dose of a) 0, b) 76×10^{-6} Einstein, and as well of c) a mixture of Ph_3B and Et_3N and d) Et_3N

Liberation of the phosphazene base, namely *t*-butyliminotris(dimethylamino) phosphorane (*t*-BuP_1(dma)), from the photolysis of *t*-BuP_1(dma)•$HBPh_4$ upon 254-nm irradiation under nitrogen was studied by ^{31}P NMR spectroscopy (Figure II.17). With the increase of irradiation dosage, the peak at 50.00 ppm representing the protonated form of the phosphazene base (*t*-BuP_1(dma)·H^+, Figure II.17a) decreased, and a new peak at 20.87 ppm, which was identical to the chemical shift for *t*-BuP_1(dma), appeared gradually (Figure II.17b, c and d). With irradiation of 102×10^{-6} Einstein, the peak at 50.00 ppm was fully shifted to 20.87 ppm, indicating 100 % conversion. These spectral changes indicated the efficient photogeneration of *t*-BuP_1(dma) from *t*-BuP_1(dma)•$HBPh_4$.

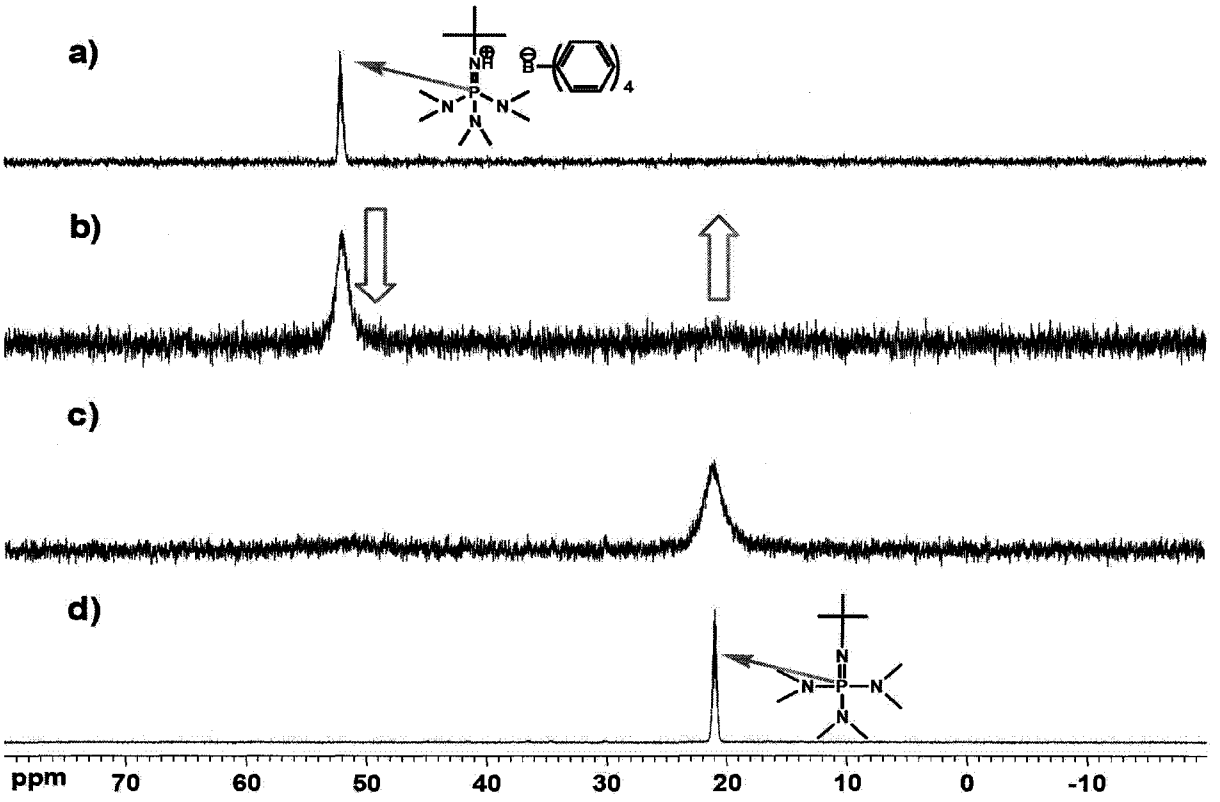

Figure II.17. ^{31}P NMR spectra (DMSO-d_6) of *t*-BuP$_1$(dma)•HBPh$_4$ after irradiation at 254 nm with a dose of a) 0, b) 10×10^{-6} Einstein, c) 102×10^{-6} Einstein, and as well of d) *t*-BuP$_1$(dma)

Based on the results from the pH indicator tests and the NMR studies, the versatile base-generating ability of tetraphenylborate salts is confirmed. Nitrogen bases, from phosphazene base to tertiary amines, are successfully released through photolysis of the corresponding tetraphenylborate salts.

These photogenerated bases are believed to have the same basicity and catalytic activities as free bases, even though they may form the ate-complexes with another photoproduct triarylborane (Ph_3B). The interaction between the nitrogen lone-pair electrons and the unoccupied P orbital of boron is deemed too weak to decrease the activity of generated bases. Regarding the Ph_3B-Et_3N complex, Neckers et al. already proved that the weak

interaction of Ph_3B-Et_3N did not affect the catalytic activity of photogenerated Et_3N for cross-linking of epoxides.[20] It was also reported that Et_3N formed a poor complex with borane, which had a bonding energy of N-B close to zero and decomposed at room temperature, due to the steric effect.[21] In comparison, DBU, TBD and *t*-BuP_1(dma) are of much more steric hindrance than Et_3N. Therefore, their complexes with Ph_3B should have even weaker interactions than Ph_3B-Et_3N, and thus less effect on the catalytic activities of free bases. The NMR study shows that all photogenerated bases complexed with Ph_3B exhibit a so-called "cation shift", as the methylene proton adjacent to nitrogen atom shifts to lower fields (the proton of H_e in Figure II.13 for Ph_3B-TBD, H_f in Figure II.15 for Ph_3B-DBU and H_d in Figure II.16 for Ph_3B-Et_3N). This "cation shift" is resulted from the electron density of the amine being donated to the boron empty P orbital. Table II.7 lists the observed changes of proton shifts for the complexes. A lower value of "cation shift" indicates a higher electron density remaining on the nitrogen atom due to a weaker interaction with the complexed boron. As predicted, the interactions of complexes decreased in the following order: $Et_3N{\cdot}HBPh_4$ > DBU·$HBPh_4$ > TBD·$HBPh_4$. Furthermore, Ph_3B in the amine-borane complex is known to be very easily oxidized by the oxygen in air at room temperature, which consequently releases the nitrogen base.[22] Thus, in our study, Ph_3B acts basically as a NMR shifting reagent to the photogenerated bases in NMR study, rather than an effective complexing agent to block the basicity of the photogenerated bases in any chemical reactions.

Table II.7. ^{1}H NMR resonance peak position of amine-borane complexes and free amines, and proton shifts

Amine-borane complexes	δ_H in complex [a] (ppm)	δ_H in free amine [a] (ppm)	"Cation Shift" (ppm)
Ph_3B-Et_3N	2.62	2.40	2.2
Ph_3B-DBU	3.13	3.04	0.9
Ph_3B-TBD	3.08	3.07	0.7

[a] in DMSO-d_6 at room temperature

Therefore, we demonstrated that the synthesized tetraphenylborate salts, which are capable of releasing the reactive forms of four strong nitrogen bases with the acceptable quantum efficiency parallel to most of commercially available cationic PIs,[23] can represent a new class of photobase generators. Among them, photogeneration of *t*-BuP_1(dma) and TBD is reported for the first time. Comparing with *t*-BuP_1(dma), TBD shows much higher catalytic activity in both polymerization and transesterification reactions due to its unique bicyclic structure. Thus, from here, our attention are focused on TBD•$HBPh_4$ and exploration for its potential applications as a photocatalyst.

II.2.3.2 Mechanism Study

Steady-State Photolysis

To investigate the photobase-generating mechanism, the kinetics of steady-state photolysis of TBD•$HBPh_4$ under nitrogen was studied by UV-vis spectroscopy, with reference to the known photochemistry of $NaBPh_4$ (Figure II.18).[1,2] Both compounds show nearly identical absorption before irradiation. By monitoring the spectral changes

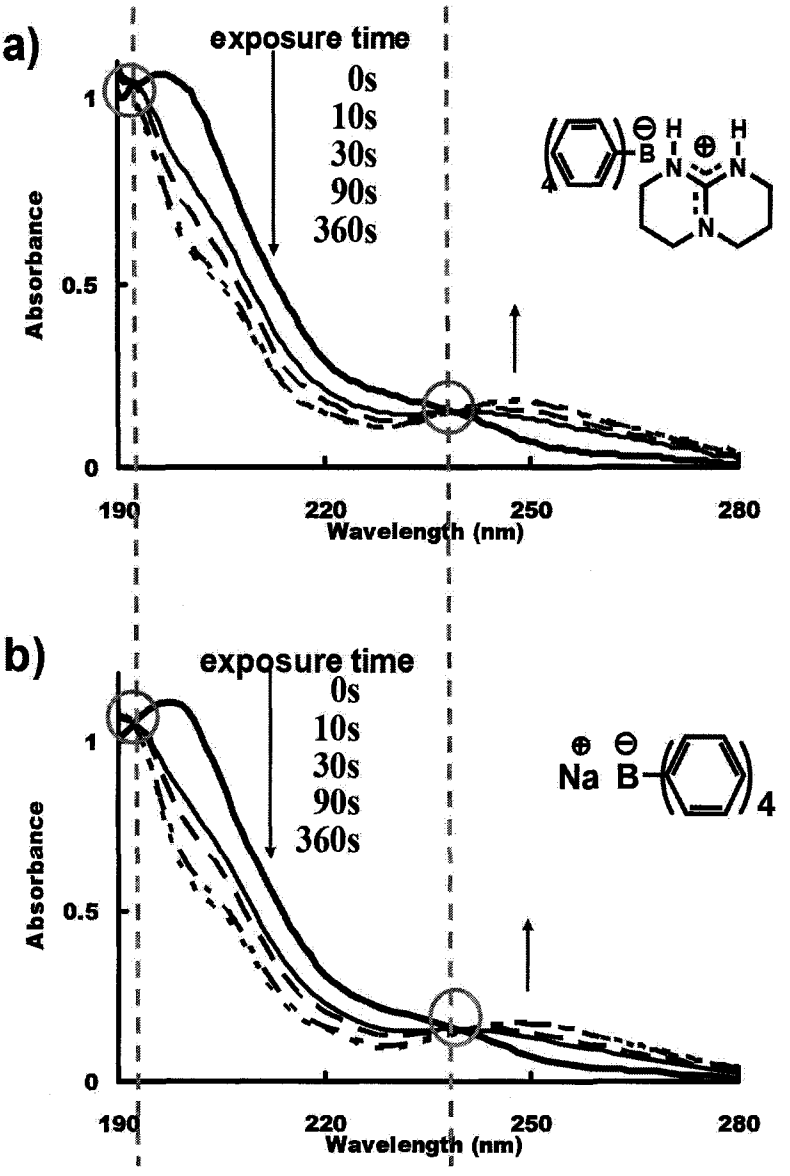

Figure II.18. UV-Vis absorption spectral changes of TBD•$HBPh_4$ and $NaBPh_4$ upon irradiation at 254 nm in acetonitrile (2×10^{-5} M) under nitrogen

during the photolysis of TBD•$HBPh_4$ and $NaBPh_4$ under the same conditions, the following were observed: (1) a drastic decrease in absorbance at 200 nm and an increase in absorbance at 250 nm with the two tight isosbestic points (192 and 239 nm) for both

salts and (2) virtually identical rate constants of photodissociation of 0.0370 ± 0.002 s^{-1} and 0.0368 ± 0.002 s^{-1} for TBD•$HBPh_4$ and $NaBPh_4$, respectively (see Experimental Part 9.). The results strongly suggest that photolysis of TBD•$HBPh_4$ proceeds in the same pathway as $NaBPh_4$. Accordingly, the excited tetraphenylborate anion rearranges and then abstracts a proton from the neighboring TBD•H^+ cation to release TBD (Scheme II.4). The resulting trivalent arylborane further decomposes to aromatic fragments. Considering the higher absorption coefficients in the deep UV region of TBD•$HBPh_4$ (Figure II.18a), TBD can be photogenerated below 200 nm, for example, at 193 nm from ArF excimer laser, in a higher quantum yield than being done at 254 nm. There are clear advantages of using sub-200 nm light in photolithography and other photoinduced processes.[24]

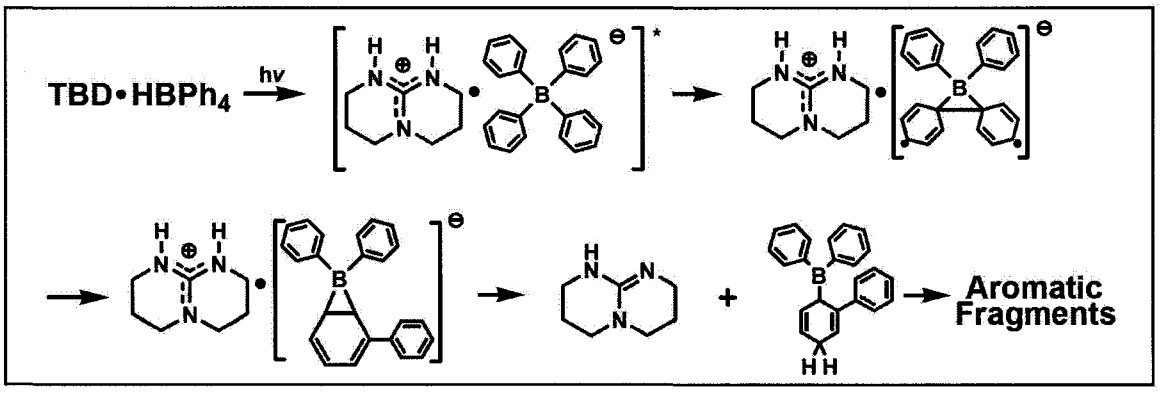

Scheme II.4. Proposed mechanism for the photogeneration of TBD from TBD•$HBPh_4$

Atmosphere Sensitivity of Photolysis (Air vs. Nitrogen)

PBGs capable of releasing bases under ambient conditions (e.g., air) are desirable for practical applications, since UV curing or imaging processes normally proceed in an open-to-air environment. Bearing this in mind, we studied the atmosphere sensitivity of

the photolysis of tetraphenylborate salts. Photodissociation of TBD•$HBPh_4$ upon 254-nm irradiation in air and nitrogen saturated acetonitrile solutions were monitored by UV-vis spectroscopy, respectively. As shown in Figure II.19, the observed absorption spectral changes for photolysis in air and nitrogen were fairly close. The decreasing rate of absorbance at λ_{max} = 196 nm in air was similar to that in nitrogen (Figure II.20). These

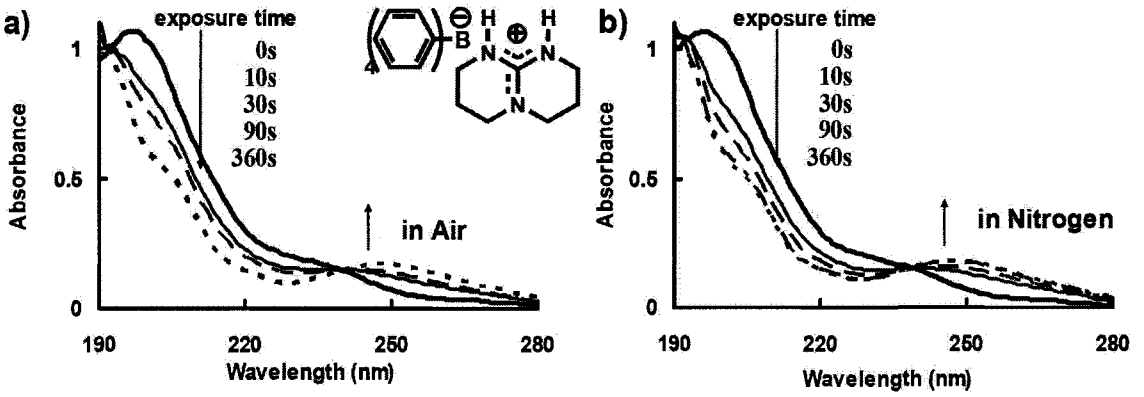

Figure II.19. UV-Vis absorption spectral changes of TBD•$HBPh_4$ upon irradiation at 254 nm in a) air and b) nitrogen saturated acetonitrile (2×10^{-5} M)

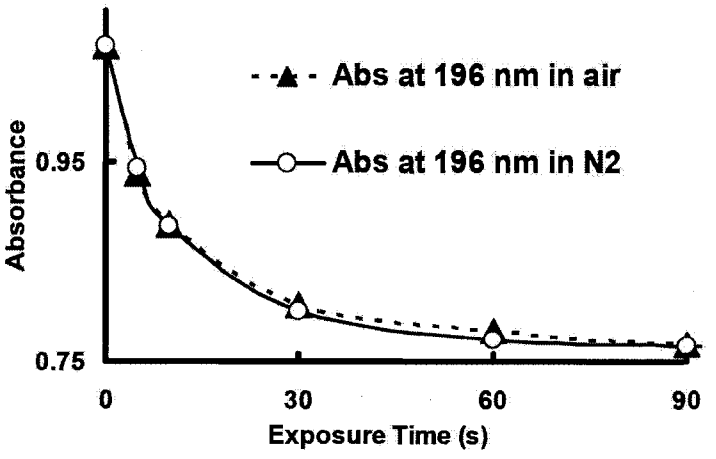

Figure II.20. Changes in absorbance at 196 nm against exposure time of TBD•$HBPh_4$ upon irradiation at 254 nm in a) air and b) nitrogen saturated acetonitrile (2×10^{-5} M)

facts suggest that the photodissociation of TBD•$HBPh_4$ in air undergo the same process as in nitrogen. In the study by Williams et al., photolysis of $NaBPh_4$ in air and nitrogen saturated aqueous solution produced the same photoproducts with similar yields.[1] Thus, TBD•$HBPh_4$ can work as a PBG in air as well.

II.3 Applications of $HBPh_4$ Salts as PBGs

Since TBD can be released from TBD•$HBPh_4$ in the presence of alcohols (methanol and ethanol), due to its much lower pK_a than alcohols ($^{water}pK_a$ = 13.6 vs 15.5-16.1), this salt can be utilized as a photocatalyst for some base-catalyzed reactions and polymerizations.

II.3.1 Photoinduced Anionic Living ROP of Cyclic Esters

Polymerization of monomers or macromers by light-induced initiation (excitation of a photoinitiator) is one of the main methods that are widely used in UV curing and micro-imaging systems. As mentioned in the previous chapter, the photoinduced anionic living ROP have some advantages to compete with the free-radical photopolymerization. However, the bases released from reported PBGs are not strong enough to initiate the anionic photopolymerization. For example, DBU generated from the known PBGs is insufficient to trigger the ROP of caprolactone (CL).[25] Realization of the photoinitiated anionic ROP using TBD•$HBPh_4$ will offer opportunities for new UV curing and other industrial applications.

Thus, bulk polymerization of CL was attempted using 1 mol % of TBD•$HBPh_4$ in

the presence of 1 mol % of n-hexanol as an initiator. After irradiation for 5 min at 254 nm, polymerization proceeded for 8 h at 60 °C. Poly(CL) with a molecular weight (Mn) of 16,537 $g \cdot mol^{-1}$ or degree of polymerization (DP) of 144 was obtained with 70 % monomer conversion (Scheme II.5). The ROP rate increased with longer irradiation time (Figure II.21 a), indicating the release of more base catalysts. The living nature of this ROP is evident by the observed linear relationship between the monomer conversion and molecular weight of poly(CL) (Figure II.21 b and c). $NaBPh_4$ was also tested as a possible photocatalyst in the control experiment. Under the same conditions, no polymerization of CL was observed at all. Additionally, no poly(CL) was formed using Ph_3B, eliminating its possible role as in-situ generated Lewis catalyst for ROP. Therefore, TBD•$HBPh_4$ is able to work as an efficient photocatalyst for anionic living ROP of CL and the photogenerated base TBD is the actual catalyst in the polymerization.

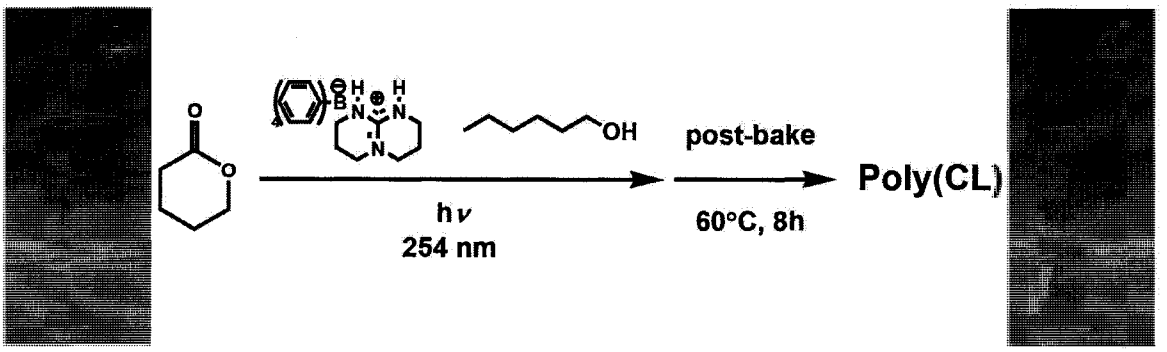

Scheme II.5. Photoinduced anionic ROP of CL catalyzed by TBD•$HBPh_4$. (left image) CL mixed with 1 mol % of TBD•$HBPh_4$ and 1 mol % of n-hexanol. (right image) Poly(CL) obtained after irradiation for 5 min at 254 nm followed by post-baking for 8 h at 60 °C.

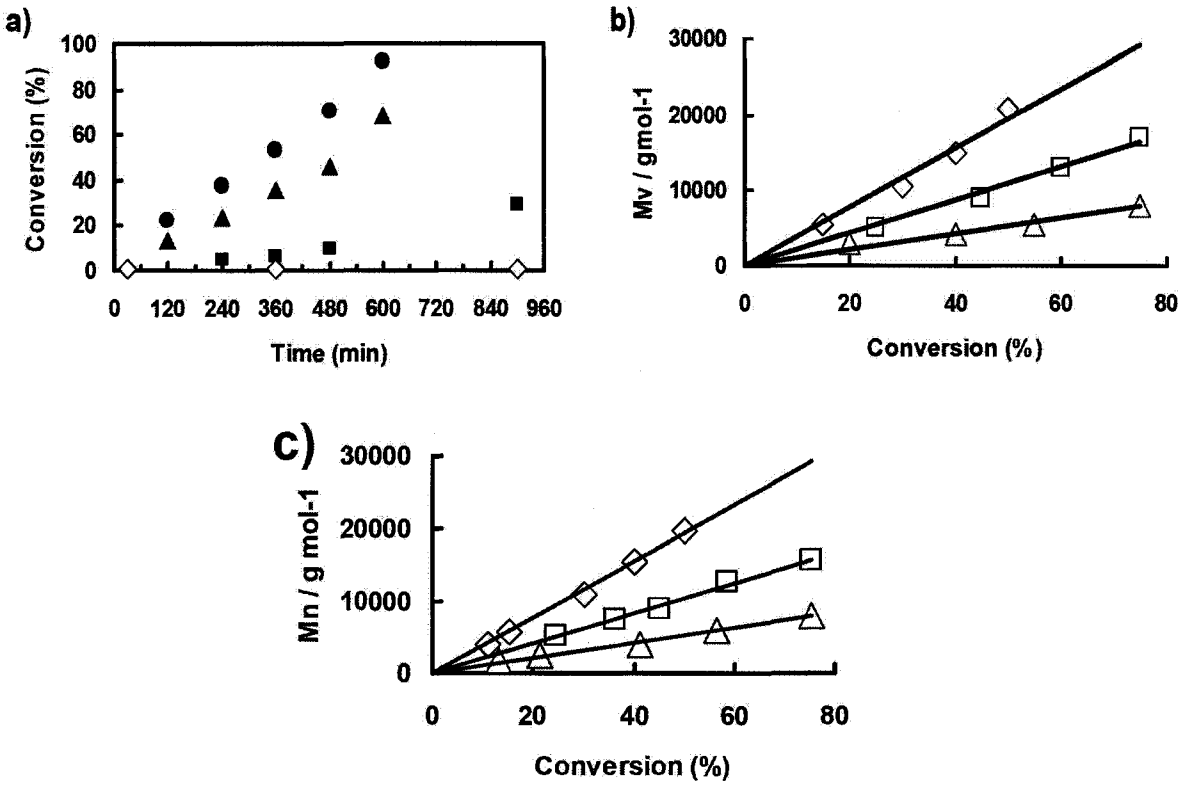

Figure II.21. a) Conversion versus time of polymerization for ROP of CL by 1 mol % of TBD•HBPh$_4$ with exposure at 254 nm for ● 5, ▲ 3, ■ 2 min, ◇ control experiment with NaBPh$_4$. b) The viscosity-average molecular weight M_v versus conversion with 5 min UV exposure (◇) DP = 200 (□) DP = 100 (Δ) DP = 50. c) The number-average molecular weight M_n versus conversion with 5 min UV exposure (◇) DP = 200 (□) DP = 100 (Δ) DP = 50

II.3.2 Photoinduced Cross-linking of Polymeric Materials Bearing Hydroxy and Ester Groups

Encouraged by the high activity of TBD•HBPh$_4$ in anionic polymerization, we further explored its ability in other base-catalyzed reactions. TBD has been proved to be an effective catalyst for transesterification reaction between an ester and an alcohol.[26, 27]

Thus, the photoinduced cross-linking of polymeric materials bearing hydroxy and ester groups in the presence of TBD•$HBPh_4$ can be envisioned.

Photoinduced Cross-linking of Cellulose and PMMA

Cellulose bearing pedant hydroxy groups and poly(methyl methacrylate) (PMMA) with ester groups on the side chain are selected. The former is water-soluble and the latter is not soluble in water and protic solvents, such as methanol. Due to the large difference in polarity, it is difficult to mix these two polymers together and to form a uniform blend without phase separation. The cross-linking is one way to deal with this blending problem.

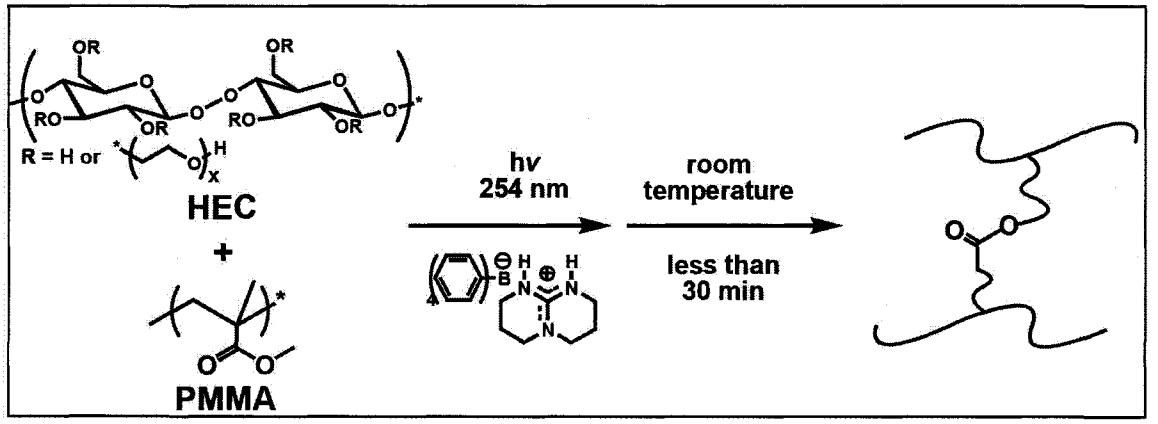

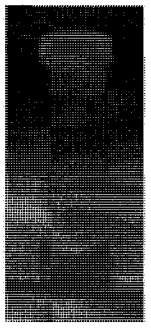

Scheme II.6. (left) a DMF solution of 1:1 (wt/wt) ratio of PMMA / HEC with 5mol% TBD•$HBPh_4$ irradiated at 254 nm light for 3 min; (right) a gel was formed in 30 min at room temperature

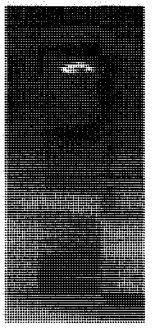

Upon addition of the irradiated TBD•$HBPh_4$ to a mixture at a 1:1 (wt/wt) ratio of

poly(methyl methacrylate) (PMMA) and 2-hydroxyethyl cellulose (HEC) in *N,N*-dimethylformamide, a gel was formed in 30 min at room temperature, indicating polymer cross-linking (Scheme II.6). The chemical bonding formed between these two polymers in solution through the TBD-catalyzed transesterification reaction can also be obtained in a solid-state. With post-irradiation baking at temperature higher than glass transition temperature (PMMA, T_g = 100 °C), the side chains containing hydroxy or ester groups can move around easily in the rubber state, which facilitates the cross-linking reaction. By removing of a molecule of methanol (boiling point at 64.7 °C at 760 mmHg), a new ester bond can be formed to link two polymer chains, and consequently minimizes the interfacial actions that induce phase separation in the blend, such as hydrogen bonds between hydroxy groups in cellulose, thus, results a uniform polymeric material. Furthermore, this photoinduced cross-linking catalyzed by TBD•$HBPh_4$ provides a feature known as "cross-linking on demand". Thus, the phase separation in the blend of PMMA/cellulose can be controlled. Upon UV irradiation through a mask, followed by post-baking, the uniformed blend is formed in irradiated area, while, phase separation still occurs in masked place.

Blending polymers is commonly tried because the properties of plastic materials can be tailored to meet various demands, which is not possible with a single polymer. In combinations of polymers that are immiscible, phase separation always occurs and plays a significant role in determining their properties. In some cases, this phase separation is needed to achieve ordered meso- and microphase-separated structures.[28-30] While, in most

of blends, it is a barrier to get homogeneous materials.[31,32] Obviously, the photocross-linking by TBD•$HBPh_4$, which is capable of controlling the phase separation property of polymer blends, would be fundamentally and practically interesting. Herein, one example we demonstrate is the interfacial photocross-linking catalyzed by TBD•$HBPh_4$ between two polymer films of PMMA and cellulose to modify their surface properties.

Photoinduced Surface Modification of Cellulose

Cellulose is the primary structural component of green plants. Its content in wood is higher than 50 percent. The bare surfaces of wooden furniture are all cellulose-based materials. Thus, the development of a new photoinduced method for cellulose surface modification will be beneficial to improving UV curable-coatings for wooden furniture.

Upon irradiation of a thick film of HEC coated with a thin layer of PMMA containing 5 mol % TBD•$HBPh_4$, only PMMA on the irradiated areas were left on HEC after washing off the top layer, as evident by a large change in the contact angle of water from 45° (for HEC) to 86° (for PMMA) (Figure II.22). This photoinduced surface modification was further monitored by attenuated total reflection infrared (ATR-IR) spectroscopy. As seen in Figure II.23, after washing off the unreacted PMMA thin film, the spectrum of modified HEC shows the depletion of the alcohol's O-H stretch at 3500-3700 cm^{-1}, with concomitant appearance of carbonyl C=O stretches at 1770 cm^{-1} due to the transesterification reaction.

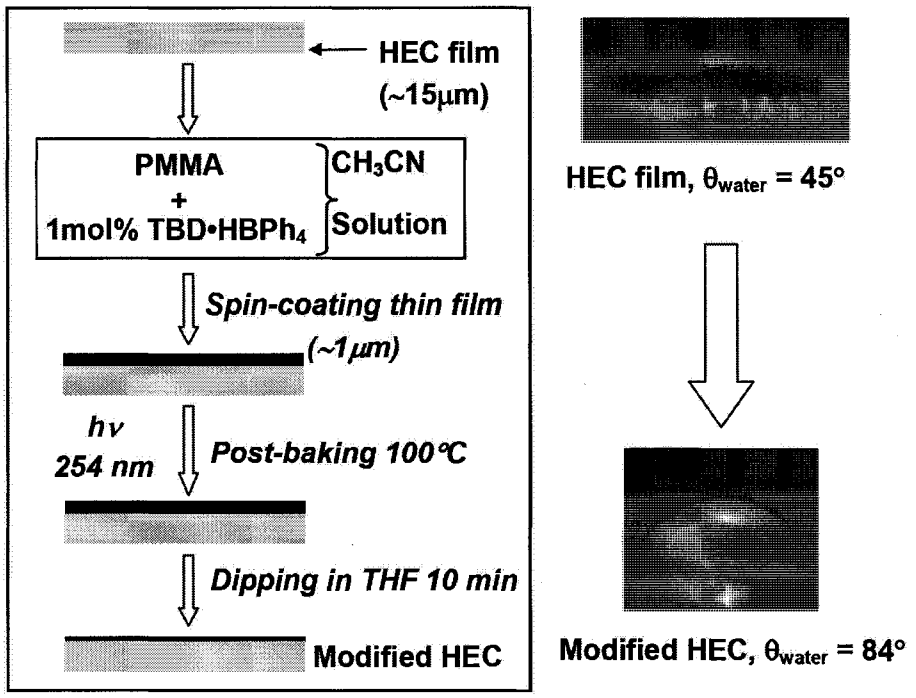

Figure II.22. Schematic illustration of photoinduced surface modification of HEC

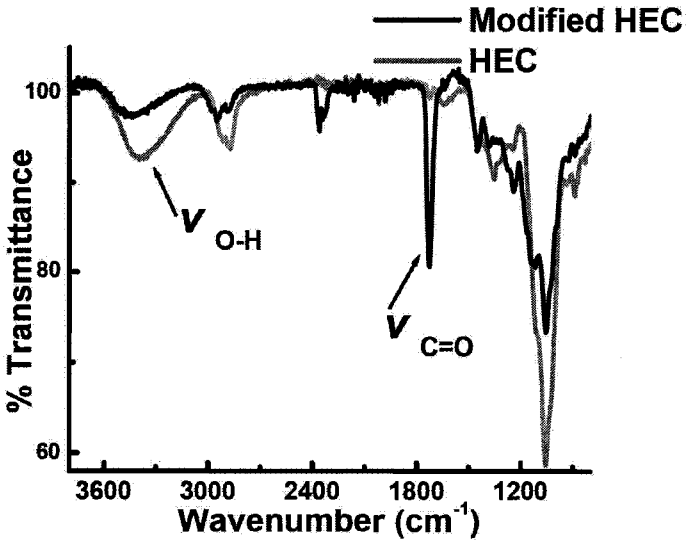

Figure II.23. ATR-IR spectral changes of HEC film before and after the surface modification catalyzed by TBD·$HBPh_4$

In addition, by carefully controlling the post-baking temperature or exposure time, the degree of this photoinduced interfacial cross-linking can be controlled. The HEC surface is gradually changed from hydrophilic (θ_{water} = 45°) to hydrophobic (θ_{water} = 86°) (Figure II.24).

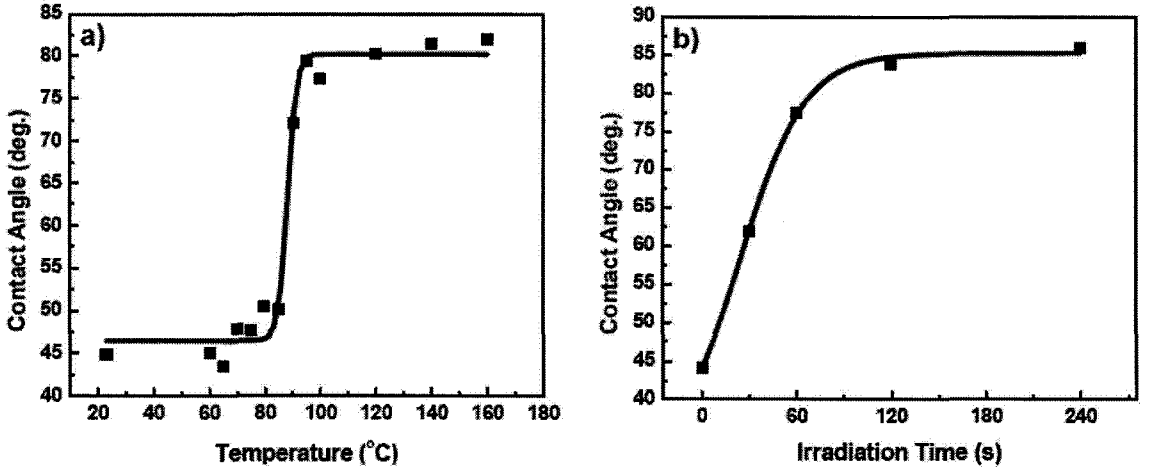

Figure II.24. a) Water contact angle variation of HEC surfaces modified by photocrosslink of PMMA containing 5 mol % of TBD•HBPh$_4$ on irradiation (10 mW/cm^2) of 3 min followed by postbaking at different temperature for 5 min. b) Water contact angle versus exposure time of HEC surfaces modified by photocrosslink of PMMA containing 5 mol % of TBD•HBPh$_4$ with postbaking at 100 °C for 5 min

Photoinduced Cross-linking of Copolymers P(MMA-co-HPA) and P(VP-co-HPA)

The photocross-linking catalyzed by TBD•HBPh$_4$ through transesterification reaction is not limited to the system involving cellulose and PMMA. Polymeric materials containing hydroxy and ester groups are all in principle possible to be cross-linked in the same manner.

Herein, one example we demonstrated is the use of hydroxypropyl acrylate (HPA) as a self-cross-linkable unit in the copolymers with methyl methacrylate (MMA) and

N-vinylpyrrolidone (VP), respectively. Films of the two copolymers, P(MMA-co-HPA) (1:1) and P(VP-co-HPA) (1:1), containing 5 mol % TBD•HBPh$_4$ were irradiated at 254 nm and then baked at 100 °C for 3 mins (Scheme II.7).

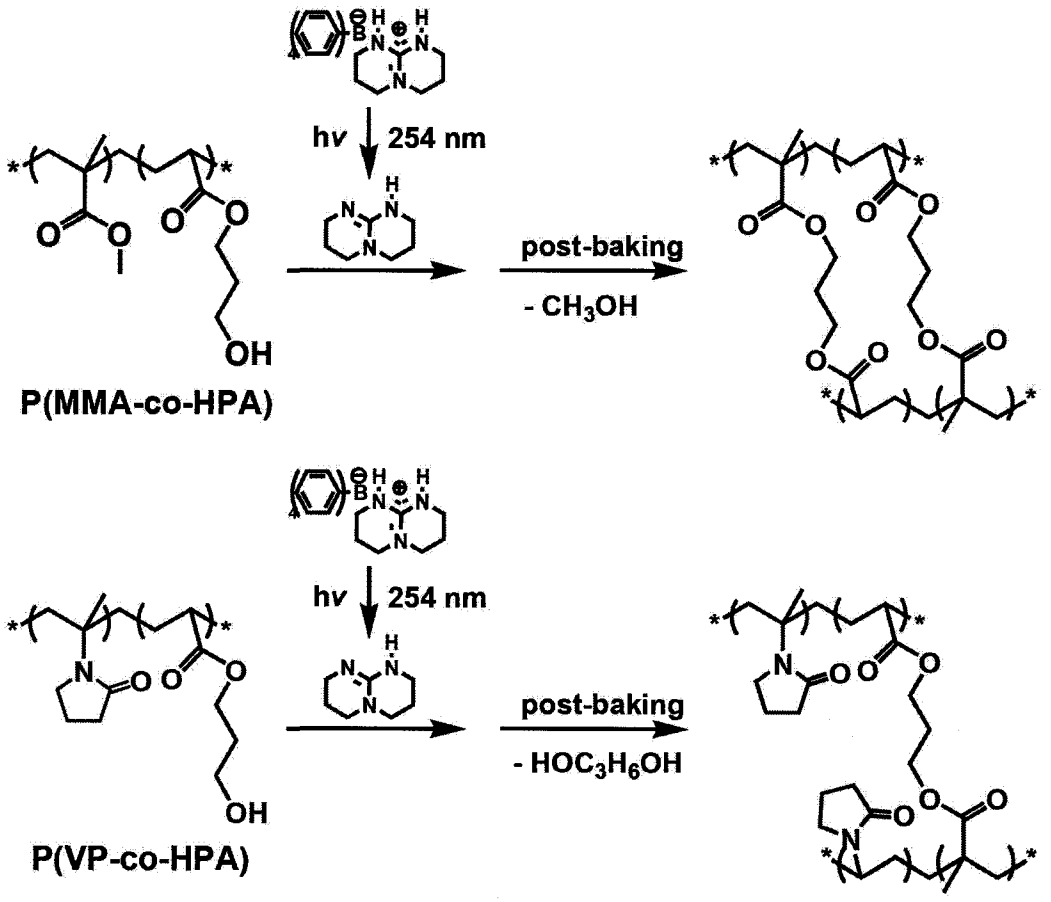

Scheme II.7. Photocross-linking of P(MMA-co-HPA) (1:1) and P(VP-co-HPA) (1:1) catalyzed by TBD•HBPh$_4$

Both polymer films became insoluble in organic solvents, including acetonitrile, THF and $CHCl_3$, due to polymer cross-linking, as a result of transesterification and subsequent loss of methanol or/and 1,3-propylenediol (Figure II.25a). In comparison, P(MMA-co-HPA) could not be cross-linked using 5 mol % Ph_3B or $NaBPh_4$. The cross-linking of copolymers was also monitored by IR spectroscopy (Figure II.25b).

Upon irradiation and post-baking, the IR spectra of P(MMA-co-HPA) thin film showed a decrease of the O-H stretch at 3300-3700 cm^{-1}, indicating the loss of alcohols. To avoid the influence of moisture in air, all the films dried in vacuum oven at 80 °C overnight. Additionally, the irradiation and post-baking all proceeded under the protection of argon. Thus, polymers or blends containing hydroxyl and ester groups can be photocross-linked with a catalytic amount of TBD•$HBPh_4$.

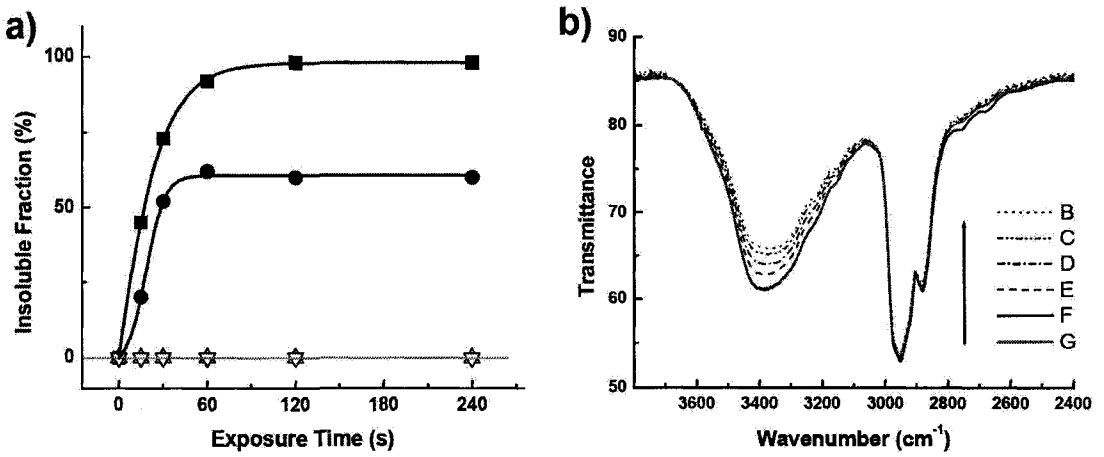

Figure II.25. a) Insolubilization of P(MMA-co-HPA) ■ and P(VP-co-HPA) ● films containing TBD•$HBPh_4$ as photocatalyst on irradiation (10mW/cm^2) followed by baking at 100 °C for 3min, ∇ and Δ are control experiments with Ph_3B or $NaBPh_4$. b) IR spectral changes in the films of P(VP-co-HPA) on irradiation (2 min) with postbaking times of (E) 5, (D) 10, (C) 20 and (B) 30 min at 100 °C. To removing residue of solvent and moisture in air, films were dried in vacuum oven at 80 °C for (G) 8h and (F) overnight

II.4. Conclusions

A series of tetraphenylborate salts are prepared. They show good thermo-stability with onset decomposing temperature up to 200 °C and absorb light in the UV-C region. Nitrogen bases, from phosphazene to tertiary amines, are released upon photolysis of their corresponding tetraphenylborate salts. Several applications using TBD·$HBPh_4$ as

photocatalyst have been demonstrated, including the photoinduced living ROP of cyclic esters and photocross-linking of polymeric materials containing the hydroxyl-ester groups.

II.5. Experimental Section

1. Materials

Triethylamine (Et_3N), 1,8-diazabicyclo[5.4.0]undec-7-ene (DBU), 1,5,7-triaza -bicyclo[4.4.0]dec-5-ene (TBD), tert-butylimino-tris(dimethylamino)phosphorane (t-BuP_1(dma)), sodium tetraphenylborate ($NaBPh_4$), hydroxypropyl acrylate (mixture of isomers) (HPA), methyl methacrylate (MMA), 1-vinyl-2-pyrrolidone (VP), PMMA (average Mw ~120,000 by GPC, powder), HEC (average Mv ~90,000), triphenylborane (Ph_3B) and phenol red were used as received (Aldrich). Caprolactone (CL), and n-hexanol were received from Aldrich and distilled from CaH_2.

2. Instruments

^1H NMR spectra were measured on a Bruker Advance 300 instrument at 300 MHz. IR and ATR-IR spectra were recorded on a Varian 1000 FT-IR Scimitar Series. UV-vis spectra were measured on a Perkin ELMER Lambda 900. Differential scanning calorimetry and thermogravimetric analyzers were conducted on a TA Q100 and a Hi-Res TGA 2950, at a heating rate of 10 °C/min.

3. Irradiation Methods

Photolysis in solution was performed in a Rayonet Photochemical Reactor RPR100

equipped with RPR2537 Å lamps. Photoirradiation of solid films was carried out with EFOS Novacure UV light source equipped with a high pressure 100 Watt mercury vapour short arc. The light intensity (10 Mw/cm^2) at 250-300 nm was determined with a built-in radiometer. Film thickness was determined by alpha-step 200 Tencor instrument.

4. Synthesis of Et_3N·$HBPh_4$, DBU·$HBPh_4$, TBD•$HBPh_4$ and *t*-BuP_1(dma)•$HBPh_4$

The base (10 mmol) was firstly dissolved in 10 mL of 10 % HCl (aq), and then, a slight excess of $NaBPh_4$ solution in 10 mL of water was added. The precipitated salt was filtered, washed several times with water followed by washing with MeOH, recrystallized from a mixture of MeOH and $CHCl_3$ (4:1), and dried in vacuo.

Et_3N·$HBPh_4$: White needle crystals; yield 89 %; mp 136-138 °C; T_{dec} 188 °C;^{1}H NMR (300 MHz, DMSO-d_6) 1.17 (m, 9H), 3.08 (q, 6H), 6.78 (t, 4H), 6.92 (t, 8H), 7.17 (m, 8H); ^{13}C NMR (75 MHz, DMSO-d_6) 9.3, 47.8, 122.0, 125.9, 137.1, 165.1.

DBU·$HBPh_4$: Colorless cubic crystals; mp 200-201 °C; T_{dec} 252 °C; ^{1}H NMR (300 MHz, DMSO-d_6) 1.64 (m, 6H), 1.90 (m, 2H), 2.64 (m, 2H), 3.24 (m, 2H), 3.46 (m, 2H), 3.55 (m, 2H), 6.78 (t, 4H), 6.92 (t, 8H), 7.17 (m, 8H); ^{13}C NMR (75 MHz, DMSO-d_6) 9.3, 47.8, 122.0, 125.9, 137.1.

TBD•$HBPh_4$: Colorless cubic crystals; yield 93 %; mp 223-224 °C; T_{dec} 251 °C; ^{1}H NMR (300 MHz, DMSO-d_6) 1.80 (m, 4H), 3.16 (t, 4H), 3.26 (t, 4H), 6.78 (t, 4H), 6.92 (t, 8H), 7.17 (m, 8H); ^{13}C NMR (75 MHz, DMSO-d_6) 17.3, 26.9, 36.8, 48.0,121.8, 125.7, 137.2, 165.2.

t-BuP_1(dma)•$HBPh_4$: White needle crystals; yield 90 %; mp 206-207 °C; T_{dec} 276 °C; ^{1}H NMR (300 MHz, DMSO-d_6) 1.22 (d, 9H), 2.68 (d, 18H), 5.46 (d, 1H), 6.78 (t, 4H), 6.92 (t, 8H), 7.17 (m, 8H); ^{13}C NMR (75 MHz, DMSO-d_6) 31.5, 37.8, 40, 121.9, 125.7, 136.2.

5. Determination of PL Quantum Yield

The general procedure is as follows:

(1) Record the UV-vis absorbance spectrum of standard sample (quinine sulphate) in 0.1*N* H_2SO_4 aqueous solution. Note down the absorbance at the excitation wavelength (254 nm) to be used.

(2) Record the fluorescence spectrum of the same solution in the 10 mm fluorescence cuvette. Calculate and note down the integrated fluorescence intensity (that is, the area of the fluorescence spectrum).

(3) Repeat steps (1) and (2) for five solutions with increasing concentrations of quinine sulphate. (There will be six solutions in all, corresponding to absorbances at the excitation wavelength of 0.02, 0.04, 0.06, 0.08 and 0.10.)

(4) Plot a graph of integrated fluorescence intensity vs absorbance. The result should be a straight line with gradient (Grad), and intercept = 0.

(5) Repeat steps (1) to (4) for another standard sample (naphthalene) and synthesized tetraphenylborate salts.

The gradients of the gradients (Grad) obtained in (4) above are proportional to the

quantum yield of the different samples. Absolute values are calculated using the standard samples which have a fixed and known fluorescence quantum yield value, according to the following equation:

$$\Phi_X = \Phi_{ST} (Grad_X / Grad_{ST}) (\eta^2_X / \eta^2_{ST})$$

Where the subscripts ST and X denote standard sample and synthesized tetraphenylborate salts respectively, Φ is the quantum yield of PL emission, Grad is the gradient from the plot of integrated fluorescence intensity vs absorbance, and η the refractive index of solvents.

6. Detection of Basic Species from Tetraphenylborate Salts by Phenol Red

An acetonitrile solution containing tetraphenylborate salts (0.5 mL, 2×10^{-5} M) was put into a quartz cell and degassed by freeze–pump–thaw cycles; then, N_2 gas was introduced. After the solution in the quartz cell was irradiated at 254 nm in a Rayonet photoreactor, an aqueous solution of phenol red (0.5 mL, 2×10^{-5} M) was added. The UV-vis spectra of the aqueous solutions were measured.

7. Photolysis of Tetraphenylborate Salts Monitored by NMR Spectroscopy

In a quartz cell (1×1×4 cm) connected with a tube, 4 mL of tetraphenylborate salts solution (3.81×10^{-3}M in acetonitrile) was degassed by freeze–pump–thaw cycles; then, N_2 gas was introduced. The tube was cocked and the cell was irradiated in a Rayonet RPR-100 photoreactor with stirring by a magnetic stirrer. The light intensity was measured by azobenzene actinometer to be 1.702×10^{-8} Einsteins•cm^{-2}•s^{-1} at 254 nm. After

irradiation for a given time, the solvent was removed by evaporation. To the residue, 0.70 mL of DMSO-d_6 was added, and ^{1}H or ^{31}P NMR was recorded.

8. Determination of Quantum Yield for Photogeneration of TBD from TBD•HBPh$_4$

A standard actinometer (azobenzene)[33] was used for the quantum yield determination. In a quartz cell (1×1×4 cm) connected with a tube, 4 mL of TBD·HBPh$_4$ solution (3.81×10^{-3}M in acetonitrile) was degassed by freeze–pump–thaw cycles; then, N_2 gas was introduced. The tube was cocked and the cell was irradiated in a Rayonet photoreactor with stirring by a magnetic stirrer. The light intensity was determined as 1.702×10^{-8} Einsteins·cm^{-2}·s^{-1} at 254 nm. After irradiation for a given time, the solvent was removed by evaporation. To the residue, 0.70 mL of DMSO-d_6 was added, and ^{1}H NMR spectra were measured.

Generation of TBD by irradiation of TBD·HBPh$_4$ was monitored by ^{1}H NMR. The amount of free TBD was measured by calculation based on the area of peak at 3.08 ppm (shown in Figure II.13b). Based on the peak area, the degree of photogeneration of TBD was plotted as a function of the absorbed photons (Figure II.14), and the slope gave the quantum yield of photogeneration of TBD (ϕ= 0.18).

9. Kinetics of Photolysis of TBD•HBPh$_4$ Studied by UV-vis Spectroscopy

The conversion of a photodissociation of HBPh$_4$ salts can be expressed as:

$$a = (A_0 - A_t) / (A_0 - A_\infty)$$

where A_0 is the absorbance of $HBPh_4$ salts in acetonitrile without irradiation, A_t is the absorbance after irradiation for a given time and A_∞ is the absorbance of fully decomposed $HBPh_4$ salts whose absorption spectra are constant even with further irradiation. The change in absorbance at 224 nm was recorded, since the photoproducts absorb least at this wavelength. Plotting ln (1-a) against irradiation time gives a straight line, and the slope gives the rate constant of photodissociation of the corresponding $HBPh_4$ salts.

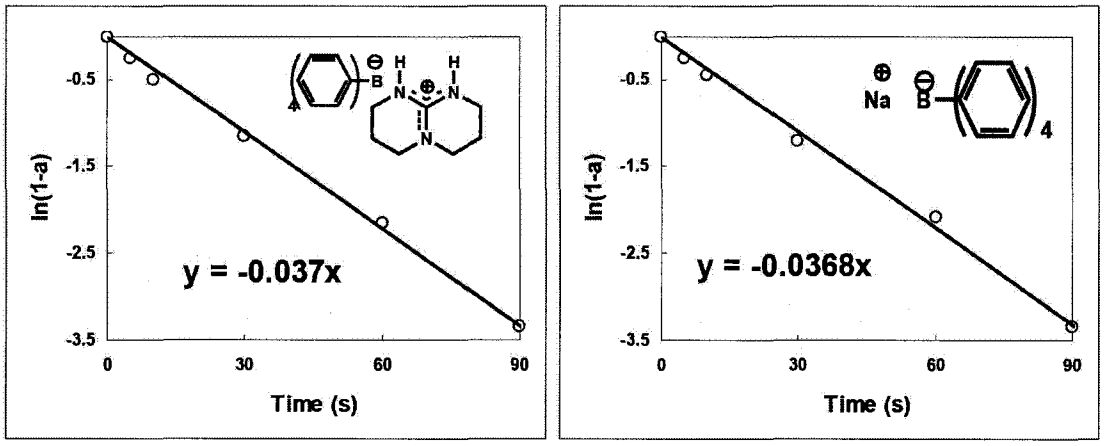

Figure II.26. ln(1-a) versus irradiation time for TBD•$HBPh_4$ and $NaBPh_4$ at 254nm in (2×10^{-5} M) acetonitrile

The tests of $HBPh_4$ salts solution in acetonitrile were done with different concentrations (1×10^5 M, 2×10^5 M, 4×10^5 M and 6×10^5 M), which gave the rate constants of photodissociation of 0.0368(±0.002) s^{-1} and 0.0370(±0.002) s^{-1} for $NaBPh_4$ and TBD•$HBPh_4$ (Figure II.26), respectively.

10. Photoinitiated Living Anionic ROP of CL using TBD·$HBPh_4$

The conversion was determined from the ratio of the α-methylene or methine

protons of the monomer to those of the polymers in ^{1}H NMR. The number-average molecular weight (M_n) was determined by end-group analysis, based on the ratio of the methyl protons of the end-group on the polymer chain, resulting form the initiator (n-hexanol), to the methylene protons within the repeat units.[34] Intrinsic viscosity was measured with an Ubbelohde viscometer in DMF at 30.0 °C. The viscosity-average molecular weight (M_v) was calculated according to the following equation: [33] $[\eta]$ (dL/g) $= 1.94 \times 10^{-4} Mv^{0.73}$.

11. Surface Modification of HEC by PMMA through Photocrosslink by TBD·HBPh$_4$

A PMMA thin film (1 μm) containing 5 mol % TBD•HBPh$_4$ was spin-coated on a HEC film (13 μm). The films were irradiated with EFOS Novacure UV light source (light intensity = 10 mW/cm^2 at 250-300 nm) in air, followed by post-baking at a given temperature in an oven. After irradiation and post-baking, the films were dipped in THF for 10 min at room temperature to remove unreacted PMMA. The surface property of the treated HEC film was evaluated by contact angle measurement using the drop shape method. Contact angle $\theta = 2 \tan^{-1}(2h/d)$, h – the height of droplet, d – the diameter of droplet.

12. Photocross-linking of P(MMA-co-HPA) and P(VP-co-HPA) using TBD·HBPh$_4$

An acetonitrile or 1-propanol solution of P(MMA-co-HPA) and P(VP-co-HPA) (Table II.8) containing TBD•HBPh$_4$ (5 mol % against the HPA unit) was cast onto a glass plate to form thin films (ca. 1.5 μm). The films were irradiated with EFOS Novacure UV

light source (light intensity = 10 mW/cm^2 at 250-300 nm) in air, followed by post-baking was at a given temperature in an oven. After irradiation or baking, the films were measured with IR spectroscopy and then dipped in THF or water for 10 min at room temperature. The insoluble fraction was determined by the ratio of the film thickness before and after dipping.

Table II.8. Physical properties of P(MMA-co-HPA) (1:1) and P(VP-co-HPA) (1:1)

Copolymers	Polymer Composition (mol %)[a]	T_g (°C)[b]	T_d (°C)[c]	M_n[d]	PDI[d]
P(MMA-co-HPA) (1:1)	MMA : HPA 56.1 : 43.9	57.9	327.6	24100	1.88
P(VP-co-HPA) (1:1)	VP : HPA 47.2 : 53.8	62.8	300.9	21623	1.58

[a] Calculated with NMR, [b] DSC, 10 °C/min under a nitrogen atmosphere, [c] TGA, 10 °C/min under a nitrogen atmosphere, [d] GPC, in $CHCl_3$.

II.6 References

1. Williams, J. L. R.; Doty, J. C.; Grisdale, P. J.; Searle, R.; Regan, T. H.; Happ, G. P.; Maier, D. P. *J. Am. Chem. Soc.* **1967**, *89*, 5153.

2. Williams, J. L. R.; Doty, J. C.; Grisdale, P. J.; Regan, T. H.; Happ, G. P.; Maier, D. P. *J. Am. Chem. Soc.* **1968**, *90*, 53.

3. Wilkey, J. D.; Schuster, G. B. *J. Org. Chem.* **1987**, *52*, 2117.

4. Room, E.; Kiitt, A.; Kaljurand, I.; Koppel, I.; Leito, I.; Koppel, I. A.; Mishima, M.; Goto, K.; Miyahara, Y. *Chem. Eur. J.* **2007**, *13*, 7631.

5. Kaljurand, I.; Kuett, A.; Soovaeli, L.; Rodima, T.; Maeemets, V.; Leito, I. *J. Org. Chem.* **2005**, *70*, 1019.

6. Rodima,T.; Kaljurand, I.; Pihl, A.; Maemets, V.; Leito, I.; Koppel, I. A. *J. Org. Chem.* **2002**, *67*, 1873.

7. Meisters, M.; Vandeberg, J.T.; Moore, C.E. *Anal. Chim. Acta.* **1970**, *49*, 481.

8. Copper, J.N.; Powbll, R.E. *J. Am. Chem. Soc.* **1963**, *85*, 1590.

9. Kiviniemi, S.; Nissinen, M.; Alaviuhkola, T.; Rissanen K.; Pursiainen, J. *J. Chem. Soc., Perkin Trans.* **2001**, 2, 2364.

10. Lindeman, S. V.; Kosynkin, D.; Kochi, J. K. *J. Am. Chem. Soc.* **1998**, *120*, 13268.

11. Chatterjee, S.; Davis, P. D.; Gottschalk, P.; Kurz, M. E.; Sauerwein, B.; Yang, X.; Schuster, G. B. *J. Am. Chem. Soc.* **1990**, *112*, 6329.

12. McCosar, B. H.; Schanze, K. S. *Inorg. Chem.* **1996**, *35*, 6800.

13. Lide, D. R., *CRC Handbook of Chemistry and Physics, 88th Edition.* **2007**

14. Aoai, T.; Kodama, K.; Yamanaka, T.; Yagihara, M. *J. Photopolym. Sci. Technol.* **1998**, *11*, 409.

15. Williams, A. T. R.; Winfield, S. A.; Miller, J. N. *Analyst*, **1983**, *108*, 1067.

16. Demas, J. N.; Crosby, G. A. *J. Phys. Chem.* **1971**, *75*, 991.

17. Eastman, J. W. *J. Chem. Phys.* **1968**, *49*, 4617.

18. Dawson, W. R.; Windsor, M. W. *J. Phy. Chem.* **1968**, *72*, 3251.

19. Tachi, H.; Yamamoto, T.; Shirai, M.; Tsunooka, M. *J. Poly. Sci., Part A: Poly. Chem.* **2001**, *39*, 1329.

20. Mejiritski, A.; Sarker, A. M.; Wheaton, B.; Neckers D. C. *Chem. Mater.* **1997**, *9*, 1488.

21. Sonnenschein, M. F.; Webb, S. P.; Redwine, O. D.; Wendt, B. L. *Macromolecules* **2006**, *39*, 2507.

22. Johnson, J. R.; Snyder, H. R.; Van Campen, M. G. *J. Am. Chem. Soc.* **1938**, *60*, 115.

23. Shirai M.; Tsunooka M. *Prog. Polym. Sci.* **1996**, *21*, 1.

24. Ito, H. Deep-UV Resist Systems. In: *Radiation Curing in Polymer Science and Technology-Vol.4: Practical Aspects and Applications*; Fouassier, J. P., Rabek, J. F., Eds.; Elsevier Applied Science Publishers: London, **1993**; pp 237-360.

25. Zhang, L.; Nederberg, F.; Pratt, R. C.; Waymouth, R. M.; Hedrick, J. L.; Wade, C. G. *Macromolecules* **2007**, *40*, 4154.

26. Schuchardt, U.; Vargas, R.M.; Gelbard, G. *J. Mol. Catal. A: Chemical* **1995**, *99*, 65.

27. Kantam, M. L.; Sreekanth, P. *Catal. Lett.* **2001**, *77*, 241.

28. Jenekhe, S. A.; Zhang, X. J.; Chen, X. L.; Choong, V. E.; Gao, Y. L.; Hsieh, B. R. *Chem. Mater.* **1997**, *9*, 409.

29. Tarkka, R. M.; Zhang, X. J.; Jenekhe, S. A. *J. Am. Chem. Soc.* **1996**, *118*, 9438.

30. Croce, F.; Appetecchi, G. B.; Persi, L.; Scrosati, B. *Nature* **1998**, *394*, 456.

31. Xanthos, M. *Polym. Eng. Sci.* **1988**, *28*, 1392.

32. Koning, C.; Pagnoulle, C.; Jerome, R. *Prog. Polym. Sci.* **1998**, *23*, 707.

33. Brode, G. L.; Koleske, J. V. *J. Macromol. Sci., Chem.* **1972**, *6*, 1109.

34. Ling, J.; Zhu, W.; Shen, Z. *Macromolecules* **2004**, *37*, 758.

CHAPTER III

INTRODUCTION TO THERMODEGRADABLE POLYMERS

As shown in Chapter II, successful photogeneration of a strong nitrogen base of TBD triggers a number of new applications in radiation curing, such as photoinduced ROP of cyclic esters and photo-cross-linking via transesterification. TBD is also able to amplify thermodegradation of polycarbonates.[1] Therefore, the following chapters of this thesis describe the studies on the structure-performance relationship of thermodegradable polycarbonates and the amplification effect of bases for the development of PC-based photoimageable sacrificial materials and dry-developing photoresists.

III.1 Brief Description of Thermodegradable Polymers

III.1.1 Definition of TD-polymers

Thermodegradable polymers (TD-polymers) refer to a class of polymeric materials that are able to completely degrade into volatile compounds upon heating in an inert atmosphere under standard atmospheric pressure. In other words, these polymers are decomposed solely by heating.

A key feature of TD-polymers is no or very low residue upon thermolysis. TD-polymers are widely used as sacrificial materials to temporarily add plastic properties or hold a shape or volume in processing, such as fabrication of the shaped parts from ceramic or metal powders and formation of air-cavities in encapsulants.[2]

III.1.2 Typical Examples of TD-polymers

Some vinyl polymers, such as poly(methyl methacrylate) and polystyrene, aliphatic polyesters and aliphatic polycarbonates all belong to the family of TD-polymers.[3, 4] These polymers are thermodegradable because: (1) they undergo nearly complete degradation at temperatures in a range of 220-600 °C, and (2) all degradation products are sufficiently volatile and can be completely evaporated off. Most of other polymers (e.g., nylons and polysulfone) only undergo a partial and complex degradation at elevated temperatures. The degradation products are usually non-volatile and char-like materials when being heated up to ~650-700 °C. The char-like materials can remain even at ~1000 °C. Therefore, both the degradation mechanism and the volatility of degradation products play an important role in thermal degradation of TD-polymers.

TD-polymers are typically composed of aliphatic chains. The reason is that aliphatic compounds (e.g., alkenes and alcohols) have much higher vapor pressure and weaker C-H and C-C bond energies than aromatic compounds. One typical example is poly(propylene carbonate) (PPC). It can be completely decomposed to cyclic carbonates, diols, dienes and carbon dioxide at approximately 350 °C in nitrogen (Scheme III.1).[5, 6] The thermogravimetry analysis (TGA) trace of PPC, which records the weight loss upon heating, is shown in Figure III.1.[7] The ash content (residue mass, M_{res}) of PPC is 0.9 wt.% at 353 °C, indicating that the polymer is completely degraded and removed by heating. The minimum temperature required to cleanly degrade a polymer in an inert atmosphere is defined as the clean-burn-off temperature ($T_{burn\text{-}off}$).

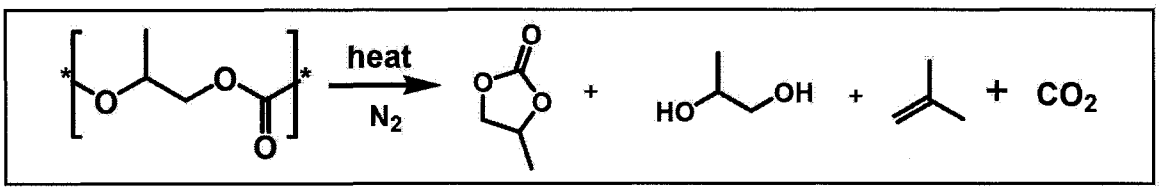

Scheme III.1. Thermal degradation reaction of poly(propylene carbonate)

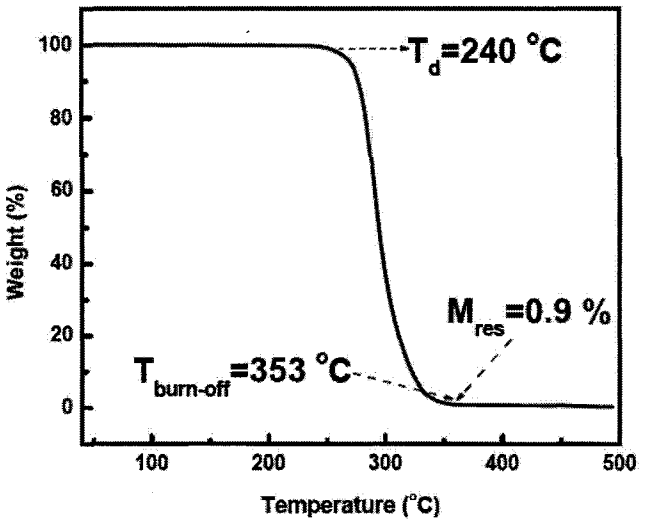

Figure III.1. TGA trace of poly(propylene carbonate) (M_n ~50,000 by GPC, available from Aldrich) in nitrogen with a heating rate of 10 °C/min

Thus, $T_{burn-off}$ is 353 °C for PPC (with a heating rate of 10 °C/min). It should be noted that experimental conditions such as atmosphere and heating rate should be given, since the $T_{burn-off}$ value is dependent on these conditions. A lower heating rate tends to give a lower $T_{burn-off}$ value.

In comparison with aliphatic polymers, only very few aromatic polymers are thermodegradable.[8] Polystyrene (PS) contains a pendent benzene ring and has an aliphatic backbone. PS can be cleanly burned off at ~450 °C (Figure III.2)[9] because it basically depolymerizes thermally in a single step to yield styrene as a principle product, along with small amounts of benzene and toluene (Scheme III.2).[10]

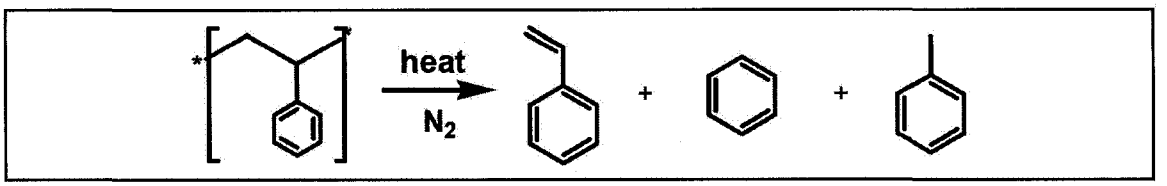

Scheme III.2. Thermal degradation reaction of polystyrene

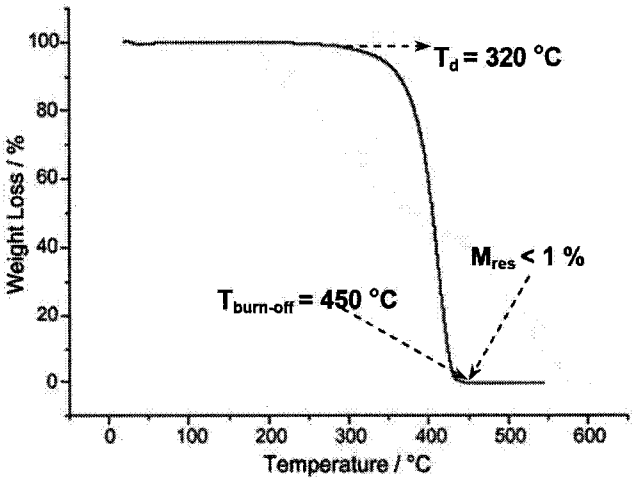

Figure III.2. TGA trace of polystyrene (commercial product from Aldrich, M_w 35,000) in nitrogen with a heating rate of 10 °C/min

III.1.3 Thermal Degradation Reactions in TD-polymers

Thermal degradation of TD-polymers is basically depolymerisation, which may start at the chain ends or randomly cleave in the main chain. Depolymerization is characterized by breaking the polymer backbone or "unzipping" the polymer main chain and yielding the starting monomer(s). For example, PMMA is depolymerized at 450 °C to yield methyl methacrylate (Scheme III.3).

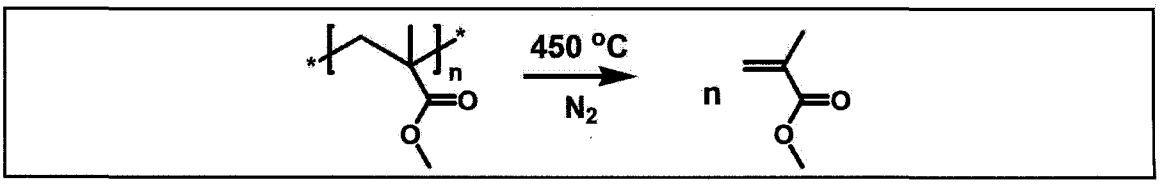

Scheme III.3. Thermally induced depolymerization of PMMA

III.1.4 Characteristics of TD-polymers

The TD-polymers have several characteristics that distinguish them from conventional polymeric materials.

- Ash content (residue mass, M_{res})

The ash content refers to the amount of non-volatile residue left after thermolysis of a polymer. To be a TD-polymer suitable for most of known processing applications, the M_{res} value should be lower than 1 wt.%. Besides the nature of polymer, the M_{res} value is also dependent on the purity of polymer, since any residual initiators, catalysts or additives can be charred at elevated temperatures. TD-polymers with zero M_{res} are desirable for many practical applications.

- Onset degradation temperature (T_d)

T_d refers to the onset temperature at which a polymer loses 5% of its original weight upon heating. It is also a measure for the onset degradation. Above the T_d, the polymer begins to degrade rapidly and release volatile materials and also begins to lose its elasticity and film-forming ability. Thus, T_d is the upper limit of processing temperature for TD-polymers. The T_d values can vary dramatically, such as 190 °C for polypropiolactone and 500 °C for polyethylene.[10]

- Clean-burn-off temperature ($T_{burn\text{-}off}$)

The minimum temperature required to cleanly degrade a polymer (weight loss ≥ 99%) in an inert atmosphere is defined as the clean-burn-off temperature ($T_{burn\text{-}off}$). There are two major factors governing $T_{burn\text{-}off}$. One is the polymer structure and another is

volatility of thermolysis by-products. The lowest $T_{burn\text{-}off}$ for all the known TD-polymers is 220 °C for poly(2,5-dimethyl-2,5-hexylene carbonate), with a heating rate at 10 °C/min in nitrogen.[7] In comparison, polyethylene has a $T_{burn\text{-}off}$ of 600 °C.[8] PMMA and PS undergo the similar depolymerization reaction. However, PMMA has a lower $T_{burn\text{-}off}$ than PS (~400 °C vs. ~450 °C) because methyl methacrylate has a lower boiling point (100 °C) than styrene (145 °C).

$T_{burn\text{-}off}$ may determine applications of TD-polymers. TD-polymers that can be burned off at a relatively lower temperature are desirable for making metal conductors or forming air-cavities on common substrates (e.g., low grade float glass).[11,12] TD-polymers with a high $T_{burn\text{-}off}$ are used as binders in the powder injection molding of ceramic or metal parts that are to be sintered at 700-900 °C. The polymer binders are required to hold the parts in shape during the sintering process.[13,14]

III.1.5 TD-polymers as Sacrificial Materials

TD-polymers have been used as sacrificial plastic binders in the manufacturing and electronics industry since the early 1970s, such as binders in powder injection molding and photoimageable silver conductor paste.[15,16,17] The main function is to impart sufficient strength and add elastic properties to ceramic powders or metal nano-particles during the shape or image-forming stage. Afterwards, the binders can be completely removed by thermolysis. To prevent the oxidation of metal nano-particles, the de-binding process is required to proceed under an inert atmosphere. The shaped ceramic and metal

products are obtained after sintering at temperature several hundred degrees lower than the melting point and possess the same mechanical and electronic properties as those made by the metal founding process. Thus, the manufacturing process using TD-polymers as binders is cost-effective and energy-saving in comparison with other traditional methods.

TD-polymers are also used as sacrificial templates or "place-holders" to form air-cavities buried in a variety of encapsulants. This approach is well accepted in the fabrication of microfluidic devices, microelectromechanical systems (MEMS), porous inorganic network, such as porous titanium dioxide in dye sensitized solar cell, and electrical interconnects (low dielectric constant).[18,19,20] During the process, TD-polymers, or so-called "place-holders", are patterned into a desired shape, encapsulated with a second material, and then decomposed upon heating, giving rise to a hollow cavity with no residue. This approach is much more versatile than the soft lithography process based on silicon rubber (polydimethylsiloxane, PDMS),[21] as it allows for the formation of structured air-cavities in any thermally stable materials, such as polyimides, epoxy resins and glass.

III.2 Types of Thermodegradable Polymers

III.2.1 Vinyl Polymers

As early as 1930s, several important vinyl polymers, notably PMMA, PS and PE, were reported to readily depolymerize by heating, leading to the recovery of a substantial

proportion of the original monomers or other low molecular weight products.[23,24,25] All of them can be cleanly removed through thermolysis at 450-600 °C in nitrogen (Table III.1).

The thermal degradation of these vinyl polymers follows a three-step radical reaction mechanism (Scheme III.4),[10] in which n is the chain length of the starting material and M_i, M_j, etc. and $M_i^\bullet$, $M_j^\bullet$, etc. represent respectively degraded polymer molecules and long chain radicals, i, j, etc. monomer units in length.

Table III.1. Thermal degradation properties of PMMA, PS and PE

TD-polymers	Source	Molecular Weight (M_w)	M_{res} (wt.%)	T_d (°C)	$T_{burn-off}$ (°C)
PMMA [a]	Aldrich	~120,000	< 1.0	370	445
PMMA [a]	Aldrich	~350,000	< 1.0	387	462
PS [a]	Aldrich	~35,000	< 1.0	377	451
PS [b]	Polystyrene BASF 473D	-	< 1.0	389	477
PE [b]	LDPE Dow 780R	-	< 1.0	437	517

[a] *Data obtained from a TA Hi-Res TGA 2950 with a heating rate at 10 °C/min in nitrogen;*
[b] *Data from reference [22].*

(1) Initiation	Random Initiation	$M_n \rightarrow M_j^\bullet + M_{n-j}^\bullet$
	Terminal Initiation	$M_n \rightarrow M_{n-1}^\bullet + M^\bullet$
(2) Depropagation	Unzipping Scission	$M_j^\bullet \rightarrow M_{j-1}^\bullet + M$
	Intramolecular Transfer and Unbuttoning Scission	$M_j^\bullet \rightarrow M_{j-z}^\bullet + M_z$
(3) Termination		$M_i^\bullet + M_j^\bullet \rightarrow M_i + M_j$ or M_{I+j}

Scheme III.4. Three-step radical depolymerization reaction mechanism of thermodegradable vinyl polymers

Poly(methyl methacrylate)

The depolymerization reaction of PMMA yields monomer in quantitative yield.[26,27,28,29] In the initiation stage of depolymerization, the random scission of the polymer along its backbone forms radicals. The generated radicals then depropagate through the unzipping scission which is the exact reverse of the propagation process in polymerization reaction (Scheme III.5). Since the radicals are stabilized on the tertiary carbon atoms by the carboxyl groups, the intramolecular radical transfer reaction of radicals is completely suppressed. It makes the whole depolymerization reaction quite simple.

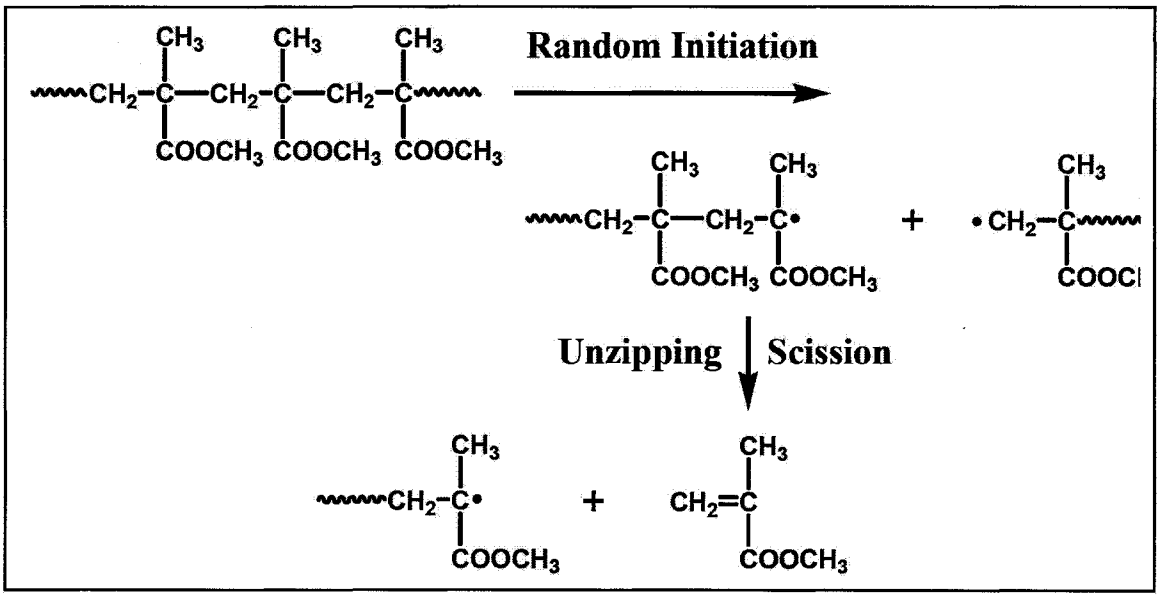

Scheme III.5. The unzipping reaction in thermal degradation of PMMA

Polystyrene

The depolymerization of polystyrene proceeds in the similar mechanism as for PMMA, except that the intramolecular radical transfer reaction competes strongly with

the unzipping scission.[30,31,32,33] Thermal analysis shows that styrene is the major degradation product (approximately 40%), together with small amounts of benzene and toluene. In addition, there is also a large fraction that consists of the decreasing amounts of dimer, trimer, tetramer and pentamer of styrene. These oligomers are formed as a result of the intramolecular radical transfer reactions (Scheme III.6), which are in direct competition with the monomer-producing process. By analogy with the description of depolymerization as unzipping, these radical transfer reactions have described as "unbuttoning".

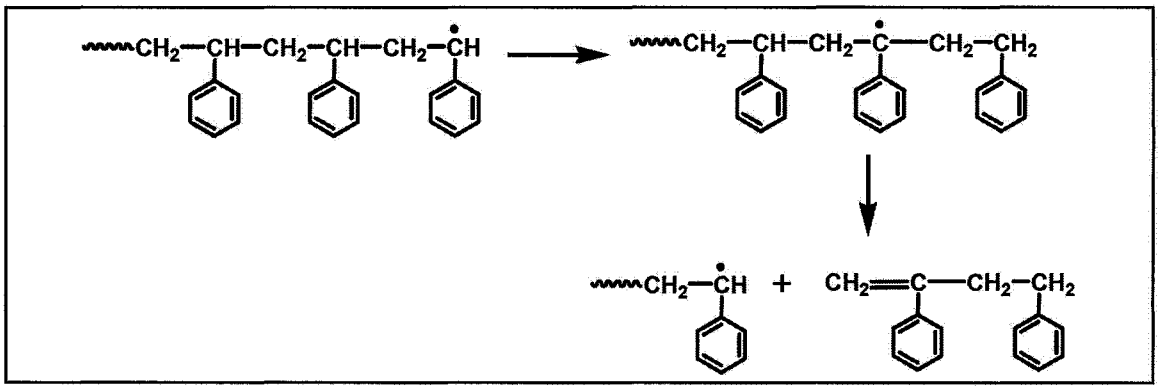

Scheme III.6. Intramolecular radical transfer reaction in thermal degradation of PS

Comparison of the monomer yields from the polymers derived from styrene, α- and β-deuterostyrenes and α-methyl styrene (Table III.2) clearly indicates that it is the α hydrogen atom that is involved in the radical transfer process. Replacement of the α hydrogen atom by deuterium has a strong suppressant effect on the transfer reaction, while the presence of the methyl group at the α position completely eliminates the transfer process. In contrast, the deuteration at the β position or methylation on the benzene ring has no significant effect.

Table III.2. Monomer yields from thermal degradation of vinyl polymers [10]

Polymer	Monomer (%)
Poly(methyl methacrylate)	100
Polystyrene	42
Poly(α-deuterostyrene)	70
Poly(β-deuterostyrene)	42
Poly(α-methyl styrene)	100
Poly(β-methyl styrene)	52
Polyethylene	<1
Poly(methyl acrylate)	Trace

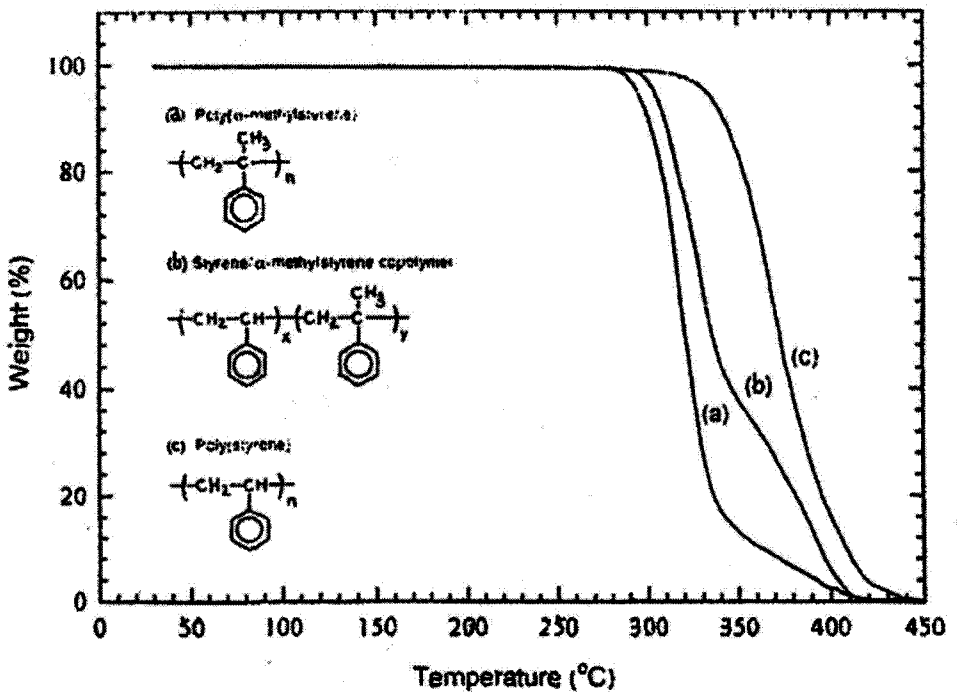

Figure III.3. TGA traces of polystyrene, poly(α-methyl styrene) and copolymer[10]

Since this α-hydrogen involved radical transfer process happened in thermal degradation of polystyrene produces the less volatile oligomers, the clean-burn-off temperature of polystyrene is higher than poly(α-methyl styrene) (Figure III.3).[10]

Polyethylene

The depolymerization of polyethylene is even more complex than that of polystyrene.[34-38] The radicals generated in the initiation stage are much less stable and tend to migrate. Thus, in the depropagation stage, the unzipping reaction has little significance. Only a trace amount of monomer is produced (Table III.2). A large proportion of mono-olefins are formed through the intramolecular radical transfer process.

Thermal analysis shows that the volatile products from degradation of polyethylene consist of an apparently continuous spectrum of hydrocarbons with 1-30 carbon atoms.[10] Of all the volatile products, propene and 1-hexene are the most abundant and this is undoubtedly because of the fact that reaction of a radical with a hydrogen atom on the fifth carbon atom should be geometrically very favourable since the transition state is a six membered ring (Scheme III.7). Since mono-olefins with more than 20 carbon atoms are low-volatile compounds, polyethylene can only be degraded completely at higher temperatures than polystyrene and PMMA (Table III.1).

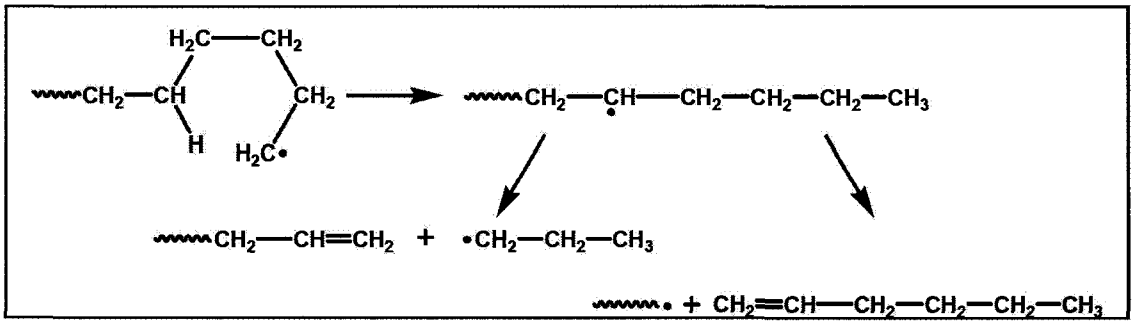

Scheme III.7. Intramolecular radical transfer reaction in thermal degradation of polyethylene

For vinyl polymers, the clean-burn-off temperature is found to increase in an order of PMMA > polystyrene > polyethylene. In general, a vinyl polymer with substituents on the α-carbon tends to undergo a relatively simple depolymerization reaction and thus has a lower clean-burn-off temperature.

III.2.2 Aliphatic Polyesters

Aliphatic polyester is another important class of TD-polymers. In 1932, Carothers et al. first noticed that polyesters formed by ring-opening polymerization of six-membered cyclic compounds undergo a complete depolymerization to yield the cyclic starting material at elevated temperatures.[39] Later on, aliphatic polyesters with less than five carbon atoms in the repeat unit were reported to be able to cleanly burned out in an inert atmosphere.[40,41] In contrast to vinyl polymers, polyesters are much more labile to thermal degradation. The clean-burn-off temperatures of thermodegradable polyesters (TD-polyesters) are in the range of 350-500 °C, being 50 °C lower on average than those of vinyl polymers.

Intramolecular ester exchange and β–hydrogen transfer are the two processes mainly responsible for thermal degradation of TD-polyesters.[42] However, degradation reactions are different according to the ring size of the monomer lactones, α-, β-, γ-, δ- or ε-polylactones.

Polyglycolide

Polyglycolide, the unsubstituted α-polylactone, is depolymerized upon heating into a

six-membered cyclic dimer through the intramolecular ester exchange.[40] The resulting cyclic dimer, glycolide, is further decomposed to highly volatile small molecules, including carbon dioxide, formaldehyde and ketenes (Scheme III.8).

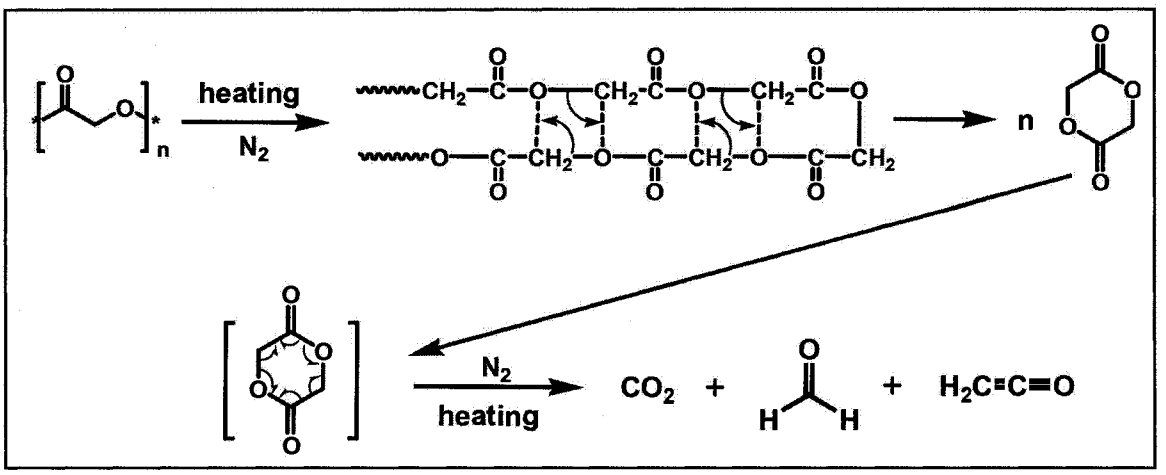

Scheme III.8. Intramolecular ester exchange process in thermal degradation of polyglycolide

Poly(lactic acid)

The alkyl substituted α-polylactones, notably poly(lactic acid), when heated, also yield cyclic dimers by intramolecular ester exchange.[43,44,45] But this process is accompanied by a β-hydrogen transfer which leads to formation of acrylic acid (Scheme III.9).

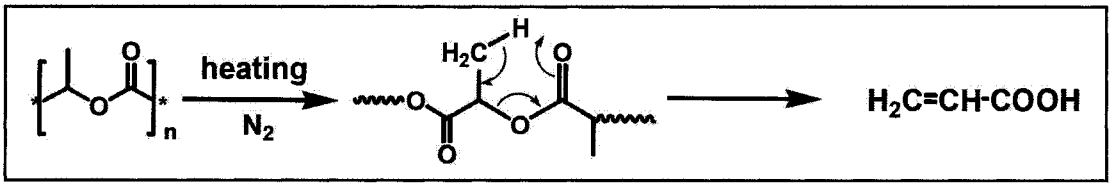

Scheme III.9. β-Hydrogen transfer process in thermal degradation of polylactide

Polypropiolactone

The thermal degradation of polypropiolactone, which is the unsubstituted

β-polylactone, mainly involves the β-hydrogen transfer process. Acrylic acid is the main thermolysis product (Scheme III.10).[46,47] The intramolecular ester exchange process is suppressed in thermal degradation because the cyclic compounds formed via intramolecular ester exchange are eight membered rings, which are quite unstable.

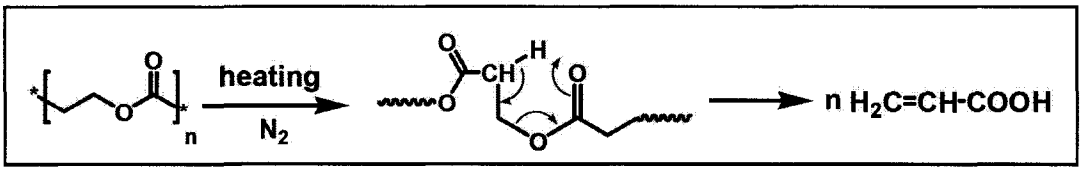

Scheme III.10. Thermal degradation of polypropiolactone

Poly(δ-valerolactone) and Poly(ε-caprolactone)

The intramolecular ester exchange process prevails again in thermal degradation of poly(δ-valerolactone) and poly(ε-caprolactone), which give quantitative yields of the six and seven-membered δ-valerolactone and ε-caprolactone respectively, as the principal thermolysis products (Scheme III.11).[48,49]

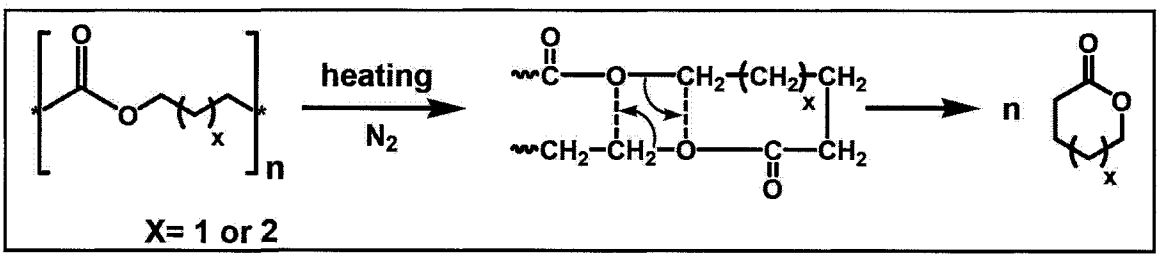

Scheme III.11. Thermal degradation of poly(δ-valerolactone) and poly(ε-caprolactone)

By comparing the degradation temperatures of TD-polyesters (Table III.3), it is obvious that a polyester containing a β-hydrogen favours the hydrogen transfer process, is able to fully degrade in the primary step of thermal degradation, and thus has a lower clean-burn-off temperature.

Table III.3. Thermal properties of thermodegradable polyesters

TD-polymer	Mechanism	Thermolysis Product: Product in Primary Step	Thermolysis Product: Final Product	M_{res} (wt.%)	T_d (°C)	$T_{burn-off}$ (°C)
-[CO-$(CH_2)_2$-O]$_n$-[a]	β-CH transfer	Acrylic acid	Acrylic acid	< 1.0	190	280
-[CO-CCH_3-O]$_n$-[b]	β-CH transfer plus Ester exchange	Acrylic acid, Lactide	Acrylic acid, CO_2, HCOH, Methylket-enes	< 1.0	290	380
-[CO-CH_2-O]$_n$-[c]	Ester exchange	Glycolide	CO_2, HCOH, Ketenes	< 1.0	300	430
-[CO-$(CH_2)_4$-O]$_n$-[a]	Ester exchange	Valerolact-one	Valerolact-one	< 1.0	389	427
-[CO-$(CH_2)_5$-O]$_n$-[a]	Ester exchange	Caprolact-one	Caprolact-one	< 1.0	415	470

[a] *Data from reference [42].* [b] *Data from reference [50].* [c] *Data from reference [51]*

III.2.3 Aliphatic Polycarbonates

Aliphatic polycarbonates with less than ten carbon atoms in each repeat unit can also be completely degraded upon heating.[42] Their clean-burn-off features were first discovered by Dixion et al. in 1980.[52] As the new generation of TD-polymers, thermodegradable polycarbonates (TD-polycarbonates) have several advantages over traditional thermodegradable polymers.[53,54,55] (1) TD-polycarbonates undergo complete degradation in the range of 200-400 °C, which is nearly 100 °C lower than vinyl

polymers and polyesters. The low burn-off temperatures allow for TD-polycarbonates being used as sacrificial materials in the conventional material processing at relatively low temperatures (200-250 °C). Thus, a wider range of substrates and structural materials can be selected and used. (2) Olefins, carbon dioxide, and alcohols are major degradation products from the thermolysis of TD-polycarbonates. In comparison, TD-polyesters, notably poly(lactic acid), generate acrylic acid and lactic acid that are more acidic than acetic acid ($^{water}pK_a$: 4.35, 3.85 vs. 4.76). Thus, TD-polycarbonates are more suitable for applications in the acid-sensitive systems. (3) While traditional TD-polymers are petroleum based products, some important TD-polycarbonates, such as poly(propylene carbonate) and poly(ethylene carbonate), are derived from carbon dioxide and epoxides.

Except for poly(ethylene carbonate) and poly(propylene carbonate), other TD-polycarbonates are still not commercially available. The thermal degradation of TD-polycarbonates undergoes two different mechanisms.[42,56] One is "back-biting" initiated by the reactive hydroxy end-groups via intramolecular ester exchange. This "back-biting" mechanism always involves a cyclic intermediate and repeatedly releases five or six-membered cyclic carbonates from the chain ends. The other mechanism is a "random main chain scission" by the thermolytic cleavage of carbon-oxygen bonds. Unsaturated fragments, CO_2 and alcohols are generated as primary thermolysis products through the "random main chain scission" process. The formation of stable five-membered rings in the "back-biting" process requires a lower activation energy than

the carbon-oxygen bond cleavage in the "random main chain scission".

Poly(ethylene carbonate) (PEC) and Poly(propylene carbonate) (PPC)

PEC and PPC are prepared by copolymerization of CO_2 with epoxides and undergo thermal degradation by the "back-biting" mechanism (Scheme III.12).[56,57]

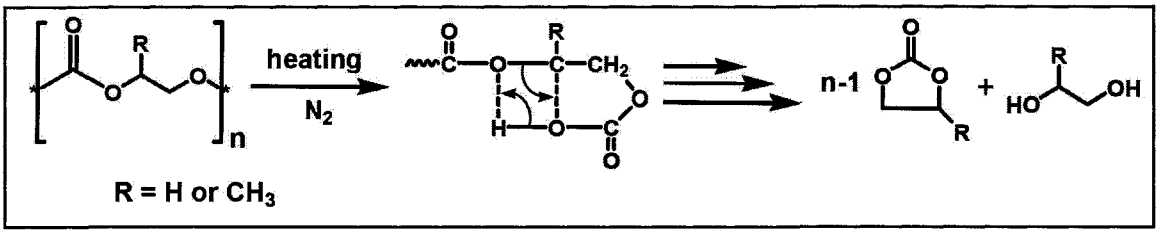

Scheme III.12. Thermal degradation of PEC and PPC via a "back-biting" process

However, PEC and PPC with capped end-groups and high molecular weights mainly exhibit the "random main chain scission" mechanism (Scheme III.13). The "back-biting" process is suppressed since the hydroxy end-groups, the necessary functional groups to initiate "back-biting", are not accessible.

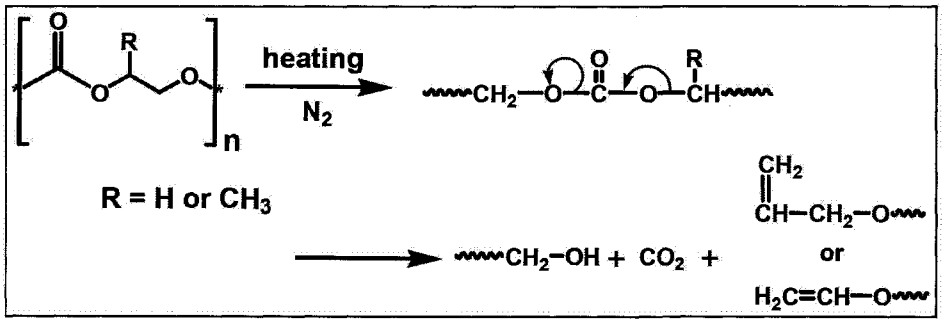

Scheme III.13. Thermal degradation of the end-capped PEC and PPC via a "random main chain scission" process

Poly(1,4-butylene carbonate) (PBC), Poly(2,5-hexylene carbonate) (PHC) and Poly(2,5-dimethyl-2,5-hexylene carbonate) (PDHC)

Thermal degradation of PBC, PHC and PDHC mainly involve the "random main

chain scission" process.[54, 58] Thermolytic cleavage is known to proceed via a β-hydrogen elimination process (Scheme III.14), in which the C_α-O bond dissociates before the C_β-H bond does and a carbocation character at the C_α position is being developed in the transition state. The presence of alkyl groups on the α carbon can stabilize the positive charge in the transition state, thus substantially lowers the activation energy and increases the rates of thermal degradation. Therefore, PDHC is able to be burned off at a lower temperature than PHC and PBC (Figure III.4).

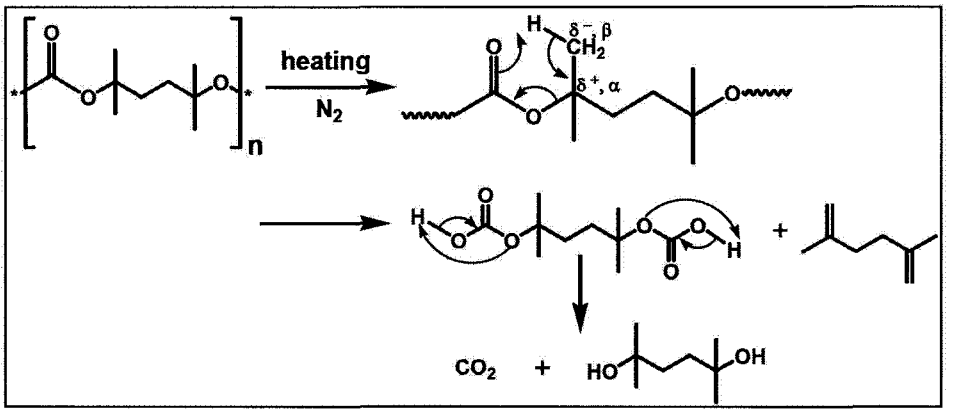

Scheme III.14. Thermal degradation of PDHC

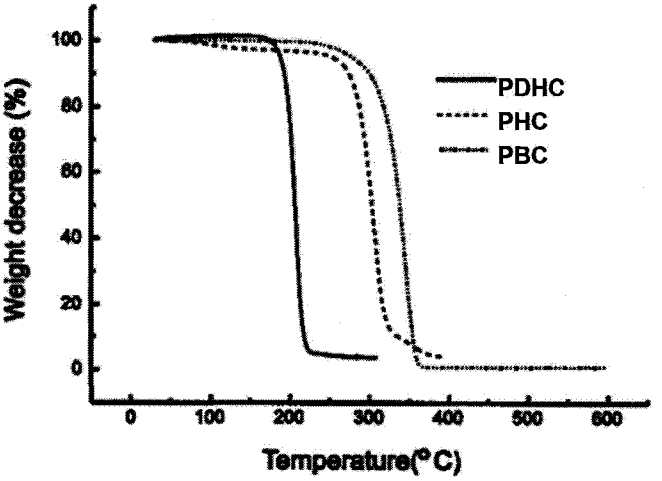

Figure III.4. TGA traces of PBC, PHC and PDHC

Poly(1,4-cyclo-hexylene carbonate) (PCHC)

Thermal degradation of PCHC only goes through the "random main chain scission" mechanism.[59] The "back-biting" process is fully suppressed as the 1,4-cyclo-hexane moiety is quite bulky and does not permit the formation of cyclic carbonates. Cyclohexene, CO_2 and cyclohexane-1,4-diol are final thermolysis products from PCHC (Scheme III.15).

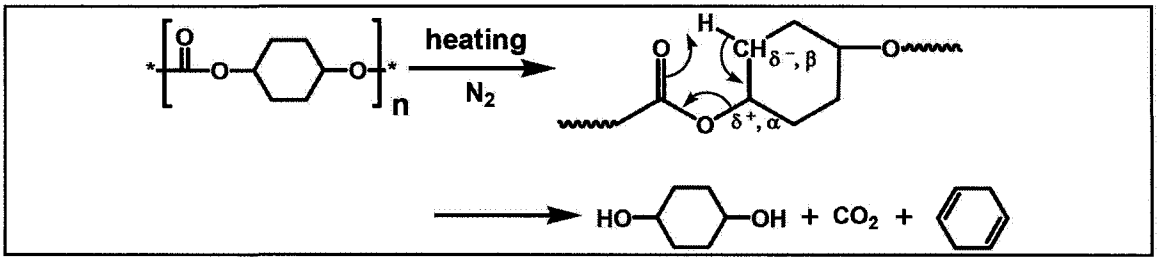

Scheme III.15. Thermal degradation reaction of PCHC

The thermal properties of TD-polycarbonates are summarized in Table III.4. It can be seen that a polycarbonate containing the electron-donating groups on the α carbon, which can stabilize the carbocation in the transition state, has lower activation energy for thermal degradation, and thus possesses a lower clean-burn-off temperature. The chain rigidity also affects the chain motion or the glass transition temperature, which in turn affects the activation energy or the clean-burn-off temperature. For example, more rigid PCHC undergoes the same degradation mechanism as more flexible PHC but degrades at a higher temperature.

Table III.4. Thermal properties of thermodegradable polycarbonates

TD-polycarbonates		Activation Energy (kJ/mol)	M_{res} (wt.%)	T_d (°C)	$T_{burn-off}$ (°C)
Primary Polycarbonate	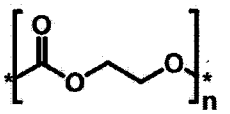 PEC	152 [a]	< 1.0	220	350
	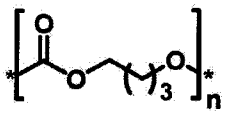 PBC	175 [b]	< 1.0	340	380
	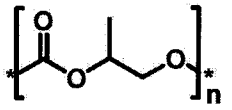 PPC	163 [a]	< 1.0	240	360
Secondary Polycarbonate	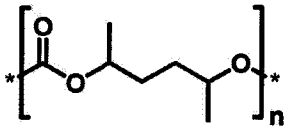 PHC	162 [b]	< 1.0	300	370
	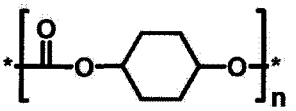 PCHC	-	< 1.0	340 [c]	384 [c]
Tertiary Polycarbonate	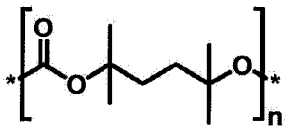 PDHC	136 [b]	< 1.0	190	220

[a] *Data from reference [7], PPC and PEC are products from Empower Materials Inc.*
[b] *Data from reference [54].* [c] *Data from reference [59].*

III.3 Application of Thermodegradable Polymers

For decades, the thermodegradable property of TD-polymers is only regarded as a

drawback in many applications. It was not until the end 1970s that TD-polymers were first applied as sacrificial binders in powder injection molding of inorganic solid parts.[60,61] Nowadays, thermally labile polymers, whose properties change drastically when exposed to heat, are of great interest in numerous applications as binders, templates, degradable cross-linking agents, recyclable thermosets, self-imaging resists, etc.

III.3.1 Sacrificial Binder in Powder Injection Molding

The powder injection molding (PIM) is a standard process for the high volume production of shaped parts (e.g., automobile parts and telecommunication devices) from fine metal or ceramic powders. Its market reached a worldwide turnover of € 800 million in 2000[4] and still keeps growing each year.

In the PIM process, TD-polymers are applied as a sacrificially plastic binder, which provides the metal or ceramic powder with the flowability and formability necessary for molding. The assistance of binders allows metals to be injected into a mold using standard plastic injection molding machines. After removal of the binder, followed by sintering of the resultant metal part at temperatures much lower than the melting point of metal, the product of metal injection molding is obtained and is normally up to 98% as dense as wrought iron (Figure III.5).[4, 62]

In a traditional founding process, metal objects are produced in the form of castings after molten metal is spread into a mold. Thus, by using TD-polymers as sacrificial binders the PIM process is obviously much more cost efficient and energy saving.

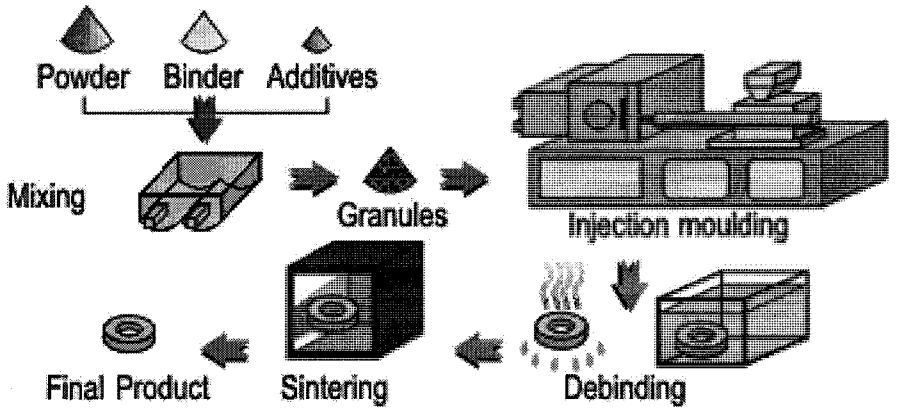

Figure III.5. Schematic illustration of the powder injection molding process

III.3.2 Sacrificial Vehicles in Photoimageable Conductor Paste

The microelectronic industry is undergoing rapid expansion and miniaturization, demanding for semiconductor integrated circuit devises which are increasingly smaller, faster and of high density.[63,64] DuPont introduced a photoimageable Ag conductor paste (DuPont Fodel®) two decades ago, for fabrication of silver electrodes in flat panel displays by a photopatterning process.[65] In 2008, DuPont upgraded the Fodel® paste to its eighth generation and extends its application in the metallization of plasma display panel (PDP) front bus electrodes for large format, full high definition televisions.

In the Fodel® paste, 30 wt.% component is a TD-polymer as a sacrificial organic vehicle for dispersion of the finely divided silver particles.[66] During the photopatterning process (Figure III.6), the entire substrate is first covered (printed, sprayed, coated or laminated) with the photoimageable paste. An image of the pattern is generated by exposure of the paste with UV radiation through a photomask. The irradiated substrate is then developed in aqueous base solution (e.g., 0.4-2.0% sodium carbonate solution). The

unexposed part is washed away. The remaining photo-patterned silver paste on the substrate is then heated in an inert atmosphere to remove organic vehicles and sinter sliver particles. A line resolution of about 50 microns can be obtained, depending on the substrate smoothness, silver particle size distribution, and exposure and development variables.

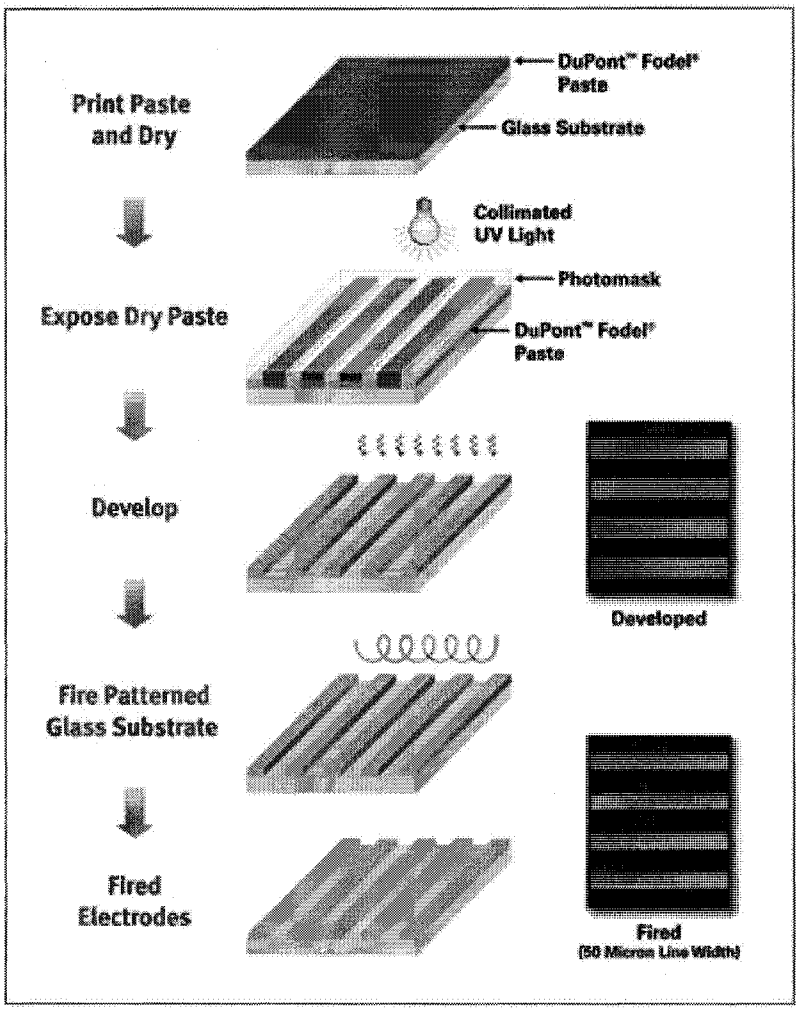

Figure III.6. Photo-patterning process of DuPont Fodel® Ag conductor paste

In contrast to chemical vapor deposition or other physical vapor deposition methods (e.g., sputtering, molecular-beam epitaxy), the DuPont Fodel® technology allows for

fabrication of the fine lines of silver conductor with a good space resolution without a need for high vacuum systems and is more suitable for fabrication of large-size devices in high-volume production.

III.3.3 Acid-Catalyzed TD-Polymers in Dry-Developing Photoresists

Photoresists produce positive or negative images via the solubility changes after exposure to light. The images developed by solvents often suffer a severe distortion due to the solvent swelling of resist materials (Figure III.7).[67, 68]

To overcome the swelling problem, Frechet et al. used the acid catalyzed TD-polycarbonates to create self-developing images without solvents.[69,70,71] The photoresist material is a mixture consisting of a tertiary TD-polycarbonate and a photoacid generator (e.g. triarylsulfonium salts), as shown in Figure III.8.

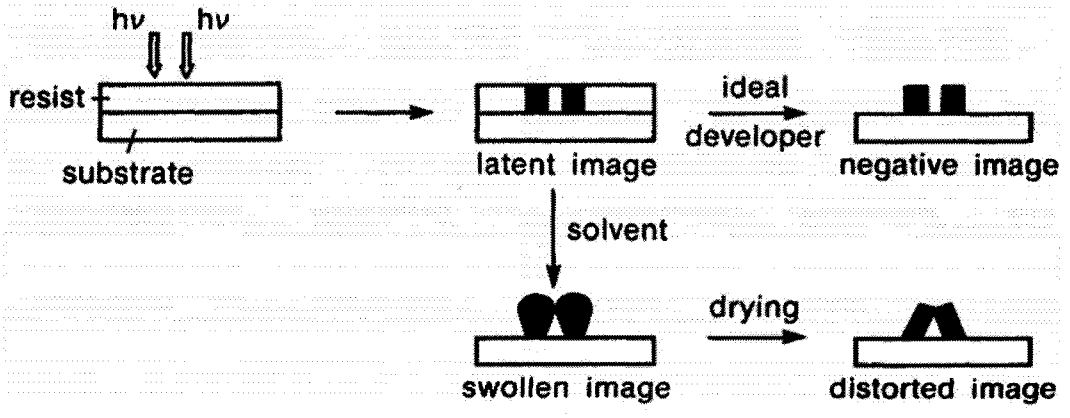

Figure III.7. Image distortion due to solvent swelling in photoresist

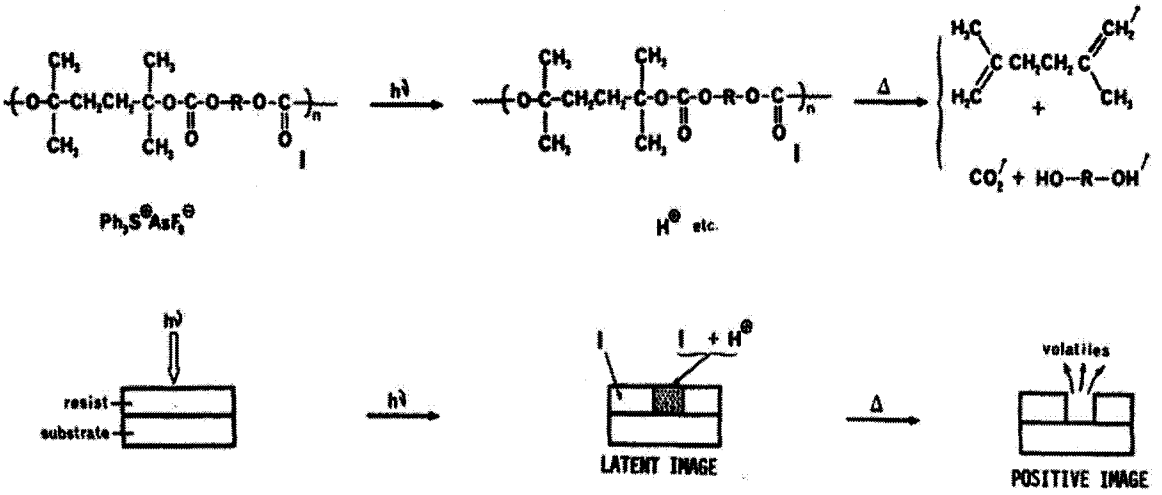

Figure III.8. Imaging process of dry-developing photoresist based on acid-catalyzed TD-polycarbonates

Upon irradiation, the area exposed to the UV light releases a strong acid from the photoacid generator, which catalyzes the degradation of the tertiary polycarbonate at low temperatures around 100 °C (Figure III.9). Without the acid, the thermal degradation takes place at a higher temperature. By utilizing the difference in thermolysis temperatures between the normal and acid-catalyzed depolymerization process, images are developed without using solvents. However, due to the relatively low volatility of the diols generated in degradation, a complete image development is not possible at the temperatures below 100 °C. Heating above the glass transition temperature (T_g = 70-80 °C) of the polymer tends to result in image distortion. Therefore, the development under vacuum is necessary.

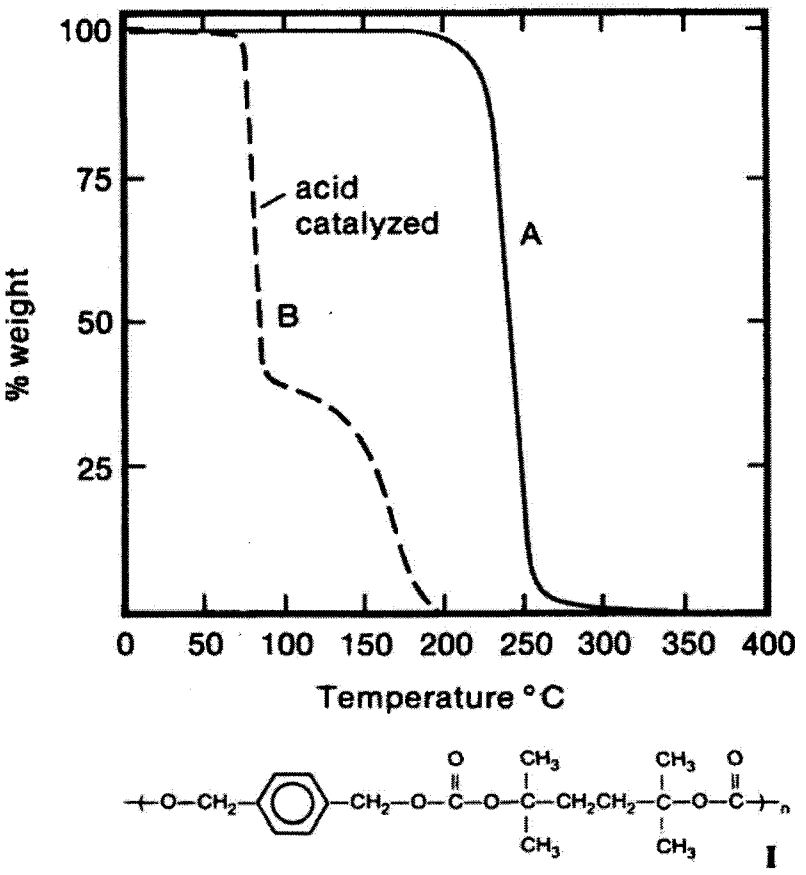

I

Figure III.9. TGA traces of (A) polycarbonate **I** and (B) **I** with acid catalyst

The line edge roughness (LER) of the formed images is another issue. For TD-polycarbonate photoresist, the degradation proceeds via a main chain scission mechanism, rather than the cleavage of the pendent groups for most common photoresists. The main chain scission is believed to be able to improve the LER of the images. The LER is mainly caused by polymer aggregates remaining at the pattern edges after development (Figure III.10). Polymer chains with the partially cleaved pedant groups may be fully removed, which leave cavities in the structure side wall. The polymer chains sticking out the wall can aggregate to a diameter of 20-30 nm.

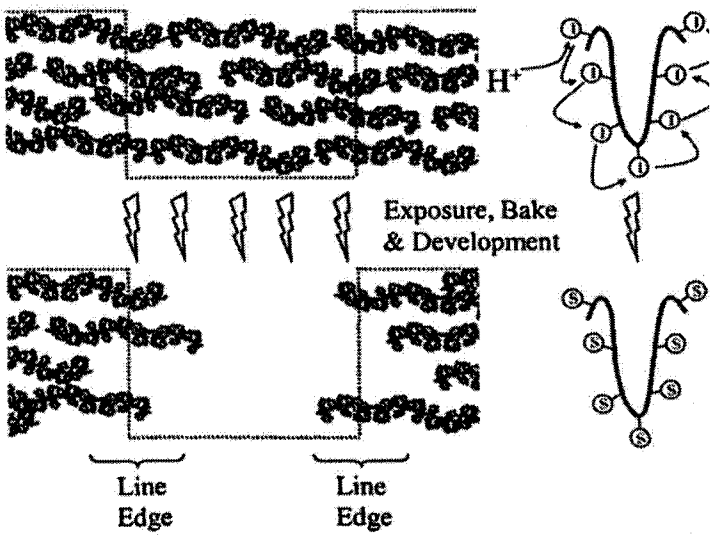

Figure III.10. Schematic drawing of a common chemical amplified resist before and after exposure, bake and development; "I" stands for insoluble, "S" for soluble groups

In contrast, in the main chain scission process, the polymer chain is totally chopped off into small molecules, thus leaving no holes or aggregated polymer coils in the structure side wall (Figure III.11).

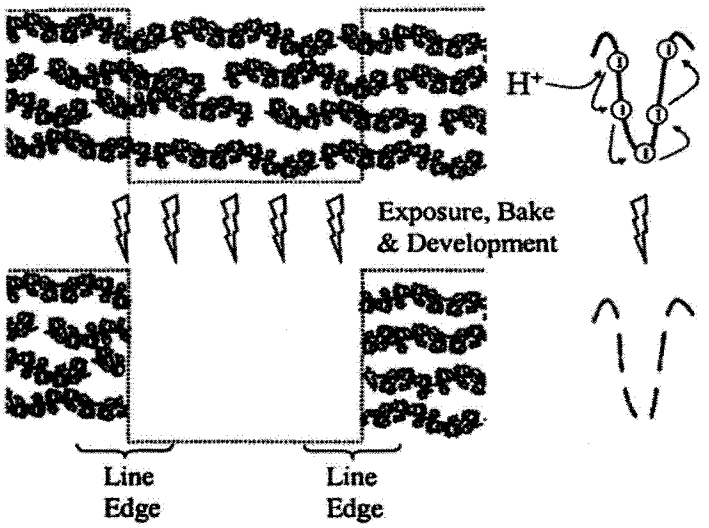

Figure III.11. Schematic drawing of a chemical amplified resist with protection groups in the polymer backbone before and after exposure, bake and development

III.4 Rationale and Objectives

In the development of TD-polymers, research efforts have been mainly focused on the replacement of traditional vinyl polymers and polyesters with polycarbonates, such as replacement of polynorbornene ($T_{burn\text{-}off}$ = 450 °C) with PPC ($T_{burn\text{-}off}$ = 360 °C), which is driven by the needs for low-temperature burn-off applications.

As the applications of the photoimageable paste products are getting increasingly sophisticated and expanding into new technology areas, there is a growing need for low-burning sacrificial organic materials. For large flat panel display devices, the high-grade glass plates are currently used to support the electrode grid, because sacrificial materials (vinyl or acrylate polymers) can only be cleanly burned off at temperatures of 550-600 °C, being close or higher than the softening temperature (~550 °C) of conventional cheaper float glass sheet. Although TD-polycarbonates can be completely degrade below 380-450 °C, only a few example of sacrificial vehicles based on polycarbonates have been reported.[72] Accordingly, the second part of this thesis deals with functional polycarbonates that are potentially applicable as a sacrificial vehicle in photoimageable conductor pastes.

Being efficient sacrificial vehicles in photoimageable conductor pastes, the TD-polycarbonates must possess the following functionalities: (1) photo-cross-linkable groups for photopattern generation, (2) acidic groups that are able to impart the solubility in aqueous base solutions during the image development, and (3) metal-binding groups, such as amide, sulfide and carboxyl groups, that can hold the metal particles at a high

loading. Considering the synthetic methods available at present, a variety of functional polycarbonates are designed and to be synthesized by condensation polymerization of the corresponding bis-chloroformate and diol monomers (Scheme III.16).

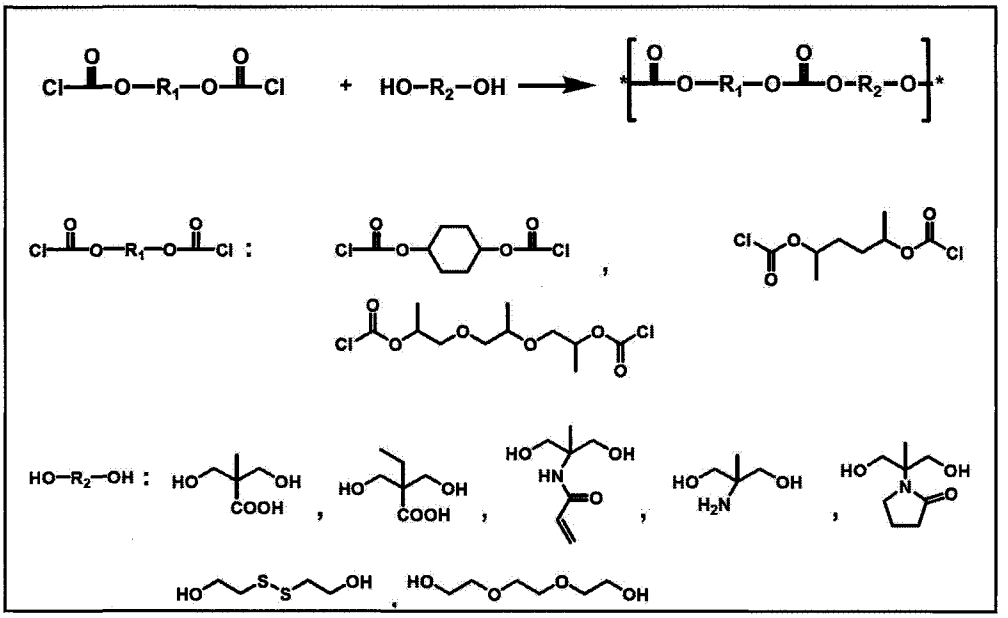

Scheme III.16. Proposed functionalized polycarbonates

By design, the bis-chloroformate monomers containing the secondary and tertiary carbon moieties will be selected, in order to achieve low burn-off temperatures. The carboxylic acid groups are designed in the diol monomers for soluble in aqueous base solution. The diols containing the polar amine, pyrrolidone, disulfide, and diether groups are used for the purpose of binding or chelating metal particles. The acrylate in the diol monomers is for photo-crosslinking. By polymerization of different monomers, a wide range of polycarbonates with various functional groups and properties can be obtained.

The relationships between the structures of functional polycarbonates and their

thermal degradation properties will be investigated in detail under various conditions. One of the variables to be investigated is the base catalyst in thermal degradation. Organic bases, such as DBU, are also proved to be able to accelerate thermolysis of polycarbonates.[73] Thus, by utilizing our newly developed photobase generator that is capable of releasing TBD (being hundred times more basic than DBU), a dry-developing photoresist based on polycarbonates and PBGs can be envisioned.

Accordingly, the overall objectives of the part two of this thesis are:

1. to synthesize functionalized thermodegradable polycarbonates containing photocross-linkable, aqueous-solution developable and metal-binding groups,
2. to study the relationships between the structure, thermal degradation and patterning properties of synthesized polycarbonates and silver conductor pastes, and
3. to explore the dry-developing photoresists based on base-catalyzed thermolysis of polycarbonates.

III.5 References

1. Endo,T.; Kakimoto.K.; Ochiai, B. *Macromolecules* **2005**, *38*, 8177.
2. Holland, B. T.; Blanford, C.; Stein, A. *Science* **1998**, *281*, 538.
3. Salamone, J. C. (eds.) *Polymeric Materials Encyclopedia*; CRC Press, **1996**.
4. Uskokovic, D. P.; Milonjic, S. K.; Rakovic, D. I. (eds.) *Recent Developments in Advanced Materials and Processes*; Trans Tech Publications Ltd, **2006**.
5. Lua, X. L.; Zhub, Q.; Meng, Y. Z. *Polym. Degrad. Stab.* **2005**, *89*, 282.

6. Lai, M. F.; Li, J.; Liu, J. J. *J. Therm. Anal. Calorim.* **2005**, *82*, 293.

7. Reed, H. A.; Henderson, C. L.; Kohl, P. A. *J. Micromech. Microeng.* **2001**, *11*, 733.

8. Mark, H. F.; Kroschwitz, J. I. (eds.) *Encyclopedia of Polymer Science and Engineering*; Wiley, **1985.**

9. Zhang, Z. B.; Zhou, S. Y.; Nie, J. *J. Mol. Cat. A: Chem.* **2007**, *265*, 9.

10. Grassie, N.; Scott, G. (eds.) *Polymer Degradation and Stabilisation*; Cambridge University Press, **1988**.

11. Bgrall, P. A.; Gue, A. M. *J. Micromech. Microeng.* **2007**, *17*, R15.

12. Kohl, P. A.; Allen, S. B. *WO2004042797* (2004).

13. Lam, Y. C.; Ying, S. G.; Tam, K. C. *Metall. Mater. Trans. A* **2000**, *31A*, 2597.

14. Lewis, J. A. *Ann. Rev. Mater. Sci.* **1997**, *27*, 147.

15. Asthana, R.; Kumar, A.; Dahotre, N. B. (eds.) *Materials Processing and Manufacturing Science*; Elsevier, **2006**.

16. Rivers, R. D. *U.S. Patent 4113480* (1978).

17. Liu, Z. Y.; Loh, N. H.; Tor, S. B.; Murakoshi, Y.; Maeda, R. *Mater. Let.* **2001**, *48*, 31.

18. Datta, M.; Osaka, T.; Schultze, J. W. (eds.) *Microelectronic Packaging*; CRC Press, **2005**.

19. Monajemi, P.; Joseph, P. J.; Kohl, P. A. *J. Micromech. Microeng.* **2006**, *16*, 742.

20. Joseph, P. J.; Henderson, C. L.; Kohl, P. A. *J. Micromech. Microeng.* **2003**, *12*, 147

21. Xia, Y.; Whitesides, G. *Angew. Chem. Int. Ed.* **1998**, *37*, 550.

22. Marcilla, A.; Menargues, A. G. S.; Ruiz, R. *Polym. Degrad. Stab.* **2005**, *88*,456.

23. Jellinek, H. H. G. (eds.) *Degradation of Vinyl Polymers*; Academic Press, **1955**.

24. Grassie, N.; Melville, H. W. *Bull. Soc. Chim. Belges* **1948**, *57*, 142.

25. Reid, W. S. *J. Soc. Chem. Ind. London* **1949**, *68*, 244.

26. MacCallum, J. R. *Makromol. Chem.* **1965**, *83*, 137.

27. Martin, J. W.; Dickens, B.; Waksman, D.; Bentz, D. P.; Byrd, W. E.; Embree, E.; Gaithersburg, M. D. *J. Appl. Polym. Sci.* **1987**, *34*, 377.

28. Lomakin, S. M.; Aseeva, R. M.; Zaikov, G. E. *Int. J. Polym. Mater.* **1996**, *31*, 153.

29. Holland, B. J.; Hay, J. N. *Polymer* **2001**, *42*, 4825.

30. Wall, L. A.; Straus, S.; Flynn, J. H.; Simha, R. *J. Phys. Chem.* **1966**, *70*, 53.

31. Gies, A. P.; Vergne, M. J.; Hercules, D. M. *Macromolecules* **2007**, *40*, 7493.

32. Levine, S. E.; Broadbelt, L. J. *Polym. Prepr.* **2007**, *48*, 601.

33. McNeill, I. C.; Zulfiqar, M.; Kousar, T. *Polym. Degrad. Stab.* **1990**, *28*, 131.

34. Bailey, W. J.; Liotta, C. *Polym. Prepr.* **1964**, *5*, 333.

35. Bailey, W. J.; Baccei, L. J. *Polym. Prepr.* **1971**, *12*, 313.

36. Day, M.; Cooney, J. D.; Shaw, K.; Watts, J. *J. Therm. Anal. Calorim.* **1998**, *52*, 261.

37. Dickens, B. *J. Polym. Sci., Polym. Chem.* **1982**, *20*, 1065.

38. Albertsson, A. C.; Karlsson, S. *Polym. Mater. Sci. Eng.* **1990**, *62*, 976.

39. Carothers, W. H.; Dorough G. L.; Natta, F. J. *J. Am. Chem. Soc.* **1932**, *54*, 761.

40. Garozzo, D.; Giuffrida, M.; Montaudo, G. *Macromolecules* **1986**, *19*, 1643.

41. Bikiaris, D. N.; Chrissafis, K.; Paraskevopoulos, K. M.; Triantafyllidis, K. S.; Antonakou, E. V. *Polym. Degrad. Stab.* **2007**, *92*, 525.

42. Grassie, N. and Scott, G. (eds.) *Development in Polymer Degradation. Vol. 7;* Elsevier, **1987**.

43. Garozzo, D.; Montaudo, G.; Giuffrida, M. *Polym. Degrad. Stab.* **1986**, *15*, 143.

44. Kopinke, F. D.; Mackenzie, K. *J. Anal. Appl. Pyroly.* **1997**, *40*, 43.

45. Kopinke, F. D.; Remmler, M.; Wachsen, O. *Polym. Degrad. Stab.* **1996**, *53*, 329.

46. Iwabuchi, S.; Jaacks, V.; Galil, F.; Kern, W. *Makromol. Chem.* **1973**, *165*, 59.

47. Grseham, T. L.; Jansen, J. E. Shaver, F. W. *J. Am. Chem. Soc.* **1948**, *1004*, 998.

48. Iwabuchi, S.; Jaacks, V.; Kern, W. *Makromol. Chem.* **1976**, *177*, 2675.

49. Luderwald, I. *Makromol. Chem.* **1977**, *178*, 2603.

50. McNeill, I. C.; Leiper, H. A. *Polym. Degrad. Stab.* **1985**, *11*, 309.

51. McNeill, I. C.; Leiper, H. A. *Polym. Degrad. Stab.* **1985**, *12*, 373.

52. Dixion, D. D.; Mantel, G. J. *J. Polym. Sci., Polym. Lett. Ed.* **1980**, *18*, 131.

53. Peng, S. W.; An, Yu. X.; Dong, Li. S. *Polym. Degrad. Stab.* **2003**, *80*, 141.

54. Speybroeck, V. V.; Martele, Y.; Schacht, E. *J. Am. Chem. Soc.* **2001**, *123*, 10650.

55. Speybroeck, V. V.; Martele, Y.; Schacht, E. *J. Phys. Chem. A.* **2002**, *106*, 12370.

56. Lua, X. L.; Zhub, Q.; Meng, Y. Z.; *Polym. Degrad. Stab.* **2005**, *89*, 282.

57. Liu, B. H.; Chen, L. B.; Yu, A. F. *Macromol. Rapid Commun.* **2002**, *23*, 881.

58. Schild, H. G.; Horner, M.G. *Pure Appl. Chem.* **1994**, *A31*, 1955.

59. Labadie, J. W.; Haidar, B. *Polym. Prepr.* **1995**, *36*, 735.

60. Pett, R. A.; Rao, N.; Qaderi, S. B. A. *U.S. Patent 4158689* (1979).

61. Pett, R. A.; Qaderi, S. B. A.; Tabar, R. J. *U.S. Patent 4158688* (1979).

62. Rak, Z. S. *Powder Metal. Metal Ceramics* **1999**, *38*, 3.

63. Lee, S. M.; Park, S. D.; Kang, N. K.; Nahm, S. *Adv. Appl. Ceram.* **2008**, *107*, 96.

64. Ketkar, S. A.; Umarji, G. G.; Amalnerkar, D. P. *Mater. Sci. Eng., B.* **2006**, *132*, 215

65. Leberzammer, E.; Roos, L. U.S. Patent 4273857 (1981).

66. Yang, H. X.; Mckeever, M. R. WO/2006/017791 (2006).

67. Reichmanis, E.; Thompson, L. F. *Chem. Rev.* **1989**, *89*, 1273.

68. Reichmanis, E.; Neenan, T. X. *Adv. Mater. Optic. Electron.* **1994**, *4*, 83.

69. Frechet, J. M. J.; Willson, C. G. *Makromol. Chem., Rapid Commun.* **1986**, *7*, 121.

70. Frechet, J. M. J.; Bouchard, F.; Kryczka, B.; Willson, G. *Polym. J.* **1987**, *19*, 31.

71. Frechet, J. M. J.; Willson, C. G. *J. Photopolym. Sci. Technol.* **1990**, *3*, 235.

72. Choi, J. H.; Drysdale, N. E. U.S. Patent 6194124 (2001).

73. Endo, T.; Nagai, D. *Macromolecules* **2005**, *38*, 8177.

CHAPTER IV

SYNTHESIS AND CHARACTERIZATION AND THERMOLYSIS STUDY OF FUNCTIONALIZED THERMODEGRADABLE POLYCARBONATES

IV.1 Synthetic Strategy and Polymer Design

IV.1.1 Synthetic Method of TD-polycarbonates

Aliphatic polycarbonates can be synthesized by a number of methods, including (a) the condensation reaction of aliphatic diols with phosgene or aliphatic bis-chloroformates,[1-5] (b) the carbonate interchange reaction of aliphatic diols with dialkyl carbonates,[6,7] (c) the solid-liquid phase-transfer-catalyzed reaction of aliphatic diols with carbonyldiimidazole,[8] (d) the polymerization of epoxides with CO_2,[9] and (e) the ring-opening polymerization (ROP) of six or seven-membered cyclic carbonates (Scheme IV.1).[10, 11]

Of all these synthetic methods, process (a) is a general route to a variety of aliphatic polycarbonates. It has been well studied and applied in commercial produciton.[12] In addition, the aliphatic diols bearing the pendant acid, amine, and amide groups are all commercially available. Therefore, we select condensation polymerization of bis-chloroformates and aliphatic diols as the synthetic method in this thesis work.

To safely handle the reaction, bis-chloroformates are prepared from the corresponding diols by using bis(trichloromethyl)carbonate (BTC), rather than highly

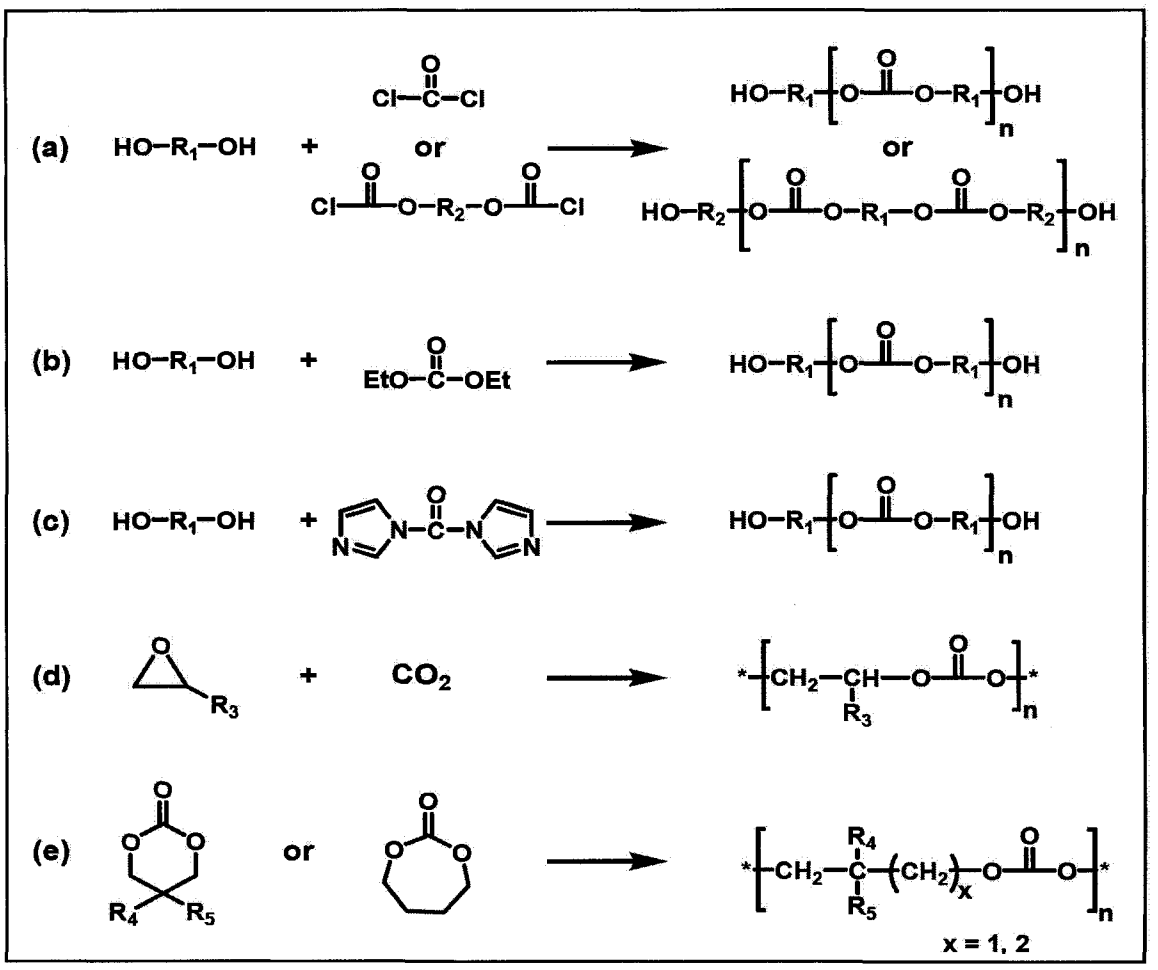

Scheme IV.1. Synthetic routes to thermodegradable polycarbonates

toxic gaseous phosgene. BTC is a crystalline solid, stable up to 130 °C and inert to moisture in air.[13] In the reaction of BTC with diols, according to the mechanism proposed by Eckert et al. (Scheme IV.2),[14] 1/3 mole of BTC reacts with 1/3 mole of nucleophile, such as pyridine, to form 1/3 mole of phosgene. In the next step a second and a third mole of phosgene evolve which are "quenched" by 2/3 mole of nucleophile, and finally react with alcohol to produce chloroformate. Thus, in the preparation of bis-chloroformates, one mole of BTC equals to three moles of phosgene and the exact amounts of BTC can be weighed for a given reaction.

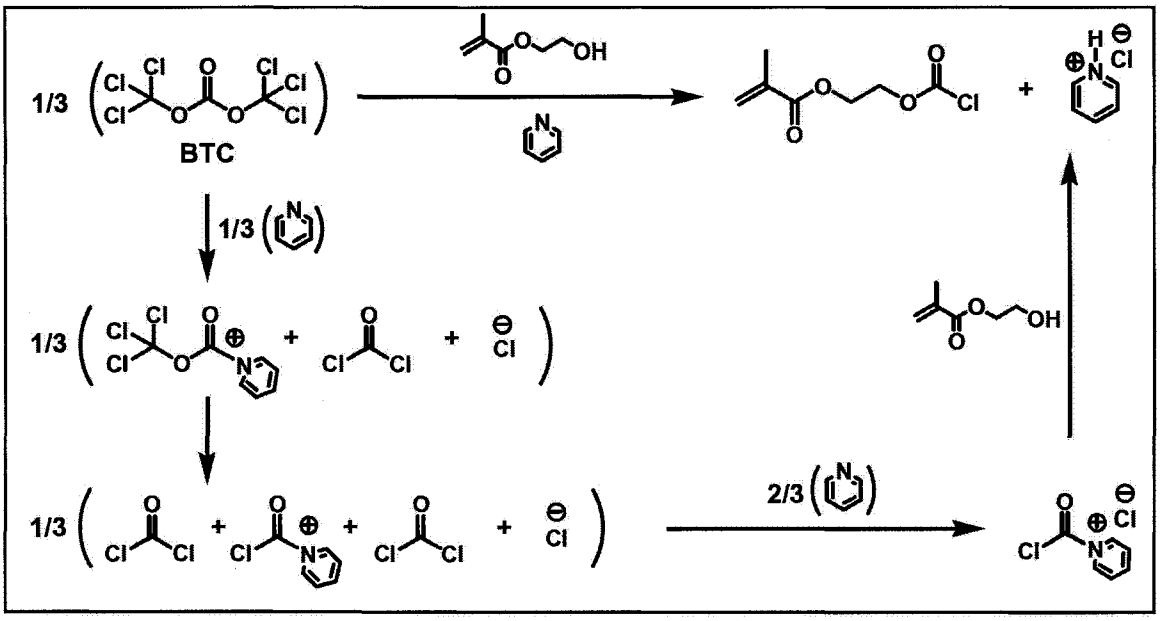

Scheme IV.2. Phosgenation reaction using BTC

Furthermore, for the polymerization alkyimidazoles, such as 1-methylimidazole or 1-ethylimidazole, are used as HCl acceptor instead of triethylamine or pyridine to ensure the clean-burn-off property of products (M_{res} < 1wt.%). The hydrochloride salt by-products may easily be trapped in polymer and can not be burned off cleanly.[15] Even 1% of salts left in the polymer will introduce char-like ashes after thermal degradation. This may be worse in functionalized TD-polymers containing acid or amide groups, which are capable of holding the hydrochloride salts even more strongly. A conventional purification method is to precipitate the polymer solution into methanol or water to wash off the salts. However, TD-polycarbonates tend to be "gum up" in water or methanol, making the salt washing or extracting extremely inefficient. This problem can be overcome by taking an advantage of low melting alkylimidazolium chloride salts (Table IV.1). In toluene or ethyl acetate, when heated up to 70 °C, the polymer dissolves and the

salts melt. Therefore, no solid salts suspend in the solution. After extractive washing, the salts solidify at room temperature, since they do not dissolve in toluene and ethyl acetate.[19] The purified polymer can be easily obtained by simply decanting and evaporating solvents.

Table IV.1. Melting points of hydrochloride salts of nitrogen bases

Salts	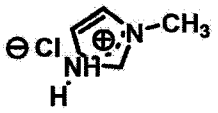 1-methylimidazolium chloride	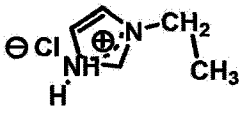 1-ethylimidazolium chloride	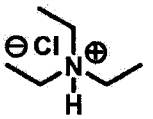 trimethylammonium chloride	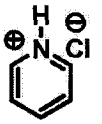 pyridinium chloride
M.P. (°C)	70 [a]	55 [a]	251 [b]	146 [c]

[a] *Data from reference [16],* [b] *Data from reference [17],* [c] *Data from reference [18],*

IV.1.2 Functionalities in TD-polycarbonates

As described in the last chapter, TD-polycarbonates are designed to be applied as potential sacrificial vehicles in photoimageable conductor pastes. Generally, the sacrificial vehicles are composed of three components: (1) aqueous-developable acidic polymer (70-75 wt.%), typically poly(methyl methacrylate-co-methylacrylic acid) (PMMA-co-PMAA) with a T_g of 50-150 °C and M_w in the range of 2,000-10,000, (2) 15-20 wt.% of photo-cross-linkable methacrylate monomers and (3) 10 wt.% of other additives, such as stabilizers, dispersants and plasticizers.[20,21] Therefore, three functionalities including aqueous developability, photo-cross-linkability and metal-binding ability are required.

The aqueous developability can be realized by incorporating carboxylic acid groups

in the polymer side chain. Aliphatic diols containing acid groups, such as propanoic acid, and buyanoic acid, are commercially available. Thus, the corresponding polycarbonates can be obtained by condensation of bis-chloroformates with acid-containing diols or the diols containing the benzyl ester which can be easily removed later by hydrogenolysis (Scheme IV.3). Previous experience in using PMMA-co-PMAA as sacrificial vehicles indicates that the appropriate concentration of acidic groups is in the range of 15-30 mol.% in order to obtain high resolution images.[21] Accordingly, polycarbonates with acid numbers in a range of 95-187 are desired. However, the final content of acid groups in TD-polycarbonates may change considering the difference in polarity between the carbonate chain and the carbon-carbon backbone.

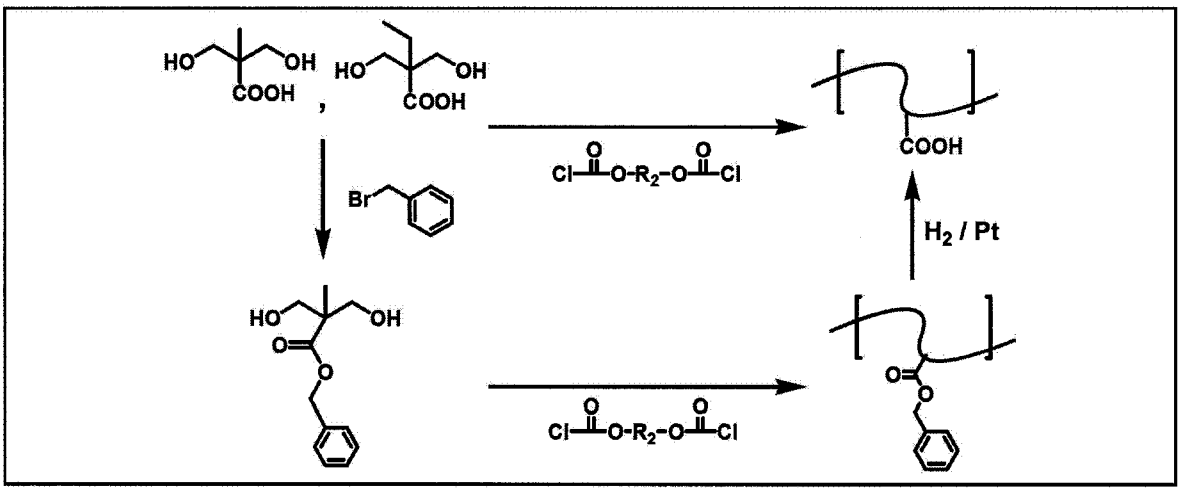

Scheme IV.3. Synthetic routes to aqueous developable polycarbonates

To implement the photo-cross-linkability, two approaches are considered. One is to prepare cross-linkable diols containing vinyl or acrylate groups and then polymerize with bis-chloroformates. The advantage of this approach is that the resulted cross-linked network can be burned out at relatively low temperatures since the network is mainly

composed of thermally labile carbonate bonds. However, the weight ratio between inorganic particles and sacrificial vehicles must be around 7:3 in photoimageable conductor pastes. Such a high volume of inorganic component will no doubt block UV light and TD-polycarbonates may not be cured enough to hold inorganic particles in the image-developing step.

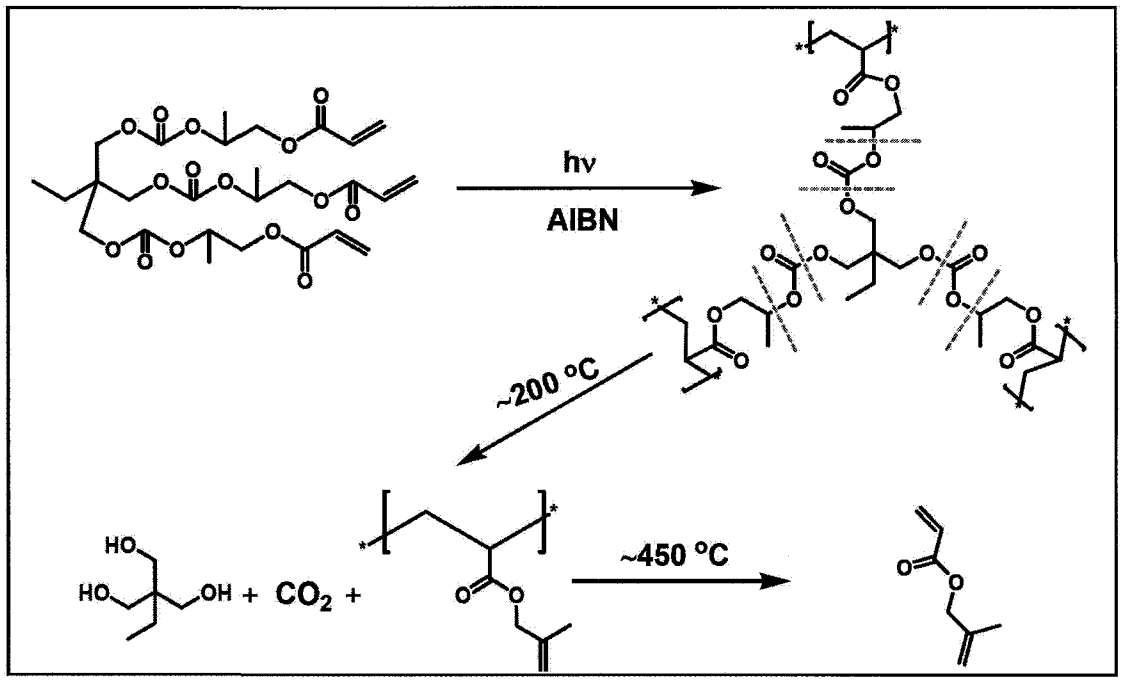

Scheme IV.4. Thermal degradation of carbonate-based cross-linked network

Another approach is to prepare carbonate-based methacrylate cross-linkers (Scheme IV.4) and then physically mix them with polycarbonates to provide photo-cross-linkability. These cross-linkers are more mobile and have a higher reactivity than the pendant acrylate groups, and thus may increase curing efficiency. Meanwhile, the resulted cross-linking network can be still thermally broken at ~200 °C due to the presence of carbonate bonds. The linear oligmers derived from cross-linkers possess a

similar structure as PMMA and thus should undergo same depolymerization reaction and may be completely removed below ~450 °C. Although this temperature is higher than $T_{burn\text{-}off}$ of TD-polycarbonates, it is still acceptable since the softening temperature of conventional float glass sheet is ~550 °C.

The diols containing the amine, disulfide and diether groups are also commercially available. Thus, the preparation of metal binding polycarbonates is quite straightforward. According to literature data, 10 mol.% of metal binding groups are needed to hold high loading of inorganic particles in photoimageable conductor pastes.

IV.2 Synthesis and Characterization

IV.2.1 Synthesis and Characterization of Monomers

IV.2.1.1 Bis-Chloroformates

Three aliphatic diols are selected to prepare bis-chloroformate monomers (Scheme IV.5). The selection is based on the following considerations. (1) These diols have 6-9 carbon atoms which ensure a good volatility once they are released during the polymer degradation and avoid a possible competing cyclization to form five- or six-membered cyclic carbonates.[22] (2) Reactions of these secondary diols with BTC are controllable to produce stable bis-chloroformates. In contrast, the reaction of BTC with primary diols yields a large amount of carbonates. Tertiary chloroformates are quite unstable making them little use in the preparation of polycarbonates.[23] (3) The presence of alkyl substituents on the α-carbon position in these diols will decrease the clean-burn-off

temperature of synthesized polymers. (4) In particular, tripropylene glycol bearing the ether moiety imparts a metal-binding ability to synthesized polymers.

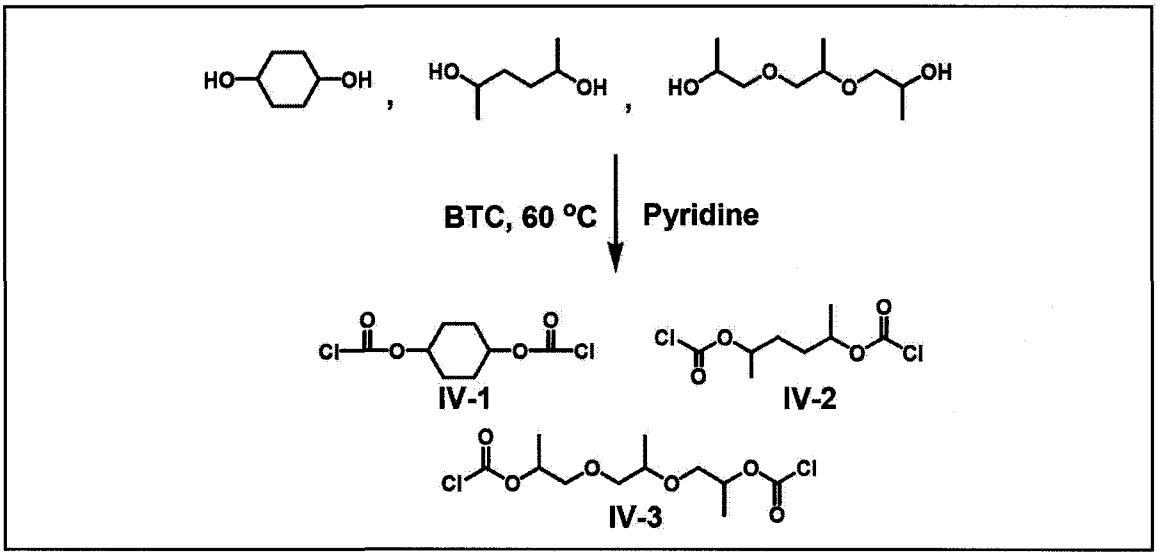

Scheme IV.5. Synthesis of bis-chloroformate monomers **IV-1**, **IV-2** and **IV-3**

The bis-chloroformate monomers **IV-1**, **IV-2** and **IV-3** were prepared from the corresponding diols and BTC in toluene with a catalytic amount of pyridine. The reaction was monitored by IR spectroscopy (Figure IV.1). Peaks at 1823 and 1185 cm^{-1} were assigned to BTC (Figure IV.1a). After adding diols and heated up to 60 °C, intense peaks at 1764 and 1166 cm^{-1} appears due to formation of chloroformates and the peak at 3400 cm^{-1} indicates the unreacted hydroxy groups (Figure IV.1b). The reaction was terminated when the peak at 3400 cm^{-1} completely disappeared (Figure IV.1c). The absence of peaks at 1740 or 1260 cm^{-1} indicated no carbonate by-products produced. Bis-chloroformates were further purified by recrystallization from hexane for **IV-1** or vacuum distillation for **IV-2** and **IV-3**. These monomers are easily handled under ambient conditions and stable in fridge for more than 3 months.

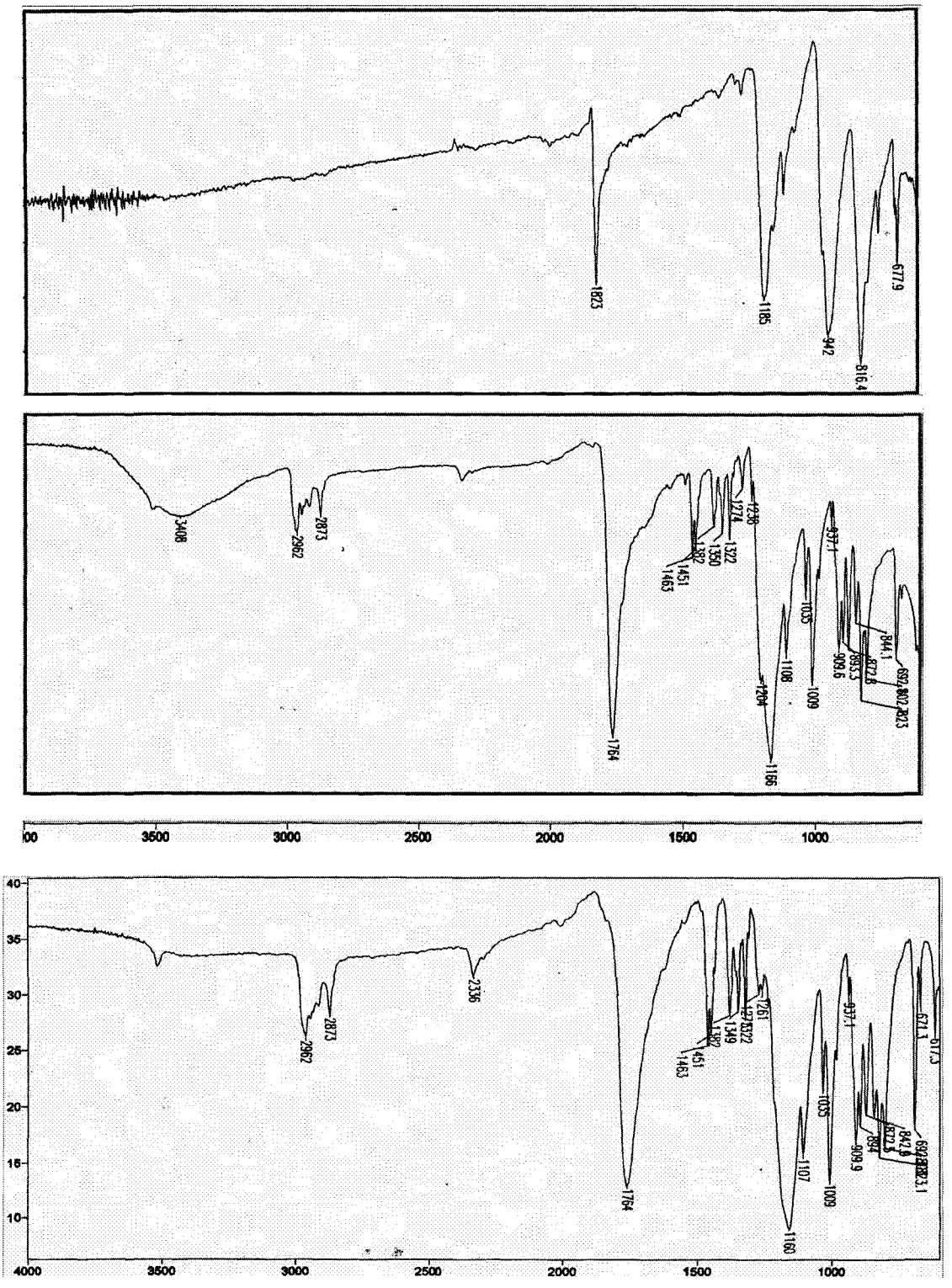

Figure IV.1. Preparation of bis-chloroformate (**IV-1**) monitored by IR spectroscopy (NaCl plates) (a) BTC dissolved in toluene, (b) 1,4-cyclohexanediol and pyridine added into solution and heating to 60 °C for 1 h, (c) heating to 60 °C for 2 h

The ^{1}H and ^{13}C NMR and IR spectroscopic data of these bis-chloroformates are consistent with their expected chemical structures (Figure IV.2). From the NMR data, their purities were estimated to be around 95-98%.

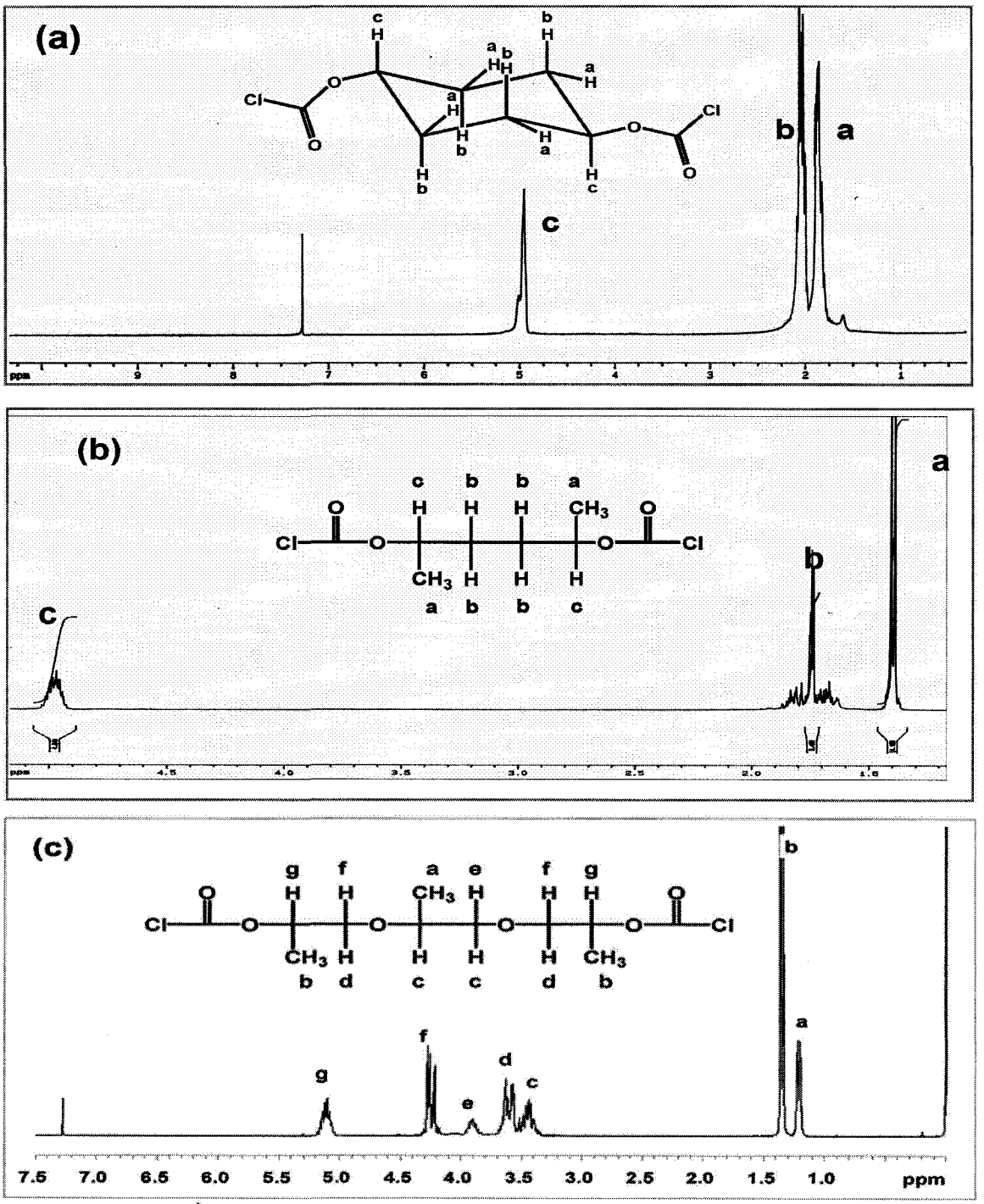

Figure IV.2. ^{1}H NMR spectra of bis-chloroformates (a) **IV-1**, (b) **IV-2** and (c) **IV-3**

IV.2.1.2 Functional Diols

Diols Containing Carboxylic-Acid Groups

2,2-Hydroxymethylpropionic acid (DMPA) and 2,2-hydroxymethylbutanoic acid (DMBA) were used as carboxylic-acid containing diol monomers for the preparation of aqueous developable polycarbonates. To prevent the possible reaction between the acid group and chloroformates during polymerization, the carboxylic acid was protected as a benzyl ester (Scheme IV.6).

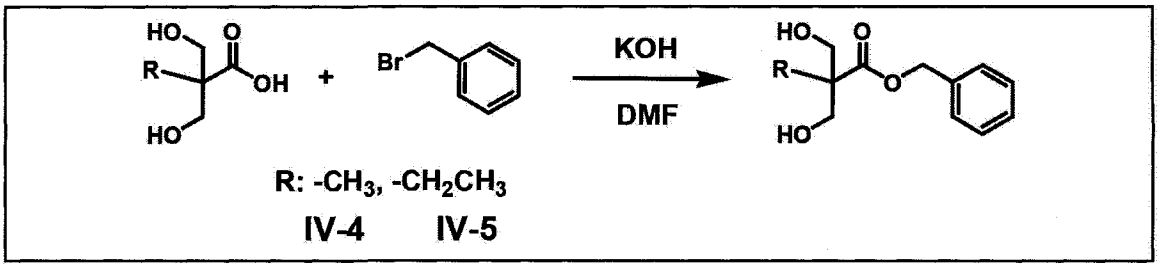

Scheme IV.6. Synthesis of diols **IV-4** and **IV-5** containing protected acid groups

The benzyl esters of DMPA (**IV-4**) and DMBA (**IV-5**) were prepared by first forming the potassium salts and then reacting the salts with benzyl bromide. The benzyl ester can be cleaved selectively in high yield by catalytic hydrogenolysis[24] without affecting the carbonate bonds formed in the later condensation polymerization. The reaction was monitored by TLC (hexane/ethyl acetate 1:1 v/v) for the formation of product ($R_f = 0.17$). The crude product was purified by chromatography on silica gel. The ester formation was verified by IR with characteristic peaks at 1580 and 1500 $cm^{-1}$for aromatic rings. The ^1H NMR spectrum of **IV-4** with complete assignment is shown in Figure IV.3.

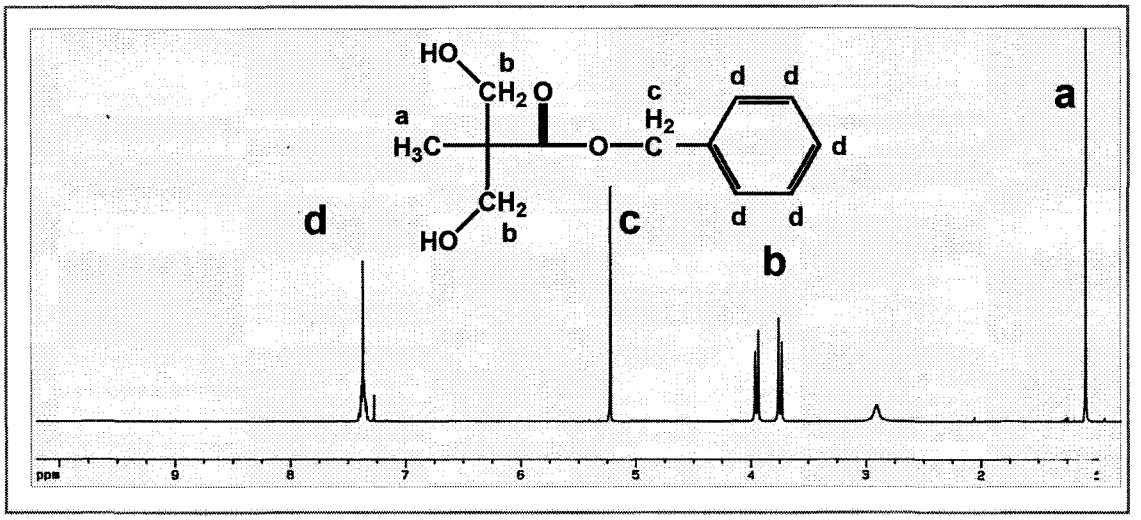

Figure IV.3. ^{1}H NMR spectrum (400 MHz, $CDCl_3$) of benzyl ester of DMPA (**IV-4**)

Diols Containing Acrylate Groups

N-[1,1-Bis(hydroxymethyl)ethyl]acrylamide (**VI-6**) was selected as the cross-linkable diol monomer. According to reports in literature,[25,26] this unsaturated diol can be polymerized readily in the presence of a free radical initiator. Thus, polycarbonates derived from this functional diol should be photo-cross-linkable.

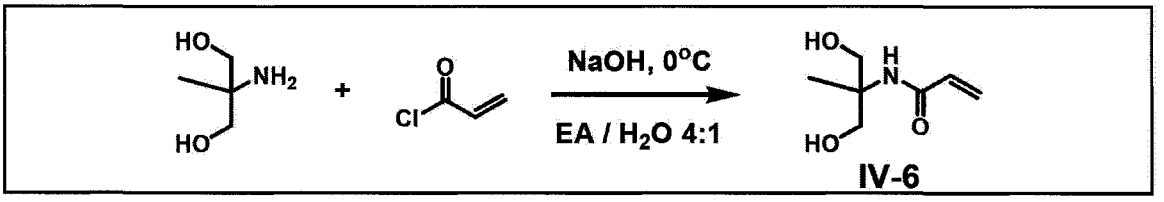

Scheme IV.7. Synthesis of diol **IV-6** containing a vinyl group

Monomer **VI-6** was synthesized from a two-phase reaction of 2-amino-2-methyl-1,3-propanediol (AMPD) and acryloyl chloride (Scheme IV.7). AMPD and acryloyl chloride were dissolved in water and ethyl acetate, respectively. An excess amount of AMPD (1.2 mole equivalent) was used and the reaction temperature was

controlled at near zero degree (ice bath). The reaction was monitored by TLC (R_f = 0.69 for acryloyl chloride in 20:1 ethyl acetate/ethanol). The crude product was isolated after removal of ethyl acetate and then purified by recrystallization from ethyl acetate/ethanol (10:1 v/v). The IR and NMR data are all consistent with its expected structure. Peaks at 1687 and 1633 cm^{-1} in the IR spectrum indicate the presence of the carbonyl and carbon-carbon double bonds. Its ^1H NMR spectrum is shown in Figure IV.4.

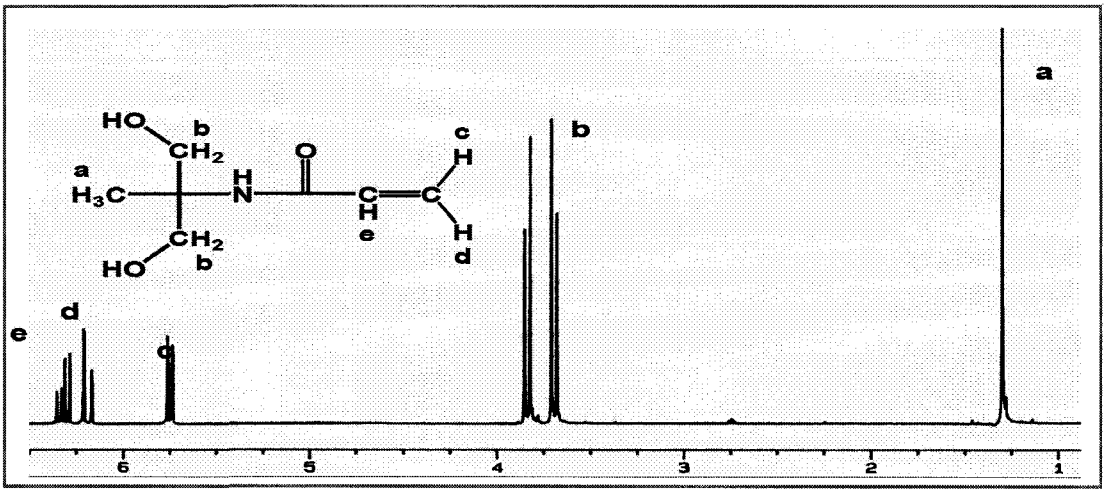

Figure IV.4. ^1H NMR spectrum (400 MHz, $CDCl_3$) of diol **VI-6**

Diols Containing Metal Binding Groups

2,2'-Dithiodiethanol (DTDE) and 2-amino-2-methyl-1,3-propanediol (AMPD) containing amide, disulfide or amine groups were used as metal-binding diol monomers (Figure IV.5).

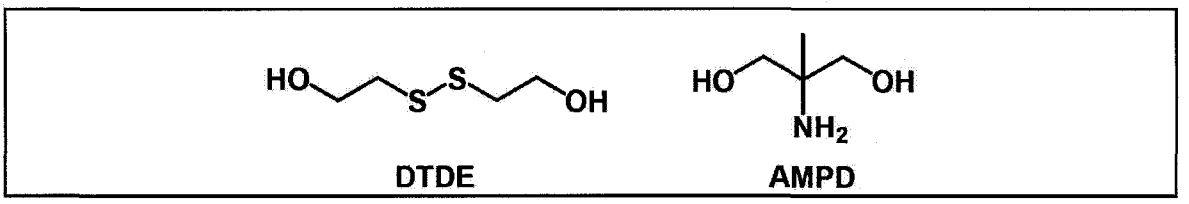

Figure IV.5. Metal-binding monomers DTDE and AMPD

DTDE were used as received without further purification. AMPD was converted to its HCl salt to block its reaction with chloroformate during polymerization. The HCl salt of AMPD (**IV-7**) was obtained as white solids by adding dry HCl gas into a solution of AMPD in isopropyl alcohol. The reaction was monitored by color changes of reaction solution in responding to a pH indicator, methyl red. The red color indicated that the reaction solution turned to acidic and the amine was consumed. The diol monomer **IV-7** was further purified by recrystallization from methanol/isopropanol (10:1, v/v). The structure of **IV-7** was confirmed by NMR spectroscopy.

Furthermore, diols bearing pendant pyrrolidinone moiety were synthesized as metal-binding monomers. The study on polymer–metal complexes shows that poly(vinyl pyrrolidinone) works as an efficient polymeric ligand for binding copper and cobalt.[27, 28] Thus, the pedant pyrrolidinone group should be a good choice for imparting metal-binding ability to polycarbonates.

The synthesis of diol monomer containing pyrrolidinone group was first attempted by a two-step reaction of converting 1-(2-hydroxyethyl)-2-pyrrolidone (HEP) to its corresponding chloroformate (HEPC) and then reacting with 1,1,1-tris(hydroxymethyl) propane (THMP) (Scheme IV.8). In the first step, a dichloromethane solution of HEP was

added dropwise to BTC solution at 0 °C to prevent formation of carbonate by-product. The reaction was monitored with FT-IR. The appearance of peaks at 1775 and 1155 cm^{-1} indicates the formation of the chloroformate, and the disappearance of O-H stretching at 3340 cm^{-1} indicates the completion of the reaction. HEPC was purified by vacuum distillation (bp = 131 °C/3 mmHg). In the second step, a solution of THMP in dry THF was added dropwise to the HEPC solution in the presence of pyridine. Although the molar ratio between the triol and chloroformate was controlled at 1.2:1, the product was still a mixture of mono-substituted and di-substituted triols. The product was purified by column chromatography twice. From the integration ratio for the α–methylene protons in the ^1H NMR spectrum, 10-15 mol.% of the di-substituted compound was still present in the product. This di-substituted compound has one hydroxy group that would act as a chain terminator in the condensation polymerization of bis-chloroformate and diol. Thus, the mixture can not be used as a diol monomer.

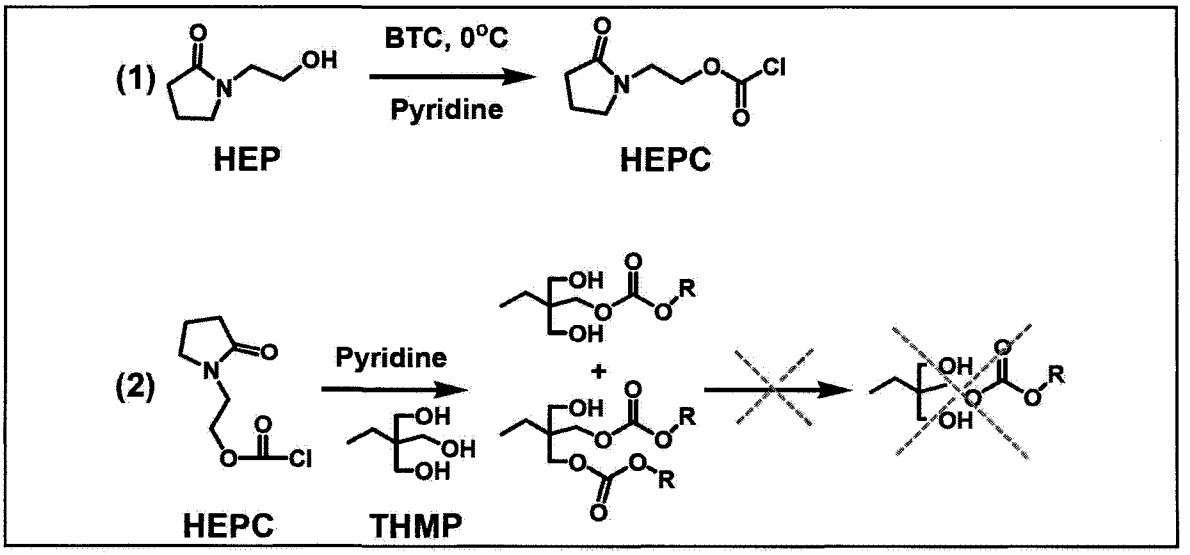

Scheme IV.8. Synthesis of diols containing pyrrolidinone groups – method A

Later on, we tried another method to prepare diol monomers containing pyrrolidinone groups. According to reports in literature, N-alkylated pyrrolidines were easily synthesized in high yields by the *gem*-cyclodialkylation between five- or six-membered cyclic esters and primary amines over a heterogeneous titania catalyst.[29,30,31] Thus, diols bearing secondary amine (APD) and tertiary amine (AMPD) could react with γ-butyrolactone (γ-BL). If the *gem*-cyclodialkylation proceeds in the same way for secondary and tertiary amines, diols bearing pyrrolidinone groups, namely 1-(1,3-dihydroxypropan-2-yl)pyrrolidin-2-one (DHPP) (**IV-8**) and 1-(1,3-dihydroxy -2-methylpropan-2-yl)pyrrolidin-2-one (DHMPP), could be obtained (Scheme IV.9).

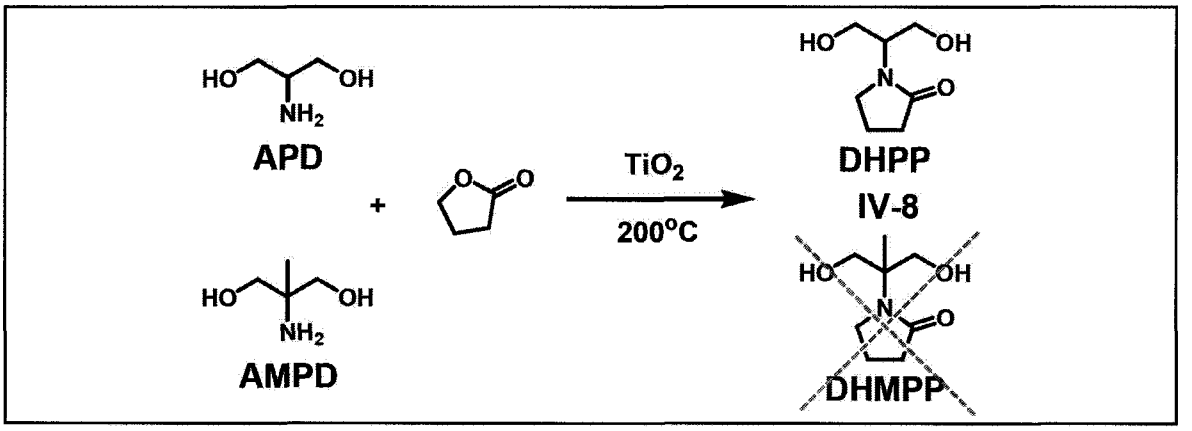

Scheme IV.9. Synthesis of diols containing pyrrolidinone groups – method B

In the reaction involving secondary amines, an excess amount of APD (1.2:1 in molar ratio) was dissolved in γ-BL in the presence of a catalytic amount of TiO_2. The γ-BL works as both a reactant and a solvent. The solution was heated up to 200 °C. The reaction was monitored by FT-IR (Figure IV.6).

It was found that the *gem*-cyclodialkylation proceeded in two steps. In the first step,

the lactone was attacked by the amine and the ring opened quickly, as evident by complete disappearance of the peak at 1770 cm^{-1} for the cyclic ester and appearance of an intense peak at 1669 cm^{-1} due to the newly generated amide (Figure IV.6a and b). Another strong peak at 1560 cm^{-1} was also shown up gradually, being assigned to the N-H bending, by comparing with the authentic IR spectra of N-methylacetamide {CH_3-CO-NH-CH_3} and N,N-dimethyl- acetamide {CH_3-CO-N-$(CH_3)_2$}. The second step was a slow cyclization. After heating overnight, the disappearance of N-H bending bond at 1560 cm^{-1} accompanied by the presence of multiple peaks in the C-H bending region (1470-1370 cm^{-1}) indicated the formation of pyrrolidinone ring. This IR spectrum was similar to the authentic one of 1-(2-hydroxyethyl)-2-pyrrolidone (Figures IV.6c and d), suggesting that the reaction was finished.

Pure DHPP, diol monomer **IV-8** was obtained by vacuum distillation (bp = 153 °C/0.25 mmHg). NMR and MS spectroscopy confirmed its chemical structure. However, the yield was much lower than the reported value in the *gem*-cyclodialkylation of primary amines (34% vs. 68%). It was believed that the conversion of the second step-cyclization was decreased by the steric hindrance effect due to the presence of alkyl substituents on α–carbon atom. As expected, the reaction involving tertiary amines did not work. Although, the amide was formed in the first step, the N-H peak at 1560 cm^{-1} did not change even with overnight heating. The cyclization of pyrrolidinone ring was totally suppressed in tertiary amines.

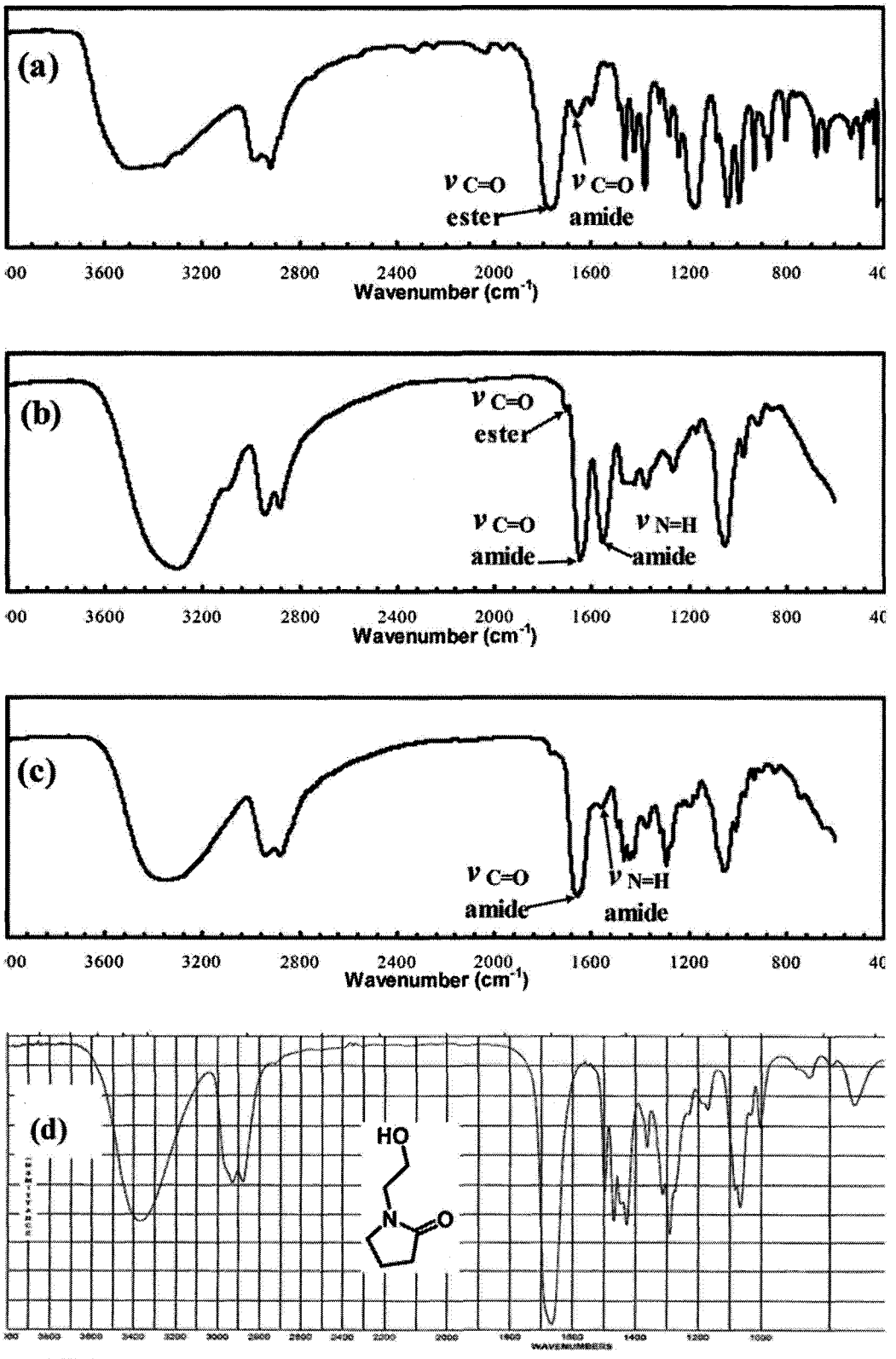

Figure IV.6. IR spectral changes of the *gem*-Cyclodialkylation between APD and γ-BL (a) before heating, (b) heated at 200 °C for 1 h, (c) overnight, and (d) authentic IR spectrum of 1-(2-hydroxyethyl)-2-pyrrolidone

IV.2.2 Synthesis and Characterization of Thermodegradable Cross-Linkers

A difunctional acrylate (**IV-9**) and a trifunctional acrylate (**IV-10**), containing thermally labile secondary carbonate moieties, were synthesized (Scheme IV.10) from the corresponding diol or triol with a secondary acrylic chloroformate.

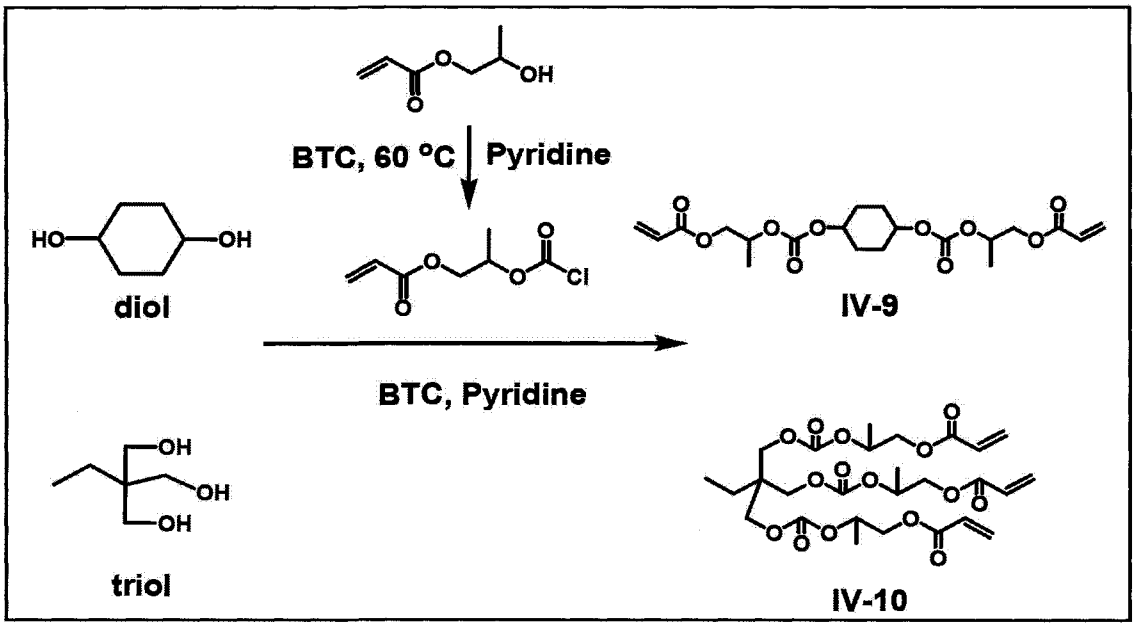

Scheme IV.10. Synthesis of thermodegradable cross-linkers **IV-9** and **IV-10**

2-Hydroxypropyl acrylate reacted with BTC in the presence of pyridine as a catalyst. The reaction was monitored by FT-IR. Disappearance of O-H stretching at 3340 cm^{-1} indicates the completion of the reaction. The product was purified by vacuum distillation. Its structure was confirmed by IR and NMR spectroscopy. An excess of this chloroformate was then used in the reaction with the diol or triol in the presence of equal molar amount of pyridine. The reaction was terminated once the IR band at 3340 cm^{-1} disappeared. **IV-9** and **IV-10** were purified by column chromatography on silica gel with ethyl acetate (R_f = 0.24 for **IV-10**, 0.32 for **IV-9** and 0.72 for chloroformate).

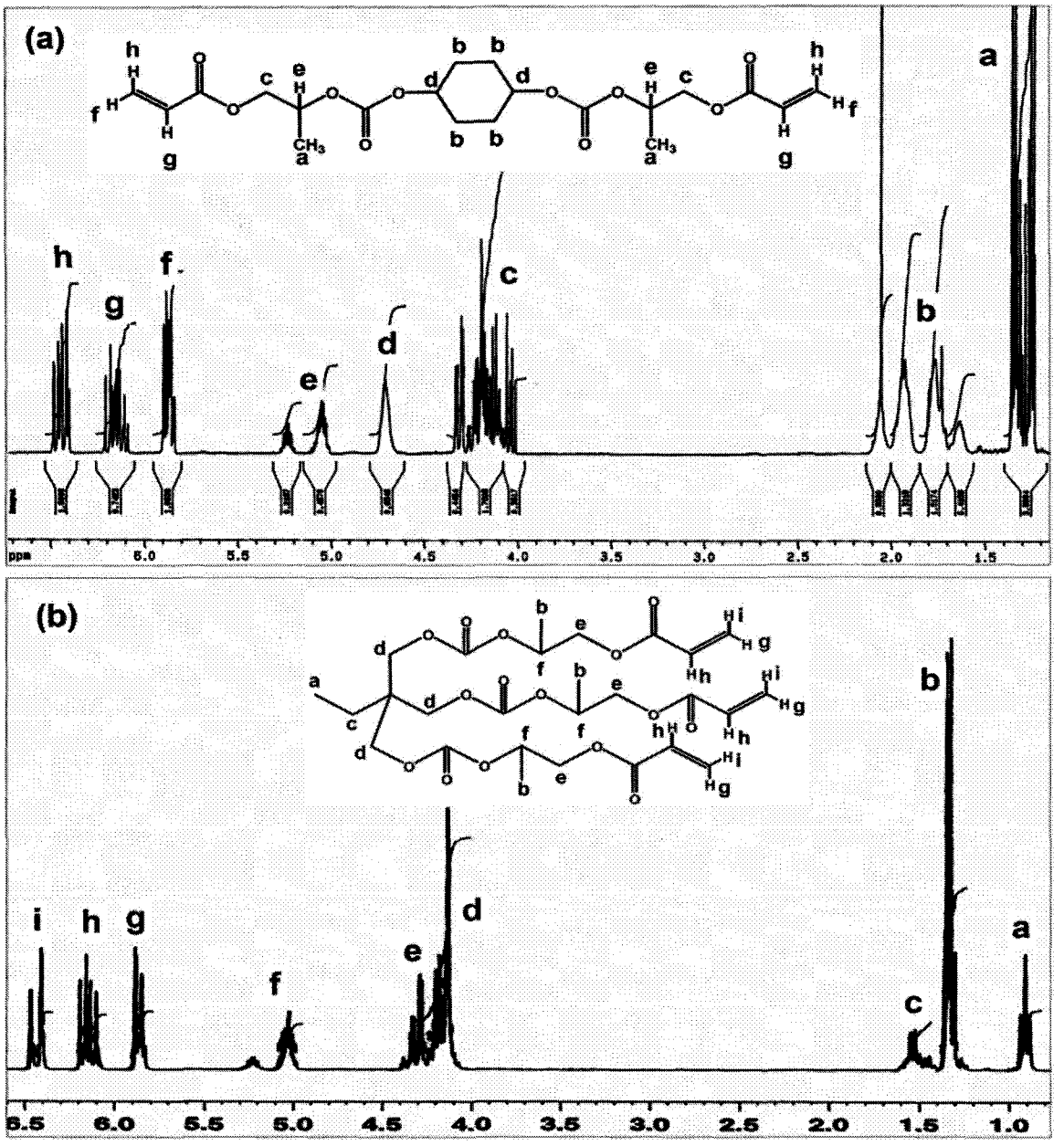

Figure IV.7. ^{1}H NMR spectra (300 MHz, $CDCl_3$) of (a) **IV-9** and (b) **IV-10**

The ^{1}H and ^{13}C NMR and IR spectra of **IV-9** and **IV-10** are consistent with their expected structures. The IR spectra showed the characteristic bands of the carbonate (C=O, 1740 cm^{-1}, C-O, 1261 cm^{-1} for **IV-9**; C=O, 1747cm^{-1}, C-O, 1266 cm^{-1} for **IV-10**) and acrylate (C=C, 1638 cm^{-1}; C=O, 1713 cm^{-1}). The ^{1}H-NMR spectra showed the vinyl

protons at 5.85-5.89 ppm, 6.10-6.19 ppm and 6.40-6.47 ppm (Figure IV.7). Both compounds are quite stable without noticeable changes in properties after storage in fridge over 2 years.

The photoinduced cross-linking experiments of **IV-9** and **IV-10** as a potential TD-cross-linker were carried out by using azobisisobutyronitrile (AIBN) as a photoinitiator. A thin films of both compounds containing 2 wt.% AIBN were cast on a NaCl plate and irradiated with 365-nm UV light followed by post-baking. The cross-linking process was monitored by FT-IR. The successful cross-linking was verified by observing the disappearance of the band at 1637 cm^{-1} (Figure IV.8) and the solubility changes of photo-irradiated films (completely insoluble in any organic solvents). Furthermore, after irradiation and post-baking, the onset temperature for initial weight loss increased from 87 °C to 201 °C for **IV-9**, indicating the formation of cross-linked network.

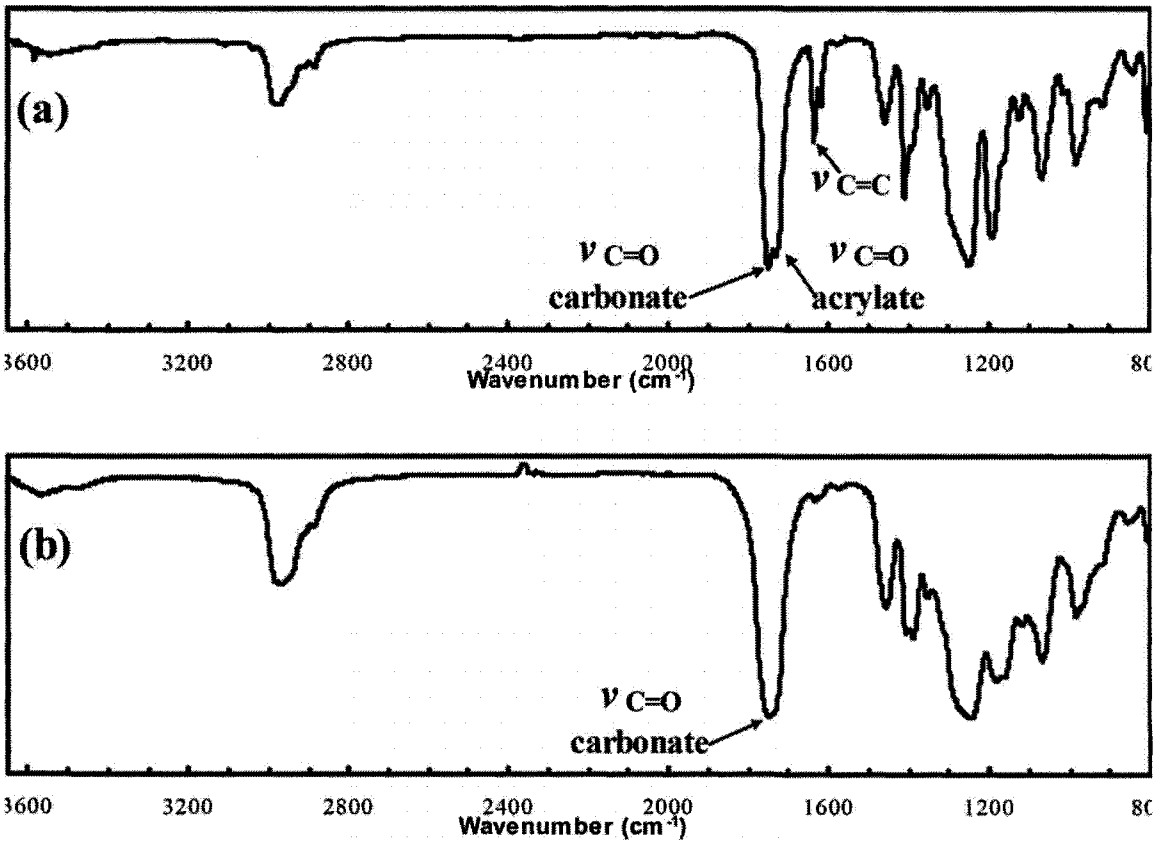

Figure IV.8. IR spectra changes of **IV-9** containing 2 wt% AIBN upon irradiation at 365-nm UV light, (a) before irradiation, (b) after irradiated (60 mJ/cm^2 at 365 nm) and post-baking (3 min at 80 °C)

The cross-linked **IV-9** and **IV-10** were studied by thermogravimetric analysis (TGA) under nitrogen at a heating rate of 10 °C/min. Figure IV.9 showed the TGA traces of cross-linked **IV-9** and **IV-10**. The onset temperatures for initial weight loss of cross-linked **IV-9** and **IV-10** were at 201 and 218 °C, respectively. According to the TGA data, there are two degradation stages (300-340 °C and 370-440 °C) in each network. In the first stage (300-340 °C), the weight-loss rates of cross-linked **IV-9** and **IV-10** were the same (-0.8 %/°C). This suggests that the cleavage of carbonate bonds takes place mainly during this stage. The activation energy (E_a) of **IV-9** was calculated to be lower than that of **IV-10** (145.3 vs. 176.2 KJ/mol), according to Chang's method.[29] This difference can be

explained by their chemical structures. The network of **IV-9** has two thermally labile secondary carbonate bonds per repeat unit, while **IV-10** has only one.

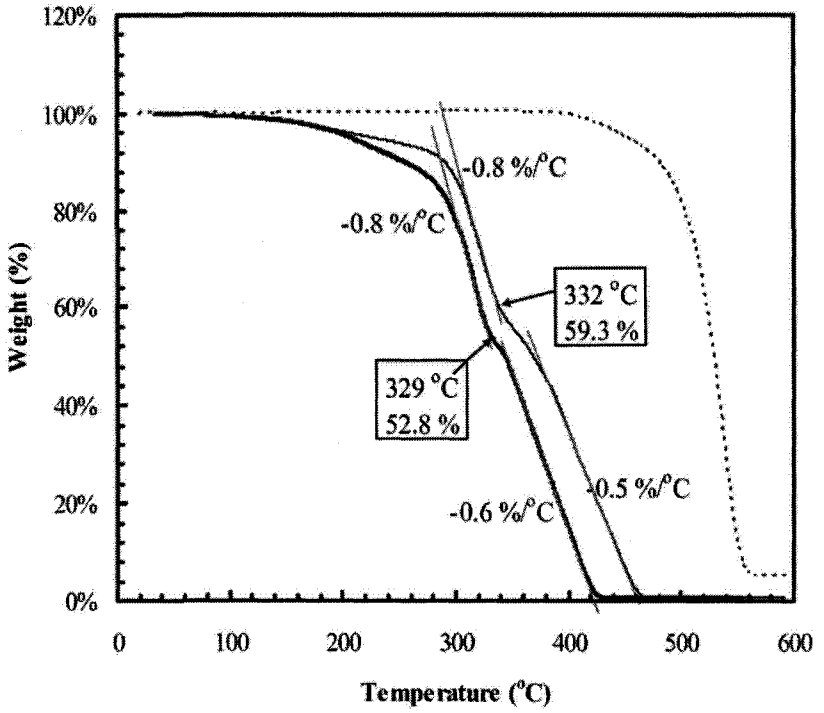

Figure IV.9. TGA traces of cross-linked **IV-9** (*Bold Line*), **IV-10** (*Solid Line*) and trimethylolpropane triacrylate (TMPTA) (*Broken Line*) under nitrogen with a heating rate of 10 °C/min

At the end of the first degradation stage, the residual weight of cross-linked **IV-9** was 52.8% at 329 °C. The lost weight corresponds to the loss of carbon dioxide and the corresponding diol (53% by weight), suggesting complete cleavage of carbonate linkages in cross-linked **IV-9** (Figure IV.10). The residual weight of cross-linked **IV-10** was 59.3% at 332 °C, being slightly higher than the expected value of 56% for the evolution of carbon dioxide and the corresponding triol. This suggests that not all the three carbonate linkages in cross-linked **IV-10** decomposed. In the second stage (370-440 °C), **IV-9** had a

higher degradation rate than **IV-10** (-0.6 vs. -0.5 %/°C), being acceptable if considering that **IV-9** had been reduced to linear oligmers and **IV-10** still was partially crosslinked.

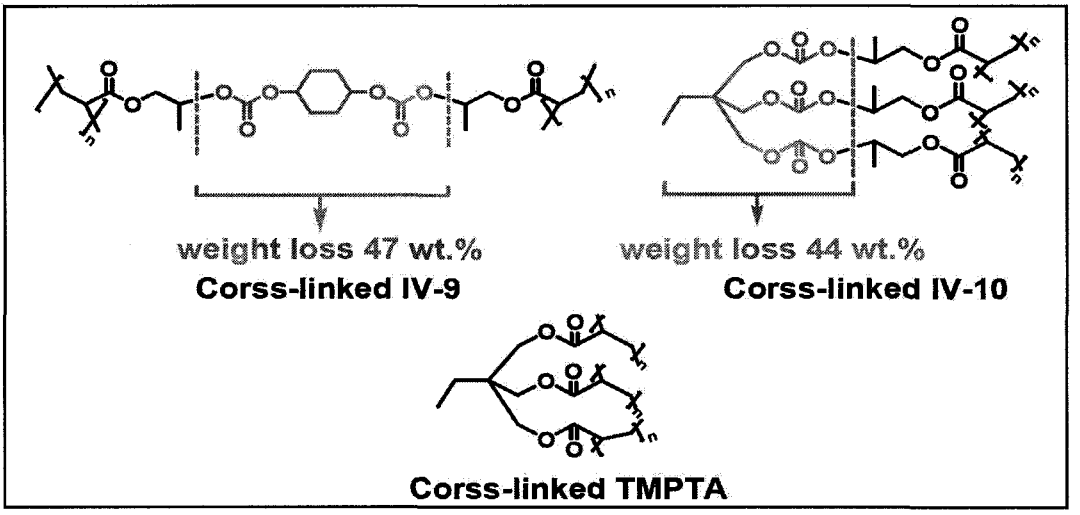

Figure IV.10. Calculation of weight loss in cross-linked **IV-9**, **IV-10** and TMPTA at 300-350 °C by thermal cleavage of carbonate linkages

Both cross-linkers **IV-9** and **IV-10** are thermally degradable in an inert atmosphere, with the residual weight less than 1 wt.% below 450 °C. Thus, their clean-burn-off temperatures are 100 °C below the softening temperature of conventional float glass sheet (~550 °C), making them suitable for the development of new photoimageable conductor pastes. In comparison, commercial acrylate cross-linkers, such as TMPTA, leave 12 wt.% char-like residues even at 550 °C.

IV.2.3 Synthesis and Characterizations of Functionalized Polycarbonates

IV.2.3.1 Synthesis

A series of functionalized polycarbonates **PC-1~PC-16** were synthesized by the

polycondenzation of bis-chloroformate and diol (Scheme IV.11) in acetonitrile and characterized by GPC, DSC and spectroscopic methods (Table IV.2). N-methyl imidazole (MIM) was added dropwise during the polymerization at such a rate that the insoluble chloroformate-MIM complex was not accumulated in a large quantity. The polymerization was monitored by IR (carbonyl peak at 1770 cm^{-1} and peak at 1160 cm^{-1} for the ether) and viscosity changes. The reaction solution became viscous after 2 h at 60 °C. The MIM HCl salt was easily separated by washing with warm toluene or ethyl acetate. The complete removal of salt can be verified by the absence of signals at 6.8-7.3 ppm in the ^1H NMR spectrum. The polymers were then purified by re-precipitation in water and methanol.

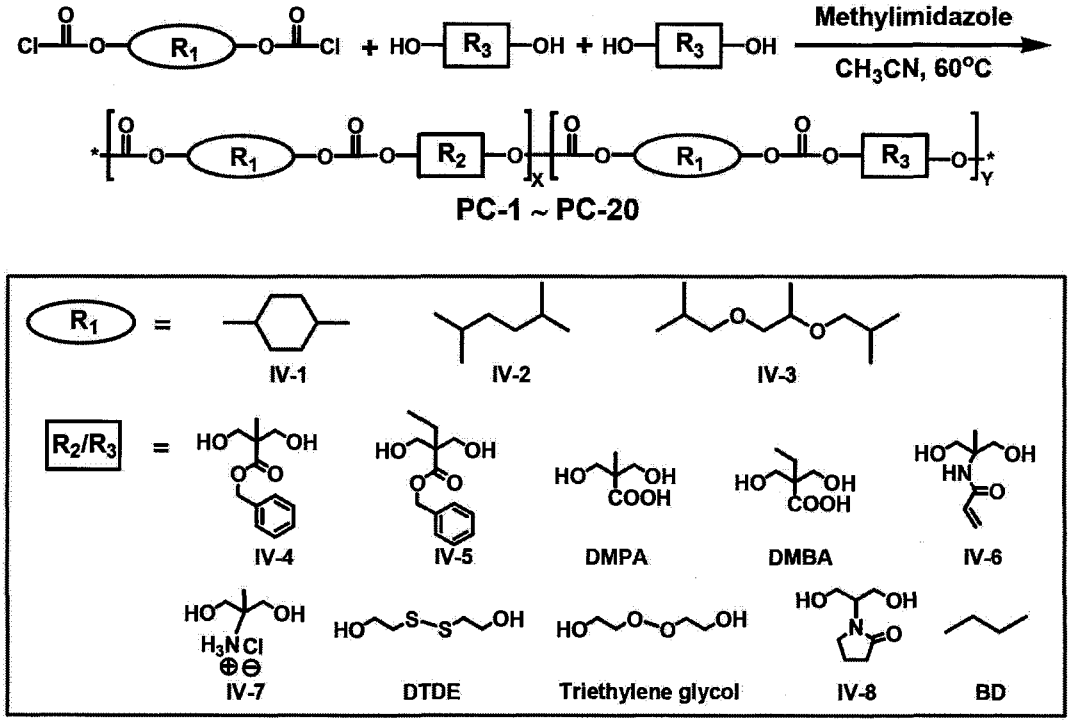

Scheme IV.11. Synthesis of functionalized polycarbonates **PC-1~PC-16**

Table IV.2. Characterization of functionalized polycarbonates **PC-1~PC-16**

Polymers		Monomer		M_w[a] ×10^3	T_g (°C)[b]	Content of Functionality
		Bis-Chloroformate	Diol(s)			
						[acrylate][c]
Cross-linkable PC	**PC-1**	IV-1	IV-6 (20%) + BD (80%)	11.2	32	18.9%
	PC-2	IV-1	IV-6 (10%) + BD (90%)	10.8	30	9.7%
	PC-3	IV-1	IV-6 (5%) + BD (95%)	10.3	30	4.6%
						Acid Number[d]
Aqueous developable PC	**PC-4**	IV-1	IV-4	8.9	-	-
	PC-5	IV-1	IV-5	9.4	-	-
	PC-6	IV-1	DMPA	7.8	72	185
	PC-7	IV-1	DMBA	8.1	68	177
	PC-8	IV-2	DMPA	9.4	17	184
	PC-9	IV-2	DMPA (80%) + BD (20%)	9.2	15	145
	PC-10	IV-2	DMPA (50%) + BD (50%)	9.7	12	89
	PC-11	IV-3	DMPA	13.2	5	136
						[disulfide][f]
	PC-12	IV-1	DTDE	11.5	46	100%
						[pyrrolidinone][g]
Metal binding PC	**PC-13**	IV-1	IV-8	-	58	93%
	PC-14	IV-1	IV-8 (10%) + BD (90%)	-	31	8%
						[amine][e]
	PC-15	IV-1	IV-7	6.7	45	91%
Reference PC	**PC-16**	IV-1	BD	15.7	28	-

[a] Measured by GPC in $CHCl_3$ and calibrated with polystyrene standards. [b] Measured by DSC with a heating rate of 10 °C/min. [c,e,f] Measured by ratio of integration of ^{1}H NMR peaks. [d] Measured by titration of polymer aqueous solution with NaOH. [g] Measured by ratio of intensity of IR peaks.

IV.2.3.2 Solubility and Glass transition Temperature

All the polycarbonates had a good solubility in acetonitrile. Polycarbonates containing carboxylic acid, amide or amine groups were also soluble in $CHCl_3$, THF, acetone, DMF and DMSO. The glass transition temperatures (T_g) of polymers containing the rigid cyclohexane moiety (**IV-1**) are normally 20 °C higher than other polycarbonates containing acyclic units. Polycarbonates containing acid or amide groups had a higher T_g (30-50 °C) due to the hydrogen bonding. In comparison, polymers derived from bis-chloroformates **IV-2** and **IV-3** are more flexible and consequently have a lower T_g in the range of 0-10 °C. They exist as colorless viscous liquids at room temperature.

IV.2.3.3 Determination of Functional Groups and Thermal Analysis

The distribution or total number of the functionality in polycarbonates can be adjusted using 1,4-butanediol (BD) as a co-monomer or a spacer. The use of BD does not affect the thermal degradation behaviour of the resulting polymers. The copolymer resulted from BD and **IV-1** was confirmed to be thermodegradable.[15] BD like other diol monomers is a primary alcohol and thus the resulting polycarbonates should undergo the same degradation process. Accordingly, the effect of a functional group on thermal degradation can be studied by comparing TGA data of a series of polymers containing a different amount of BD spacer, such as **PC-1~PC-3**. Copolymer **PC-16** with no functionality was prepared as a reference.

Thermal degradation of the functionalized polycarbonates is studied by

thermogravimetric analysis (TGA). From TGA data, M_{res}, T_d, $T_{burn\text{-}off}$, and activation energy (E_a) can be obtained. These data will allow for establishment of the relationship between the functionality and thermal degradation property and understanding of the influence of functional groups on the reaction mechanism and degradation process. In particular, by exploring the M_{res} changes of a series of polycarbonates containing different amounts of the same functional group, the upper limit content of this functional group which still allows the host polymer to be thermodegradable (M_{res} <1 wt.%) can be obtained. This allows for recommendation of a possible formulation of polycarbonates as sacrificial vehicles.

Polycarbonates Containing Acrylate Groups

Introduction of acrylate groups into polycarbonates was confirmed by FT-IR and ^1H NMR spectroscopic methods. **PC-1~PC-3** displayed carbon-carbon double bond peaks at 1639 cm^{-1} in their IR spectra, corresponding exactly to the one in the diol **IV-6**. The ^1H NMR spectra of **PC-1~PC-3** showed the presence of the vinyl protons from **IV-6** at 5.75-5.79 ppm, 6.01-6.09 ppm and 6.26-6.28 ppm, further indicating the incorporation of the acrylate moiety. The actual amount of acrylate group in polymers was calculated using the integral ratio of the vinyl proton at 6.28 ppm and α–methylene proton of cyclohexane ring at 4.79 ppm. The calculated values were consistent to the feed ratio (18.9±0.3% vs. 20% for **PC-1**; 9.7±0.4% vs. 10% for **PC-2**; 4.6±0.4% vs 5% for **PC-3**).

Considering that these cross-linkable polycarbonates were firstly cured and then

burned out when they were used as sacrificial vehicles, thermal degradation of cross-linked **PC-1~PC-3** was studied by TGA. The polymers were photo cross-linked in the same way as for curing of TD-cross-linkers **IV-9** and **IV-10**. The cross-linked polymer films were insoluble in any organic solvents and the vinyl band at 1638 cm^{-1} in the IR spectra disappeared.

TGA traces of cross-linked **PC-1~PC-3** and reference polymer **PC-16** was shown in Figure IV.11. They were heated in nitrogen with a heating rate of 10 °C/min. The onset temperature for initial weight loss (T_d) and clean-burn-off temperature ($T_{burn-off}$) of cross-linked polymers were in the same level. But the ash contents (M_{res}) were greatly raised with the increasing of acrylate content (Table IV.3).

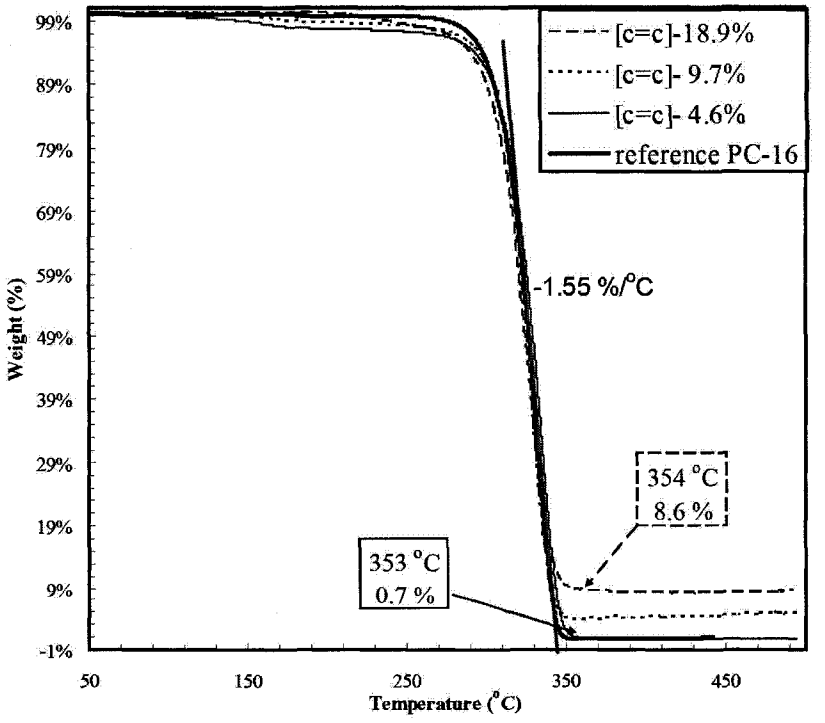

Figure IV.11. TGA traces of cross-linked **PC-1** (*Broken Line*), **PC-2** (*Dotted Line*), **PC-1** (*Solid Line*) and **PC-16** (*Bold Line*) under nitrogen with a heating rate 10 °C/min

Table IV.3. Thermodegradation properties of cross-linkable polycarbonates **PC-1, 2, 3**

Polymer	[acrylate][a] (mol%)	M_{res} (wt.%)	T_d (°C)	$T_{burn\text{-}off}$ (°C)	$R_{weight\ loss}$ (wt.%/°C)	E_a[b] (KJ/mol)
PC-1	18.9±0.3	0.7	292	352	-1.54	175±2
PC-2	9.7±0.4	3.8	298	354	-1.53	173±1
PC-3	4.6±0.4	8.6	303	354	-1.55	178±1
PC-16	0	0.0	289	348	-1.56	169±2

[a] Measured by integration ratio of ^{1}H NMR peaks. [b] Calculated according to Chang's method.[29]

Polycarbonates Containing Acidic Groups

In **PC-4** and **PC-5**, the carboxylic acid groups were protected as benzyl esters. The benzyl groups were removed later from the polymers by hydrogenation. Figure IV.12 is the ^{1}H NMR spectrum of **PC-4** after deprotection and clearly shows the absence of aromatic (7.31 ppm) and benzylic (5.07 ppm) protons after hydrogenation. Likewise, the peak denoted as **a** (-CH_3) is shifted downfield. In the IR spectrum of deprotected **PC-4**, a broad peak appears at 3300 cm^{-1} indicating the presence of carboxylic acid groups. GPC of **PC-4** and **PC-5** showed no change in molecular weights and molecular weight distributions before and after deprotection.

PC-6 and **PC-7** were prepared by direct polycondensation without the protection of acid groups. The IR spectra of these polymers showed the characteristic acid bands centered at 3350 cm^{-1}, and their ^{1}H NMR spectra were identical to those of deprotected **PC-4** and **PC-5**. This suggests that the acid groups are inert during the polymerization. Thus, **PC-8~PC-11** were all prepared by the direct polycondensation.

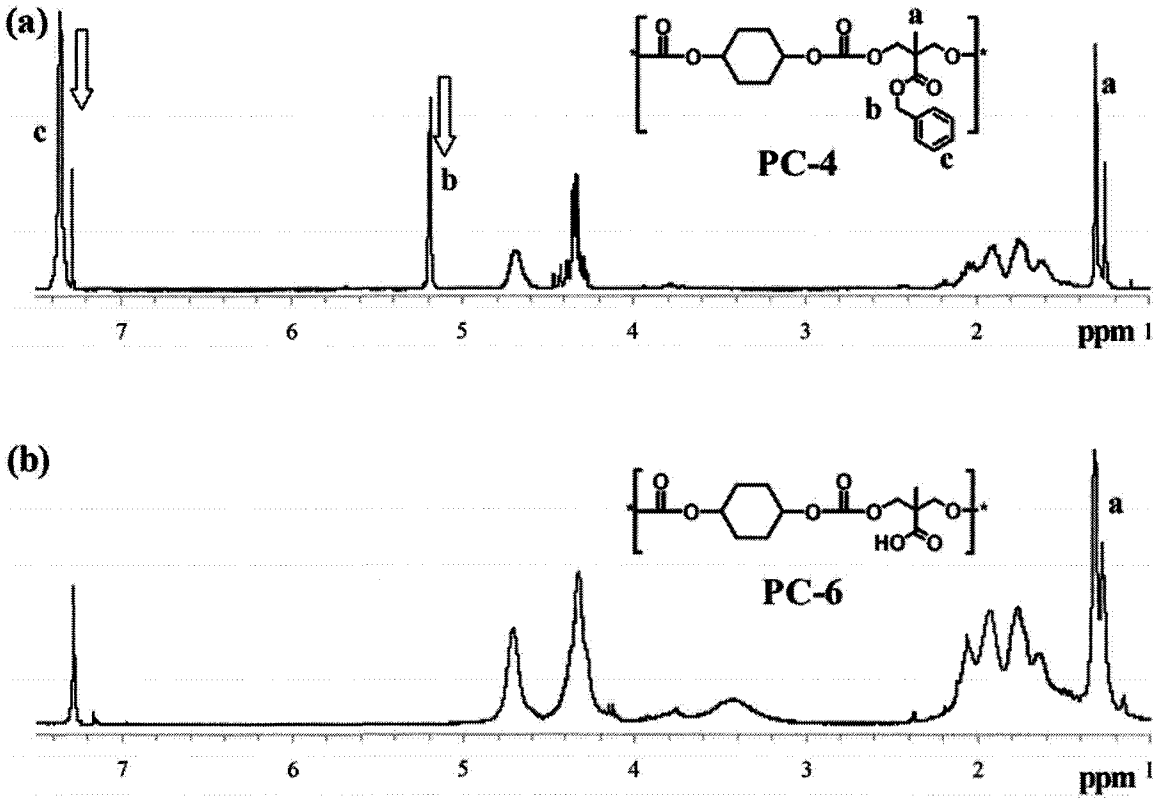

Figure IV.12. ^{1}H NMR spectra (300 MHz, $CDCl_3$) of **PC-4** (a) before and (b) after deprotection

The actual content of carboxylic acid groups in the **PC-6~PC-11** was measured by acid-base titration. The polymer was suspended in distilled water and titrated with 0.1 M NaOH solution. Phenolphthalein was used as an indicator. During the titration, the polymer was gradually dissolved and then the colorless solution turned red, indicating the equivalence point. The acid number of a polymer is defined as the mass of potassium hydroxide (KOH) in milligrams that is required to neutralize one gram of chemical substance. Thus, the amount of consumed NaOH in titration was normalized and converted to the mass of KOH. The acid numbers of **PC-6~PC-11** were around 89~185 ± 3. These values are just located in the desired range of 85-187 for aqueous developable

polymers suitable for use in photo-imaging conductor pastes. Furthermore, thermal degradation of **PC-6~PC-11** was studied by TGA (Table IV.4). All these acidic polymers were able to be cleanly burned out below 420 °C in nitrogen. Thus, **PC-6~PC-11** were all applicable as sacrificial vehicles.

Table IV.4. Thermodegradation properties of **PC-6~PC-11**

Polymer	Acid Number [a]	M_{res} [b] (wt.%)	T_d [b] (°C)	$T_{burn-off}$ [b] (°C)	$R_{weight\ loss}$ (wt.%/°C)	E_a [c] (KJ/mol)
PC-6	185±3	0.9	261	335	-1.21	155±2
PC-7	177±3	0.7	258	329	-1.23	153±2
PC-8	184±4	0.6	212	317	-1.15	138±1
PC-9	145±3	0.5	245	324	-1.17	142±1
PC-10	89±4	0.4	248	329	-1.22	148±2
PC-11	136±3	0.6	249	348	-1.13	166±3

[a] Measured by acid-base titration. [b] Measured by TGA with a heating rate of 10 °C/min in nitrogen. [c] According to Chang's method.[29]

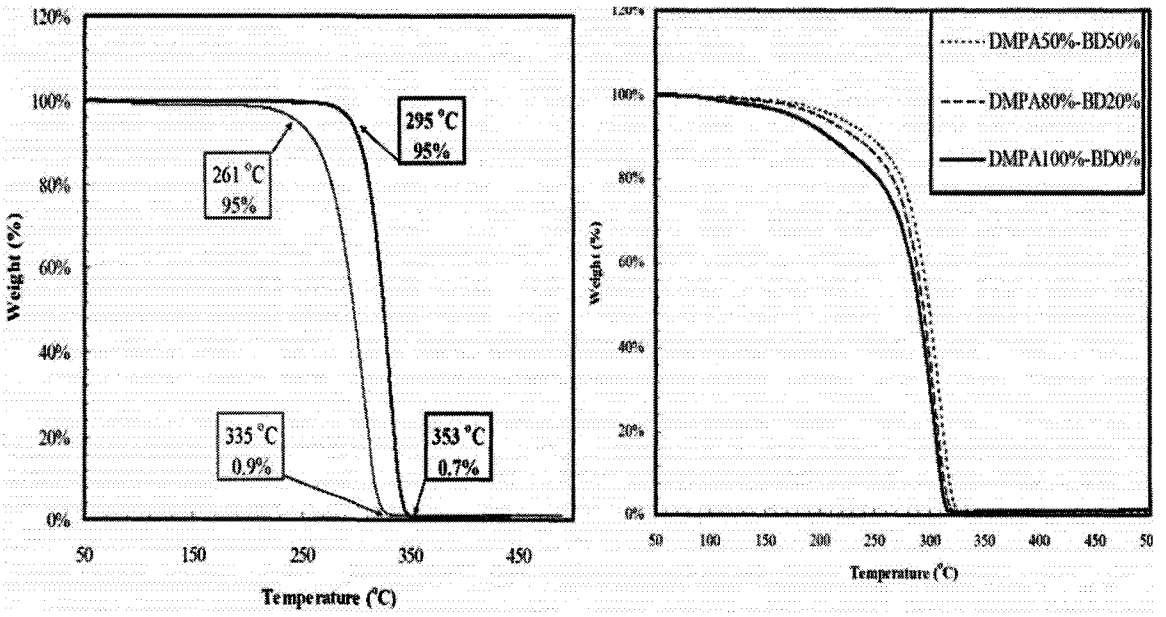

Figure IV.13. TGA traces of (left) **PC-6** (*Solid Line*) and **PC-16** (*Bold Line*), (right) **PC-8** (*Bold Line*), **PC-9** (*Broken Line*) and **PC-10** (*Dotted Line*) under nitrogen with a heating rate 10 °C/min

The effect of the acid group on thermal degradation of polycarbonates was studied by comparing TGA data of **PC-6** with reference **PC-16**. As shown in Figure IV.13 (left), **PC-6** was thermally degraded about 20 °C lower than **PC-16**, indicating that the pendant acid group can facilitate the degradation (see **PC-8~PC-10** in Figure IV.13). The results are consistent to the study on the acid-catalyzed thermolytic depolymerization of polycarbonates by Frechet et al,[30] in which the thermal cleavage of carbonates proceeds through a polar transition state stabilized by the carboxylic acids.

Polycarbonates Containing Metal-binding Groups

The presence of disulfide groups in polycarbonate **PC-12** was verified by NMR spectroscopy. The peaks at 3.02 and 4.40 ppm are assigned to the methylene protons in the disulfide diol segment. The disulfide content was determined from the ratio of integration of peaks at 3.02 and 4.83 ppm assigned to the methylene protons in the disulfide diol segment and α–methylene protons in the cyclohexane ring, respectively. The actual content of disulfide was found to be same as the feed ratio. As shown in Figure IV.14, the disulfide groups seem to slow down a bit the degradation process of polymer relative to reference **PC-16**. The weight loss rate was lower for **PC-12** (-1.01%/°C) than for **PC-16** (-1.55%/°C). The small change can be explained by low volatility of the thermolysis products resulted from **PC-12**, e.g., dienes and diols.[8]

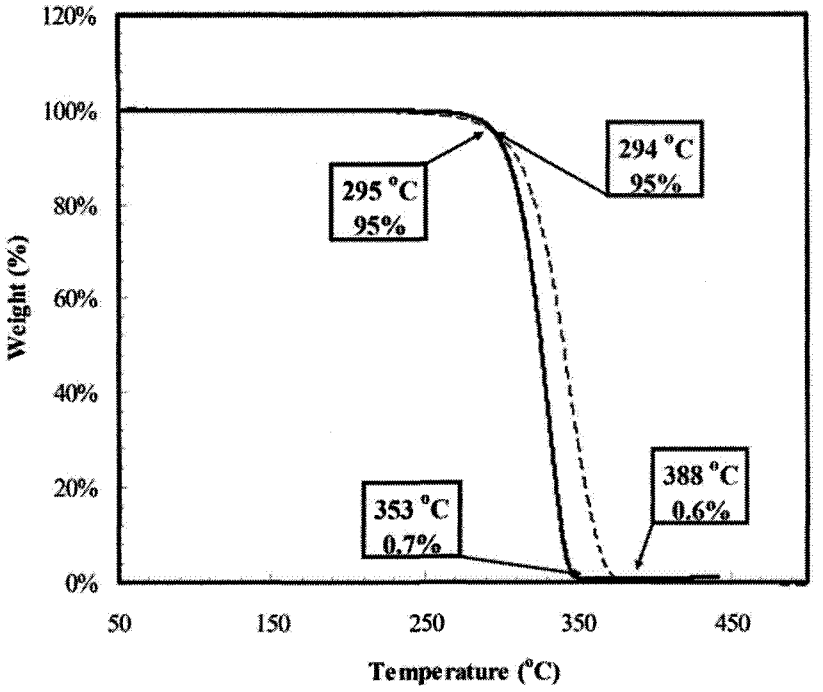

Figure IV.14. TGA traces of **PC-12** (*Solid Line*) and **PC-16** (*Bold Line*) in nitrogen with a heating rate 10 °C/min

As shown in Table IV.5, dienes or diols containing disulfide groups have higher boiling points and thus are less volatile. Nevertheless, **PC-12** can be cleanly burned out (M_{res} = 0.6%) at 388 °C in nitrogen and thus is applicable as a sacrificial material.

Table IV.5. Boiling points of thermolysis products from **PC-12** and **PC-16**

Compound				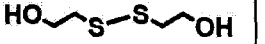
bp	-4.5 °C	-	230 °C	158 °C /3.5mmHg

Introduction of the pyrrolidinone groups into polycarbonates **PC-13** and **PC-14** was confirmed by IR and NMR spectroscopy. The IR spectra of these polymers show the characteristic carbonyl band at 1686 cm^{-1} for the pyrrolidinone group. The ^1H NMR spectra of **PC-13** and **PC-14** display the peaks at 2.20, 2.40 and 3.48 ppm, assigned to the

methylene protons on the pyrrolidinone ring. In order to quantify the content of pyrrolidinone groups in **PC-13** and **PC-14**, IR spectroscopy was used to establish a calibration curve using the intensity of peak at 1686 cm^{-1} versus concentration of monomer **IV-8** in the reference polycarbonate **PC-16**. From the calibration curve, the content of pyrrolidinone groups in **PC-13** and **PC-14** were determined to be 93% and 8%, respectively, quite close to the feed ratio in polymerization. The TGA study indicated that polymers containing the pyrrolidinone ring had the same T_d and same initial weight loss rate as the reference **PC-16** (Figure IV.15). This means that the presence of pyrrolidinone groups does not affect thermal cleavage of carbonate bonds.

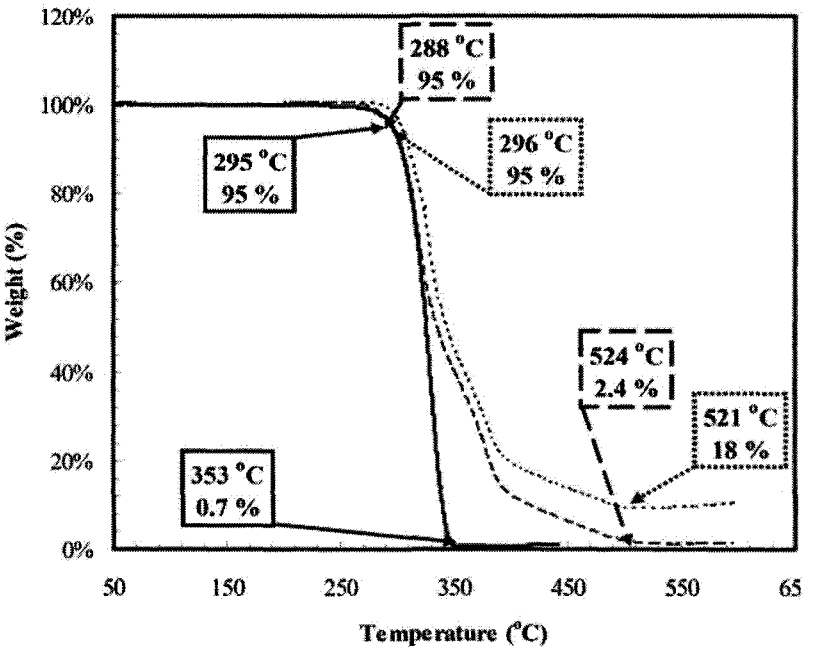

Figure IV.15. TGA traces of **PC-13** (*Dotted Line*), **PC-14** (*Broken Line*) and **PC-16** (*Bold Line*) in nitrogen with a heating rate 10 °C/min

However, due to low volatile by-products containing pyrrolidinone the degradation proceeded slowly for **PC-13** and **PC-14** in comparison with **PC-16**. **PC-14** containing

only 8% pyrrolidinone groups still left more than 2 wt.% of char-like residue after degradation. Thus, **PC-13** and 14 can not be used as sacrificial vehicles.

The amine group was protected as its hydrochloride salt in **PC-15**. The amine function in **PC-15** can be freed by extensive washing with 10% Na_2CO_3 solution, as evident by a negative test using $AgNO_3$. The IR spectrum of **PC-15** shows the N-H stretching centered at 3450 cm^{-1}. The amine content was determined by ^1H NMR from the ratio of the methylene proton in the amine diol segment at 4.31 ppm and α–methylene proton of the cyclohexane moiety at 4.79 ppm and found to be close to the feed ratio (91% vs. 100%). The TGA study of **PC-15** indicates that this polymer is thermally degradable, leaving almost no residue (0.8 wt.%) at 339 °C in nitrogen. Its thermolysis proceeded at temperature of 40 °C lower than that of the reference **PC-16** (Figure IV.16).

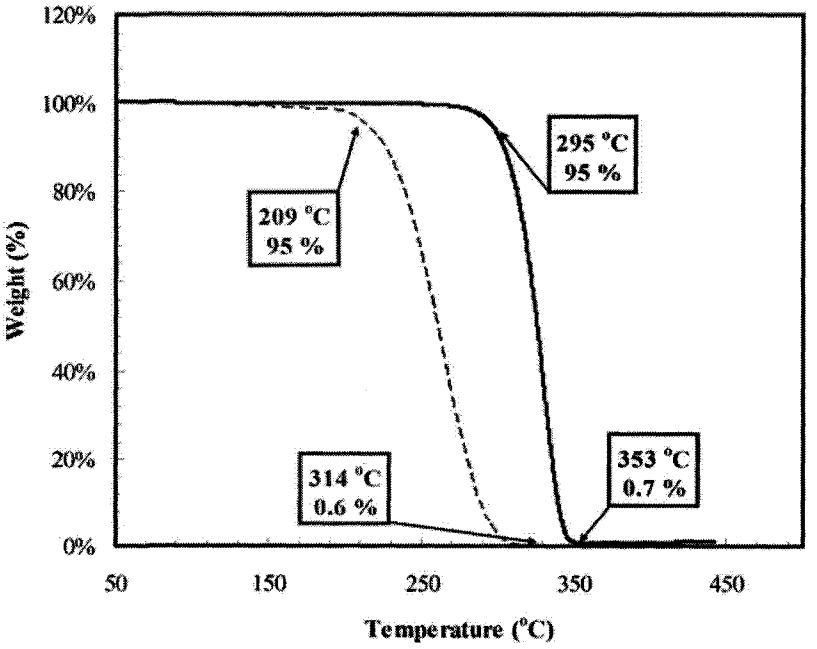

Figure IV.16. TGA traces of **PC-15** (*Broken Line*) and **PC-16** (*Bold Line*) under nitrogen with a heating rate 10 °C/min

Thus, the amine group can act as a base and also facilitates thermal degradation of polycarbonates. Comparing with the acid amplification (Figure IV.13, left), the base amplification seems to be much more efficient (40 °C drop by amine group vs. 20 °C decrease by carboxylic acid groups), despite lower molecular weight of **PC-15** than **PC-16** (6.7×10^3 vs 1.6×10^4).

IV.3 Functionalized Polycarbonates as Sacrificial Vehicles in Photoimageable Silver Pastes

The sacrificial vehicles in photoimageable conductor pastes generally consist of (1) 70-75 wt.% aqueous-developable acidic polymer, (2) 15-20 wt.% of photo-cross-linkable components and (3) 10 wt.% of metal-binding additives. Based on thermolysis properties of the prepared functional polycarbonates, a suitable formulation (**SV-1**) of sacrificial vehicles can be recommended (Figure IV.17). The functionalized TD-polycarbonate and trifunctional cross-linker **IV-10** were selected.

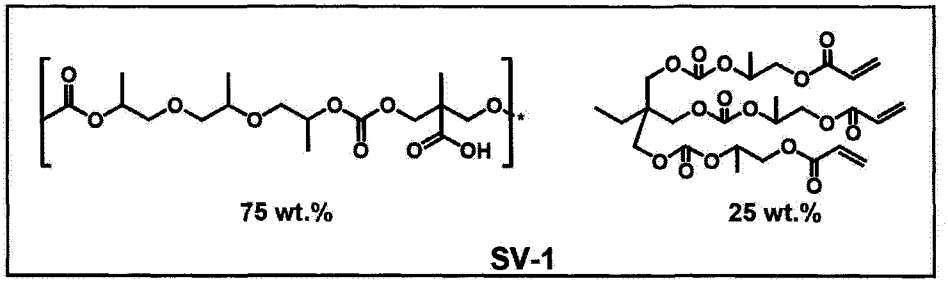

Figure IV.17. Sacrificial vehicle **SV-1**

Although **PC-3** is thermally degradable, its low cross-linker content (less than 5% of acrylate) may not provide enough crosslinked networks to hold a high loading of metal powders. **PC-11** was chosen because of its higher acid content and metal-binding ability.

Thus, sacrificial vehicle **SV-1** is composed of 75 wt.% of **PC-11** and 25 wt.% of **IV-10**.

The preparation of photoimageable Ag pastes is as follows. **SV-1** was mixed with silver nano-powders at the ratio of 3:7 by weight in a motor. AIBN was added as photoinitiator. Acetonitrile and isopropanol (2:1, v/v) were used as solvent and lubricant. The paste was then cast on a glass plate and dried in an oven at 50 °C. The resulted film with a thickness of 5 μm was exposed to 365-nm UV light, followed with post-baking. The patterns were then developed with 0.5% Na_2CO_3 aqueous solution. The commercial paste available from DuPont was used as a reference and treated in the same procedure.

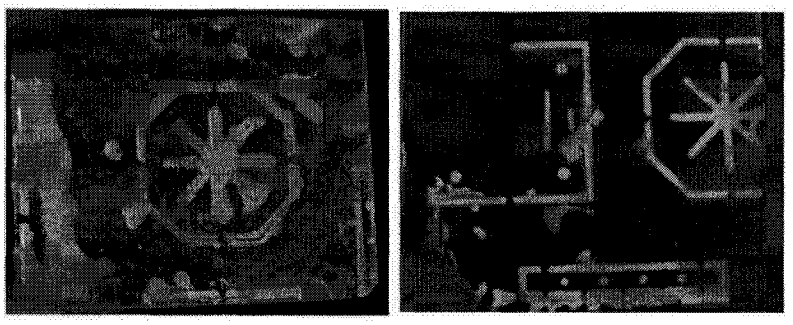

Figure IV.18. Photo-images of Ag patterns using **SV-1** (left) and DuPont paste (right)

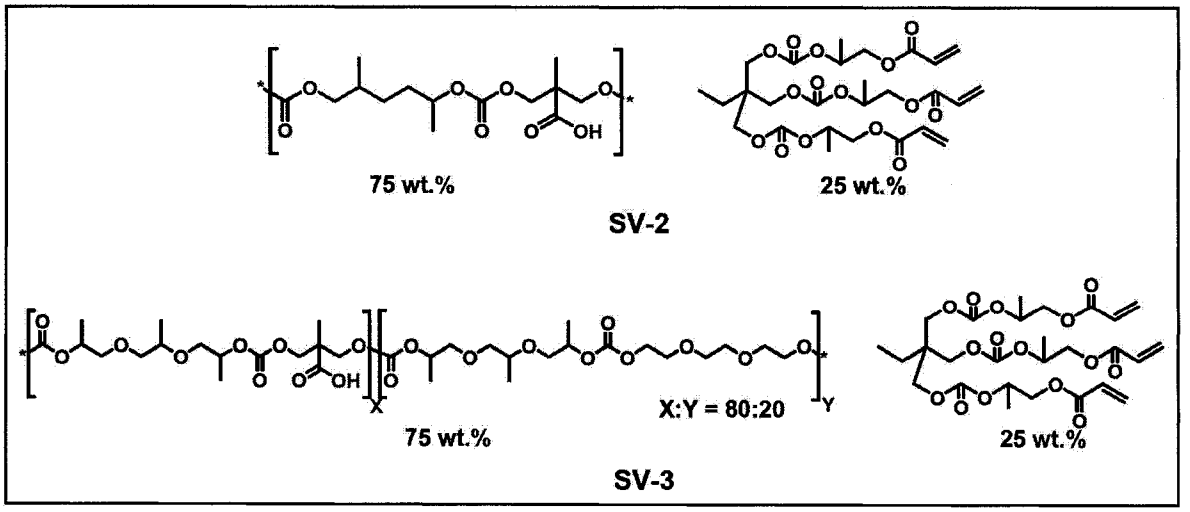

Figure IV.19. Sacrificial vehicle **SV-2** and **SV-3**

As shown in Figure IV.18, the quality of Ag patterns formed by **SV-1** is rather poor comparing with the patterns formed by DuPont paste. The unexposed part can not be cleanly washed off, which might be due to low acid content or less water soluble and poor hydrophilicity of **SV-1**. Accordingly, **SV-2** and **SV-3** were proposed (Figure IV.19).

In **SV-2**, **PC-6** possessing a high acid number (185 for **PC-6** vs. 136 for **PC-11**) was used. In **SV-3**, 20% of PEG segment was introduced to increase hydrophilicity. However, the patterns formed by **SV-2** were even worse (Figure IV.20). Only **SV-3** gave the patterns (Figure IV.21) with the same quality as the one from DuPont paste, attributing the PEG segment. Thus, a polycarbonate-based photoimageable Ag conductor paste has been demonstrated.

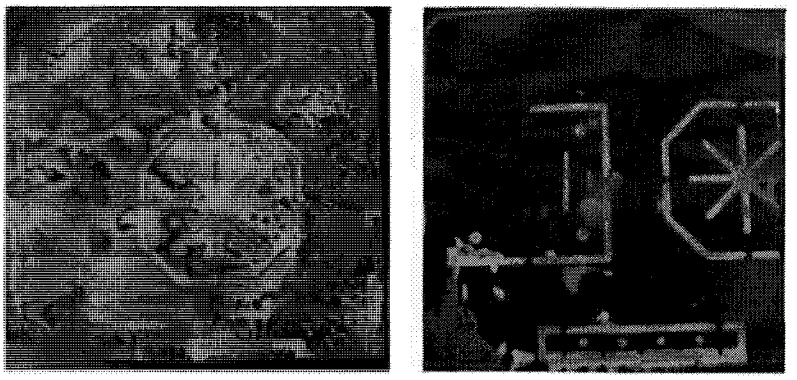

Figure IV.20. Photo-images of Ag patterns by **SV-2** (left) and DuPont paste (right)

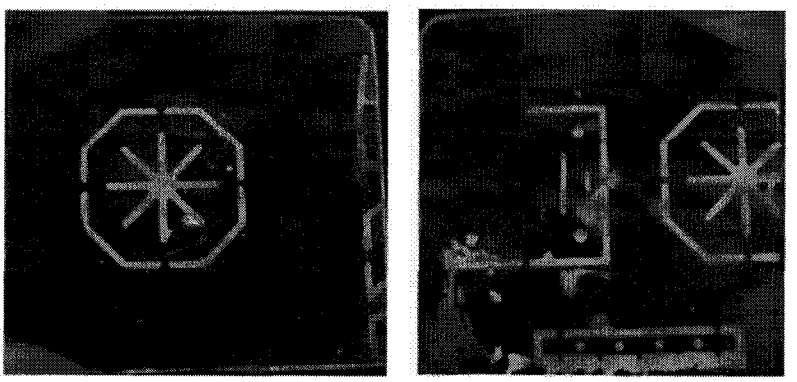

Figure IV.21. Photo-images of Ag patterns by **SV-3** (left) and DuPont paste (right)

One important advantage of this new paste is its low burn-off temperature. As shown in Figure IV.22, **SV-3** can be completely removed at 400 °C, which is 120 °C lower than that of DuPont paste. This lower burn-off temperature allows the cheaper float glass sheet (softening temperature ~550 °C) to be used as a substrate instead of silicon wafer or specialty glass.

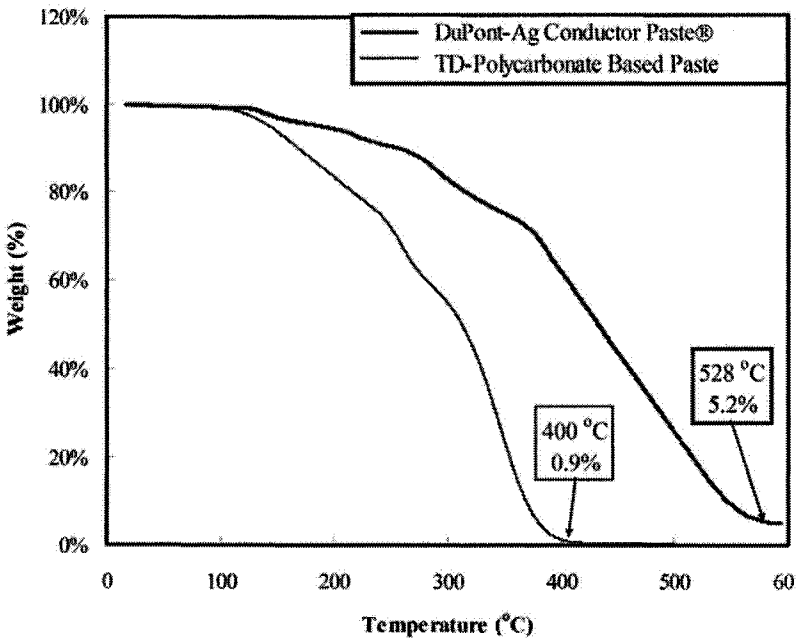

Figure IV.22. TGA traces of (left) **SV-3** (*Solid Line*) and DuPont paste (*Bold Line*) under nitrogen with a heating rate 10 °C/min

IV.4 Base-Catalyzed Thermolysis of TD-Polycarbonates: An Approach to Dry-Developing Resist Materials

To study the base amplification effect, a catalytic amount (3 wt.%) of an amine base was added into a polycarbonate, and the thermal degradation was then monitored by TGA. By comparing TGA traces of this polymer before and after adding the base, the effect of the base catalyst on thermal degradation of polycarbonates can be determined. A series of amine bases with different basicity including phenylhydrazine ($PhNHNH_2$), triethylamine

Table IV.6. The basicity of phenylhydrazine, triethylamine, DBU and TBD

Amine Bases	Phenylhydrazine[a]	Triethylamine[a]	DBU[a]	TBD[a]
pK_a (AN)	12.33	18.8	24.34	26.03

[a] pK_a Values tested in acetonitrile solution, data from reference [31]

(TEA), DBU and TBD were evaluated (Table IV.6). The goal is to identify the maximal chemical amplification effect with a catalytic amount (~3 wt.%) of amine bases, and ideally, to identify a strong base capable of lowering the thermolysis temperature of polycarbonates close to the room temperature. Thermal degradation of polycarbonates can undergo either the "back-biting" process initiated at the reactive hydroxy chain ends to form cyclic monomers or the main-chain random scission process via a syn-elimination to produce dienes and diols. Accordingly, two typical polycarbonates were selected in the study (Table IV.7) : poly(1,4-cyclohexylene carbonate) (PCHC) that only undergoes the main-chain scission and poly(propylene carbonate) (PPC) that is mainly degraded by the "back-biting" process. This allows us to determine which the degradation process was preferred in the base-catalyzed thermolysis and identify which polycarbonates were most sensitive to amine bases.

Table IV.7. Properties of polycarbonates used in base-catalyzed thermolysis study

Polycarbonates		Source	M_n	T_g (°C)[a]	$T_{burn-off}$ (°C)[c]	M_{res}[b] (wt.%)
PPC	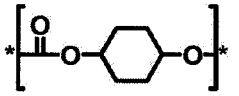	Aldrich	50,000	34	351	0.5
PCHC	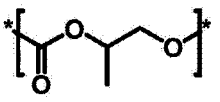	Prepared in Our Lab	16,000	112	353	0.9

[a,b] Measured by DSC and TGA with a heating rate of 10 °C/min in nitrogen.

IV.4.1 Base-Catalyzed Thermolysis of PPC

As shown in Figure IV.23, the thermolysis temperature was lowered considerably when a catalytic amount of amine base was added to PPC. The decrease in temperature is strongly related to the amine's basicity (Table IV.8). With the strongest base TBD, both the onset degradation temperature and clean-burn-off temperature of PPC were lowered by 200 °C. By adding DBU, the thermolysis temperatures of PPC dropped around 100 °C. However, tertiary amines (TEA) and phenylhydrazine showed no amplification effect. The results suggest that strong amine bases have a higher catalytic reactivity towards polycarbonate degradation (Scheme IV.12).

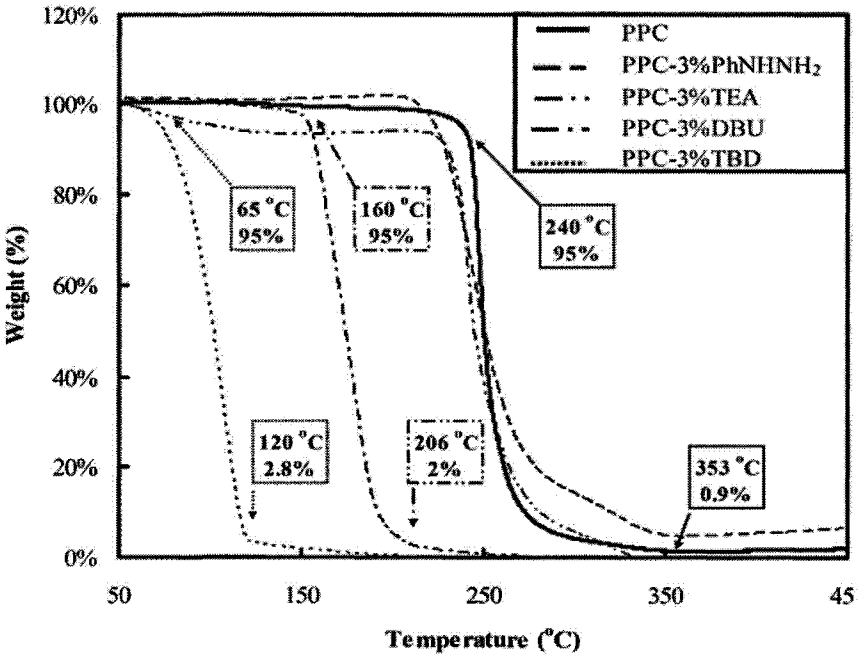

Figure IV.23. TGA traces of PPC, PPC with 3 wt.% of $PhNHNH_2$, TEA, DBU and TBD, in nitrogen at a heating rate of 10 °C/min

Table IV.8. Effect of amine bases on degradation of PPC

Bases	$^{AN}pK_a$	ΔT_d (°C)	$\Delta T_{burn-off}$ (°C)	M_{res} (wt.%)
TBD	26.03	175	233	0.3
DBU	24.34	80	150	0.7
TEA	18.8	10	0	0.9
$PhNHNH_2$	12.33	10	0	4.8

In addition, the rates of weight loss for PPC, PPC with 3 wt.% of DBU and PPC with 3 wt.% of TBD were evaluated by TGA to be -1.79%/°C, -1.74%/°C and -1.73%/°C, respectively. Since the weight loss depends on the degradation mechanism and the volatility of thermolysis products, the same rates for weight loss indicate that the base-catalyzed thermolysis goes through the same "back-biting" process as PPC and releases the same cyclic propylene carbonate. To determine the products resulted from base-catalyzed thermolysis of PPC, the degradation was monitored with real time FT-IR spectroscopy. A thin film of PPC doped with 3 wt.% of TBD was sandwiched in two NaCl plates for IR measurement before and after heating at 80 °C for 5 min and then at 120 °C for 5 min under nitrogen (Figure IV.24). The disappearing bands at 1740 and 1260 cm^{-1} indicate degradation of PPC. The newly formed intense peak at 1800 cm^{-1} is assigned to the cyclic carbonate by comparing with the authentic IR spectrum of propylene carbonate. Thus, the product generated in the base-catalyzed thermolysis of PPC was proved to be a cyclic carbonate.

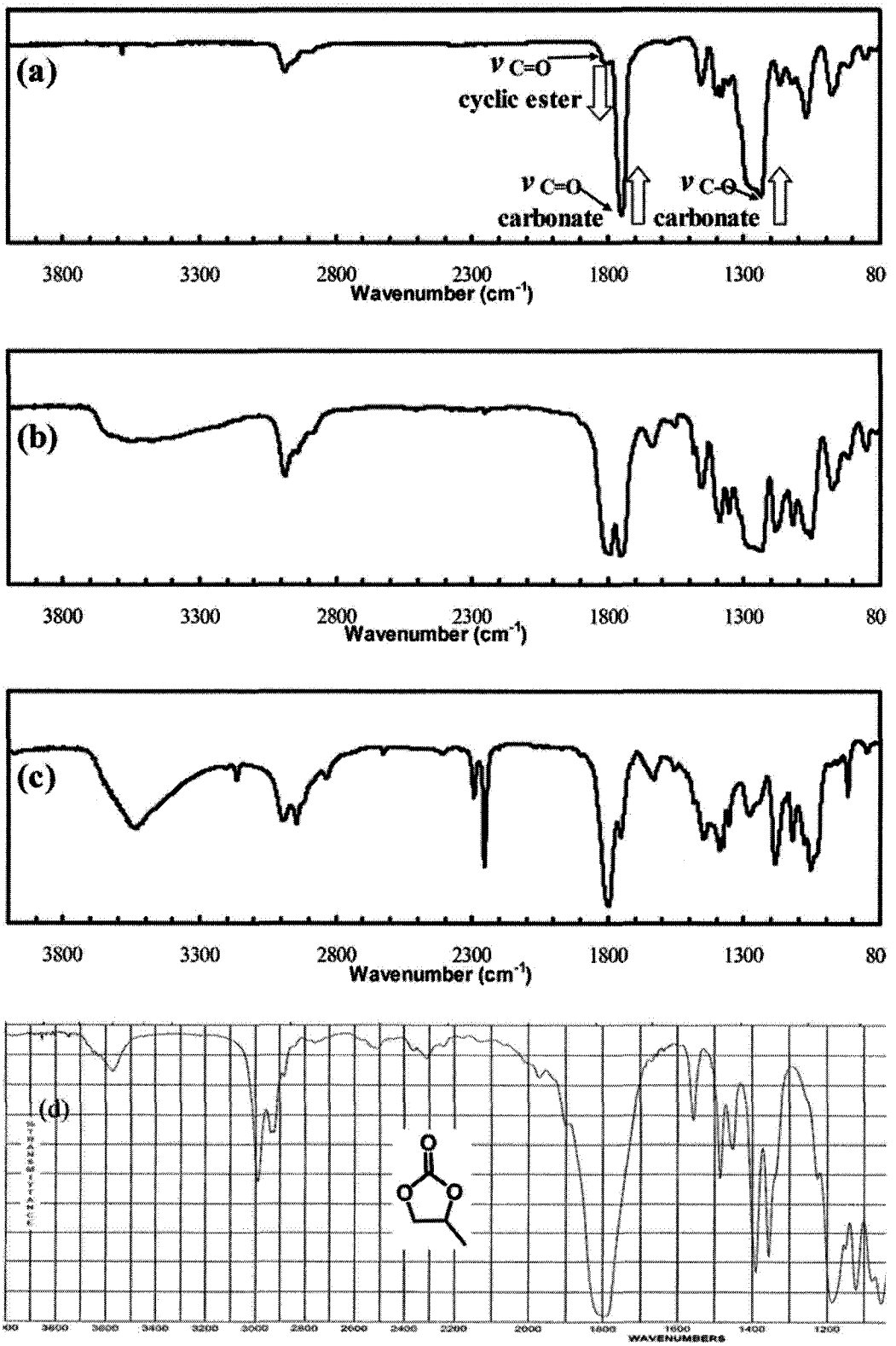

Figure IV.24. Thermolysis of PPC with 3 wt.% of TBD monitored by FT-IR, (a) before heating, (b) after heating at 80 °C for 5 min, (c) after heating at 120 °C for 5 min in nitrogen and (d) the authentic IR spectrum of propylene carbonate

To further identify the structure of this cyclic carbonate, PPC containing 3 wt.% of TBD was sealed in a tube filled with nitrogen and then heated at 120 °C for 30 min. The resulting liquid was first tested by GPC (Figure IV.25), which shows complete degradation of PPC to small molecules. After isolation and purification by column chromatography on silica gel with ethyl acetate, the product was isolated in 92% yield and identified as propylene carbonate by IR and NMR spectroscopy. The base-catalyzed thermolysis of PPC is thus believed to go through the nucleophilic attack of the imine nitrogen in DBU or TBD to the carbonyl group to produce an alkoxide that further back bites the carbonate bonds to release cyclic monomers (Scheme IV.12). Accordingly, the base amplification effect should be further enhanced in the presence of an alcohol. The strong bases including DBU and TBD should be able to deprotonate alcohols to generate alkoxides, which should be quite mobile in the polymer matrix and thus more react towards the carbonate bonds.

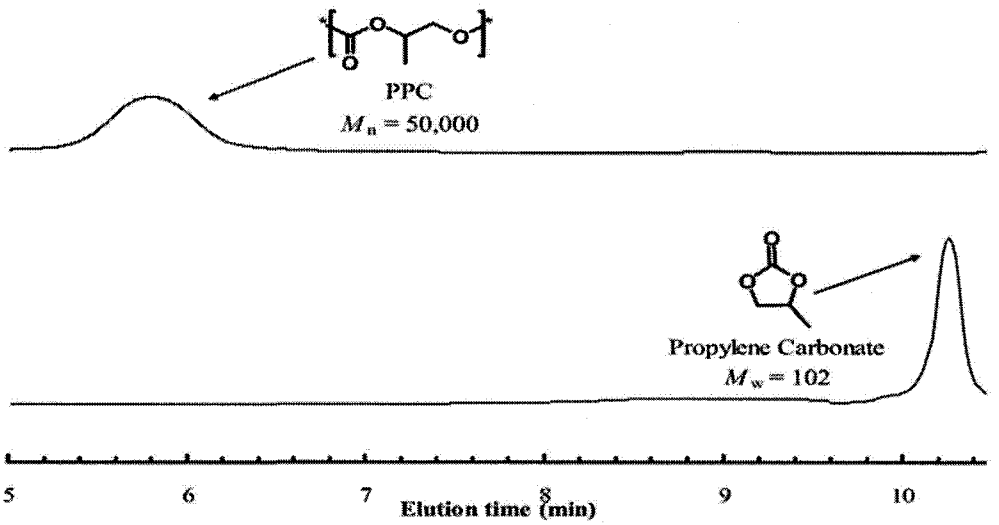

Figure IV.25. GPC profiles of PPC and the crude liquid product from degradation of PPC with 3 wt.% of TBD at 120 °C for 30 min in nitrogen

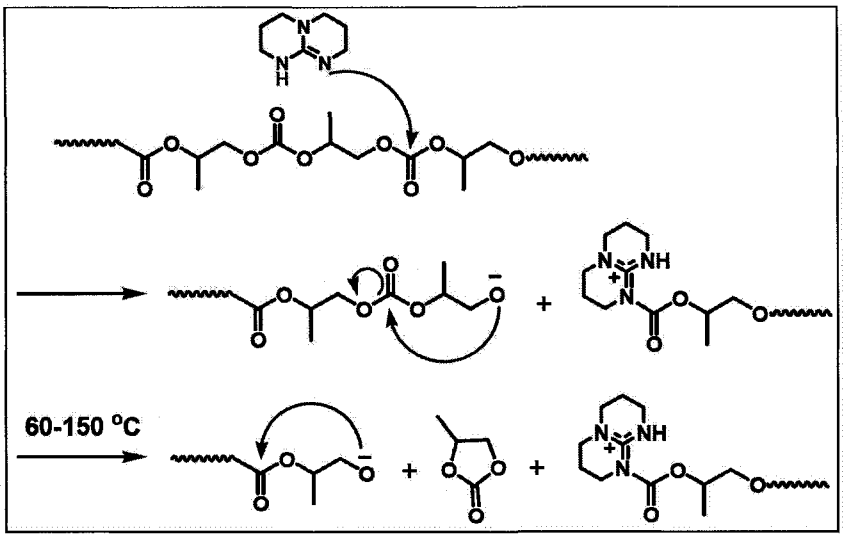

Scheme IV.12. Plausible mechanism for TBD-catalyzed thermolysis of PPC

Indeed, as shown in Figure IV.26, the thermolysis temperature is further lowered by 60 °C in the presence of 3 wt.% glycerol (GL) in PPC containing DBU. The effect of glycerol is more significant in thermal degradation of PPC containing TBD. After mixing 3 wt.% of TBD and glycerol with PPC at room temperature, the solid polymer degraded to a non-viscous liquid in less than 30 min.

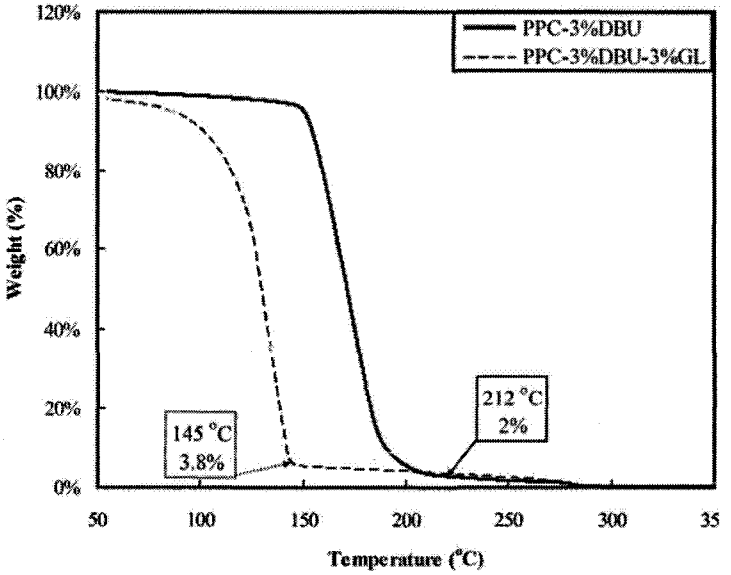

Figure IV.26. TGA traces of PPC with 3 wt.% of DBU and PPC with 3 wt.% of DBU Plus 3 wt.% of glycerol in nitrogen at a heating rate of 10 °C/min

IV.4.2 Base-Catalyzed Thermolysis of PCHC

In contrast, all the selected amine bases showed no amplification effect in thermal degradation of PCHC (Figure IV.27). Although 10-20 wt.% weight was observed at 120 °C, the clean-burn-off temperature for base-doped PCHC was still the same as that of the polymer alone. DBU and TBD should be able to cleave the carbonate bonds, but the resulting alkoxide can not further trigger the back-biting process due to the bulky cyclohexane ring (Scheme IV.13). The resulting non-volatile oligmers could only undergo further degradation via syn-elimination at higher temperatures.

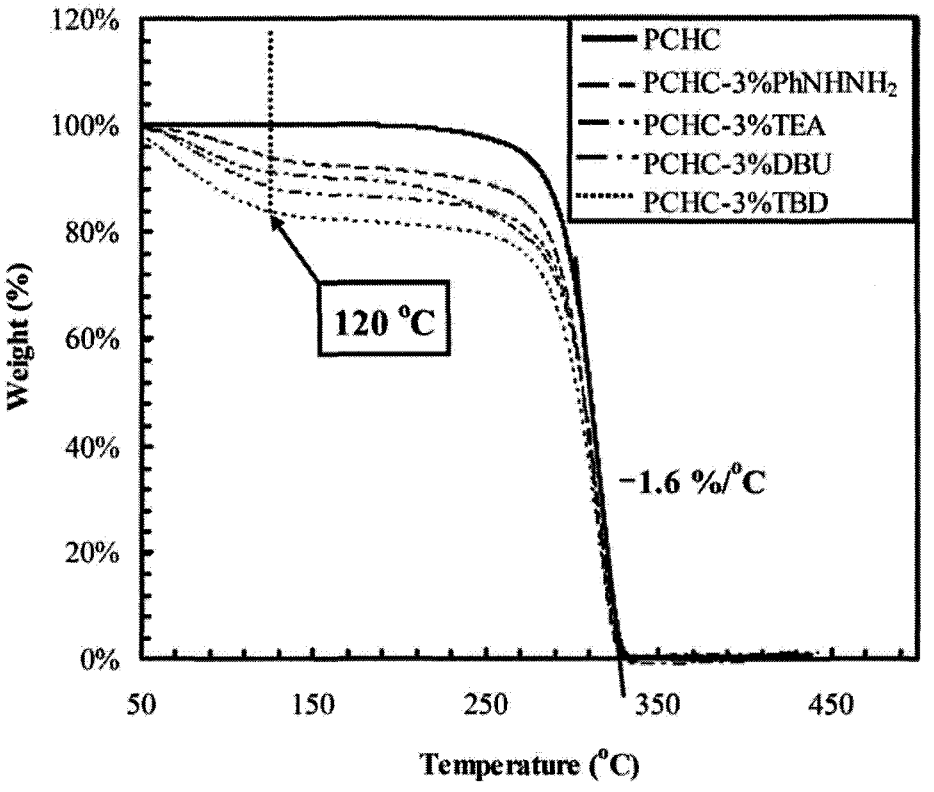

Figure IV.27. TGA traces of PCHC, PCHC with 3 wt.% of $PhNHNH_2$, TEA, DBU and TBD in nitrogen at a heating rate of 10 °C/min

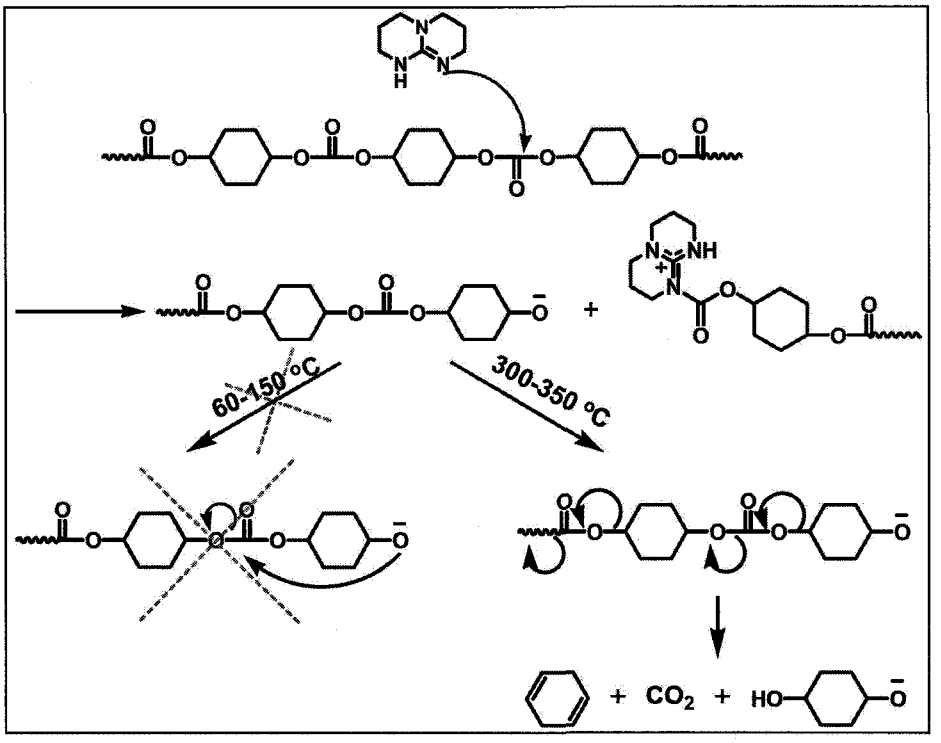

Scheme IV.13. Plausible mechanism for base-catalyzed thermolysis of PCHC

IV.4.3 Dry-Developing Photoresist Materials Based on TBD-catalyzed Thermolysis of PPC

PPC itself is normally stable up to 240 °C; while, in the presence of TBD and glycerol, it can start to degrade at the temperature close to room temperature and over 98 wt.% of the polymer is cleanly removed below 150 °C. This large difference in thermolysis temperatures between the two different formulations of PPC was exploited for a dry-developing photoresist system (Figure IV.28). Our newly developed photobase generator TBD·$HBPh_4$ (see Chapter II) can provide the TBD base by photolysis. Thus, a photosensitive system that consists of a thin film of PPC with a catalytic amount of TBD·$HBPh_4$ and glycerol can be realized. Exposure of this photosensitive film through a pattern mask to UV radiation causes decomposition of TBD·$HBPh_4$ with the liberation of

a catalytic amount of TBD within PPC. Image development can then be done simply by heating the film, which triggers the base-catalyzed thermolysis of PPC in the exposed areas only. This would lead to the appearance of a positive-tone image as volatile thermolysis products evaporate off.

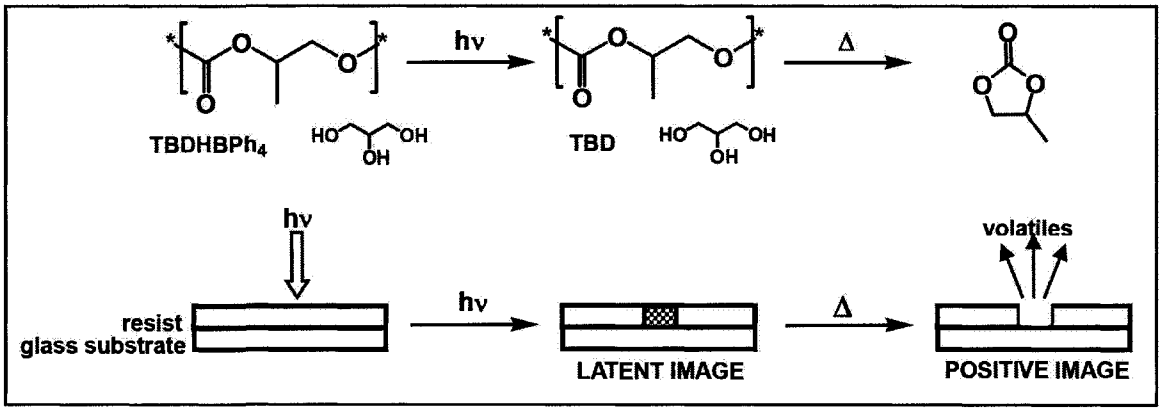

Figure IV.28. Imaging process of a base-catalyzed thermodegradable polycarbonate resist system

To optimize the conditions for the imaging development, the irradiated and non-exposed films were examined by TGA (Figure IV.29). As expected, the irradiated part of film started to degrade at a lower temperature (i.e., 60 °C) and lost 98% of its weight below 120 °C, but at the same temperature the non-exposed film was stable and had no weight loss. Considering that the resulting liquid propylene carbonate can lower the glass transition temperature of PPC and deform the film or patterns at elevated temperatures, the development was carried out in a vacuum oven under 8-10 Torr by heating from room temperature to 100 °C at a rate of 10 °C/min, followed by isothermal heating at 100 °C for 5 min.

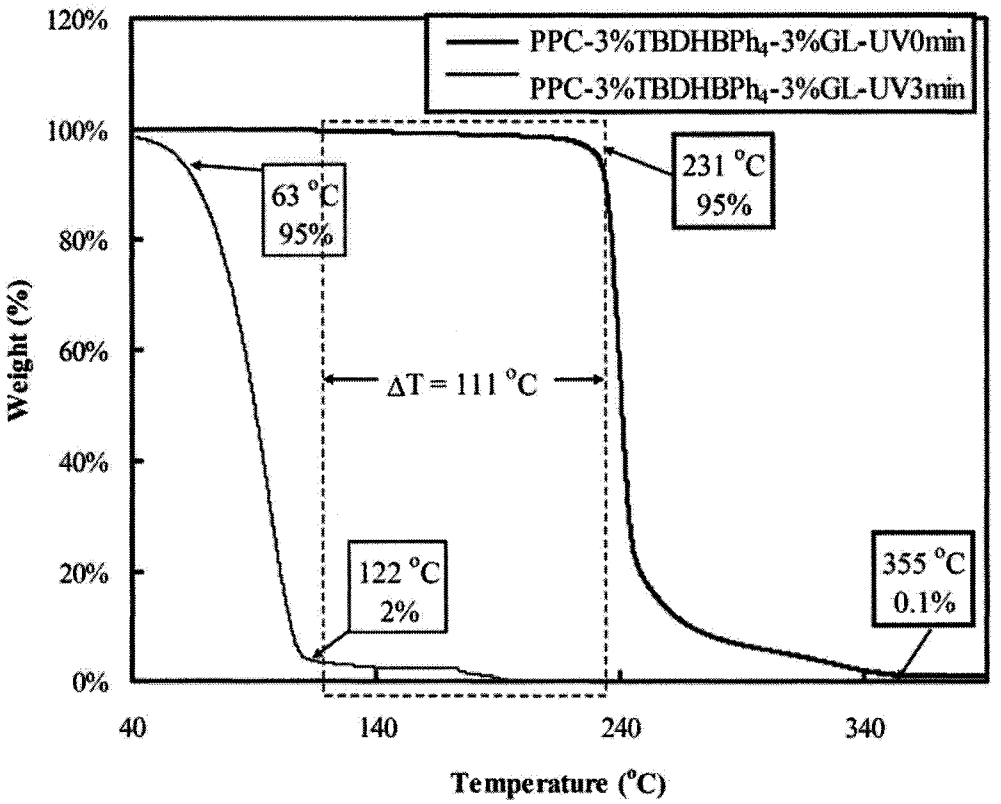

Figure IV.29. TGA traces (in nitrogen at a heating rate of 10°C/min) of PPC containing 3 wt.% TBD and glycerol with or without 254-nm irradiation

Figure IV.30 shows the scanning electron micrographs of positive tone images obtained from PPC containing 3 wt.% of TBD·$HBPh_4$ and glycerol by dry-developing process. The dark circular areas represent the developed patterns and the bright area indicates the PPC film. This positive image was consistent to the photomask patterns with a resolution better than 80 μm. The aspect ratio of the formed images, which is defined as the height of a feature divided by the width, was measured to be 3 to 1. As shown in Figure IV.31, the images have sharp side-walls indicating that deformation of PPC film did not happen during the development. Therefore, a new dry-developing photo-imaging resist material based on the base-catalyzed thermolysis of polycarbonate is demonstrated.

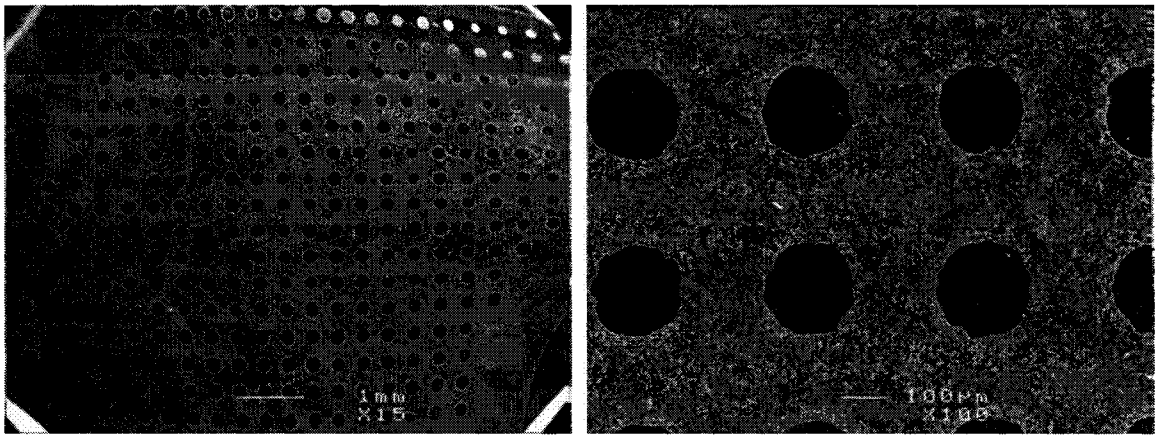

Figure IV.30. Scanning electron micrographs of positive-tone images obtained from PPC containing 3 wt.% of TBD·$HBPh_4$ and glycerol

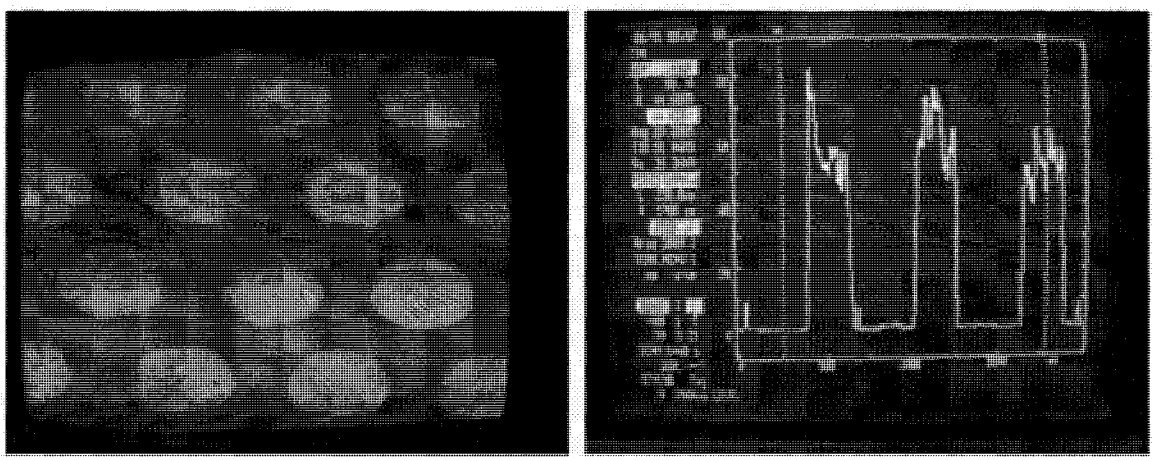

Figure IV.31. Microscopic photos of positive images and depth profiles

This new photoresist system was then applied to patterning ITO films. The ITO glass was spin-coated with PPC containing 3 wt.% of TBD·$HBPh_4$ and Glycerol, followed by UV exposure and thermal treatment. Chemical etching of ITO was then carried out using aqueous hydrochloric acid solution containing $FeCl_3$ as an oxidizing agent. The rest of PPC resist film was then easily removed by further heating or washing with acetone. The patterned ITO with an 80-μm resolution is showed in Figure IV.32, in which the dark circular spots represent the glass substrate after removal of ITO coating.

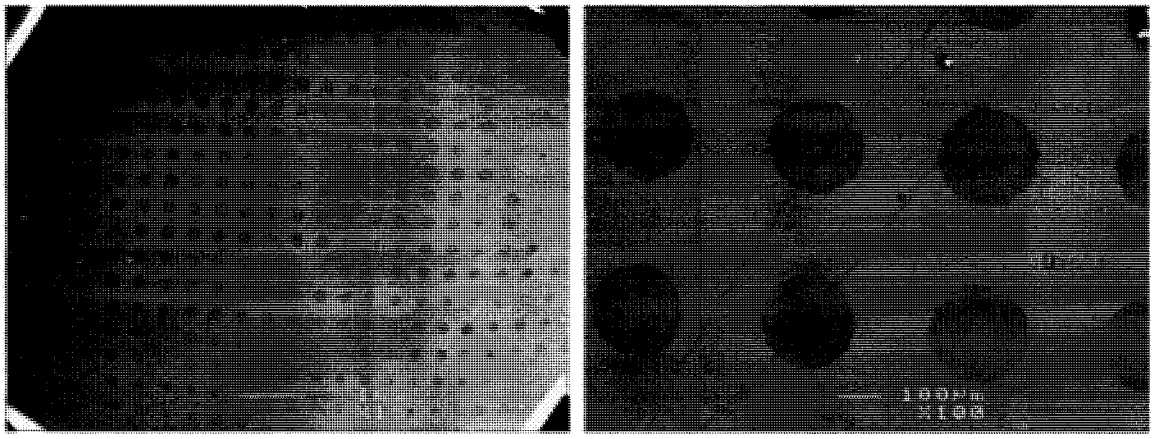

Figure IV.32. Scanning electron micrographs of patterned ITO glass using dry-developing photoresist of PPC containing 3 wt.% of TBD·$HBPh_4$ and glycerol

IV.5 Conclusion

In this chapter, a series of functionalized aliphatic polycarbonates are prepared and characterized. By studying their thermodegradation behaviours and photo-patterning abilities, PC-based formulations have potential to be sacrificial vehicles in photoimageable conductor pastes are recommended. The base-amplification effect on thermolysis of PPC is also investigated. As a result, a dry-developing photoresist material with TBD·$HBPh_4$ as a photocatalyst has been demonstrated.

IV.6 Experimental

1. Materials

1,4-Cyclohexanediol, 2,5-dimethyl-2,5-hexanediol, tripropylene glycol, triphosgene (BTC), 2,2-hydroxymethylpropionic acid, 2,2-hydroxymethylbutanoic acid, benzyl bromide, 2-amino-2-methyl-1,3-propanediol, 2,2'-dithiodiethanol,

1,1,1-tris(hydroxymethyl)propane, γ-butyrolactone, 2-hydroxypropyl acrylate, and azobisisobutyronitrile were received from Aldrich and used without purification. All the solvents used in reactions with bis-chloroformates were dried prior to use.

2. Instruments and Methods

IR spectra were recorded on a Varian 1000 FT-IR Scimitar Series. ^{1}H NMR spectra were measured on a Bruker Advance 300 instrument at 300 MHz. Differential scanning calorimetry and thermogravimetry were conducted on a TA instruments Q100 and Hi-Res TGA 2950. Both thermal techniques used a heating rate of 20 °C/min.

Photoirradiation of solid films were carried out by EFOS Novacure UV light source equipped with a high pressure 100 Watt mercury vapour short arc. The light intensity (10 Mw/cm^2) at 250-300 nm was determined by the built-in radiometer. Film thickness and depth profile were determined using the alpha-step 200 Tencor instrument.

3. Monomer Synthesis

Synthesis of Bis-Chloroformate Monomers

In a 250-mL magnetically stirred three-neck round-bottomed flask fitted with a condenser was dissolved 20.8 g (0.07 mole) of BTC in 100 mL of toluene, followed by addition of 0.1 mole of diols and 0.1 mL of pyridine. The mixture was stirred for 2 h at 60 °C. The reaction was monitored by IR. Once all the diols were consumed, a strong stream of nitrogen gas was passed through the solution mixture and exhausted through two

sodium hydroxide scrubbers in series to remove the excess of BTC and/or HCl. The remaining toluene solution was filtered and evaporated to give crude products. **IV-1** was purified by recrystallization in hexane. **IV-2** and **IV-3** were purified by distillation.

1,4-Cyclohexanediol bis(chloroformate) (IV-1): White needle crystal; yield 46%; mp 113-114 °C; ^{1}H NMR (300 MHz, $CDCl_3$) δ = 1.82 (m, 4H), 2.03 (m, 4H), 4.94 (s, 2H); ^{13}C NMR (75 MHz, $CDCl_3$) δ = 24.4, 74.6, 150.6; IR: 1764 cm^{-1} (C=O), 1166 cm^{-1} (C-O).

2,5-Dimethyl-2,5-hexanediol bis(chloroformate) (IV-2): Colorless liquid; yield 88%; bp 85-87 °C / 1.0 mmHg; ^{1}H NMR (300 MHz, $CDCl_3$) δ = 1.39 (d, 6H), 1.74 (m, 4H), 4.98 (m, 2H); ^{13}C NMR (75 MHz, $CDCl_3$) δ = 21.2, 30.1, 72.1, 152.6; IR: 1770 cm^{-1} (C=O), 1164 cm^{-1} (C-O).

Tripropylene glycol bis(chloroformate) (IV-3): Colorless liquid; yield 76%; bp 68-71 °C/0.5 mmHg; ^{1}H NMR (300 MHz, $CDCl_3$) δ = 1.21 (d, 3H), 1.35 (d, 6H), 3.42 (m, 2H), 3.62 (m, 2H), 3.91 (m, 1H), 4.25 (m, 2H), 5.11 (m, 2H); ^{13}C NMR (75 MHz, $CDCl_3$) δ = 17.1, 19.2, 67.2, 75.8, 76.7, 78.1, 154.3; IR: 1770 cm^{-1} (C=O), 1165 cm^{-1} (C-O).

Synthesis of Diol Monomers Containing Protected Acid Groups

DMPA (9.00 g, 67.11 mmol) and KOH (4.30 g, 76.79 mmol) were dissolved in 50 mL of DMF. The potassium salt was allowed to form at 100 °C for 1 h. Benzylbromide (13.80 g, 80.71 mmol) was then added. After 15 h of stirring at 100 °C, DMF was evaporated. The residue was dissolved in 200 mL of diethyl ether and washed with two

portions (50 mL) of water. The crude product was purified by chromatography on silica gel eluting with hexane first and then gradually with 20:80 hexane/ ethyl acetate.

Benzyl-2,2-bis(methylol)propionate (IV-4): White crystals: yield 67%; ^{1}H NMR (300 MHz, $CDCl_3$) δ = 1.08 (s, 3H), 3.74 (d, 2H), 3.95 (d, 2H), 5.22 (s, 2H), 7.36 (m, 5H); ^{13}C NMR (75 MHz, $CDCl_3$) δ = 17.1, 49.3, 66.6, 67.5, 127.8, 128.3, 128.6, 175.7.

Benzyl-2,2-bis(methylol)butanonate (IV-5): White crystals: yield 71%; ^{1}H NMR (300 MHz, $CDCl_3$) δ = 1.10 (t, 3H), 1.68 (m, 2H), 3.74 (d, 2H), 3.95 (d, 2H), 5.22 (s, 2H), 7.36 (m, 5H); ^{13}C NMR (75 MHz, $CDCl_3$) δ = 11.2, 22.1, 52.2, 63.6, 67.4, 127.8, 128.2, 128.6, 175.6.

Synthesis of Diol Monomers Containing Acrylate Groups

Acryloyl chloride (5.32 g, 58 mmol) in dry ethyl acetate (40 mL) was added dropwise into a cold solution of 2-amino-2-methyl-1,3-propanediol (5.15 g, 49 mmol) and NaOH (2.32 g, 58 mmol) in 10 mL of water. The reaction continued for 4 h at 0-5 °C. Then, the ethyl acetate layer was partitioned and dried over anhydrous Na_2SO_4. Ethyl acetate was evaporated and and the residue was fractionated, using a silica gel column with ethyl acetate/ethanol (20:1 v/v) as an eluent. The eluted fractions, after being examined by TLC, were collected (R_f = 0.37). The product was further purified by recrystallization in ethyl acetate/ethanol (10:1 v/v) and dried in vacuo.

N-[1,1-Bis(hydroxymethyl)ethyl]acrylamide (IV-6): White plate crystal; yield 68%; mp 83-84 °C; ^{1}H NMR (300 MHz, $CDCl_3$) δ = 1.16 (s, 3H), 3.69 (d, 2H), 4.83 (d, 2H),

5.72 (d, 1H), 6.15 (d, 1H), 6,33 (d, 1H); ^{13}C NMR (75 MHz, $CDCl_3$) δ = 18.7, 58.6, 63.8, 124.7, 132.6, 164.8; IR: 1687 cm^{-1} (C=O), 1633 cm^{-1} (C=C).

Synthesis of Diol Monomers Containing Metal Binding Groups

Concentrated sulphuric acid (3 mL, 55 mmol) was added dropwise to sodium chloride (7.0 g, 120 mmol) with stirring at room temperature. The HCl gas was bubbled into an isopropanol (40 mL) solution of AMPD (5.0 g, 50 mmol) with aid of purging argon. The resulted white precipitate (**IV-7**) were filtered and washed with acetone. Further purification was done by recrystallization in methanol/isopropanol (10:1 v/v): White crystal; yield 78%; mp 90-91 °C, ^{1}H NMR (300 MHz, DMSO-d_6) δ = 1.83 (s, 3H), 4.22 (s, 4H).

In a three-necked, round-bottomed flask fitted with a condenser, APD (2.0 g, 22 mmol) was dissolved in γ-BL (1.57g, 18 mmol) with a catalytic amount of TiO_2 (0.1 g). The solution was heated up to 200 °C and refluxed overnight. The cooling water was removed from the condenser and argon was slowly bubbled through the reaction solution for 2 h. The product was collected by distillation (bp = 153 °C/0.25 mmHg).

1-(1,3-dihydroxypropan-2-yl)pyrrolidin-2-one (IV-8): White solid; yield 34%; ^{1}H NMR (300 MHz, DMSO-d_6) δ = 1.88 (m, 2H), 2.21 (t, 2H), 3.34 (t, 2H), 3.77 (m, 5H); ^{13}C NMR (75 MHz, DMSO-d_6) δ = 18.1, 32.7, 44.4, 56.2, 68.9, 173.1; IR: 3400 cm^{-1} (O-H), 1669 cm^{-1} (C=O).

4. Synthesis of TD-Cross-linkers

BTC (4.40 g, 15 mmol) was dissolved in toluene (50 mL), followed by addition of 2-hydroxypropyl acrylate (40 mmol) and pyridine (0.05 mL). The mixture was stirred for 2 h at 60 °C and overnight at room temperature. Then, the reaction solution was filtered and evaporated. The product chloroformate was collected by vacuum distillation (68 °C/5 mmHg).

2-Hydroxypropyl acrylate chloroformate: Colorless liquid; yield 84%; ^{1}H NMR (300 MHz, $CDCl_3$) δ = 1.39 (d, 3H), 4.34 (m, 2H), 5.12 (m, 1H), 5.85 (d, 1H) 6.16 (t, 1H), 6.40 (d, 1H); ^{13}C NMR (75 MHz, $CDCl_3$) δ = 18.3, 67.7, 71.2, 128.3, 130.9, 151.8, 167.5; IR (C=O, chloroformate) 1770 cm^{-1} , (C=O, acrylate) 1713 cm^{-1}, (C=C) 1637 cm^{-1}.

2-Hydroxypropyl acrylate chloroformate (8.0 g, 41.7 mmol) was dissolved in dry dichloromethane (150 mL) and added slowly to a dichloromethane solution (200 mL) of corresponding diol or triol (34.7 mmol) and pyridine (3.2 g, 40 mmol) over a period of 1 h at 0 °C. The mixture was further stirred at room temperature for 7 h. After removal of solvent, the residue was washed with dry ethyl acetate and filtered to remove pyridine chloride salt. The product was purified by column chromatography on silica gel with ethyl acetate. TLC (silica) ethyl acetate, R_f = 0.24 for **IV-10** and 0.32 for **IV-9**.

IV-9: Colorless liquid; yield 79%; ^{1}H NMR (300 MHz, $CDCl_3$) δ = 1.31 (m, 6H), 1.75 (dd, 4H), 1.92 (dd, 4H), 4.26 (m, 4H), 4.71 (m, 2H), 5.08 (m, 2H), 5.87 (m, 2H), 6.18 (m, 2H), 6.42 (m, 2H); ^{13}C NMR (75 MHz, $CDCl_3$) δ = 17.1, 27.1, 71.0, 73.3, 80.2, 129.2, 156.3, 166.7; IR (C=O, carbonate) 1743 cm^{-1}, (C=O, acrylate) 1723 cm^{-1}, (C=C) 1638 cm^{-1}.

IV-10: Colorless liquid; yield 74%; ^{1}H NMR (300 MHz, $CDCl_3$) δ = 0.91 (t, 3H), 1.34 (d, 9H), 4.21 (m, 6H), 4.32 (m, 6H), 5.08 (m, 3H), 5.87 (m, 3H), 6.16 (m, 3H), 6.41 (m, 3H); ^{13}C NMR (75 MHz, $CDCl_3$) δ = 9.1, 17.6, 21.2, 34.6, 72.0, 74.3, 129.2, 156.7, 165.7; IR (C=O, carbonate) 1741 cm^{-1}, (C=O, acrylate) 1717 cm^{-1}, (C=C) 1636 cm^{-1}.

5. Polymer Synthesis

The general procedure is described for the polymerization of hexanediol-dichloroformate with bis(hydroxymethyl)propionic acid. An argon-flushed, three-necked, round-bottomed flask fitted with a magnetic stir was charged with hexanediol-dichloroformate (40 g, 0.165 mol) and bis(hydroxymethyl)propionic acid (22.0 g, 0.165 mol) and 10 mL of anhydrous acetonitrile. The mixture was heated to 50 °C in water bath while 1-methylimidazole (26.3 mL, 0.33 mol) was added dropwise via a dropping funnel over 40 min. After 2 h at 50 °C, the reaction mixture was cooled to room temperature and stirred overnight. Hydroxypropyl acrylate (1 mL, 0.008 mol) was added in one portion and the mixture was heated to 50 °C for 30 min. Toluene (300 mL) was then added and acetonitrile was removed by distillation at 80 °C. After cooling to room temperature, the polymer solution was easily decanted as the imidazole salt remained at the bottom of the reaction flask. Toluene was evaporated on a rotary evaporator. The resulting polymer was further purified by dissolving in acetonitrile and re-precipitated in water. The yield of polymer was 81-90%.

PC-1: Colorless solid; yield 81%; $[\eta]_{inh}$= 0.21 dL/g (C = 0.5 g/dL, 30 °C, $CHCl_3$); GPC

M_w = 11,200, M_n = 6,227, M_w/M_n = 1.8 (based on polystyrene standards); Tg = 32 °C (DSC, 10 °C/min);

PC-2: Colorless solid; yield 84%; $[\eta]_{inh}$= 0.20 dL/g (C = 0.5 g/dL, 30 °C, $CHCl_3$); GPC M_w = 10,800, M_n = 6,360, M_w/M_n = 1.7 (based on polystyrene standards); Tg = 30 °C (DSC, 10 °C/min);

PC-3: Colorless solid; yield 77%; $[\eta]_{inh}$= 0.18 dL/g (C = 0.5 g/dL, 30 °C, $CHCl_3$); GPC M_w = 10,270, M_n = 5,700, M_w/M_n = 1.8 (based on polystyrene standards); Tg = 30 °C (DSC, 10 °C/min);

PC-6: White powder; yield 74%; $[\eta]_{inh}$= 0.32 dL/g (C = 0.5 g/dL, 30 °C, $CHCl_3$); GPC M_w = 7,800, M_n = 5,008, M_w/M_n = 1.56 (based on polystyrene standards); Tg = 72 °C (DSC, 10 °C/min);

PC-7: White powder; yield 74%; $[\eta]_{inh}$= 0.28 dL/g (C = 0.5 g/dL, 30 °C, $CHCl_3$); GPC M_w = 8,080, M_n = 4,588, M_w/M_n = 1.76 (based on polystyrene standards); Tg = 68 °C (DSC, 10 °C/min);

PC-8: Colorless liquid; yield 76%; $[\eta]_{inh}$= 0.22 dL/g (C = 0.5 g/dL, 30 °C, $CHCl_3$); GPC M_w = 9,200, M_n = 4,798, M_w/M_n = 2.05 (based on polystyrene standards); Tg = 17 °C (DSC, 10 °C/min);

PC-9: Colorless liquid; yield 72%; $[\eta]_{inh}$= 0.20 dL/g (C = 0.5 g/dL, 30 °C, $CHCl_3$); GPC M_w = 9,400, M_n = 4,878, M_w/M_n = 1.96 (based on polystyrene standards); Tg = 15 °C (DSC, 10 °C/min);

PC-10: Colorless liquid; yield 68%; $[\eta]_{inh}$= 0.20 dL/g (C = 0.5 g/dL, 30 °C, $CHCl_3$);

GPC M_w = 9,700, M_n = 5,160, M_w/M_n = 1.88 (based on polystyrene standards); Tg = 12 °C (DSC, 10 °C/min);

PC-11: Colorless liquid; yield 65%; $[\eta]_{inh}$= 0.17 dL/g (C = 0.5 g/dL, 30 °C, $CHCl_3$); GPC M_w = 13,200, M_n = 6,160, M_w/M_n = 2.2 (based on polystyrene standards); Tg = 5 °C (DSC, 10 °C/min);

PC-12: Light yellow solid; yield 87%; $[\eta]_{inh}$= 0.37 dL/g (C = 0.5 g/dL, 30 °C, $CHCl_3$); GPC M_w = 11,507, M_n = 8,784, M_w/M_n = 1.31 (based on polystyrene standards); Tg = 46 °C (DSC, 10 °C/min);

PC-13: Light yellow solid; yield 71%; $[\eta]_{inh}$= 0.32 dL/g (C = 0.5 g/dL, 30 °C, $CHCl_3$); Tg = 58 °C (DSC, 10 °C/min);

PC-14: Light yellow solid; yield 73%; $[\eta]_{inh}$= 0.30 dL/g (C = 0.5 g/dL, 30 °C, $CHCl_3$); Tg = 31 °C (DSC, 10 °C/min);

PC-15: Light yellow liquid; yield 69%; $[\eta]_{inh}$= 0.11 dL/g (C = 0.5 g/dL, 30 °C, $CHCl_3$); GPC M_w = 6,763, M_n = 5,591, M_w/M_n = 1.12 (based on polystyrene standards); Tg = 45 °C (DSC, 10 °C/min);

PC-16: White powder; yield 84%; $[\eta]_{inh}$= 0.21 dL/g (C = 0.5 g/dL, 30 °C, $CHCl_3$); GPC M_w = 15,780, M_n = 8,971, M_w/M_n = 1.76 (based on polystyrene standards); Tg = 28 °C (DSC, 10 °C/min).

Deprotection by Hydrogenation

To a flame-dried round-bottomed flask equipped with a magnetic stir bar, the benzyl or benzylidene protected dendrimer was dissolved in a 1:1 mixture of CH_2Cl_2 and MeOH

(total of 20 mL). Pd/C (10%) was added and the flask was evacuated and back-filled with hydrogen three times (H_2 pressure: 1 atm). After vigorous stirring for 24 h, the reaction mixture was filtered through a Celite plug in a fritted glass funnel and the filtrate was evaporated to dryness on a rotary evaporator in vacuo. The product was obtained as white foam in quantitative yield.

6. Method for Calculating Kinetic Parameters of Thermal Degradation from TGA

The reaction rate is expressed as a product of a temperature dependent function, *K(T)* and a composition- or conversion-dependent term, f(α),

$$d\alpha / dt = K(T) \times f(\alpha) \qquad \text{Eq.(1)}$$

where α , t and T are the conversion (weight of polymer volatilized/initial weight of polymer), the time (min) of reaction and the absolute temperature of reaction (*K*), respectively. *K(T)* is the reaction rate constant, which is assumed to obey the usual Arrhenius relationship:

$$K(T) = A\exp(-E / RT) \qquad \text{Eq.(2)}$$

where *A*, *E* and *R* are the pre-exponential factor, the activation energy ($Jmol^{-1}$) and the universal gas constant (8.314 $Jmol^{-1}K^{-1}$), respectively. If reaction of polymer degradation is assumed to be a simple nth-order reaction, $f(\alpha)$ can be written as follows:

$$f(\alpha) = (1- \alpha)^n \qquad \text{Eq.(3)}$$

Then a new equation can be obtained by combining Eqs. (1), (2) and (3).

$$d\alpha / dt = A(1- \alpha)^n \exp(-E / RT) \qquad \text{Eq.(4)}$$

Although there are many methods for the calculation of kinetic parameters of the thermal degradation by TG measurements, they are all based on this equation Eq.(4). From Eq. (4) it follows:

$$\ln (d\alpha / dt) = \ln A + n \ln (1- \alpha) - E/RT \qquad \text{Eq.(5)}$$

Eq. (5) can be further rewritten as:

$$\ln (d\alpha / dt) - n \ln (1- \alpha) = \ln A - E/RT \qquad \text{Eq.(6)}$$

By plotting the left term of Eq. (6) versus 1/T, a straight line should be obtained if the selected n value is correct, and the E and ln A values can be obtained from the slope and intercept of the straight line, respectively. This is the Chang's method[29] for analyzing the thermal degradation of a polymer.

IV.7 References

1. Penco, M.; Sartore, L.; Samperi, F. *Macromol. Chem. Phys.* **2006**, *207*, 1492.
2. Moratti, S. C.; Charalambides, Y. C. *Science of Synthesis* **2005**, *8*, 451.
3. Kim, W. B.; Lee, J. S. *Angew. Chem., Int. Eng. Chem. Res.*, **2004**, *43*, 1897.
4. Hata, S.; Goto, H.; Tanaka, S.; Oku, A. *J. Appl. Polym. Sci.* **2003**, *90*, 2959.
5. Suresh, S.; Gulotty, R. J.; Cummins, C.; Smith, D. W. *Polymer* **2003**, *44*, 5111.
6. Carothers, W. H.; Hill, J. W. *J. Am. Chem. Soc.* **1933**, *55*, 5031.
7. Jiang, Z.; Gross, R. A. *Macromolecules* **2007**, *40*, 7934.
8. Houlihan, F. M.; Bouchard, F.; Frechet, J. M. J. *Macromolecules* **1986**, *19*, 13.
9. Aida, T.; Inoue, S. *Macromolecules* **1981**, *14*, 1166.

10. Yasuda, T.; Aida, T.; Inoue, S. *Macromolecules* **1983**, *16*, 1792.

11. Yasuda, T.; Aida, T.; Inoue, S. *Macromolecules* **1984**, *17*, 2217.

12. Mark, H. F.; Kroschwitz, J. I. (eds.) *Encyclopedia of Polymer Science and Engineering*; Wiley, **1985**.

13. Cotarca, L.; Delogu, P.; Nardelli, A.; Sunjic, V. *Synthesis* **1996**, *5*, 553.

14. Eckert, H.; Forster, B. *Angew. Chem., Int. Ed. Engl.* **1987**, *26*, 894.

15. Labadie, J. W.; Haidar, B. *Polym. Prepr.* **1995**, *36*, 735.

16. Ohno, H.; Yoshizawa, M. *Solid State Ionics* **2002**, *154*, 303.

17. Harmon, K. M. *J. Mol. Struc.* **2005**, *740*, 75.

18. Kolmakov, Kirill A. *Can. J. Chem.* **2007**, *85*, 1070.

19. Gabel, D.; El-Zaria, M. B. *Science of Synthesis* **2004**, *6*, 541.

20. Smith, J. D.; Yang, H.X.; Suess, T.R. *US Patent 20050014091*, **2005**.

21. Glicksman, H. D.; Yang, H. X. *US Patent 20030138708*, **2003**.

22. Corey, E. J.; Winters, R. A. E. *J. Am. Chem. Soc.* **1963**, *85*, 2677.

23. Choppin, A. R.; Rogers, J. W. *J. Am. Chem. Soc.* **1948**, *70*, 2967.

24. Vogel, Vogels's Textbook of Practical Organic Chemistry; Longman Scientific & Technical: Essex.

25. Martin, F. D.; Oxley, J. C. *Polym. Mate. Sci. Eng.* **1984**, *51*, 688.

26. Sausaman; D. K.; Purcell, R. F. *US Patent 3785855,* **1974**.

27. Esperanza Diaz, R. B.; Valenciano, I. A. K. *J. Appl. Polym. Sci.* **2004**, *93*, 1512.

28. Wohrle, D.; Pomogailo, A. D. (eds.) *Metal Complexes and Metals in Macromolecules:*

Synthesis, Structure and Properties; Wiley-VCH, **2003**.

29. Chang, W. L. *J. Appl. Polym. Sci.* **1994**, *53*. 1759.
30. Frechet, J. M. J.; Willson, C. G. *J. Photopolym. Sci. Technol.* **1990**, *3*, 235.
31. Kaljurand, I.; Kuett, A.; Soovaeli, L.; Rodima, T.; Maeemets, V.; Leito, I. *J. Org. Chem.* **2005**, *70*, 1019.

Summary

The tetraphenylborate salts represent a new family of shortwave UV PBGs. They are able to generate nitrogen bases, from phosphazene to tertiary amines, with quantum efficiency similar to most of commercially available cationic PIs. Among them, *t*-BuP_1(dma)·$HBPh_4$ and TBD·$HBPh_4$ are the first examples capable of releasing strong bases *t*-BuP_1(dma) and TBD, which are 100-1000 times more basic than DBU generated from the previously reported PBGs. Realization of photogeneration of the super strong organic bases offers new opportunities for further advances in deep-UV curing and photoresist technology. Examples include using TBD·$HBPh_4$ as a photocatalyst for photo-induced ring-opening polymerization of cyclic esters, surface modification of cellulose, and dry-developing photoresist based on PPC.

Regarding photoimageable polymeric materials, polycarbonates containing a variety of functional groups have been developed, including acrylate, carboxylic acid, metal-binding disulfide, amine and pyrrolidinone groups. The correlation between the functional groups and thermal degradation of polycarbonates has been established.

Polycarbonates containing carboxylic acid groups can be completely degraded at about 350 °C. The base-catalyzed thermolysis of polycarbonate proceeds in a "back-biting" process to release cyclic carbonates as by-products and accelerates in the presence of a catalytic amount of glycerol and TBD, resulting in complete degradation of PPC below 180 °C. Using TBD·$HBPh_4$, the dry-developing photoresist material based on PPC has been demonstrated with an image resolution better than 80 μm and an aspect ratio of 3:1. With PBGs, the functionalized polycarbonates have been applied as photoimageable sacrificial vehicles in silver conductor pastes that can be cleanly 'burned' out at 400 °C in nitrogen, which is 120 °C lower than the DuPont Fodel pastes.

CONTRIBUTIONS TO KNOWLEDGE

1. Tetraphenylborate salts are proved to be a new family of shortwave UV PBGs and capable of releasing nitrogen bases including *t*-BuP_1(dma), TBD, DBU and Et_3N, with quantum efficiency similar to most of commercially available cationic PIs.

2. *t*-BuP_1(dma)·$HBPh_4$ and TBD·$HBPh_4$ are the first examples capable of releasing strong bases *t*-BuP_1(dma) and TBD, which are 100 times more basic than the strongest base (DBU) generated among all the previously reported PBGs.

3. TBD·$HBPh_4$ has been demonstrated to be an efficient photocatalyst for photoinduced living ROP of cyclic esters and the photocross-linking of polymeric materials containing the hydroxyl-ester groups.

4. Photo-cross-linkable polycarbonates containing acrylate groups, aqueous developable polycarbonates bearing carboxylic acid groups, and metal-binding polycarbonates containing ether, disulfide, amine and pyrrolidinone groups are prepared.

5. The sacrificial vehicle based on synthesized polycarbonates is applied in silver conductor pastes, which can be cleanly burned out at the temperature of 120 °C lower than the commercial DuPont paste.

6. Using $TBDHBPh_4$, the dry-developing photoresist material based on PPC has been demonstrated. The photo-patterned images have a resolution better than 80 μm and an aspect ratio of 3:1.

PUBLICATIONS:

1. Sun, Xun; Gao, Jian Ping; Wang, Zhi Yuan. "Bicyclic guanidinium tetraphenylborate:

2. a photobase generator and a photocatalyst for living anionic ring-opening polymerization and cross-linking of polymeric materials containing ester and hydroxy groups" *J. Am. Chem. Soc.* **2008**, *130*, 8130.

3. Bai, Yaowen; Song, Naiheng; Gao, Jian Ping; Sun, Xun; Wang, Xiaomei; Yu, Guomin; Wang, Zhi Yuan. "A New Approach to Highly Electrooptically Active Materials Using Cross-Linkable, Hyperbranched Chromophore-Containing Oligomers as a Macromolecular Dopant" *J. Am. Chem. Soc.* **2005**, *127*, 2060.

AWARD:

1. Xerox-CSC graduate Student Award - MSED Poster Award at the IUPAC/CSC conference in 2003, "Organic Template-Based Soft Processing: A New Strategy for One-Step Processing of Advanced Materials and Fabrication of Microstructures".